POLLUTANT REMOVAL FROM WATER USING PLANT MATERIALS

BEATRICE KATHEU KAKOI

DOCTOR OF PHILOSOPHY

(Environmental Engineering and Management)

JOMO KENYATTA UNIVERSITY OF

AGRICULTURE AND TECHNOLOGY

2018

Pollutant removal from water using plant materials

Beatrice Katheu Kakoi

A Thesis Submitted in Partial Fulfillment for the Degree of Doctor of philosophy in Environmental Engineering and Management

2018

DECLARATION

This thesis is my original work and has not been presented for a degree in any other university.

Signature:……. Date:…….

Beatrice Katheu Kakoi

This thesis has been submitted for examination with our approval as the university supervisors:

Signature:…… Date:……

Prof. James Wambua Kaluli, PhD

JKUAT, Kenya

Signature:…… Date:……..

Dr. Peter N. Ndiba, PhD

University of Nairobi, Kenya

Signature:…… Date:…….

Prof. George Thuku Thiong'o, PhD

JKUAT, Kenya

DEDICATION

This work is dedicated to my husband, Mr Onesmus Kakoi, and my children Kevin and Pendo for inspiring me during my studies.

ACKNOWLEDGEMENT

I would like to express my sincere gratitude to my supervisors Prof. James Kaluli, Dr. Peter Ndiba and Prof. George Thiong'o for their guidance and encouragement throughout this study. I would also like to thank the technical staff in the departments of Civil Engineering, Chemistry and Soil, Water and Environmental Engineering at Jomo Kenyatta University of Agriculture and Technology (JKUAT) for their help in data collection and analysis. Special thanks to my colleagues for their moral support.

I acknowledge the administration of JKUAT for their financial support and grant of study leave. I also acknowledge the National Commission for Science, Technology and Innovation (NACOSTI) for the research grant which made it possible for me to undertake this research.

Finally, I would like to acknowledge my husband, son and daughter for their love and support.

TABLE OF CONTENTS

LIST OF TABLES

LIST OF FIGURES

LIST OF APPENDIXES

Appendix A

Appendix B

Appendix C

Appendix D

Appendix E

Appendix F

LIST OF ABBREVIATION/ACRONYMS

AAS – Atomic absorption Spectroscopy

ANOVA - Analysis of Variance

AOAC - Association of Analytical Communities

AP - Adequate precision

APHA - American Public Health Association

Bp - Banana pith

Ce - Concentration of adsorbate remaining in solution

CKD - Cement kiln dust

COD - Chemical oxygen demand

$c_x c_y$ - Particle concentrations for two particles of sizes x and y

C_{xy} - Number of collision occurring per unit time per unit volume

EPA - Environmental protection agency

FTIR - Fourier Transform infra-red

$K(v_x v_y)$ - Brownian aggregation collision factor which depends on particle

K_1 - Equilibrium rate constant of pseudo-first sorption (g/mg.s)

K_2 - Equilibrium rate constant of pseudo-second sorption (g/mg.s),

K_{AB} - Mass transfer coefficient

KB - Boltzmann's constant (J/K)

LOF - Lack-of-fit test

MD - Maerua Decumbent

MS*E* - Mean Square of residuals

MS*R* - Mean Square of regression

OS	-	Opuntia Spp.
pHpzc	-	point of zero charge
PVC	-	Polyvinyl Chloride
Qe	-	Equilibrium concentration
$\mathbf{q_t}$	-	Amount of pollutant adsorbed at time t (mg/g)
SEM	-	Scanning electron microscope size, temperature, and pressure
SS*E*	-	Sum of square caused by the residual
SS*L*	-	Sum of square due to the lack-of-fit
SS*P*	-	Sum of square due to the pure error
SS*R*	-	Sum of square caused by the regression
SS*T*	-	Total sum of square
T	-	Absolute temperature (K)
WHO	-	World Health Organisation
β_i	-	Linear regression term
β_{ij}	-	Interaction regression term
β_{ii}	-	Quadratic regression term
β_o	-	Value of the fixed response at the center point of the design
μ	-	Viscosity
α	-	Order of coag-flocculation process

ABSTRACT

Removal of pollutants from contaminated water is a necessary measure in protection of the environment and human health. The use of biomaterials for removal of heavy metal from polluted water is eco-friendly and economical technique for developing countries. This study evaluated locally available biomaterials namely; banana pith, Opuntia Spp. and Maerua Decumbent as bio-coagulants and bio-sorbents of heavy metals. Banana pith, Opuntia Spp. and Maerua Decumbent biomass were characterized using proximate, elemental and functional groups analyses. Proximate analysis followed the Standard Methods (AOAC, 1999) whereas elemental analysis was conducted using Perkin-Elmer Series II CHNS/O 2400 Elemental Analyzer and functional group analysis using Fourier Transform Infrared (FT-IR) Spectroscopy, Model 8400. Bio-coagulants and bio-sorbents were used to remove turbidity, COD and selected heavy metals; lead, chromium, copper and zinc from contaminated surface water and paint industry wastewater. Turbidity was measured using a turbidity meter SGZB while heavy metal analysis was done with the help of an atomic absorption spectrometer AAS- 6200 Shimadzu. The study applied response surface methodology (RMS) for optimization of coagulation and flocculation processes in treatment of paint wastewater. Characterization of the study biomaterials revealed that they comprised of polysaccharides, proteins and lipids with functional groups that included amino, carboxyl, sulfate and hydroxyl. An 80% removal rate of heavy metals through bio-sorption was achieved. Langmuir and Freundlich isotherm models described the sorption data for the studied biomass, ($R^2 \approx 0.9$) indicating single layer sorption on homogeneous material. Sorption kinetic data was best described by the second order kinetic models. The calculated q_e approached the experimental values

indicating that chemical sorption process may have been dominant. The highest chromium uptake of 2.36 mg/g by banana pith was achieved at an initial influent concentration of 20 mg/l, flow rate 3 ml/min and bed depth 6 cm in continuous flow studies. Coagulation –flocculation process kinetics revealed that banana pith, Maerua Decumbent and Opuntia Spp. followed second order kinetics with a peri-kinetic flocculation half-life of 1.16, 0.78 and 0.84 minutes respectively; and rate constants k of 0.0027, 0.004 and 0.00037 l/mg.min respectively. Optimization of paint wastewater treatment using Response Surface Methodology resulted in maximum turbidity removal from paint wastewater of 99.24 %, at optimum conditions of pH 5.56, Maerua Decumbent dosage of 1.0 g/l and settling time 52.3 minutes. The 100% lead removal was realized at pH 6.81 and Maerua Decumbent dosage of 1.16 g/l. Some 99.97 % removal of chromium was achieved at pH 5.78 and Maerua Decumbent dosage of 1.03 g/l. At pH 5.00 and Maerua dosage of 1.3 g/l, an optimum zinc removal rate of 81.2% and optimum iron removal rate of 85.6 % were achieved. Confirmatory experiments validated the model to within 4% error. This research demonstrates the potential use of bio-coagulants in water and wastewater treatment.

CHAPTER ONE

INTRODUCTION

1.1 Background Information

Industrial growth, rapid urbanization and high population in developing countries, results in increased generation of wastewaters, which are mainly disposed into water bodies. Industrial wastewaters usually contain pollutants such as heavy metals, dyes, phenols, inorganic anions and pesticides that are toxic to life. Heavy metals are non-biodegradable; moreover, they bio-accumulate in the environment and cause various diseases and disorders (Davis *et al.*, 2000; Gupta et al, 2009). Heavy metal pollution occurs directly by effluent outfalls from industries, refineries and waste treatment plants and indirectly by the contaminants that enter the water supply from groundwater systems and from atmosphere through rain water (Bailey *et al*., 1999; Vijayaraghavan & Yun, 2008). Consequently, many aquatic environments face metal concentrations that exceed criteria designed to protect the environment, animals and humans.

Techniques employed in removal of heavy metal pollution from water and wastewater include biological treatment, chemical coagulation and precipitation, ion-exchange, electrochemical methods, adsorption using activated carbon and membrane processes (Farooq et al., 2010). All these methods are characterized by environmental challenges and high initial and running costs. Therefore, there is need for alternative methods (Kapoor & Viraraghavan, 1995)

The use of bio-coagulants in water treatment is desirable because they are inexpensive and safe for human health and the environment. While locally available bio-materials such as banana pith (Musa spp.), Opuntia spp. and Maerua decumbent have been studied for turbidity removal, (Mwachiro et al., 2004), (Lenz *et al.*, 2011) and (Habsahalwi *et al.*, 2013) their application in removal of heavy metals has not been reported.

The removal of heavy metal from polluted water by biomass is a complex reaction involving biomass surface functional groups including carboxyl (-COOH), hydroxyl

(-CHH) and amine (-NH_2) groups among others (Vijayaraghavan et al., 2011; Bahman R. , 2014; Muhammad et al., 2015). Applicability of the bio- materials in heavy metal removal requires knowledge of their characteristics.

Operational parameters such as solution pH, biomass dose and initial concentration of the heavy metal may affect performance of bio- materials as bio-sorbents. Understanding the significance of these parameters requires evaluation of equilibrium and kinetics of bio-sorption by the materials.

Efficient application of biomaterials in the coagulation-flocculation process requires optimization of involved processes. Most optimization studies for the coagulation-flocculation process use the trial and error conventional 'change one factor at a time' approach (Mohd *et al*., 2008). These single-dimensional searches are in most cases, incapable of revealing the optimal combination of factors because they fail to capture some of the interactions (Trinh and Kang, 2011).

1.2 Statement of the problem

Discharge of harmful substances into water causes water pollution. Most of the pollutants are toxic to most life forms and, therefore, need to be removed. The conventional methods of pollutant removal from water are environmentally unfriendly and non-affordable for most communities in the developing world. Consequently, there is need for alternative methods that are affordable, locally available and eco-friendly. Some plant materials such as banana pith (Musa Spp.), cactus (Opuntia Spp.) and Maerua Decumbent have potential for pollutant removal. Application of natural materials in water treatment requires adequate information on the mechanism of pollutant removal. The fitting of experimental kinetic data to mathematical models can identify the mechanisms involved. Moreover, where several operating factors are involved, the one factor at a time approach to obtaining optimum conditions may fail to capture the interactive effects of the various factors. Therefore, it is necessary to employ an interactive tool such as the response surface methodology (RMS) that captures all the interactions.

1.3 Justification

The conventional methods of pollutant removal from water are environmentally unfriendly and non-affordable for most communities in the developing world. Use of natural materials for pollutant removal would provide readily available, non-toxic, biodegradable and less expensive alternatives. Some plant materials such as banana pith (Musa Spp.), cactus (Opuntia Spp.) and Maerua Decumbent have potential for pollutant removal. These plants are locally available in Kenya.

Exploitation of the potential of these plants in pollutant removal would address the challenges being faced in water and waste water treatment in developing countries.

1.4 Objectives

1.4.1 Objectives

The main objective of study was to investigate the potential use of plant materials as bio-coagulant/flocculants and bio-sorbents in water and waste treatment.

Specific objectives

1. To characterize the biomass in terms of their proximate and elemental composition; and functional groups.
2. To evaluate the performance and determine the equilibrium and kinetics of the plant biomass as sorbents for heavy metal removal from water.
3. Evaluation of the performance and determine the kinetics of plant biomass as bio-coagulants for turbidity removal and the effect of the coagulation-flocculation process in heavy metal removal from polluted River water.
4. Optimization of the coagulation-flocculation process in the removal of turbidity and heavy metals from paint industry wastewater.

1.5 Research questions

1. What compounds and functional groups are present in bio-sorbent and coagulant?
2. What is the kinetics of heavy metal removal by plant bio-sorbents?
3. What is the kinetics of turbidity removal by plant based coagulants?
4. How well would the response surface methodology optimization of coagulation-flocculation process for paint industry wastewater describe the optimum conditions?

1.6 Scope

This study covered coagulation and flocculation and bio-sorption of pollutants in water using three plant materials; namely, banana pith, Maerua Decumbent and Opuntia Spp. The potential use of the plant materials as natural coagulants was evaluated through removal of turbidity and heavy metal from surface water and industrial wastewater. The efficacy of natural bio-sorbents was evaluated for removal of heavy metals from synthetic wastewater. Response surface methodology was used in optimization of coagulation-flocculation process of paint wastewater treatment only.

1.7 The limitations

This study detected heavy metals in Nairobi River but it was not possible to identify specific sources the different contaminants.

By use of response surface methodology multiple response optimization was achieved for the removal of turbidity and COD using three factors (pH, dosage and settling time) and for the removal of lead, chromium, zinc and iron using two factors (pH and dosage). It was not possible to obtain overall optimum conditions for all the studied pollutants because of variation of factors used in the study.

CHAPTER TWO

LITERATURE REVIEW

2.1 Metals in the environment

Metals play an important role in life. They are used in the manufacture of many common things such as batteries, clothes, cars, computers, among others. The high demand for metals requires production of a large quantity of metal through ore mining. Metal production and release to the environment has increased dramatically during the 20th century's Industrial Revolution (Nriagu, 1996). Cumulative anthropogenic release of heavy metals into the environment has disrupted the natural biogeochemical cycles of metals, causing increased deposition of heavy metals in soils and aquatic ecosystems. On the other hand, release of these metals from industrial waste streams to the environment has become of great global environmental concern (Alluri *et al.,* 2007). Toxic metals persist in the environment. Furthermore, through a process of bio-accumulation, they can enter into the food chains and pose adverse effects on human and environmental health (Volesky, 2003). Heavy metal pollution in the aquatic ecosystems has also become a serious threat and of great environmental concern (Srivastava & Goyal, 2010) even as authorities all over the world implement strict environmental regulations it.

In Kenya, water pollution from industrial and municipal sources is among the worst pollution problems (GOK, Government of kenya Development plan, 1993).It is estimated that 85% of Kenya's rural population depends exclusively on surface sources for water supply (Otieno, 1995).These water sources are increasingly being threatened by pollution from agricultural and industrial sources (Olago & Akech, 2002). Studies on pollution of Nairobi River found that sewage, nutrients, toxic metals, human waste, solid waste dumping, industrial and agricultural chemicals are main pollutants (Wandiga, Odipo, & Jonnalagada, 1995).

2.2 Toxicity of heavy metal

The bio toxic effects of heavy metals refer to the harmful effects of heavy metals to the body when they are consumed above the recommended limits. All heavy metals have specific toxicity signs (Table 2.1). Signs common to cadmium, lead, arsenic, zinc, copper and aluminum poisoning include gastrointestinal disorders, stomatitis, tremor, hemoglobinuria, ataxia, paralysis, vomiting and convulsion and depression when volatile vapors and fumes are inhaled (Rai & Tripathi, 2007).

2.3 Removal of heavy metals from polluted water

Removal of heavy metals from industrial effluents is usually achieved through conventional adsorbents such as activated carbon, polymer resins and synthetic coagulants. It can also be achieved through the use of processes such as chemical precipitation, chemical oxidation or reduction, electrochemical treatment, evaporation, filtration, reverse osmosis, ion exchange, and membrane technologies (Dan et al., 2008). A summary of advantages and disadvantages of some metal treatment technologies is presented in Table 2.2.

Table 2.1: Sources and effects of heavy metal

Heavy metal	Major source	Toxic effect	References
Lead	Mining, paint, pigments, Pharmaceutical wastewater, electroplating, manufacturing of batteries, burning of coal	Anemia, brain damage, anorexia, malaise, loss of appetite, liver, kidney, gastrointestinal damage, mental retardation in children	(Chen & Hao, 1998) (Godt, *et al*., 2007) (Shruthi *et al*., 2016)
Copper	Plating, copper polishing, Pharmaceutical wastewater, paint, printing operations	neurotoxicity, and acute toxicity, dizziness, diarrhea	(Sharma Y. , 1995) (Shruthi *et al.*, 2016)
Cadmium	Plastic, welding, pesticide, fertilizer, mining, refining	Kidney damage, bronchitis, gastrointestinal disorder, bone marrow, cancer, lung insufficiency, hyper-tension, Itai–Itai disease, weight loss.	(Singh et al, 2006)
Zinc	Mining, refineries, brass manufacturing, plumping, Pharmaceutical wastewater,	Causes short term mental-fume fever, gastrointestinal distress	(WHO, 2001) (Shruthi, *et al.*, 2016)
Mercury	Batteries, paper industry, paint industries, mining	Damage to nervous system, protoplasm poisoning, corrosive to skin, eyes, muscles, dermatitis, kidney damage	(Manohar *et al.*, 2002)
Nickel	Porcelain enameling, non-ferrous metal, paint formulation, electroplating, Pharmaceutical wastewater.	Chronic bronchitis, reduced lung function, lung cancer,	(Ozturk, 2007) (Shruthi *et al*., 2016)
Chromium	Textile, dyeing, paints and pigments, steel fabrication, Pharmaceutical wastewater,	Carcinogenic, mutagenic, teratogenicity, epigastria pain nausea, vomiting, severe diarrhea, producing lung tumors	(Gadd G. , 2010) , (Shruthi *et al.*, 2016)

Table 2.2: Removal of heavy metal ions from wastewater

Method	Advantages	Disadvantages
Chemical precipitation	Simple, inexpensive, Most of the metal can be removed	Large amounts of sludge produced, disposal problems
Chemical coagulation	Sludge settling, dewatering	High cost, large consumption of chemicals
Ion exchange	High regeneration of materials, metal selective	High cost, less number of metal ions removed
Electrochemical methods	Metal selective, no consumption of chemicals, pure metals can be achieved	High capital cost, high running cost.
Adsorption using activated carbons	Most of the metals can be removed, high efficiency	Cost of activated carbon, performance depends upon adsorbents
Membrane processes and ultra-filtration	Less solid waste produced, less chemical consumption, high efficiency for single metal	High initial and running cost, low flow rate, removal percentage decrease with the presence of other metals.
Sources: (Farooq et al.,2010), (Volesky, 2003), (Zouboulis *et al.,* 2004;). (Fu & Wang, 2011)		

Precipitation and synthetic coagulants although very effective have the major disadvantage of high running cost and production of large volumes of sludge. Ion exchange has high operational costs even though it is often preferred by the industry. Moreover, the need for resin replacements, membrane clogging and special handling and regular cleaning, and periodic replacements are some other disadvantages of this technology for metal removal (Srivastava & Goyal, 2010).

2.4 Bio-sorption

Applying biotechnology in controlling and removing metal pollution has been paid much attention and it is gradually becoming a topic of interest in the field of metal pollution control because of its potential application (Wang & Chen , 2009). Bio-sorption is the property of certain biomolecules or types of biomass to bind and concentrate selected ions or other molecules from aqueous solutions (Volesky, 2007). Bio-sorption is a rapid phenomenon of passive metal sequestration by the non-growing biomass/adsorbents.

The bio-sorption process involves a solid phase commonly referred to as sorbent or bio-sorbent (biological material) and a liquid phase or solvent, normally water, containing a dissolved species to be sorbed or adsorbate, metal. Because of the higher affinity of the adsorbent for the adsorbate species, the latter is attracted and bound there by a variety of mechanisms. The process continues until equilibrium is established between the amount of solid-bound adsorbate species and its portion remaining in the solution. The degree of adsorbent affinity for the adsorbate determines its distribution between the solid and liquid phases (Ahalya, Ramachandra, & Kanamadi, 2003). Bio-sorption is a physico-chemical process and includes mechanisms such as absorption, adsorption, ion exchange, surface complexation and precipitation (Lawrence *et al.*, 2010).

2.4.1 Advantages of Bio-sorption Process

Several materials of biological origin bind heavy metals. Biomaterials with sufficiently high metal-binding capacity and selectivity for heavy metals are appropriate for full-scale bio-sorption process (Wang & Chen, 2009) hence the need to establish potential use of specific materials. Overall, compared with the conventional heavy metal removal methods, the potential advantages of bio-sorption process include (Wang & Chen, 2009):

a. Use of naturally abundant renewable biomaterials that can be produced cheaply;
b. Ability to treat large volumes of wastewater due to rapid kinetics;
c. High selectivity in terms of removal and recovery of specific heavy metals;
d. Ability to handle multiple heavy metals and mixed wastes;
e. High affinity, reducing residual metals to below 1 ppb in many cases;
f. less need for additional expensive reagents which typically cause disposal and space problems;
g. Operation over a wide range of physiochemical conditions including temperature, pH, and presence of other ions;
h. Relatively low capital investment and low operational cost;
i. Greatly improved recovery of bound heavy metals from the biomass, and;

j. Greatly reduced volume of hazardous waste produced.

Use of non-living biomass for large-scale applications is more applicable than bio accumulative processes that use living microorganisms, because the latter require nutrient supply and complicated bioreactor systems (Romera et al., 2006). In addition, maintenance of a healthy microbial population is difficult due to toxicity of the pollutants being extracted and other unsuitable environmental factors like temperature and pH of the solution being treated. Recovery of valuable metals is also limited in living cells because they may be bound intracellular. For these reasons, attention has been focused on the use of non-living biomass as bio-sorbents (Romera et al., 2006; Gourdon *et al.*, 2006)**.**

2.4.2 Bio-sorption Mechanism

Metal bio-sorption by biomass mainly depends on the functional groups (Table 2.3) (Volesky, 2007). The symbol R is shorthand for alkyl and its placement in a formula indicates that what is attached at that site varies from one compound to another (Talaro, 2002). The bio-sorption of heavy metals by the biomaterials might be attributed to the polysaccharides, proteins and lipids in the materials that contain hydroxyl, sulfhydryl, phosphates, carbonyl and amino groups. These functional groups can bind metal ions involving valance forces through sharing or exchange of electrons between bio sorbent and metal (Nieboer & Richardson, 1980) (Figure 2.1).

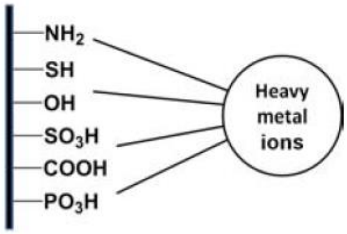

Figure 2.1: Possible binding modes between functional groups and heavy metal ions.

2.4.3 Types of Bio-sorbent Materials

Performance of different bio-sorbents for the removal of variety of heavy metals has been reported by (Larous *et al.*, 2005; Uysal & Ar., 2007; Qi & Aldrich, 2008; Atalay, Gode, & Sharma, 2010). The agricultural residues seem to be preferred (Johnson *et al*,

2002,Nasernejad et al., 2005;; Horsfall et al., 2006) and green coconut shells are a most appropriate example for the adsorption removal of inorganic and organics (Crisafully *et al.*, 2008)

Table 2.3: Biomass representative functional groups and organic compounds

Formula of functional group	Name	Class of compounds
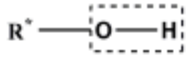	Hydroxyl	Alcohols, carbohydrates
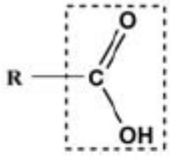	Carboxyl	Fatty acids, proteins, organic acids
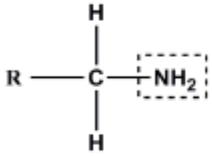	Amino	Proteins, nucleic acids
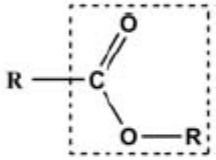	Ester	Lipids
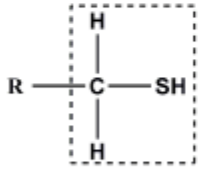	Sulfhydryl	Cysteine (amino acid), proteins
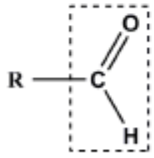	Carbonyl, terminal end	Aldehydes, polysaccharides
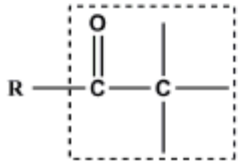	Carbonyl, internal	Ketones, polysaccharides

Source: (Volesky, 2007)

These materials can also passively bind metal ions through various physicochemical mechanisms. Mechanisms responsible for bio-sorption, although understood to a limited extent, may be a combination of ion-exchange, complexation, coordination, adsorption, electrostatic interaction, chelation and/or micro precipitation (Volesky, 2007)

2.4.4 Bio-sorption Isotherms

Bio-sorption is usually described through isotherm (Basha, Murphy and Jha, 2008). A bio-sorption isotherm is relatively simple method for determining the feasibility of using a certain bio-sorbent material for a particular application. It is a plot of the amount of adsorbate per unit weight of adsorbent (*qe)* against the equilibrium concentration of the adsorbate remaining in solution (*Ce). The* quantity described is nearly always normalized by the mass of bio-sorbent to allow comparison of different materials. Isotherms in heavy metal bio-sorption are an indication of mechanism involved in their removal.

(a) Freundlich model

The first mathematical equation fits to an isotherm was published by Freundlich and Kuster in 1907 according to (Abbas *et al.*, 2013). Freundlich showed that bio-sorption from solution could be expressed by empirical formula:

$$q_e = K_f C_e^{1/n} \tag{2.1}$$

The linearized form of Equation 2.1 is as shown in Equation 2.2

$$\log q_e = \log K_f + \frac{1}{n}\log C_e \tag{2.2}$$

Where; q_e (mg/g) is the amount adsorbed per unit mass of adsorbent and C_e is the equilibrium concentration (mg/L). The plot of log q_e versus log C_e gives a linear plot. From which the Freundlich constants K_f and n can be determined.

(b) Langmuir Model

The Langmuir adsorption model (Eq. 2.3) is applied to single-layer adsorption. It is based on the assumptions that (i) maximum adsorption corresponds to a saturated monolayer of solute molecules on the adsorbent surface; (ii) energy of adsorption is constant, and (iii) no transmigration of adsorbate in the plane of the surface (Lucas & Cocero, 2004; Sharker & Acharya, 2006)

$$q_e = \frac{q_m K_L C_e}{1 + K_L C_e} \tag{2.3}$$

The linearized form of Langmuir isotherm is given by Equation (2.4)

$$\frac{C_e}{q_e} = \frac{1}{K_L q_m} + \frac{C_e}{q_m} \tag{2.4}$$

Where; q_m (mg/g) and K_L (l/mg) are the Langmuir constants. The capacity of the bio-sorbents in binding with metal ions is determined by plotting Ce/qe against Ce.

2.4.5 Kinetic Modeling of Bio-sorption in a Batch System

For any practical applications, the process design, operation control and adsorption kinetics are very important (Ho & McKay, 1999). The bio-sorption kinetics in a wastewater treatment is significant; as it provides valuable insights into the reaction pathways and the mechanism of an adsorption reaction (Ho et al., 2000). Also, the kinetics describes the solute uptake, which in turn controls the residence time of adsorbate at the solid-solution interface (Guo et al., 2003)

a) Pseudo-First Order Kinetic Model

The Lagergren rate equation (Weber & Morris, 1963) was the first-rate equation for the adsorption of liquid/solid system based on solid capacity. The Lagergren rate equation for the adsorption of a solute from a liquid solution may be represented as:

$$\frac{dq}{dt} = K_1(q_e - q_t) \tag{2.5}$$

which is the integrated rate law for a pseudo-first order reaction, where q*e* is the amount of pollutant adsorbed at equilibrium (mg/g); *qt* is the amount of pollutant adsorbed at time t (mg/g); and K_1 is the equilibrium rate constant of pseudo-first sorption (g/mg.s). Equation (2.5) can be rearranged to obtain a linear form of Equation (2.6)

$$\ln(q_e - q_t) = \ln q_e - K_1 t \qquad (2.6)$$

b) Pseudo-Second Order Kinetic Model

This kinetic model is based on the assumptions (Ho *et al.,* 2000) that a monolayer of adsorbate on the surface of adsorbent, the energy of adsorption for each adsorbent is the same and independent of surface coverage, the adsorption occurs only on localized sites and involves no interactions between adsorbed pollutants and the rate of adsorption is almost negligible in comparison with the initial rate of adsorption.

The Pseudo second kinetic rate equation can be written as shown in Equation 2.7.

$$\frac{dq_t}{dt} = K_2(q_e - q_t) \qquad (2.7)$$

Linearized form of the equation is as shown in Equation 2.8.

$$\frac{t}{q_t} = \frac{1}{K_2 q_e^2} + \frac{1}{q_e} \qquad (2.8)$$

Where K_2 is the rate constant of adsorption, (g/mg.s), q_e *(mg/g)* is the amount of pollutant adsorbed at equilibrium in (mg/g), q_t is amount of adsorbate on the surface of the adsorbent at any time, t in (mg/g).

2.4.6 Bio-sorption in a packed column bed

Continuous flow in fixed bed column are often preferred to batch processes because there are easier to operate in full scale operation. The performance of packed bed column is analysed using the fraction of effluent concentration (C/Co) versus time curves. For Bio-sorption, the plot is usually referred to as the breakthrough curve. A

typical breakthrough curve is illustrated in Figure 2.2 and Figure 2.3. The breakthrough point is usually defined as the point when the ratio between influent concentration, C_o (mg/l) and outlet concentration C_t (mg/l) becomes 0.05 to 0.9 as illustrated in Figure 2.3. After 50 % breakthrough point, the column can still operate until the ratio Ct/Co becomes 0.9. This point is termed as the operating limit of the column. The column will be completely exhausted when the pre-determined inlet concentration is almost equal to the outlet concentration. The curves are a function of the column flow parameters, sorption equilibrium and mass transport factors and much of the information needed to evaluate the column performance is contained in these plots of effluent concentration as a function of time or throughput volume. The general slope of this breakthrough curve depends mainly on the capacity of the column with the respect to the feed concentration bed depth. (Francisco *et al.,* 2010) studied the fixed bed column using green coconut shells as adsorbent for the removal of toxic metal ions. (Upendra & Manas, 2006) carried out investigations on fixed bed of sodium carbonate treated rice husk and used for the removal of Cd (II). Different column design parameters like depth of exchange zone, adsorption rate, adsorption capacity, etc. was calculated. Effect of flow rate and initial concentration was studied. In this study performance of banana pith bio-sorbent in a fixed bed column was studied.

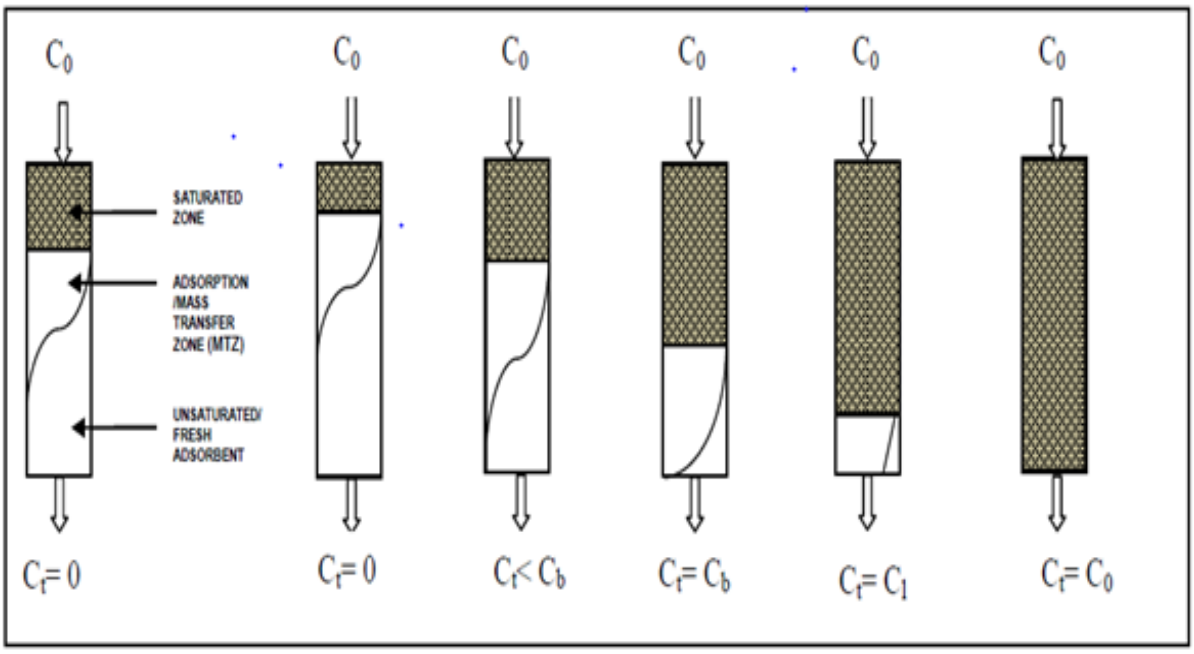

Figure 2.2: Schematic representation of saturated, mass transfer or adsorption and unsaturated/fresh adsorbent zones.

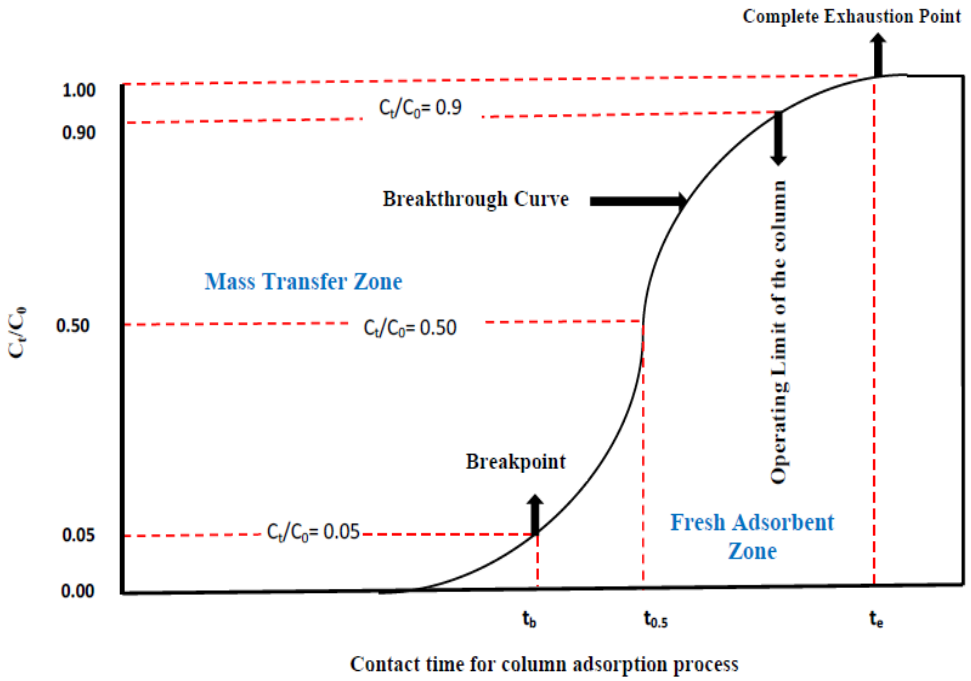

Figure 2.3: Typical breakthrough curve

2.5 Coagulation and flocculation

Coagulation and Flocculation have been used to assist in the removal of particulate and dissolved materials in water and wastewater treatment. It is the most widely applied process for the production of potable water as well as for the treating of wastewaters (Tatsi *et al*., 2003). Coagulation and flocculation require a unique combination of chemical reactions and physical transport processes which are used to destabilize and aggregate suspended particles. The factor that stabilizes colloidal particles must be overcome and individual colloids must aggregate and grow bigger if they are to be separated from suspension during coagulation. The process of destroying the stabilizing forces and causing aggregation of colloidal particles is termed coagulation. Flocculation, refers to the induction of destabilized particles in order to come together, to make contact and thereby form large agglomerates, which can be separated easier usually through gravity settling (Geng., 2005) (Bratby, 2006).

2.5.1 Theory of Coagulation

The effective coagulation is the most critical aspect of the conventional water treatment process. The method destabilizes and aggregate small stable colloidal (non-settleable) impurities, usually consist of a combination of biological organisms, bacteria, viruses, protozoans, color causing particles, organic matter and inorganic solids into larger particle units called floc, which are efficiently removed by several physicochemical processes as following rapid mixing, slow mixing, solid-liquid separation stages of sedimentation and filtration (Figure 2.4)

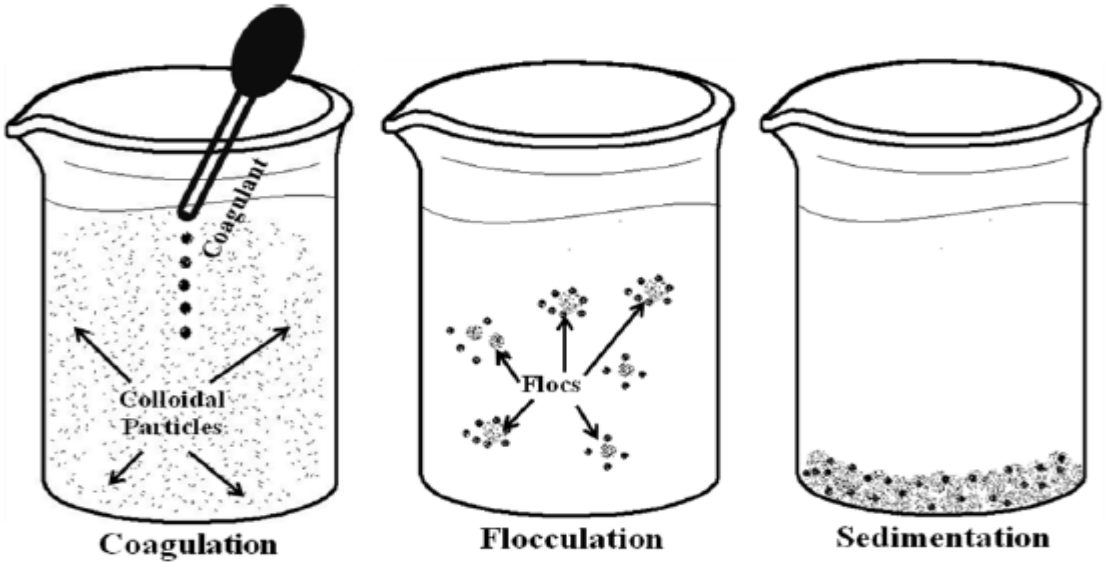

Figure 2.4: Coagulation process

2.5.2 Coagulation mechanism

Dempsey (1984) identified four mechanisms through which coagulation may be achieved. These mechanisms include double layer compression, charge neutralization, sweep coagulation and inter-particle bridging. These methods may take place individually or collectively to destabilize colloidal particles, facilitating their removal from suspension (Letterman, 1999; Davis, 2010)

Colloidal particles are stable in aqueous systems due to the electrostatic charge and/or hydration on their surfaces. The chemical structure and composition of a particle at the water-solid interface determines the net charge and stability of the particles. In most natural systems, the net charge of a colloidal particle is negative due to the ionization of surface acidic functional groups and adsorption of ions. Solution pH determines the net charge of a particle to some degree. A negatively charged colloidal particle attracts ions of opposite charge (counter ions) to its surface from the surrounding water. The layer formed from the abundance of counter ions on the surface of the colloidal particle is known as the fixed layer. As the fixed layer becomes more concentrated, diffusion will occur outside of the fixed layer (Figure 2.5). An electrostatic potential, the zeta potential exists at the boundary between. This electrostatic potential extends outward from the particle until there is a balance on ions

with the bulk solution. The zeta potential is used to determine the stability of the suspension. As zeta potential increases, repulsion forces between particles begin to increase and the colloidal suspension becomes more stable. The amount of bound water at the particle surface also effects stability by preventing particles from coming into close contact with one another. The particle destabilization can occur through addition of coagulants.

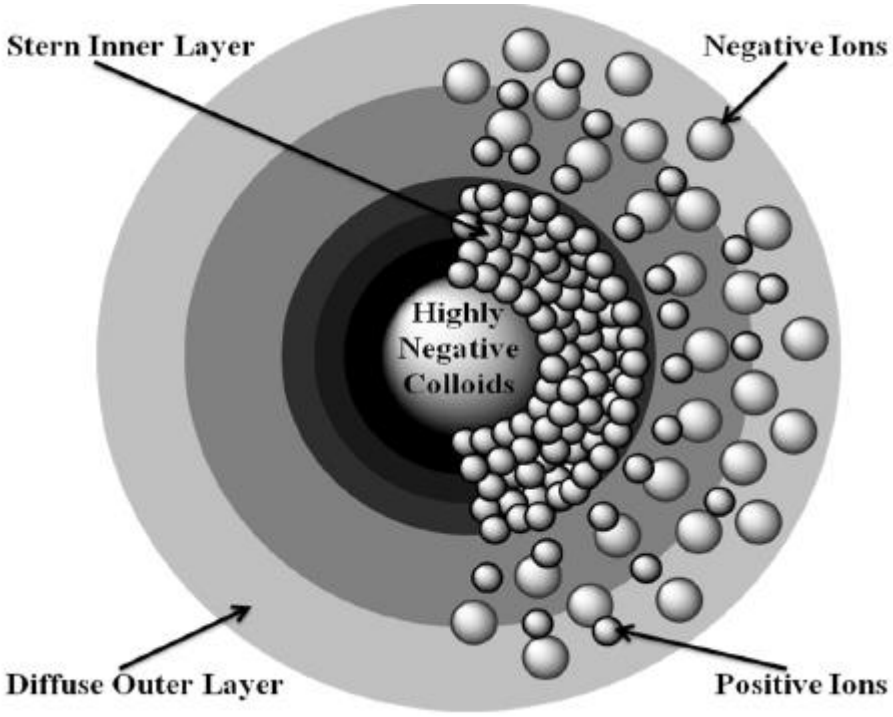

Figure 2.5: Process of destabilization of colloid particles.

a) Double Layer Compression

Double layer compression is a classical method used to describe particle destabilization. The mechanism is achieved through addition of a *coagulant* (*electrolyte*) into a suspension of colloids. Ions possessing a net charge opposite to the net charge of the colloid material are attracted to the area surrounding the outside of the particle, referred to as the diffuse layer. As more counter-ions are added to the suspension they are attracted towards the suspended particles causing the diffuse layer to become compressed. Destabilization reduces the amount of energy required to move

the two colloidal particles of like surface charge together (Figure 2.6). Double layer compression has been proven to be an important destabilization mechanism.

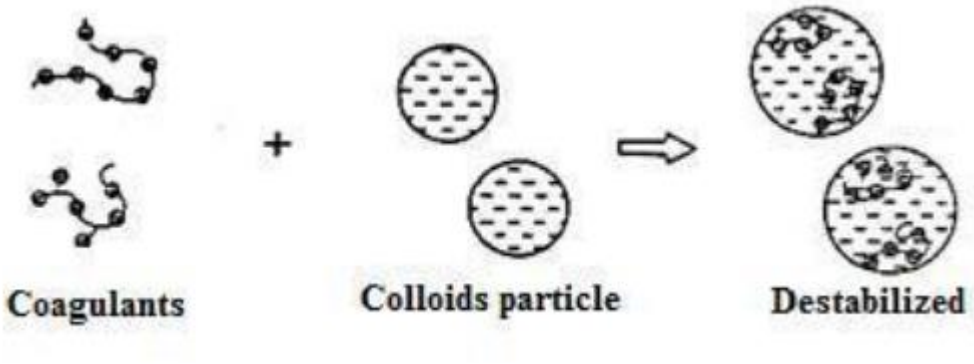

Figure 2.6: Destabilization of colloid particles

b) Surface Charge Neutralization

Surface charge neutralization harnesses the principles involved in double layer compression and occurs in two processes (Figure 2.7). The first process involves the addition of a coagulating agent with a net charge which is opposite to that of the net surface charge of the suspended particles.

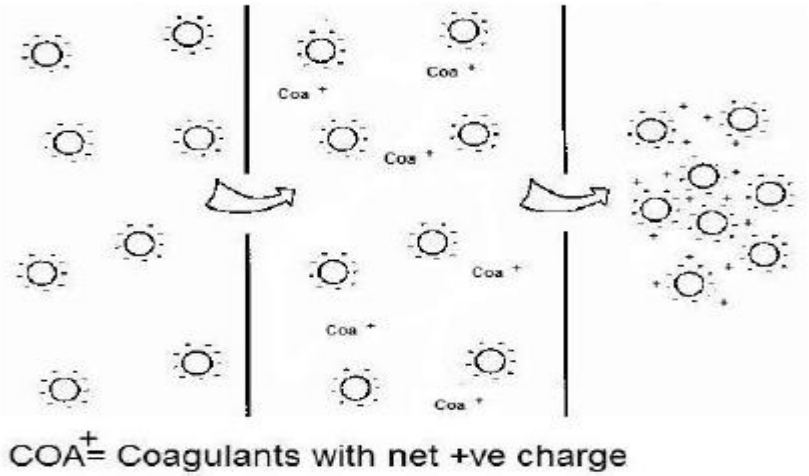

Figure 2.7: Charge neutralization during coag-flocculation process.

The reduced surface charge of the particle will lower the energy necessary for two particles to come into contact with one another, similar to double layer compression.

c) Adsorption and charge neutralization

The adsorption of positive ions provokes a change of the surface charge. It is therefore possible that ions adsorb beyond the point of neutral or zero charge, especially when ions with a high charge density are involved (Figure 2.8).

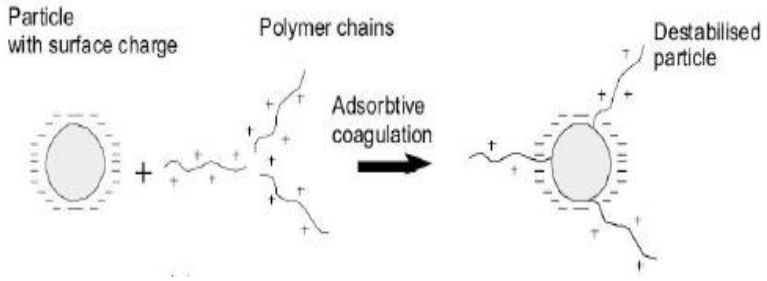

Figure 2.8: Adsorption during coagulation and flocculation process

c) Adsorption and inter-particle bridging.

Here the destabilization does not occur due to compensation of charge, but by bridge formation between the particles. Commonly, long chained synthetic polymers adsorb on different particle surfaces and thus crosslink the particulate material (Figure 2.9). The efficiency of this process depends on the number of available polymer groups and the adsorption capacity of the particles. There is an optimal polymer concentration. Once it is undercut, cross-linking is not efficient due to limited polymer molecules. If it is exceeded, cross-linking is hampered by the absence of free adsorption locations.

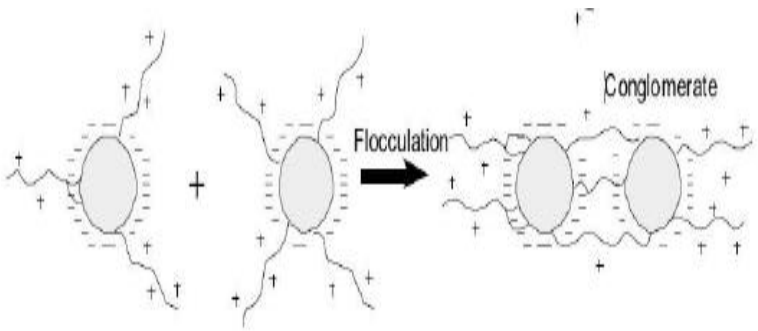

Figure 2.9: Inter-particle bridging during coagulation-flocculation process

d) Enmeshment in a precipitate

Colloid entrapment involves adding relatively large doses of coagulants, usually aluminum or iron salts which precipitate as hydrous metal oxides. The amount of coagulant used is far in excess of the amount needed to neutralize the charge on the colloid. Some charge neutralization may occur but most of the colloids are literally swept from the bulk of the water by becoming enmeshed in the settling hydrous oxide floc. This mechanism is often called sweep floc. Sweep floc is achieved by adding so much coagulant to the water that the water becomes saturated and the coagulant precipitates out. Then the particles get trapped in the precipitant as it settles downward (Hart, 2001).

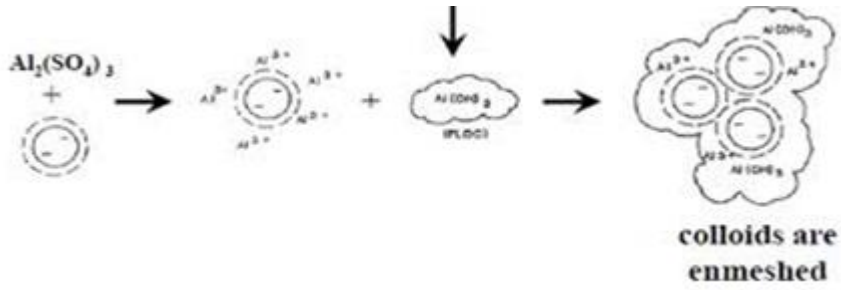

Figure 2.10: Enmeshment during coagulation-flocculation process.

e) Inter-particle bridging and sweep floc.

Inter-particle bridging occurs when high-molecular-weight polymers branch out and adsorb to multiple particles. This process may also occur when polymer chemically react with other polymer or share ions directly to form ionic bridges. The resulting aggregated particles may have reactive polymer branches extending into the aqueous suspension. The process of inter-particle bridging occurs when particles combine with other particles through this manner. The branched polymer that facilitates this process must extend past the diffuse layer to avoid repulsion tendencies of similarly charged particles. The creation of polymer branches causes particle destabilization and may cause re-stabilization. During inter-particle bridging, particles come together to form a mesh-like matrix consisting of destabilized colloids and polymer branches. As the floc begins to settle, it may entrain smaller particles. This process is referred to as

sweep floc, which includes other coagulation mechanisms to form the initial floc. Most conventional surface water treatment plants operate in the region where sweep floc is the predominate mechanism of coagulation (Amirtharajah & O'Melia, 1990).

2.5.3 Types of coagulants

a) Metal Coagulants

The metal base coagulant mainly contains metal salt of aluminum and iron such as Aluminum Sulfate (Alum), Acidified Aluminum Sulfate (Acid Alum), Aluminum Chloride, Sodium Aluminate, Ferric Sulfate, Ferrous Sulfate, Chlorinated Ferrous Sulfate, Ferric Chloride and lime.

b) Organic polymers

Organic polymers are commonly used as primary coagulants or coagulant aids in drinking water treatment. These high-molecular-weight polymers, usually referred to as *polyelectrolytes*, are synthetic compounds that strongly tend to absorb the particles on the surface in an aqueous suspension. Synthetic organic polymers have been used as an effective coagulant aid in drinking water purification systems. However, organic polymers have potential limitations. The use of organic polymers alone may be effective in particle destabilization, but produce poor quality floc additionally; the use of organic polymers has not exhibited increased disinfection by-product precursor removal (Check, 2005). Polymer formulations contain contaminants from the manufacturing process such as residual monomers, other reactants and reaction by-products that could potentially negatively impact on human health. Polymers and product contaminants can react with other chemicals added to the water treatment process to form undesirable secondary products. Organic polymers are classified according to the electric charge of their dissociated macro ions in water: *Cationic*, *Anionic* and *Nonionic*. Cationic polymers. Cationic Polyelectrolyte polymers such as Poly di-methyl di allyl ammonium chloride (PDMDAAC) produce positively charged ions when dissolved in water and widely used as primary coagulant or as an aid to such metal coagulants because, the suspended and colloidal solids commonly found in water has generally negatively charged. Anionic Polyelectrolyte: Polymers such as Copolymer acrylamide/Tri methyl amino ethyl acrylate produced negative charged ion

when dissolved in water. These are used to remove positively charged solids, used along with metal coagulants. Nonionic Polyelectrolyte: Nonionic polyelectrolyte's (e.g. Nonionic polyacrylamide) has balanced, or neutral charge ion and released both charge ions when dissolving in water.

c) Polymerized Inorganic Coagulants

Polymerized inorganic coagulants have been developed and used in water and wastewater treatment since 1980s. The polymerized inorganic coagulants have shown their superior performance in water and wastewater treatment; and these can be concluded as their wider working pH range, a lower sensitivity to water temperature, lower dosages required to achieve the equivalent treatment efficiency and lower residual metal-ion concentrations (Odegaard *et al.*, 1990). This has been attributed to the presence of a range of polymeric species having higher molecular weights. Generally, polymers carry a higher cationic charge, which enhance their surface activity and charge-neutralizing capacity, making them more competitive, which enhance the rate of colloid charge neutralization, floc development; and settlement and reduction in cost, less sludge production than the conventional coagulants (Jiang & Graham, 1998) (Hu *et al*., 2006). Polymeric coagulants include, Al or Fe (III) based Polymeric Inorganic Coagulants, Aluminum Chlorohydrate. (Jiang & Graham, 1998), Si based Polymeric Inorganic Coagulants (Moussas & Zouboulis, 2008).

d) Cement Kiln Dust

Cement Kiln Dust (CKD) is an industrial secondary product which is considered a problematic source of air pollution, especially that the quantities of these product are increasing without finding any sustainable way to handle these valuable products.

Cement Kiln Dust (CKD) has high content of calcium oxide (CaO) that results in using it as a replacement for lime in treating acidic wastewater (Mackie, Boilard, Walsh, & Lake, 2010). It has been also used as a chemical coagulant for wastewater treatment and it reveals promising results in enhancing the TSS, BOD_5, COD, and P-total (EL Zayat, Mohamed, Sherien, & Salah, 2012). (Taha, 2003) Investigated the effect of CKD on the mobility of the heavy metals present in the municipal wastewater and sewage sludge. The

capacity of CKD, as heavy metals scavenger, for chromium up take from aqueous solutions has also shown good results (El Awady & Sami, 1997)

e) **Bio-coagulants**

Use of natural materials is of interest because of reduced costs, environmental concerns of synthetic organic polymers and inorganic chemicals. Natural polyelectrolytes are virtually toxic free, biodegradable in the environment and locally available. These coagulants are derived from microorganisms, animals, plants, vegetables and derivatives of the mineral origins (Kwaambwa & Maikokera, 2007). The natural polymers may not always be effective and need to be assessed on a case by case basis, just as any other coagulant product. For example, extracts from the seeds of Moringa Oleifera reduced turbidity and suspended solids by 80 to 99.5% in raw water (Rico *et al.*, 2010). Moringa Oleifera reduced 90 to 99% of bacteria and 90 % of cercariae (Schistosomamansoni) from water. (Chaudhuri & Babu, 2005), found that Nirmali seeds could be used as coagulant removing turbidity, bacteria and viruses from water (Muyubi & Kuofu, 1995). Similarly (Diaz et al., 1999) (Raghuwanshi *et al.*, 2002) found seeds extracts of several species of chestnut and acorn could be used as natural coagulants for turbidity removal. (Renault *et al.*, 2009), found that chitosan can be used as a coagulant and that mechanisms of turbidity removal was largely charge neutralization, because of positively charged amino group and bridging. (Di Bernardo *et al*., 2000), found that corn starch and cationic waxy cassava can be used as coagulants for turbidity removal and that the mechanism of action was predominantly adsorption and bridging. (Zhang, *et al*., 2006) and (Lenz, et al., 2011) reported that polymer extracted from cactus can be used as primary coagulant for turbidity removal and that its efficiency was comparable to that of Moringa Oliefera. (Habsahalwi *et al.*, 2013), found that banana stem juice as a coagulant removed 80.1, 88.6, and 98.5%, chemical oxygen demand, suspended solids, and turbidity respectively from spent cooled wastewater. (Mwachiro *et al.*, 2004), found that Maerua decumbent can be used for turbidity removal from water.

(Ravikumar & Sheeja, 2013), found that Moringa seeds removed 95, 93, 76 and 70 % copper, lead, cadmium and chromium, while (Saidu et al., 2006)) found that Moringa

oliefera removed 71-89, 66-92, 45-48% lead, iron and cadmium respectively. (Vikashni et al., 2012) found that Moringa seeds removed 90 , 60 and 50% of copper, lead, cadmium, zinc and chromium respectively.

Research on the use of natural coagulants for heavy metal removal in addition to turbidity, COD, suspended matter is limited. This study used banana pith, Opuntia spp. and Maerua Decumbent to remove heavy metals from polluted water.

2.5.4 Kinetics of coagulation and flocculation process.

(Peavy *et al.* , 1985) suggests that Brownian motion in a colloidal system should exceed the electrostatic potential of the system in order to achieve destabilization of the colloidal system. However, when the distance between each particle of the colloid system is high and the Van der Waal forces of attraction are low, coagulants are used to achieve agglomeration. On addition of coagulants into the colloidal system quick dispersion of the coagulants to all parts of the system is important. Thus a period of rapid mixing is essential. This is usually very brief (Jiang & Graham, 1998), and it should be less than five minutes. During the period of rapid mixing the following things do occur: hydrolysis, adsorption, precipitation (Jiang & Graham, 1998). (Stumm & O'Melia, 1968) give a breakdown of the following occurrences; a reduction in potential energy between particles, and an increase in Brownian motion, which leads to collisions between small sized particles. There is also a reduction in surface potential of colloid that causes the adsorption of counter ions by colloidal particles during the period of rapid mixing. On completion of the rapid mixing period there is an onset of slow mixing, it is also a period when inter-particle bridging occurs within particles in colloid. The period of slow mix may be between fifteen to thirty minutes depending on the colloidal system. Finally, the last factor that also influences the kinetics of a system is the period of sedimentation. This is the time during which the particles formed are allowed to settle. In coagulation and flocculation experiment this period is about thirty minutes. The heavy particles drop out of the fluid due to the force of gravity.

Coagulation kinetics is described by Smoluchowski Theory (Smoluchowski, 1917). The theory defines the frequency of collisions for potential pairs of aggregating objects

as products of concentrations of the combining components and rate constants. Smoluchowski coagulation law, is a bimolecular collision law governed by diffusion of the particles toward one another in accordance with Fick's law (Debye, 1942). In this study the coagulation kinetics for removal of turbidity from surface water using the plant coagulants was studied.

The process of aggregation or coagulation has fundamental significance in many branches of science, such as colloid chemistry, biology, medicine, among others. They are also very important for environmental protection, because the treatment of water and sewage by biological or chemical methods is always accompanied by the process of aggregation and coagulation. Knowledge of the course of the coagulation process in a broad range of concentrations of the coagulant and the contaminant being coagulated is without doubt important, e.g. in the treatment of water for consumption and for industrial purposes, in the chemical treatment of municipal and industrial sewage. Coagulation is a kinetic process, occurring with a higher or lower rate. The effectiveness of the whole coagulation process, as well as the properties of the aggregate formed, depends to a high degree on the coagulation rate (Mearkin, 1991; Ehrl et al., 2009,Wardzynska & Beata, 2016).

Mwachiro *et al.,* 2004, Lenz *et al.,* 2011, Habsahalwi *et al.,* 2013 and have shown that Opuntia Spp., banana pith and Maerua Decumbent respectively have the capacity to remove turbidity from water. The kinetic studies of these plant coagulants have not been reported. The kinetics and time evolution of particle aggregation in the removal turbidity from river water using the three plant coagulant was evaluated.

2.5.5 Kinetic theory and model development for coagulation process

a) The Brownian coagulation theory.

Coagulation kinetics is described by the Smoluchowski (1917) theory. The theory defines the frequency of collisions for potential pairs of aggregating objects as products of concentrations of the combining components and rate constants, depending on the mechanism of the process and geometrical dimensions of the components of the aggregation stage.

In an aqueous suspension, where Brownian motion dominates, the number of collision occurring per unit time per unit volume, C_{xy}, for two particles of volumes Vx and Vy is expressed as Equation (2.15) (Von Smoluchowski, 1917), (Liyang, 1988) and (Holtholf *et al.*,1996)**.**

$$C_{xy} = K(v_x v_y)c_x c_y \tag{2.15}$$

Where,

$K(v_x v_y)$ is the Brownian aggregation collision factor which depends on particle size, temperature, and pressure.

$c_x c_y$ is the particle concentrations for two particles of sizes x and y.

The formation rate r_f of particles of volume v_p, as a result of collisions between particles of volumes v_x and v_y is expressed as in Equation (2.16) (Liyang, 1988; Okolo, Menkiti, & Nnaji, 2014)**.**

$$r_f = \frac{1}{2}\sum_{x+y=p} C_{xy} \tag{2.16}$$

Note that x + y = p shows that the summation is governed by collisions, for which

$$v_x + v_y = v_p \tag{2.17}$$

The rate of loss of particles r_l of volume v_p by collision with other all other particles is given by Equation (2.18) (Liyang, 1988; Okolo, Menkiti, & Nnaji, 2014):

$$r_l = \sum_{x=1}^{\infty} C_{xk} \tag{2.18}$$

Hence, the rate of change in the number of density of particles of volume Vp is

$$\frac{dc_k}{dt} = r_f - r_l \tag{2.19}$$

Substituting Equation (2.16) and (2.18) into Equation (2.19), yields

$$\frac{dc_k}{dt} = \frac{1}{2}\sum_{x+y} K(v_x v_y) c_x c_y - c_k \sum_{x=1}^{\infty} K(v_x v_p) c_x \qquad (2.20)$$

The collision factor can be obtained through the steady-state particle diffusion as:

$$K(v_x, v_y) = 4\pi(D_x + D_y)(a_x + a_y) \qquad (2.21)$$

Where,

D denotes the diffusion coefficient and ‘a’ the ‘particle’ radius

The solution for Equation (2.21) for initially mono-disperse system was obtained by smoluchowski (1917), applying the Einstein-Strokes relation,

$$D_x = \frac{K_B T}{6\pi\mu a_x} \qquad (2.22)$$

Where,

μ is the viscosity

K_B is Boltzmann’s constant (J/K)

T is Absolute temperature (K)

For a mono-disperse system ($v_x = v_y$), the collision factor function is reduced to Equation (2.23)

$$K(v_x, v_y) = 4\pi * 2 * (\frac{KT}{6\pi\mu a_x}) * 2a_x = \frac{8K_B T}{3\mu} \qquad (2.23)$$

The generic aggregation rate of particles (during coagulation / flocculation) can be derived by the combination of Equations (2.20) and (2.23) to yield Equation (2.24) according to (Von Smoluchowski, 1917).

$$\frac{dC_t}{dt} = -kC_t^{\alpha} \quad (2.24)$$

Where,

C is the total number concentration of particles at time t

k is the α^{th} order coagulation constant

α is the order of coag-flocculation process

The relationship between the Brownian aggregation collision factor and α^{th} order coagulation rate constant has been reported (Ani *et al.*, 2012) to be:-

$$K = 2k \quad (2.25)$$

For first order reaction (α = 1), integration of Equation (2.24) yields to Equation (2.26).

$$\ln\frac{C_o}{C_t} = k't \quad (2.26)$$

Where, C_t is particle concentration at time t in mg/l, and k' is the first order rate constant (l/mg. min). Similarly, for second order reaction, Equation (2.24) becomes, (2.27).

$$\frac{1}{C_t} = k''t + \frac{1}{C_o} \quad (2.27)$$

Where k'' is the second order rate constant (l/mg min).

b) Prediction of aggregation rate of particles

Equation 2.20, with appropriate K values can be used to predict the aggregation rate of particles in suspension while a flocculation process occurs. For Brownian aggregation, Equation (2.20) can be solved exactly resulting in the expression shown in Equation (2.28) for a coagulation period where the total number particles is decresased by a factor of 2. (Costa, 1995, Holthof *et al.*, 1996;; Thomas *et al.*, 1999).

$$\frac{C_{m(t)}}{C_0} = \frac{\left[\frac{KC_c t}{2}\right]^{m-1}}{\left[1+\frac{KC_o t}{2}\right]^{m+1}} \tag{2.28}$$

For

$$\tau_{\frac{1}{2}} = \frac{2}{kC_o} \tag{2.29}$$

Where,

C_o is the initial particle concentration. And coagulation half time $\tau_{1/2}$ represents a useful time scale for the identification of early stages in the coagulation process

Equation (2.28), represents a generic expression for time evolution of particle(s) of m^{th} order. Therefore for monomers (m=1), singlets;

$$\frac{C_1}{C_0} = \frac{1}{(1+(KC_0 t/2))^2} \tag{2.30}$$

Therefore,

$$C_1 t = 4C_0(2+KC_0 t)^{-2} \tag{2.31}$$

For dimmers (m = 2), doublets;

$$\frac{C_2}{C_0} = \frac{KC_0/2}{(1+(KC_0 t/2))^3} \tag{2.32}$$

Therefore,

$$C_2 t = 4C_0^2 Kt(2 + KC_0 t)^{-3} \tag{2.33}$$

For trimmers (m = 3), triplets

$$\frac{C_3}{C_0} = \frac{(KC_0/2)^2}{(1+(KC_0 t/2))^4} \tag{2.34}$$

Therefore,

$$C_3 t = 4C_0^3 (Kt)^2 (2 + KC_0 t)^{-4} \tag{2.35}$$

A general representation of equations 2.31, 2.33 and 2.35 can be expressed as:

$$C_{m(t)} = 4C_0^m (Kt)^{m-1} (2 + KC_0 t)^{-(m+1)} \tag{2.36}$$

2.5.6 Response surface methodology

Response surface methodology is a collection of statistical and mathematical methods that are useful for the modeling and analyzing engineering problem. Response surface methodology also quantifies the relationship between the controlling input parameters and the obtained response surfaces. The aim of RSM is to optimize response of interest which is influenced by numerous variables (Mason *et al.*, 2003; Montgomery, 2008;). According to (Bas & Boyanci, 2007) and (Bezerra *et al.*, 2008), RSM is an efficient statistical method to predict the best performance conditions with a minimum number of experiments. The interaction effect of the independent parameters on the response can be observed and investigated via RSM. The model equation easily clarifies these effects for binary combination of the independent parameters. Moreover, the empirical model that relates the response to the independent variables is utilized to obtain information about the process.

In order to apply RSM as an optimization tool, some stages (Steppan *et al.,* 1998) need to be followed. They include:

1. Designing of a series of experiments for adequate and reliable measurement of the response of interest.
2. Developing a mathematical model of the second order response with the best fittings
3. Finding the optimal set of experimental parameters that produce a maximum or minimum value of response
4. Representing the direct and interactive effects of process parameters through two and three -dimensional plots.

Process optimization is carried out to minimize operational costs while maximizing the process performance. Most optimization is done using conventional one factor at a time strategy, which changes a single factor while maintaining other factors constant. The approach does not demonstrate the combined effect of all factors; it is tedious, provides insufficient information and often times the optimization point could have been missed.

a) RSM-Mathematical Model

Besides analyzing the independent variables effects, this experimental methodology also generates a mathematical model. The graphical viewpoint of the mathematical model has led to the term RSM. The relationship between the responses and the inputs are represented by Equation (2.37).

$$Y = f(x_1, x_2, x_3 .... x_n) \pm \varepsilon \qquad (2.37)$$

where Y is the response, f is the unknown function of response, x_1, x_2, x_3 … x_n are the input variables which affects the response, n is the number of the independent variables and Ɛ is the statistical error that represents other sources of variability not accounted for by f.

After selection of the design, the model equation and coefficients are defined and predicted.

As a result of sequential model sum of squares, a quadratic model is selected by software (Design Expert, version 10). If total number of experiments is n and Ɛ is random error; then the response surface is expressed as Equation (2.38) using matrix notation.

$$\underbrace{\begin{Bmatrix} y_1 \\ y_2 \\ . \\ . \\ . \\ y_n \end{Bmatrix}}_{Y} = \underbrace{\begin{Bmatrix} 1x_{11}x_{12}.....x_{1k} \\ 1x_{21}x_{22}.....x_{2k} \\ . \\ . \\ . \\ 1x_{n1}x_{n2}.....x_{nk} \end{Bmatrix}}_{X} \underbrace{\begin{Bmatrix} \beta_1 \\ \beta_2 \\ . \\ . \\ . \\ \beta_n \end{Bmatrix}}_{\beta} + \underbrace{\begin{Bmatrix} \varepsilon_1 \\ \varepsilon_2 \\ . \\ . \\ . \\ \varepsilon_n \end{Bmatrix}}_{\varepsilon} \tag{2.38}$$

If N is the total number of experiments and n is the number of factors Equation (2.39) can be used to calculate the total number of experiments

$$N = n^3 + 2n + n_c \tag{2.39}$$

The selected independent variables are coded according to Equation (2.40)

$$x_i = \frac{x_i - x_o}{\Delta x}, \text{ where i=1, 2…. k} \tag{2.40}$$

RSM models generally a full quadratic equation. The second order model can be written as follows:

$$Y = \beta_o + \sum_{i=1}^{n} \beta_i x_i + \sum_{i=1}^{n} \beta_i x_i^2 + \sum_{i \neq j=1}^{n} \beta_i x_i x_{ij} + \varepsilon \tag{2.41}$$

Where,

β_o is the value of the fixed response at the center point of the design; β_i, β_{ii} and β_{ij} are the linear, quadratic and interaction effect regression terms, respectively:

x_i denotes the level of the independent variable
n is he number of independent variables and
ε is the random error.

The second order polynomial equation is derived as Equation 2.42

$$Y = \beta_0 + \beta_1 x_1 + \beta_2 x_2 + \beta_3 x_3 + \beta_{12} x_1 x_2 + \beta_{13} x_1 x_3 + \beta_{23} x_2 x_3 + \beta_{11} x_1^2 + \beta_{22} x_2^2 + \beta_{33} x_3^2 + \varepsilon \quad (2.42)$$

b) Statistical analysis by RSM wide range

The statistical and diagnostic studies are obtained from RSM (Design expert Software, 2006). The Analysis of Variance (ANOVA) including sequential F-test, lack-of-fit test and other adequacy measures is offered by RSM. ANOVA could also verify the efficiency of the developed model.

The sum of square for the deviations in all the trials is known as the total sum of square (SS*T*) (Eq.2.43). It is computed by adding the sum of square caused by the residual (SS*E*) and the sum of square caused by the regression (SS*R*).

$$SS_T = SS_E + SS_R \quad (2.43)$$

In general, an experiment is repeated for accuracy and confidence in the results. However, this leads to errors and deviations. For an experiment that involves repeatability, the SS*R* (Eq.2.44) is found by adding the sum of square due to the lack-of-fit (SS*L*) and the sum of square due to the pure error (SS*P*):

$$SS_R = SS_L + SS_P \quad (2.44)$$

The Fischer test (F-test) of a model evaluates the significance of the model by calculating the ratio of the mean square of regression (MS*R*) to the mean square of residuals (MS*E*). A small F-value for the model is not desired since it indicates that the variance is caused by random unexplained disturbances referred to as noise. The p-value (p > F) provides an indication of the significance of a model in relation with the F-value. It can be defined as the probability that a variable did not affect the

response for a given F-value. If the p > F for the model is less than 0.05 a model is said to be significant, meaning that there is 5% chance that the F-value is due to noise. If the p > F is above 0.1, the model is insignificant (Trinh & Kang, 2011)

The lack-of-fit test (LOF) determines the inability of a model to fit experimental data that are not represented in the experimental domain. This is commonly done by calculating its F-value. A small F-value for the LOF is desired, since the experimenter wants the model to fit. If the p > F is greater than 0.05 the LOF for the model is insignificant and the model is able to fit any data that are not specified in the experimental domain (Trinh and Kang, 2011). A good LOF does not guarantee the adequacy of a model, the coefficient of determination (R^2) (Eq.2.45) must be considered given the fact that it measures the overall performance of a model and its value should be close to 1 (Bas & Boyanci, 2007)**.**

$$R^2 = 1 - \left(\frac{SS_R}{SS_T} \right) \tag{2.45}$$

The adjusted R^2 (Eq.2.46) is computed by arranging the number of terms in a regression relative to the number of design points and it is usually equal to or lower than R^2. It has the particularity of being less subjected to variation than the R^2 when a new term is added to the regression (Myers *et al.*, 2009)

$$Adjusted..R^2 = 1 - \left(\frac{SS_E / df_E}{SS_T / df_T} \right) \tag{2.46}$$

$PRESS = \sum_{I=1}^{n} \left(\frac{e_i}{1 - h_{ii}} \right)^2$, PRESS-Predicted residual sum of squares

Where e_i represents the residual and h_{ii} is the leverage (Montgomery, 1997)

The PRESS is used to measure the predicted R^2, which indicates the level of change in the data using model. During the selection of a model, the aim is to maximize the

adjusted and predicted R^2 values. For a best fit, the difference between the adjusted and predicted R^2 must be less than 0.2.

Other parameters in the analysis of a model include the standard deviation (SD) expressed as Eq.2.47 and APS (Eq.2.49)

$$SD = \sqrt{MS_E} \tag{2.47}$$

The coefficient of variation (CV)(Eq.2.48) measures the unexplained changes in the data:

$$CV = \left[\frac{SD}{\overline{Y}}\right] * 100 \tag{2.48}$$

Where,

$\overline{Y}$ is the mean of the response variable.

The adequate precision statistics (AP) (Eq.2.49) determines the performance of the model in predicting the responses. A value of AP greater than four means that the model will give good predictions

$$AP = \tilde{Y}_{\max} - \tilde{Y}_{\min} \tag{2.49}$$

Where,

$\tilde{Y}_{\max}$ and $\tilde{Y}_{\min}$ represent the maximum predicted response and the minimum predicted response respectively (Myers et al., 2009)

c) Model diagnostics

Diagnostic plots provide a confirmation that the ANOVA assumptions are correctly met by analyzing the residuals (Eq.2.50) versus various other elements that will be discussed in this section.

$$\text{Re}\,sidual = e_i = Y - \tilde{Y}_i \tag{2.50}$$

Where,

Y_i is the actual response and $\tilde{Y}_i$ is the response predicted by the model.

The residuals are classified as externally studentized (ESRes) or internally studentized (ISRes). A residual is said to be studentized when it is divided by the estimate of its standard deviation (SD). The ISRes (*r*) (Eq.2.51) compares the value of a residual to the residual variance in order to measure the number of SD that separates the actual from predicted values.

$$IS\,\mathrm{Re}\,s = r = \frac{e_i}{s\sqrt{(1-h_{ii})}} \tag{2.51}$$

Where s is the standard deviation.

ESRes (*t*) (Eq.2.52) makes a comparison between the residual and the residual variance, excluding the first case of SD (s_{-1}). It represents the number of SD between the predicted value and the actual response (Montgomery, 2009).

$$ES\,\mathrm{Re}\,s = t = \frac{e_i}{S_{-1}\sqrt{1-h_{ii}}} \tag{2.52}$$

Diagnostic plots such as predicted versus actual plot, normal plot of residual, residuals versus predicted and residual versus the run predicts the reliability of the developed model. RSM also reports on predicted values and actual values.

c) The process of optimization.

Chemical engineering is mostly about optimizing processes through new designs and other methods. RSM provides models that can be used to predict optimal conditions of a particular system. Using Design Expert software, the optimization can be done graphically or numerically, where the experimenter sets goals or criteria of the conditions desired for a given process. RSM optimizes its factors through a desirability function (D) (Eq.2.53) for multiple responses. Where, N is the number of responses, r and d I are the importance of particular response and partial desirability function respectively

$$D = \left[\prod_{i=1}^{N} d_i^r i \right]^{1/\sum r_i} \tag{2.53}$$

From literature review it was found that (Jiang-Ping *et al.,* 2007) used aluminium chloride as main coagulant and chitosan as flocculant aid for removal of turbidity and optimized the process using RSM. The removal of COD, turbidity and total suspended solid using poly-aluminium chloride and alum were studied by (Shahin *et al.,* 2009) and optimized the process using RSM. The removal of nickel from wastewater using chitosan was studied and optimized by (Nor Azimah *et al.,* 2013). Optimization using RSM of colour parameters of cooked meat was optimized by (Saficoban & Yilmaz, 2010) whereas (Fathi *et al*., 2011) applied RSM to material science in optimization of a textile system. The process of biodiesel production was studied and optimized by (Salamatinia et *al.*, 2011). The removal of COD, color and turbidity removal from textile wastewater using electrochemical oxidation was studied and optimized by (Korbathi & Tanyolac, 2008). (Mahajeri, et al., 2011)-optimized COD, Color and iron removal from landfill leachate using Fenton oxidation whereas (Wang *et al.,* 2011) optimized turbidity removal, lignin removal and clean water recovery from pulp mill wastewater.

This tool was used to optimize the removal of not only turbidity and COD but also the removal of heavy metal from paint wastewater using plant coagulant, plant coagulant and alum and using plant coagulant and lime (from cement kiln dust).

2.5.7 Sensitivity Analysis

Sensitivity Analysis allows the study of how uncertainty in the output of a model can be apportioned to different sources of uncertainty in the model input (Saltelli, 2002) It may be used to determine the input variables that contribute the most to an output behavior, and the non-influential inputs, or to ascertain some interaction effects within the model (Saltelli, 2002). The SA process entails the computation and analysis of the so-called sensitivity or importance indices of the input variables with respect to a given quantity of interest in the model output. Importance measures of each uncertain input variable on the response variability provide a deeper understanding of the

modeling in order to reduce the response uncertainties in the most effective way (Kleijnen, 1997) (Ioannidis, 2005). For instance, putting more efforts on knowledge of influential inputs will reduce their uncertainties. The underlying goals for Sensitivity Analysis are model calibration, model validation and assisting with the decision-making process.

2.6 Plant biomass in water and wastewater treatment

Phytoremediation is often also referred as botanical bioremediation or green remediation (Chaney , et al., 1997) and is defined as the use of green plants to remove pollutants from the environment or to render them harmless. Bio-sorption of heavy metals from aqueous solutions is a relatively new concept that has proved to be effective in the removal of contaminants from aqueous effluents. Adsorbent materials derived from low-cost agricultural wastes can be used for the effective removal and recovery of heavy metal ions from wastewater streams (Farooq et al., 2010). Both living and dead biomasses (an inactive biomass) as well as cellular products such as polysaccharides can be used for metal removal. Various metal-binding mechanisms have been postulated to be active in bio-sorption by action of metallic ions toward the functional groups present in natural proteins, lipids and carbohydrates positioned on cell walls. Biomaterials previously investigated include use of fungal biomass (Mathialagan & Viraraghavan, 2009) , bacteria (Rani *et al.*, 2009), plants (Wankas et al., 2006) and agricultural by-products (Dang et al., 2009; Farooq et al., 2010). Studies using bio-sorbents reveal that both living and dead microbial cells uptake metal ions, hence offering a potentially inexpensive alternative to conventional adsorbents. However, living cells often die due to the toxic effects of the heavy metals.

In addition, living cells often require the addition of nutrients and hence increase the biochemical oxygen demand (BOD) and chemical oxygen demand (COD) in the effluent. Therefore, the use of dead cells or non-living biomaterials as metal sequestering agents is fast gaining ground since toxic ions do not affect them (Grimm et al., 2008). Most of these agricultural by-products are widely available and are of little or no economic value, and some of them in fact present a disposal problem.

Moreover, dead cells are cheaper, effective in reducing heavy metals to very low levels and require less care and maintenance.

This study investigated the potential use of three plants namely banana stems, Opuntia spp. and Maerua Decumbent in water and waste water treatment. These plants are widely available, non-food and have not been used for any major economic uses. Banana is an herbaceous plant of the genus Musa spp. of the family Musacea. Bananas plants are widely cultivated in the tropics. The banana stem (Figure 2.11) from which the fruit bunches are harvested usually has no much further use and has little nutritional value. There are two types of the Opuntia spp. of the family of Cactaceae (Figure 2.11): those with spiny fruits, and those that are spineless. In Kenya they grow in the wild or are planted as hedge. Maerua decumbent is a small shrub growing to 3 m high (more commonly 1.2-1.8 m), often multi-stemmed, arising from a tuberous rootstock (Figure 2.11). They grow in dry bush land and open areas in riverine vegetation and they are commonly found in sandy areas, light clay soils and rocky areas.

(a)

(b)

(c)

Figure 2.11: Images of Banana pith (a), Opuntia Spp. (b) and Maerua Decumbent (c).

2.6.1 Knowledge gaps identified by the literature review

Reviewed literature indicates that biomass materials including banana pith, Maerua Decumbent and Opuntia Spp. have been used in turbidity removal. However, their special characteristics (chemical composition, performance and kinetics) which make them useful in water treatment have not been reported. Furthermore, previous studies have considered the one factor at a time optimization strategy, which changes a single factor while maintaining other factors constant. This approach does not demonstrate the combined effect of all factors; it is tedious; it provides insufficient information and the optimization point could be missed. Therefore, the response surface methodology for optimization was applied in this research.

CHAPTER THREE

METHODOLOGY

3.1. Overview of methodology of the study.

This chapter presents the methods and materials that were used to achieve the objectives of the study. Biomaterials namely banana pith, Opuntia Spp. and Maerua Decumbent were evaluated for water and wastewater treatment (Figure 3.1).

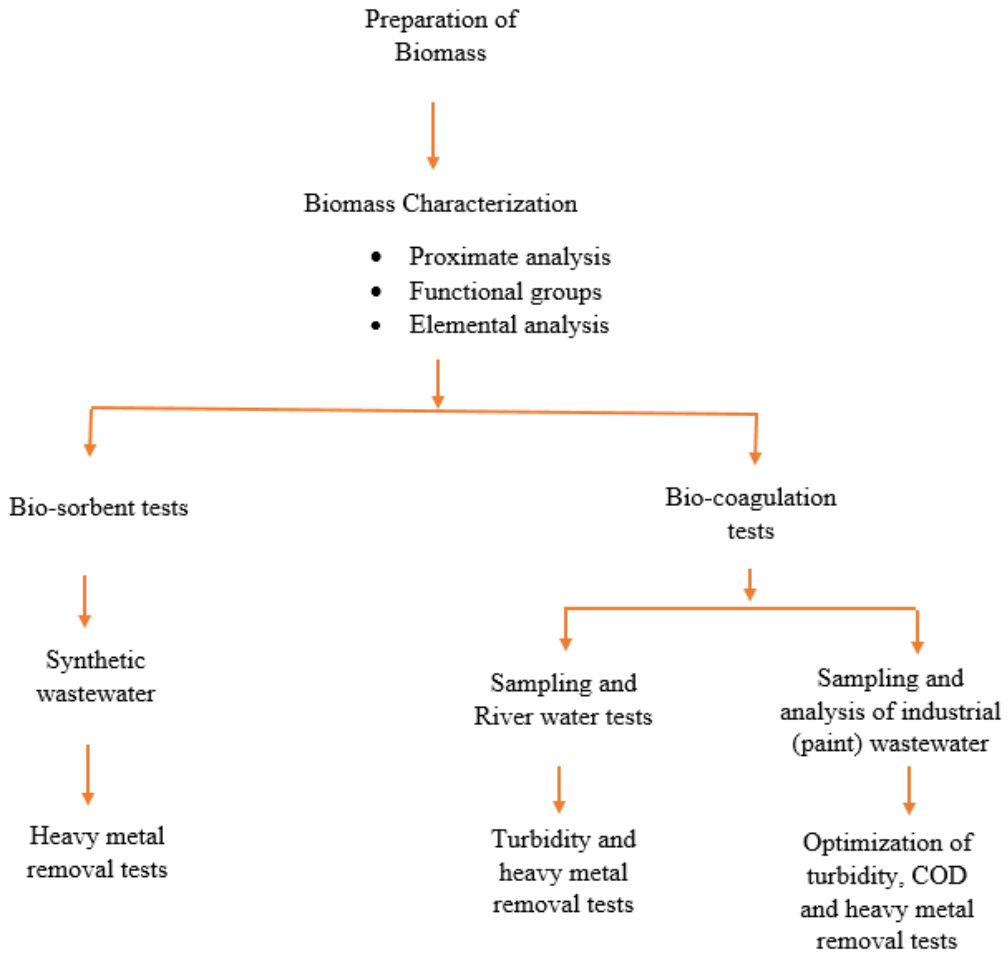

Figure 3.1: Methodology flow chart

The study first characterized the biomaterials by proximate, elemental and functional groups analyses. It then evaluated the ability of the materials to remove turbidity and heavy metal from water and paint industry wastewater through bio-sorption and bio-coagulation. Response surface methodology was then used to optimize the removal of turbidity, COD and heavy metals from paint wastewater.

3.2 Material characterization

3.2.1 Determination of proximate analysis of biomass materials

The selected biomass were analysed for proximate composition including the percentage moisture, fat (lipids), crude protein, fibre and ash following standard methods (AOAC, 1999). Total percentage carbohydrate content was determined by the difference method of totalling the other constituents and subtracting from 100. The methods used to determine these constituents are described in the sections 3.2.1.1 to 3.2.1.6

a) Determination of moisture content tests

Moisture content was determined according to (AOAC, 1999). Empty dish with a lid was dried in an oven at 105^0C for 3 hours and then transferred to desiccator to cool. The weight of the empty dish with a lid was then determined. Sample weighing 3g was then spread uniformly on the dish. The dish and contents were dried in an oven at 105 ^{o}C for one hour. After drying; the dish was transferred to the desiccator to cool with the lid partially covered and then weighed.

The moisture content was computed as shown in Equation (3.1).

$$Moisture(\%) = \frac{(W_1 - W_2)}{W_1} * 100 \quad (3.1)$$

Where,

W_1 = weight (g) of sample before drying

W_2 = weight (g) of sample after drying

b) Determination of protein content tests

The protein content was determined according to (AOAC 1999). Sample of 1.0 g was placed in a digestion flask. Kjedahl catalyst of 5g and 200 ml of concentrated sulphuric acid was added to the flask. Another tube containing the above chemical except sample was prepared as blank. The flask was then be inclined and heated gently until frothing ceased. The mixture was heated briskly until solution became clear.

The content was cooled and 60 ml of water added. Immediately the flask was connected to digestion bulb on condenser and with tip of the condenser immersed in standard acid and 5-7 drops of mix indicator in receiver. The flask was rotated to mix content thoroughly then heated until all NH_3 was distilled. The receiver was removed and the tip of the condenser washed and the excess standard acid distilled was titrated with standard NaOH solution.

The protein content was computed using Equation (3.2).

$$\text{Protein}(\%) = \frac{(A-B)*N*14.007*6.25}{W} \qquad (3.2)$$

Where,

A = Volume of ml of 0.2NHCL used sample titration

B = Volume (ml) of 0.2 N HCL in blank titration

N = Normality of HCL

W = weight (g) of sample

14.007 = atomic weight of nitrogen

6.25 = the protein-nitrogen factor

c) Determination of ash content tests

The crucible and the lid were heated in an oven at 550 ^{o}C overnight to ensure that the impurities on the surface of crucible are burned off. The crucible was then cooled in a desiccator for 30 minutes. The crucible and lid were weighed to 3 decimal places. Sample of 5 g was weighed into the crucible. The sample was heated over low Bunsen flame with lid half covered. When fumes were no longer produced, the crucible and lid was placed in the furnace. It was heated uncovered at 550^{o}C overnight. The lid was

replaced after heating to prevent loss of fluffy ash. The crucible was then cooled in a desiccator and weighed after the sample turned grey with the lid on.

The ash content was computed as shown in Equation (3.3).

$$Ash(\%) = \frac{Weight.of.ash}{Weight.of.sample} * 100 \quad (3.3)$$

d) Determination of fat (lipids) content tests

The bottle and lid were placed in the incubator at 105^{o}C overnight to ensure the weight of the bottle is stable. Sample of 4 g was then weighed to paper filter and the wrapped. The sample was taken into an extraction thimble and then placed in the extraction unit. The bottle containing 250 ml petroleum ether was thereafter heated for about 14 hours. The sample was then evaporated using the vacuum condenser and incubated at 80^{o}C until solvent was completely evaporated and bottle completely dry. After drying the bottle with partially covered lid, it was transferred to the desiccator to cool and its dried content was reweighed.

The fat content was computed as shown in Equation (3.4).

$$Fat(\%) = \frac{Weight.of.fat}{Weight.of.sample} * 100 \quad (3.4)$$

c) Determination of crude fibre tests

Defatted sample, 1 g, was placed in a glass crucible and attached to the extraction unit. To the defatted sample 150 ml boiling, 1.25 % of sulphuric acid solution was added. The sample was then digested for 30 min and then the acid was drained out and the sample was washed with boiling distilled water. After this, 1.25% of sodium hydroxide solution (150ml) was added. The sample was then digested for 30 minutes, thereafter, the alkali was drained out and the sample was washed with boiling distilled water. Finally, the crucible was removed from the extraction unit and oven dried at 110^{o}C

overnight. The sample was then cooled in a desiccator and weighed (W_1). The sample was then ashed at 550 ^oC in a furnace for 2 hours, cooled in a desiccator and reweighed (W_2).

Extracted fibre was then computed as shown in Equation (3.5).

$$Fibre(\%) = \frac{Digested.sample(W1) - Ashed.sample(W2)}{Weight.of.sample} * 100 \quad (3.5)$$

d) Determination of Carbohydrate

Carbohydrate (%) =100-(crude protein+ crude fat+ Total ash +Crude fibre) (3.6)

3.2.2 Analysis of Functional Groups in Banana Pith, Maerua Decumbent and Opuntia Spp.

The ground sample of each of the plant coagulant was mixed with potassium bromide at the ratio of 1:25. The mixture was ground and compressed using mini-hand compressor to attain a thin slate for analysis. The functional groups in the material for adsorption of pollutants were analyzed using Fourier Transform Infrared (FT-IR) Spectroscopy, model 8400.

3.2.3 Determination of point of zero charge.

The pH of a solution affects the surface charge of the biomass as well as the degree of the ionization and speciation of different pollutants. The point of zero charge for each of the plant coagulant biomass was determined by the solid addition method. A 50 ml of 0.1 M KNO_3 solution was transferred into a series of 100 ml conical flasks. The initial pH values of the solution were adjusted from 2 to 10 by the addition of 0.1N of HNO_3. 1.5 g of the biomass was added to each flask and the flask capped immediately. The flasks were placed in a constant temperature water bath shaker and shaken for 24 hours after which the pH was measured.

3.2.4 **Elemental analysis of Banana pith, Maerua Decumbent and Opuntia Spp.**

The carbon, hydrogen, nitrogen and sulphur content of each of the plant coagulant biomass were determined by the use of Perkin-Elmer Series II CHNS/O 2400 Elemental Analyser. The oxygen content was determined as the difference of the total mass and the sum of the mass of the others elements in the sample.

3.3 Bio-sorption studies

3.3.1 Batch **bio-sorption studies**

a) Bio-sorbents used in the study

Banana pith, Maerua Decumbent and Opuntia Spp. powder of size passing sieve opening 0.4 mm were studied for removal of pollutants from synthetic wastewater.

b) Water sample for bio-sorption studies.

Synthetic wastewater was used for bio-sorption studies tests. Working metal concentration was prepared from 1000 mg/l stock solution of the different heavy metals studied.

c) Batch Experiments

(i) Optimization of contact time

Wastewater of 100 ml, containing 5 mg/l of lead, copper, zinc and chromium separately were each mixed with 0.2 g of the bio-sorbents at pH 5. The solution was agitated at the speed of 250 rpm for different time period ranging from 30 to 300 minutes. After each set time period the solution was centrifuged 1500 rpm for 15 minutes and the solution was filtered using a Whattman filter paper. The amount of heavy metal remaining in the solution was determined by AAS machine (AAS- 6200 Shimadzu). The experiment was carried out at room temperature.

(ii) Optimization of dosage

Varied dosages of ranging from 0.05 to 0.4 g were mixed with 100 ml of water sample containing 5 mg/l of each metal. The solution was agitated at the speed of 250 rpm for 120 minutes. The solution was centrifuged 1500 rpm for 15 minutes and then filtered

using a Whattman filter paper. The amount of heavy metal remaining in the solution was determined by AAS machine. The experiment was carried out at room temperature.

(iii) Optimization of pH

The pH of water sample containing 5 mg/l of each metal was varied in the range 3-9. Each sample was mixed with the optimum dosage identified in sub-section 3.3.1.3(b) and the solution subjected to agitation at 250 rpm for 120 minutes. The solution was centrifuged at 1500 rpm for 15 minutes and then filtered using a Whattman filter paper. The concentration of heavy metal remaining in the solution was measured using by AAS. The experiment was carried out at room temperature

(iv) Optimization of initial Concentration

Sample water of 100 ml, containing varied initial metal concentration ranging from 5-20 mg/l was mixed with the best dosage and pH identified above. The solution was then subjected to agitation at the speed of 250 rpm for 120 minutes. The solution was centrifuged 1500 rpm for 15 minutes and then filtered using a Whattman filter paper. The amount of heavy metal remaining in the solution was determined by AAS machine. The experiment was carried out at room temperature.

d) Equilibrium studies

For the isotherm studies, the initial metal concentrations were varied from 5 to 20 mg/l using optimum dosage identified in sub-section 3.3.1.3(b) above (dry weight) adsorbent. The adsorption flasks were agitated at 250 rpm and samples were collected at specified time intervals, centrifuged at 1500 rpm for 15 minutes filtered and analyzed for the residual metal concentration.

The equilibrium data were fitted with Langmuir and Freundlich Isotherm models

e) Calculation

$$\text{Metal removal (\%)} = \left(\frac{C_o - C_t}{C_o}\right) * 100 \qquad (3.7)$$

$$\text{Adsorbed amount}, q_e = \frac{V(C_o - C_e)}{W} \quad (3.8)$$

Where,

C_o C_t and C_e are the initial concentration, concentration at time t and equilibrium concentrations of each metal (mg/l) in the solution. V is the volume of the solution (L) and W is the mass of dry adsorbent used (g).

f) Kinetic Studies

Kinetics experiments were conducted with 5, 10, 15 and 20 mg/l of the different metals in 100 ml water and with best dosages identified of the three bio-sorbents at room temperature and pH. The water samples were agitated at 250 rpm for 5 hours. At different time intervals the amount of metals remaining in the solution was determined. The kinetics data were evaluated with pseudo-first-order and pseudo-second-order kinetics equation.

3.3.2 Bio-sorption in a Fixed-Bed Column

A PVC column with 1.5 cm diameter was packed with known quantity of banana pith (Figure 3.2). The experiments were conducted by pumping chromium solution through the column in a down-flow mode using a peristaltic pump. All experiments were conducted at room temperature and at pH 5. The effects of various parameters such as flow rates (3, 5 and 7 ml/min), bed height (2, 4 and 6 cm) and initial chromium concentration (5, 10 and 20 ppm) were investigated. And the data fitted to relevant models.

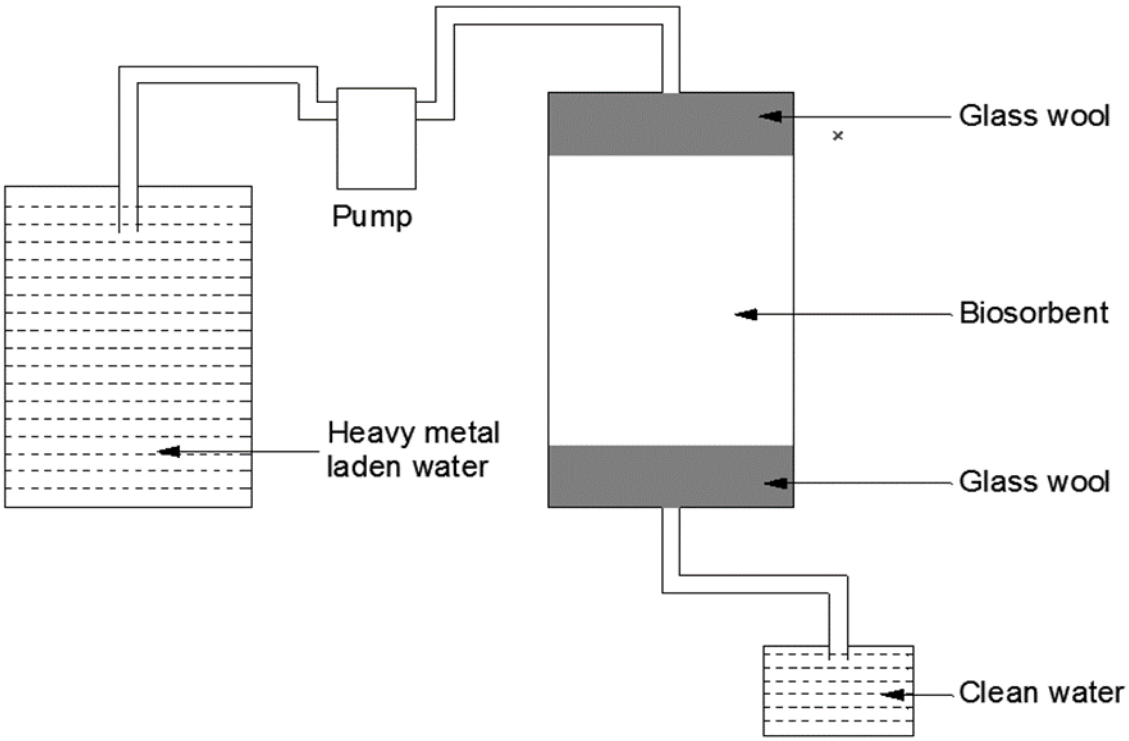

Figure 3.2: Experimental set-up for a fixed bed column

The performance of column study was evaluated in terms of maximum bed capacity q_t, adsorbed metal per cent (Y) and equilibrium metal uptake q_e.

Where,

The maximum bed capacity for a given flow rate and feed concentration was calculated using Equation (3.9)

$$q_t = \frac{Q\int C_{ad}\,dt}{1000} \qquad (3.9)$$

Where,

q_t is maximum bed capacity, mg, Q is the inlet flow rate, ml/min and C_{ad} is adsorbed metal concentration mg/l, Area under the plot of adsorbed metal concentration verses time (hours).

The total amount of metal sent to the column is given by Equation (3.10)

$$M_t = \frac{C_o Q t_{total}}{1000} \quad (3.10)$$

Where,

M_t is the total amount of metal sent to the column, g, C_o is the initial metal concentration, mg/l, Q is the volumetric flow rate, ml/min and t total is the total flow time, min.

Total percentage of metal removal (Y) is given by Equation (3.11)

$$Y = \frac{q_t}{M_t} * 100 \quad (3.11)$$

Where,

q_t is maximum bed capacity, mg and M_t is the total amount of metal sent to the column, mg.

Equilibrium metal uptake in the column is given by Equation (3.12)

$$q_e(\exp) = \frac{q_t}{x} \quad (3.12)$$

Where,

q_e (exp) is the equilibrium metal uptake, mg/g and x is the amount of adsorbent in the column in grams.

The effluent volume was calculated using Equation

$$V_{eff} = Q t_{total} \quad (3.13)$$

Where,

V_{eff} is effluent volume collected, ml, Q is the volumetric flow rate, ml/min and t_{total} is total flow time, min

Fixed bed modelling

For the successful design of a fixed bed column adsorption process, the concentration -time profile or breakthrough curve should be analysed carefully. Three different kinetic models were implemented to explain the column dynamic process in this study. The models are described below.

Break through curve analysis using Adams-Bohart Model

The Adams-Bohart model is based on the assumption that the rate of adsorption is proportional to both the concentration of the adsorbing species and the residual capacity of the adsorbent. The Adams-Bohart model is expressed as in Equation (3.14) (Loderio *et al.*, 2006).

$$\frac{C_t}{C_o} = \exp(K_{AB}C_o t - K_{AB}N_o \frac{Z}{U_o}) \qquad (3.14)$$

Where,

K_{AB} (l/min.mg)(mass transfer coefficient) is rate constant of Adams-Bohart model, z (cm) is the bed depth, N_0 (mg/L) is maximum ion adsorption capacity per unit volume of adsorbent column, and U_0 (cm/min) is the linear velocity of influent solution. The linear form of Adams-Bohart model is expressed as shown in Equation (3.15).

$$\ln(\frac{C_t}{C_o}) = K_{AB}C_o t - K_{AB}N_o \frac{Z}{U_o} \qquad (3.15)$$

Break through Curve analysis using the Thomas model

The Thomas model is widely used in column performance modeling. Its derivation assumes Langmuir kinetics of adsorption-desorption and no axial dispersion. The expression for the Thomas model for adsorption column is given as in Equation 3.16 (Thomas H. , 1944).

$$\frac{C_t}{C_o} = \frac{1}{1 - \exp\left[(\frac{K_{TH} q_e x}{Q}) - K_{TH} C_o t\right]} \quad (3.16)$$

Where,

K_{TH} (l/min.mg) is the Thomas model constant, qe (mg/g) is the predicted adsorption capacity, x is mass of adsorbent (g), Q is influent flow rate (mL/min), C_o is initial solution concentration (mg/L), and C_t is effluent solution concentration (mg/L). The linear form of Thomas model is expressed as in Equation (3.17)

$$\ln(\frac{C_t}{C_o} - 1) = \frac{K_{TH} q_e x}{Q} - K_{TH} C_o t \quad (3.17)$$

Break through Curve analysis using the Yoon-Nelson model

This model is simpler than other models and also requires no data about the characteristics of the system such as the type of adsorbent and the physical properties of the adsorption bed. The Yoon-Nelson equation is expressed as in Equation (3.18) (Yoon & Nelson, 1984).

$$\frac{C_t}{C_o - C_t} = \exp(K_{YN} t - \tau K_{YN}) \quad (3.18)$$

Where,

K_{YN} (1/min) is the rate constant and τ (min) is the time required for 50% adsorbate breakthrough. The linear form of Yoon-Nelson model is expressed as below.

$$\ln(\frac{C_t}{C_o - C_t}) = (K_{YN} t - \tau K_{YN}) \quad (3.19)$$

The values of K_{YN} and τ were calculated from the linear plot of ln (Ct/(Co-Ct)) verses time (minutes) at different flow rates, bed heights and initial concentration.

3.4 Bio-coagulant Treatment of Surface Water

The use of bio-coagulation for removal of pollutants from Nairobi River water was evaluated. The procedures used are described in the following subsections.

3.4.1 Preparation of the coagulant material

Three bio-coagulants; namely, banana pith, Maerua Decumbent and Opuntia Spp. were investigated for treatment of Nairobi River water. Banana pith was obtained from harvested banana plantain at Juja, Kiambu County. Maerua decumbent was obtained from Marakwet, Baringo County and Opuntia Spp. was obtained from Machakos County. The banana pith, Maerua Decumbent and Opuntia Spp. were cleaned and rinsed with distilled water. The materials were then cut into small pieces and dried in an oven at a temperature of 60 ^{o}C for 6 hours. The dried pieces were ground with a grinder into a powder, which was then stored in dried plastic containers for experimental use.

3.4.2 Nairobi River water sampling

Water samples were collected as grab samples from Nairobi River at Ruai (SP) (Figure 3.3) in pre-cleaned containers and treated with nitric acid (2%). The samples were stored in a cool box and transported to the laboratory. The physical and chemical characterization of the river water was conducted using Standard Methods (APHA, 1998).

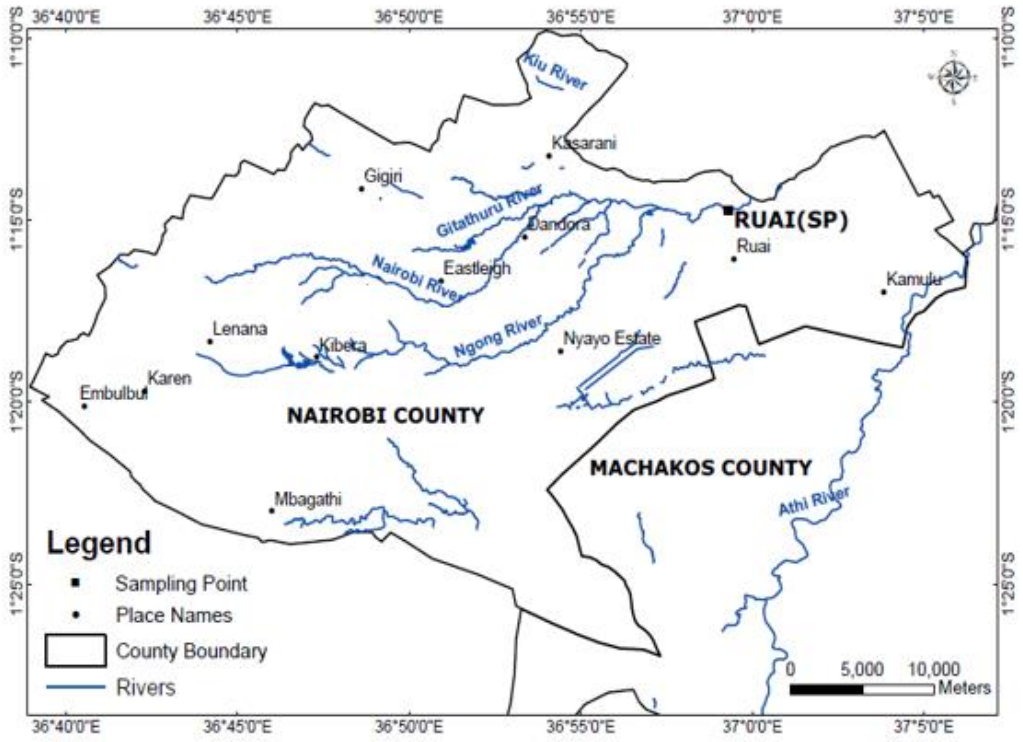

Figure 3.3: Sampling points at Ruai along Nairobi River.

3.4.3 Quality Assurance and Quality Control

All reagents used were of analytical grade. To avoid metal contamination, glassware were washed and rinsed with 10% HCL followed by distilled water. Sample preparation and analysis were carried out using standard methods of analysis (APHA, 1998).

3.4.4 Coagulation-flocculation Tests

Coagulation and flocculation tests were carried out on Nairobi River water using conventional jar test apparatus at room temperature. The pH of the water was varied using 1M HCL and NaOH. About 500 mL of the water was placed in 1 L jars and placed in the jar test apparatus. Plant material coagulant was added at dosages in the range 0.1 - 1 g/l. The mixture was subjected to 3 minutes of rapid mixing at 180 rpm, 20 minutes of mixing at 10 rpm and 30 minutes of settling. During settling, samples were withdrawn with pipette from 2 cm depth and turbidity measured using turbidity

meter (SGZB) to study perikinetic flocculation. Coagulated water samples were further filtered using filter paper No.42 to remove floating particles. The samples were stored in plastic bottles at 4 ˚ C until analysis. The samples were analyzed for COD, sulphates, nitrates, copper, chromium, iron, zinc, lead and manganese using the standard methods (APHA, 1998).

To study peri-kinetic flocculation, the observed turbidity was taken as a measure of the con-centration of colloidal particles remaining in suspension. It was converted to total suspended solids (TSS) values using the expressions (Metcalf and Eddy, 2003):

$$TSS\ (mg/L) = (TSS_f) \times T \quad (3.20)$$

Where,

T = Turbidity (NTU)

TSS_f = Conversion factor 2.3 (Metcalf and Eddy, 2003)

The coagulation performance was determined using the following equation

$$Coag..Efficiency = \frac{C_o - C_t}{C_o} * 100 \quad (3.21)$$

Where,

C_o is the initial particle concentrate

C_t final particle concentration

3.5 Bio-coagulant Treatment of Paint wastewater

Treatment of paint wastewater for removal of turbidity and heavy metals was evaluated for the following coagulants

1. Alum and bio-coagulants,
2. Bio-coagulant only and
3. Bio- coagulant with lime from cement kiln dust

3.5.1 Sampling

Paint wastewater was obtained from Crown Paints Industries. The wastewater was first mixed thoroughly before sampling (Figure 3.4). Sampling was carried out using 20 litres jerry can and preserved by addition of nitric acid. The composition of the paint wastewater was analyzed using the standard methods (APHA, 2008).

Figure 3.4: Mixing of paint wastewater before sampling

3.5.2 Treatment of paint wastewater using alum coagulant plus bio-coagulants

a) Alum coagulant turbidity removal tests

Various dosages 0.2-1.4 g/l of alum were mixed with 300 ml of paint wastewater at pH 7. Rapid mix at 180 rpm was carried out for one minute and, slow mixing at 20

rpm for 20 minutes. The content were allowed to settle for 30 minutes. The turbidity of the supernatant was analyzed after 30 minutes.

b) Alum coagulant and bio-coagulant turbidity and heavy metal removal tests

The mixing of alum coagulant and plant bio-coagulants was based on weight ratio (Table 3.1).

Table 3.1: Mixing ratio of alum and plant coagulant

Experiment No.		1	2	3	4	5	6
Alum dosage	g/l	1.0	0.8	0.6	0.4	0.2	0
	%	100	80	60	40	20	0
Bio-coagulant dosage	g/l	0	0.2	0.4	0.6	0.8	1.0
	%	0	20	40	60	80	100

3.5.3 Treatment of paint wastewater using bio-coagulant (Maerua Decumbent)

a) Effect of pH on turbidity removal using Maerua Decumbent tests

Maerua Decumbent of 0.7 g/l was mixed with 300 ml of paint wastewater at different initial pH (5-9). The contents were rapid mixed at 180 rpm for 3 minutes followed by slow mixing of 20 rpm for 20 minutes and allowed to settle for 60 minutes. The turbidity removal was there after determined for all the pH by use of a turbidity meter.

b) Effect of Maerua Decumbent dosage on turbidity removal tests.

Different Maerua dosages ranging from 0.3 g/l to 1.7 g/l were evaluated for turbidity removal, at the best pH and 60 minutes settling time.

c) Effect of Maerua Decumbent dosage and pH on heavy-metal removal tests

Wastewater of 300 ml at different initial pH was mixed with varied dosages of Maerua. The content was rapid mixed at 180 rpm for 3 minutes followed by slow mixing of 20 rpm and allowed to settle for 60 minutes. The amount of metal in the supernatant was analyzed by use of AAS.

3.5.4 Use of Plant material and cement kiln dust (CKD)

a) Characterisation of cement kiln dust

Cement kiln dust was characterised to establish its contents. This was carried out by use of x-ray diffraction machine at Kenya Portland Cement.

b) Opuntia Spp. and cement kiln dust turbidity and heavy metal removal tests

Cement kiln dust was used together with the plant materials. The cement kiln dust was obtained from Kenya Portland Cement Company. Cement Kiln dust contain high percent of calcium oxide, approximately 65.6 %. To obtain calcium hydroxide from the dust, the Cement kin dust was mixed with water at 4 ^{O}C and then the solution was stirred at speed of 200 rpm for 15 minutes. The solution was decanted and the milk like slurry was used in the experiments. Different quantities of the slurry were investigated. 300 ml of paint wastewater was mixed with varied dosages of Opuntia spp. and CKD Slurry

3.6 Optimization of coagulation-flocculation process

3.6.1. Experimental design and process optimisation

The Design Expert Software Version 10 was used for statistical analysis. The response surface experimental designs were carried out through central composite design method (Figure 3.5). Optimizations were carried out for alum coagulants only, alum plus banana pith, Maerua Decumbent only and Opuntia spp. plus CKD.

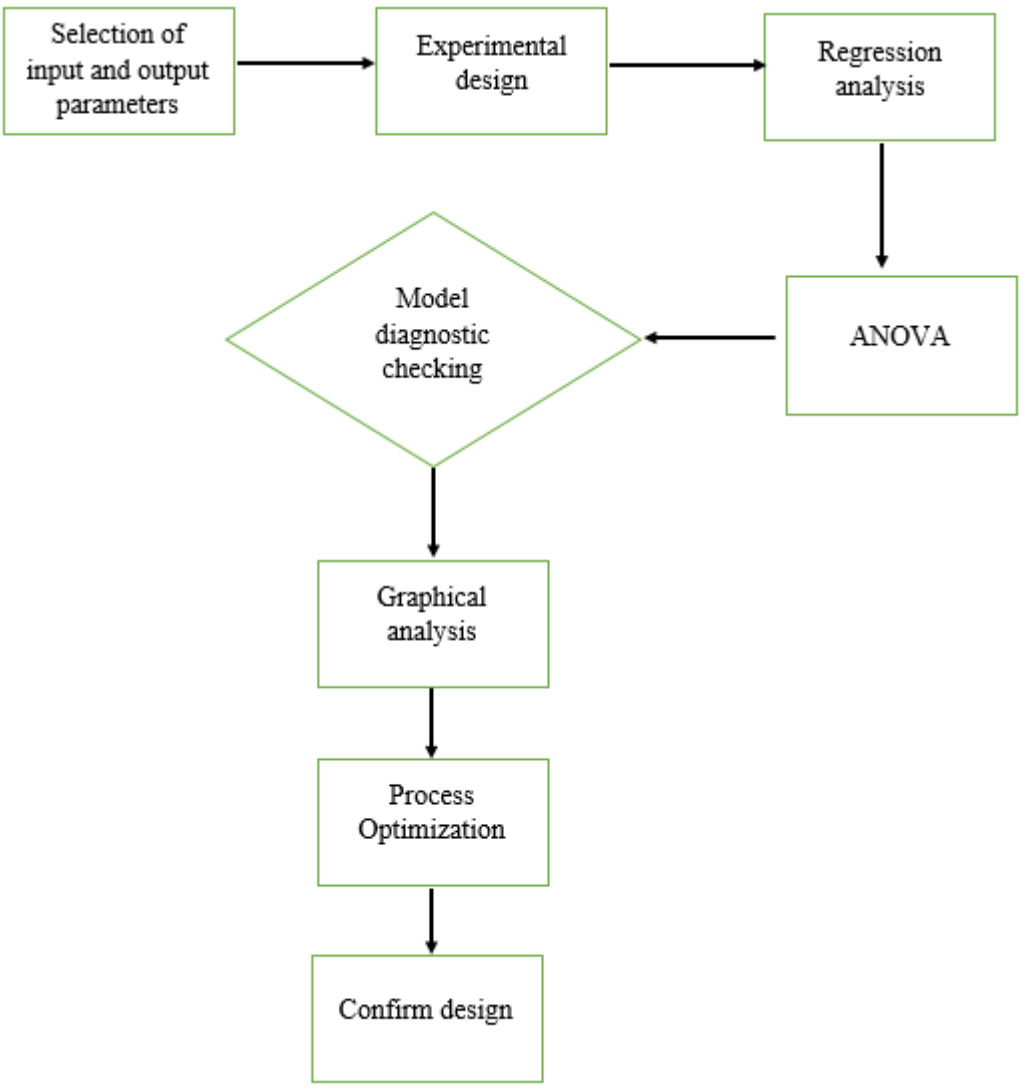

Figure 3.5: Flow chart for optimization process

Preliminary coagulation and flocculation tests supplied the range for appreciable contaminant reduction. Table 3.2 to Table 3.5 indicate the range of parameters used in the design. Because expression of variables usually use different units and/or limits of variation, the significance of their effects on responses can only be compared after they are coded (Montgomery, 2004).

Therefore, the statistical calculations coded the variables X_i as x_i according to Equation 3.22)

$$x_i = \frac{X_i - X_o}{\Delta X} \qquad (3.22)$$

Where, Xi is the un-coded value of the i^{th} independent variable; X_o is the value of X_i at the centre point of the investigation area and ΔX is the step change.

Coagulant dosage (X1), pH (X2) and settling time (X3) were the independent variable in the removal of turbidity and COD during coagulation and flocculation process. For heavy metals, only coagulant dosage (X1) and pH (X2) were significant. Therefore, the study of the heavy metal was for the full settling period of 60 minutes.

Table 3.2: Independent variables process and their corresponding levels for alum only

	Symbols		Levels		
Independent variables	uncoded	coded	-1	0	+1
Alum dosage(g/l)	X_1	x_1	0.26	0.63	1.0
pH	X_2	x_2	7	9	11
Settling time (minutes)	X_3	x_3	20	40	60

Table 3.3: Independent variables process and their corresponding levels for alum dosage and Banana pith

	Symbols		Levels		
Independent variables	uncoded	coded	-1	0	+1
Alum dosage (g/l)	X_1	x_1	0.2	0.6	0.8
Banana dosage (g/l)	X_2	x_2	0.2	0.4	0.6
pH	X_3	X_3	7	9	11
Settling time (minutes)	X_4	x_4	10	20	30

Table 3.4: Independent variables process and their corresponding levels for Maerua Decumbent

	Symbols		Levels		
Independent variables	uncoded	coded	-1	0	+1
Maerua dosage(g/l)	X_1	x_1	0.7	1	1.3
pH	X_2	x_2	5	7	9
Settling time (minutes)	X_3	x_3	20	40	60

Table 3.5: Independent variables process and their corresponding levels for Opuntia Spp. and CKD

	Symbols		Levels		
Independent variables	uncoded	coded	-1	0	+1
Opuntia Spp. dosage (g/l)	X_1	x_1	0.2	0.45	0.7
CKD (ml)	X_2	x_2	4	7	10
Settling time (minutes)	X_3	x_3	10	20	30

Three process parameters; namely, turbidity, COD and heavy metal concentrations were selected as the dependent variable or the responses. Equation 3.23 predicted the responses of contaminant removal.

$$Y = \beta_o + \sum_{i=1}^{n} \beta_i x_i + \sum_{i=1}^{n} \beta_{ii} x_i^2 + \sum_{i=1}^{n} \sum_{j=i+1}^{n} \beta_{ij} x_i x_{ij} + \varepsilon \quad (3.23)$$

Where, Y is the predicted response (turbidity, COD and heavy metal removal), β_o is the constant coefficient; β_i , β_{ii} and β_{ij} are the linear ,quadratic and interaction effect regression terms, respectively; x_i and x_j are variables, which influence predicted response Y ; n is the number of factors and Ɛ is the random error.

Graphical analyses of the data employed analysis of variance (ANOVA) to obtain the interaction between the process variables and the responses. The quality of the fit polynomial model expressed by the coefficient of determination, R^2, and its statistical

significance was checked by the Fishers F-test in the same program. Models were selected or rejected based on the p-value (probability) with 95% confidence level. Three-dimensional surface plots were obtained based on the effects of the levels of the factors studied. The plots were used for studying the simultaneous interaction of the factors on the responses.

Numerical optimization of the coagulation-flocculation process was carried out using the Design Expert Software Version 10. Results of the optimization were validated by conducting further coagulation-flocculation tests at the predicted optimal conditions.

3.6.2 Sensitivity Analysis

Sensitivity analysis yields the information about the increment or decrement tendency of the response objective function with respect to the process parameter. From the developed empirical relationships for the prediction of turbidity, COD and heavy metal removals ,the sensitivity equations were obtained differentiating Equation (3.23) for each of the response with respect to the process parameters namely dosage, pH and settling time.

CHAPTER FOUR

RESULTS AND DISCUSSION

4.1 Characteristics of Bio-material

The results for proximate analysis, elemental analysis and functional groups are presented in Table 4.1and 4.2 and Figure 4.1 to 4.3 respectively. Biomass containing polysaccharide (carbohydrates), proteins and lipids with functional groups such as amino, carboxyl, sulfate, hydroxyl etc) play an important role in the removal of contaminant from polluted water (Hamdy 2000; Karthikeyan *et al.*, 2007,; Apiratikal & Pavasant, 2008;). The removal of pollutant by natural polyelectrolytes depends on the degree of ionization of the functional groups, the degree of copolymerization and/or the number of substituted groups within the polymer structure to (Duan & Gregory, 2003; Jiang J. , 2001)

4.1.1 Proximate analysis of banana pith (Bp), Maerua Decumbent (MD) and Opuntia Spp. (C) biomass.

The proximate results (Table 4.1) indicated that the Opuntia Spp. had high percentage of lipids, crude fibre and carbohydrates, Maerua decumbent had a high percentage of protein and carbohydrates whereas banana pith had high percentage of crude fibre and carbohydrates.

Carbohydrates, lipids and proteins have been identified as the possible active agent leading to coagulation (; Raghuwanshi et al., 2001; Saenz et al., 2004; Mavura et al., 2008;Yin C.-Y. , 2010)

Table 4.1 Proximate analysis for Opuntia Spp., Maerua Decumbent and Banana pith biomass

No.	Parameter	Parameter content in percentage (%)		
		Opuntia Spp.	Maerua	Banana pith
1	Crude protein	0.82	12.33	0.81
2	Crude fibre	20.24	4.10	19.4
3	Lipids	19.20	3.30	5.00
4	Ash	14.00	5.00	16.00
5.	Moisture	4.00	12.33	8.70
6	Carbohydrates	41.74	62.94	50.10

4.1.2 Elemental analysis of banana pith, Maerua Decumbent and Opuntia Spp. biomass.

The elemental component of Opuntia Spp., Maerua and Banana pith in terms of carbon, hydrogen, nitrogen, oxygen and sulphur were determined (Table 4.2). The results indicated that the three materials contain high amount of carbon and oxygen and less amount of nitrogen, hydrogen and sulphur.

Table 4.2: Elemental analysis of Opuntia Spp., Maerua Decumbent and Banana pith.

No.	Parameter	Parameter content in percentage (%)		
		Opuntia Spp.	Maerua Decumbent	Banana pith
1	Carbon	41.71	38.51	32.34
2	Hydrogen	5.23	3.84	4.21
3	Nitrogen	1.72	1.25	1.46
4	Oxygen	40.13	42.21	43.54
5	Sulphur	0.24	0.31	0.86

4.1.3 Functional groups of banana pith, Maerua Decumbent and Opuntia Spp. biomass.

The functional groups in Maerua Decumbent, Opuntia Spp., and Banana pith coagulant were identified in the FT-IR spectrum range 500–4000 cm−1. The FT-IR results were presented in Figure 4.1 to 4.3. The bands between 3363.6 and 3859.3 cm^{-1} were attributed to O-H stretching caused by presence of alcoholic and phenolic hydroxyl groups involved in hydrogen bonding (Surkannen, 1987; Johnston & Aochi, 1996). The peak observed at 2923 and 2932 cm^{-1} were attributed to stretching vibrations of the aliphatic and aromatic -CH (Skoog & Leary, 1992). The stretching band at 1645.0 and 1647 were attributed to bending vibrations of the N-H (amino – acids), C=O stretching (aldehydes and acetones, esters) (Farinella *et al.*, 2007). The band at 1525-1550.7 was attributed to Aromatic domain and N-H bending vibrations, while those at 1415.7 and 1421.4 were attributed to C-N stretching of primary amides (Senesi *et al.,* 2003). The peaks observed at 1323 and 1384.8 cm−1 were an indication of stretching vibrations of symmetrical or asymmetrical ionic carboxylic groups (COOH) of pectin (Farinella *et al.,* 2007). The peaks at 1247.9 were attributed to C-O deformation vibrations of phenols and carboxyl (Mattoli, et al., 2006) or could have resulted from the C-O stretching vibration of ketones, aldehydes and lactones or carboxyl groups (Chandrasekhar & Pramada, 2006). The bands at 1029.9 cm−1 were associated with the vibrations of C-O-C and OH of polysaccharides (Ibarra & Moliner, 1991), while the peak at 1055.0 were attributed to C-O bonds in primary and secondary alcoholic groups. The peak at 846.6 and 1004.8 cm−1 were associated with amine groups. The observed range of functional groups in the three-biomass indicated capacity to remove a wide variety of contaminants as reported by (Vijayaraghavan et al., 2011; Bahman R. , 2014; Muhammad et al., 2015)

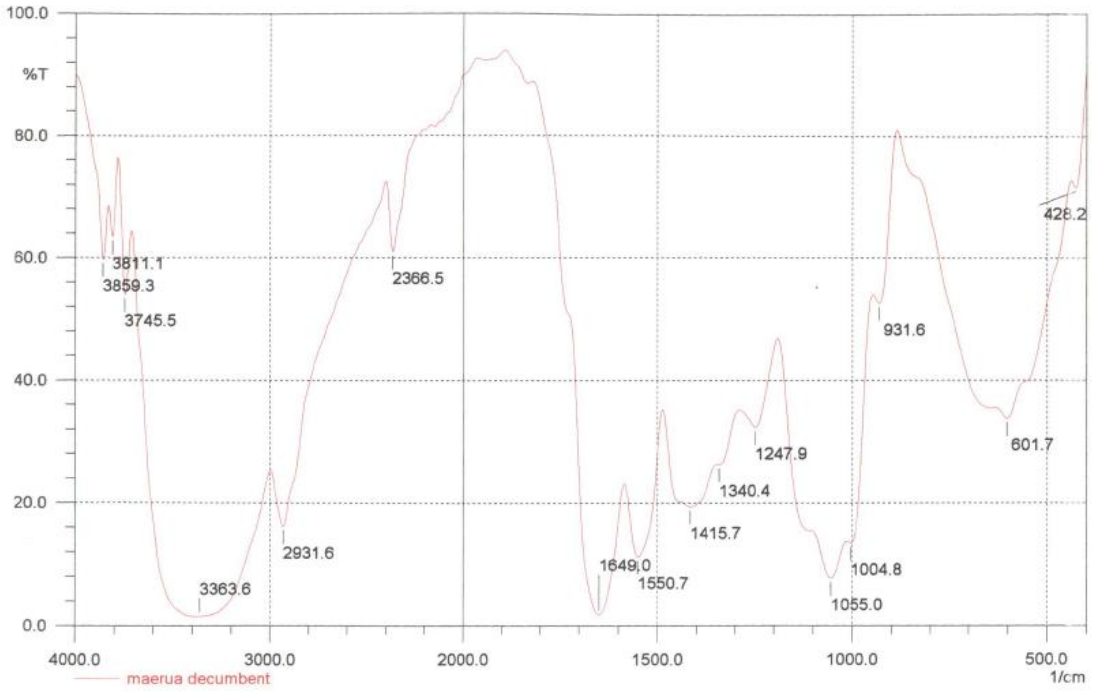

Figure 4.1: FT-IR spectra for Maerua Decumbent powder

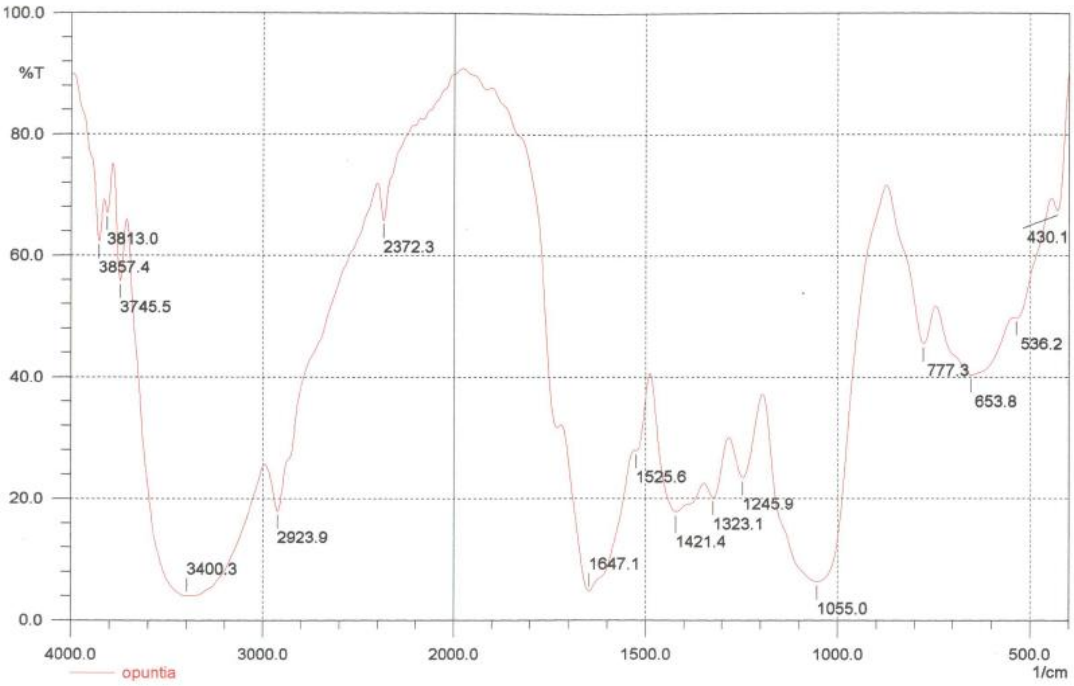

Figure 4.2: FT-IR spectra for Opuntia Spp. Powder.

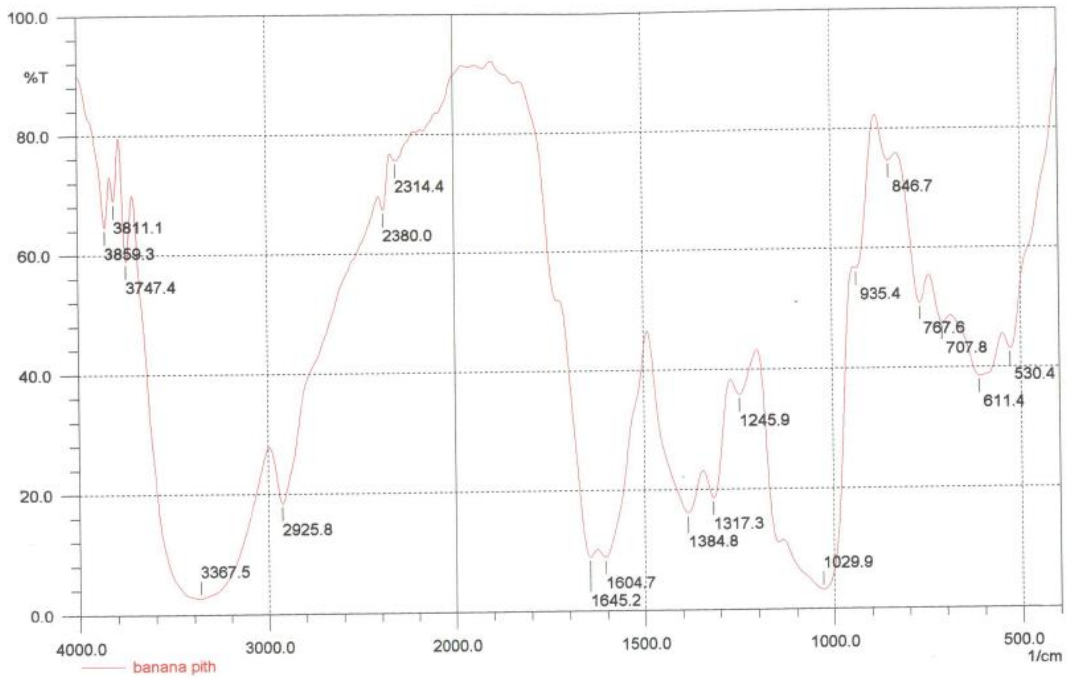

Figure 4.3: FT-IR Spectra of banana pith powder.

4.1.4 Determination of point of zero of the different plant biomass

The pH at which the biomass surface takes a zero value is defined as point of zero charge (pH pzc). At this pH, the charge of the positive surface sites is equal to that of the negative ones. The knowledge of pH pzc allows hypothesis on the ionization of the functional groups and their interaction with pollutants in solution. At pH values, greater than pH pzc, the biomass is negatively charged while at lesser pH, the solid surface is positively charged. The results for this analysis are shown in Figure 4.4 to 4.6. The point of zero charge for Maerua decumbent, Opuntia Spp. and Banana pith were 4.1, 4.8 and 4.9 respectively

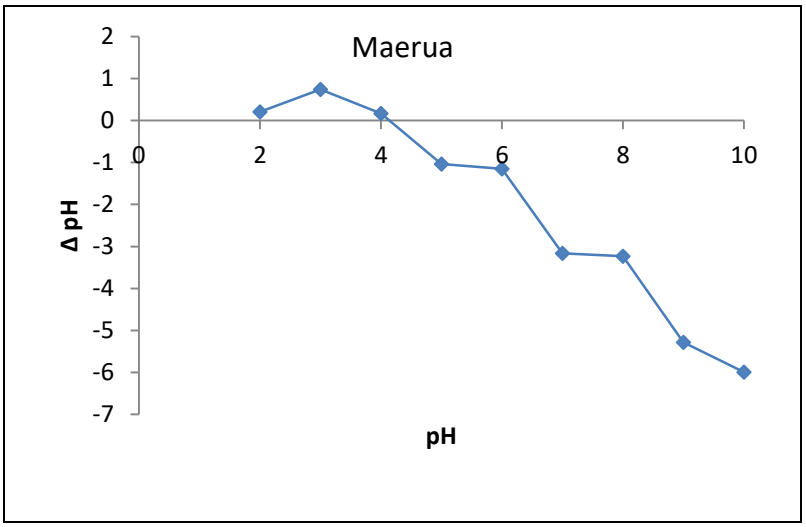

Figure 4.4: Point of zero charge of Maerua biomass.

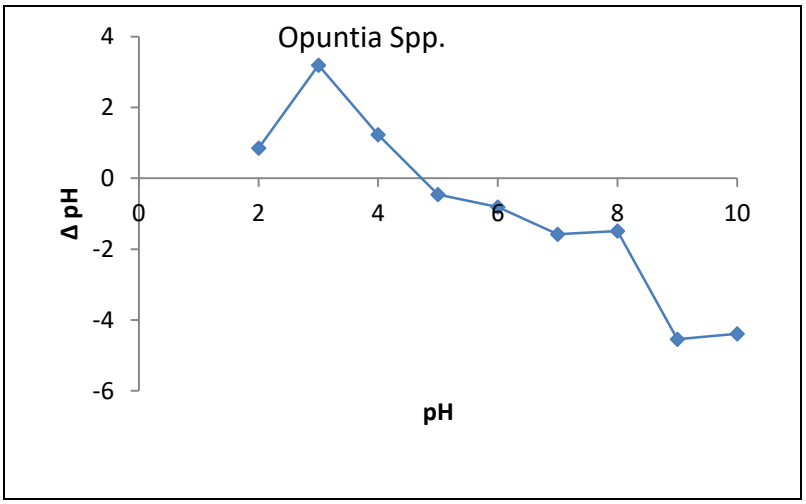

Figure 4.5: Point of zero charge of Opuntia Spp. biomass.

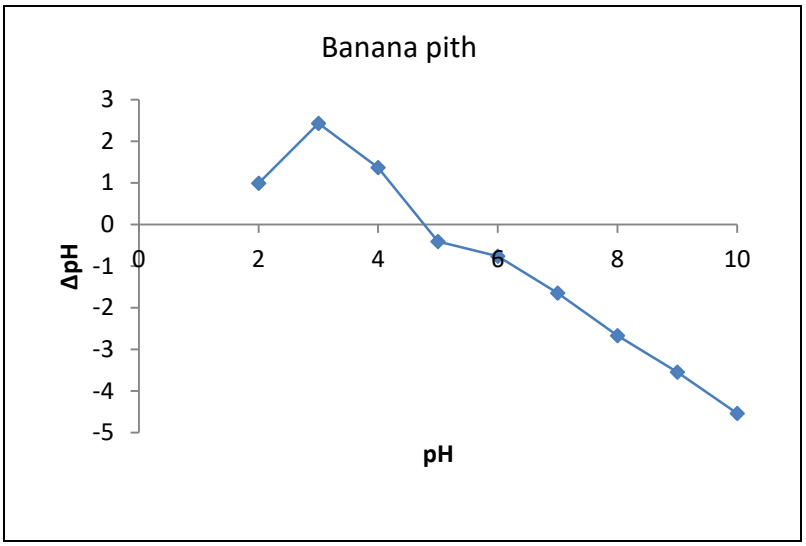

Figure 4.6: Point of zero charge of banana pith biomass.

4.2 Bio-sorption of Heavy Metals

Studies were carried out in order to determine the effects of the operational parameters on metal ion adsorption. The operational parameters studied included the time required for equilibrium, the biomass dose and the pH of the solution. The uptake of metal ions by the biomass was initially evaluated in batch condition.

4.2.1 Batch experiments for bio-sorption of heavy metal unto Banana pith (Bp), Maerua Decumbent (MD) and Opuntia Spp. (C)

(a) Effects of contact time in the removal of heavy metals

The purpose of this experiment was to determine the contact time required to reach the equilibrium between the solid phase (biomass of three materials namely banana pith, Maerua decumbent and Opuntia Spp.) and liquid phase (Wastewater). Results from the experiment (Figure. 4.7) shows that the metal uptake increases with time and after some time, it reaches a constant value where no more ions can be removed from the solution. A similar trend was reported by (Azouaou *et al.*, 2010, Adsorption of cadmium from aqueous solution onto untreated coffee grounds:equilibrium,kinetics and thermodynamics., 2010; Mohammad et al., 2011) in their study of the removal of heavy metal from aqueous solution using untreated coffee and chemically modified algae. The time required to attain this state of equilibrium is termed as the equilibrium

time. The amount of metal ion adsorbed at the equilibrium time reflects the maximum adsorption capacity of the adsorbent under these particular conditions. The result showed that the adsorption of metal ion increases with time up to 1hour and then it becomes almost constant at the end of the experiment. It can be concluded that the rate of metal binding with biomass is more predominant during initial stages, which gradually decreases and remains almost constant after 120 min.

(b) Effects of dosage in the removal of heavy metals

The effect of dosage was investigated at the range of 0.05-0.4 g/100 ml. The results (Figure 4.8) indicate that the optimum dosages were 0.2g/100 ml for banana pith and Maerua whereas for Opuntia Spp. it was 0.1g/100 ml. The percentage of metal removal increased with the increasing amount of biomass. This may be attributed to the availability of more and more binding sites for complexation of metal ions. Similar findings were reported by (Razmovski & Sciban, 2008; El-Said *et al*., 2010) as they evaluated the removal of heavy metal using fungal biomass and rice husk ash. After the optimum dosage in all the cases, decrease in bio-sorption was observed. This could be explained as a consequence of a partial aggregation of biomass, which results in a decrease in effective surface area for the bio-sorption according to (Karthikeyan et al., 2007).

(c) Effects of pH in the removal of heavy metals

The pH value influences the surface charge of the adsorbent, the degree of ionization and the species of adsorbate. So, the pH of the aqueous solution is an important controlling parameter in the heavy metal bio-sorption process (Ahamd, & Ahmad, 1998, Babu & Gupta, 2008,). The effect of pH on the bio-sorption of Cr, Pb, Zn, and Cu (II) by Banana pith, Maerua and Opuntia Spp. is shown in Figure 4.9. The effects of solution pH on the adsorption of metal ions onto the biomass studied were evaluated in the pH range of 3 to 9. High bio-sorption efficiency was obtained at pH 5 for all the bio-sorbent. At higher pH the percentage removal of heavy metal reduced. The high removal of lead metal at pH 5 may be due to the reason that in this pH heavy metal exists in solutions predominantly as free metal ions and the ionization degree of functional groups from adsorbent surface is higher enough to allow the electrostatic

interactions increasing metal adsorption as reported by (Se-Kwon Kim, 2015). At very low pH < 4 most of the functional groups are protonated and act as a positively charged species (Se-Kwon Kim, 2015). The excess of protons at this pH can compete with heavy metal ions and in consequence the amount of heavy metal, removed is low. Reduction of metal removal at higher pH>7 may be attributed to the formation of anionic hydroxide complexes and their competition with the active sites according to (Ahmet & Mustafa, 2008; Kumar *et al.,* 2006).

(d) Effect of initial concentration in the removal of heavy metals

The graph (Figure 4.10) shows metal uptake of metal ions versus different concentrations of heavy metal ions. The metal sorption was evaluated for the different metal concentrations. It was observed that metal sorption increased with increase in initial concentration. High initial concentration provides an important driving force to overcome mass transfer resistance of metal ion between the aqueous and solid phases. Similar results were reported by (Onyancha et al., 2008) in the removal of chromium using algae bio-sorbent.

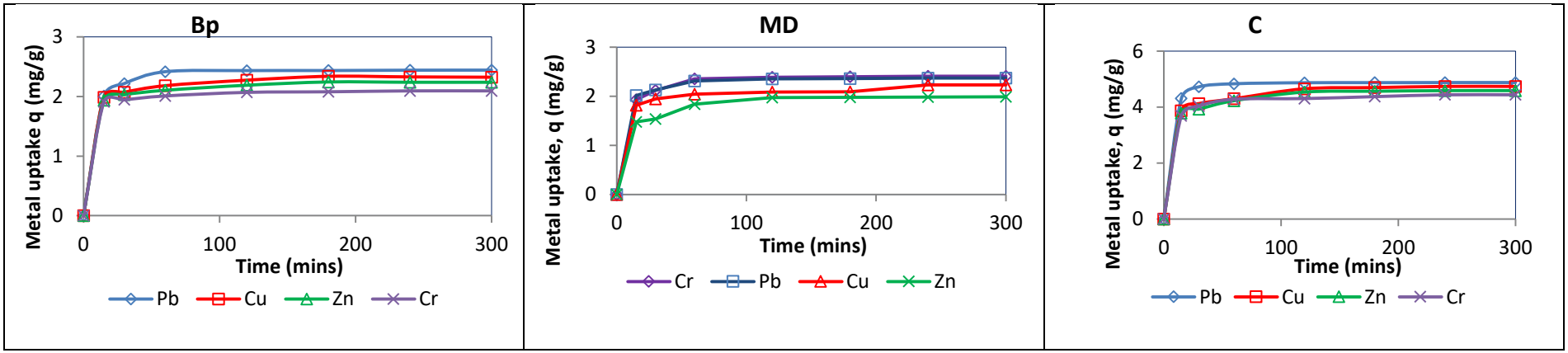

Figure 4.7: Metal uptake capacities at varying time intervals

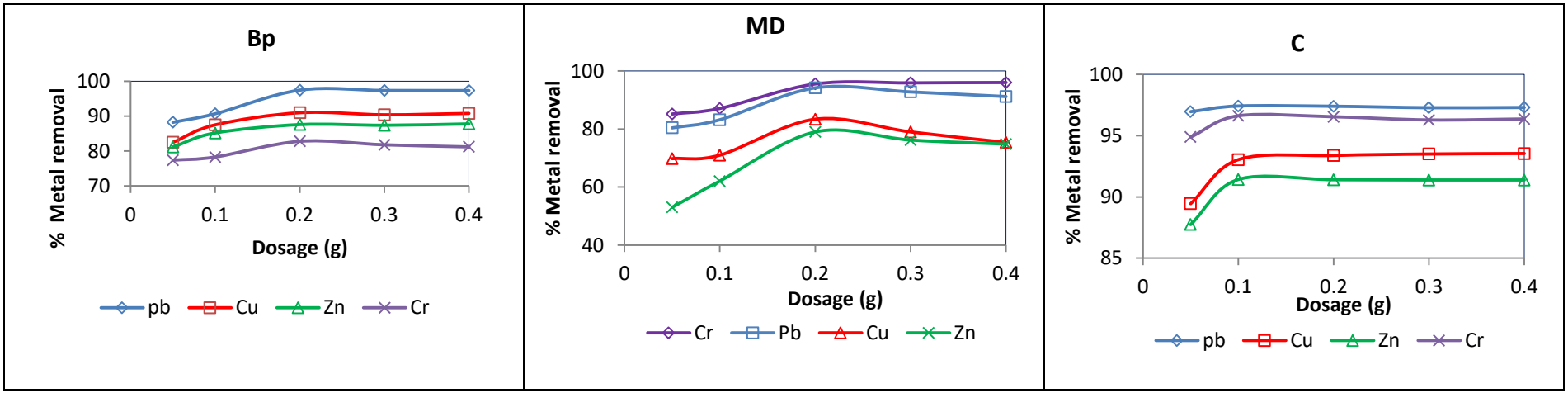

Figure 4.8: Effect of adsorbent dose on metal adsorption

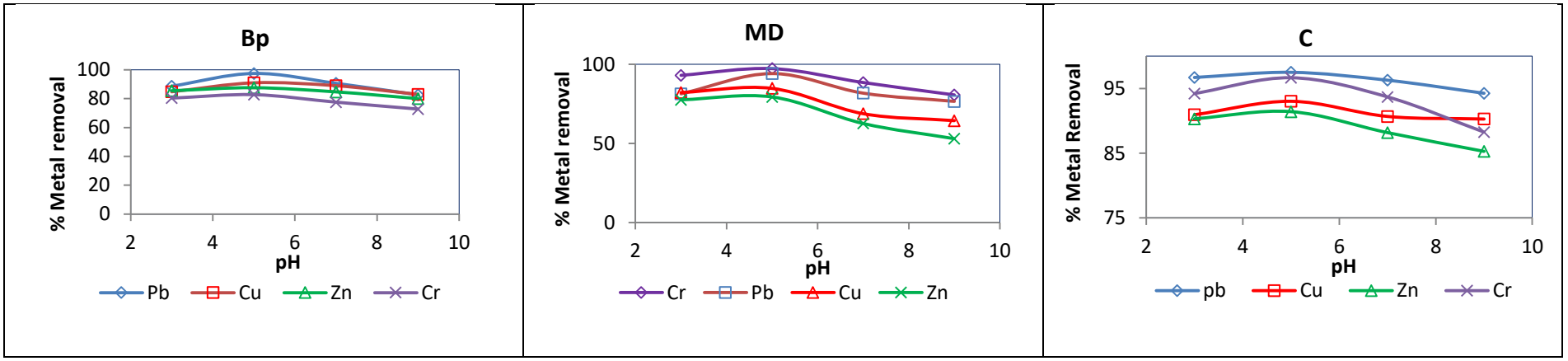

Figure 4.9: Effect of varying pH on metal ions adsorption.

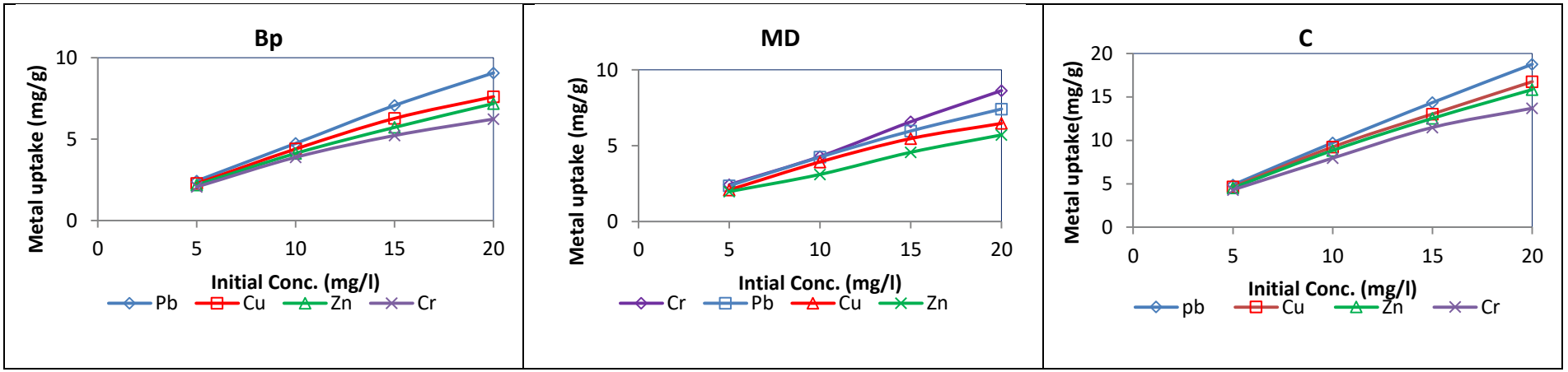

Figure 4.10: Effect of varying concentration of metal ions.

(e) Bio-sorption Isotherm modelling.

The adsorption isotherm indicates how the adsorbed molecules distribute between the liquid and the solid phase when the adsorption process reaches an equilibrium state (Kratochvil & Volesky, 1998). Freundlich (Eq.2.2) and Langmuir (Eq.2.4) isotherms were used to describe bio-sorption of lead, chromium, copper, and zinc unto banana pith, Maerua and Opuntia Spp. (Figure 4.11 to 4.16). The constants for the isotherms were determined and recorded in Table 4.3.

Table 4.3: Freundlich and Langmuir constants for banana pith

Banana Heavy metal	Langmuir R^2	q_{max}	K_L	Freundlich R^2	1/n	K_f
Banana pith						
Lead	0.983	12.210	1.954	0.991	0.524	7.859
Copper	0.993	10.000	0.502	0.994	0.482	4.044
Zinc	0.989	9.718	0.444	0.997	0.505	3.185
Chromium	0.995	9.569	0.232	0.989	0.550	2.453
Maerua Decumbent						
Chromium	0.993	11.099	1.397	0.992	0.488	5.880
Lead	0.949	8.881	1.046	0.995	0.403	4.124
Copper	0.982	8.650	0.520	0.998	0.457	2.955
Zinc	0.860	8.183	0.228	0.959	0.499	1.862
Opuntia Spp.						
Lead	0.994	26.525	1.964	0.966	0.570	17.964
Copper	0.993	24.876	0.848	0.993	0.565	10.517
Zinc	0.998	22.988	0.626	0.974	0.564	8.185
Chromium	0.996	19.268	0.548	0.965	0.524	6.437

The higher the K_L, the higher is the affinity of the adsorbent for metal ions. According to the data in Table 4.3, the affinity order for banana pith were Pb>Cu>Zn>Cr with a

q_{max} of 12.2, 10.0, 9.7 and 9.6 respectively whereas for Maerua Decumbent the affinity was Cr>Pb>Cu>Zn with of q_{max} of 11.1, 8.88, 8.65 and 8.18 respectively and finally the affinity for Opuntia Spp. was Pb>Cu>Cu>Cr with a q_{max} of 26.53, 24.88, 22.99, 19.27 respectively. The values of the q_{max} experimentally obtained were found comparable with theoretically calculated q_{max}. The theoretical q_{max} for lead, copper, zinc and chromium removal using banana pith were 11.6, 11.5, 9.8 and 10.8 respectively.

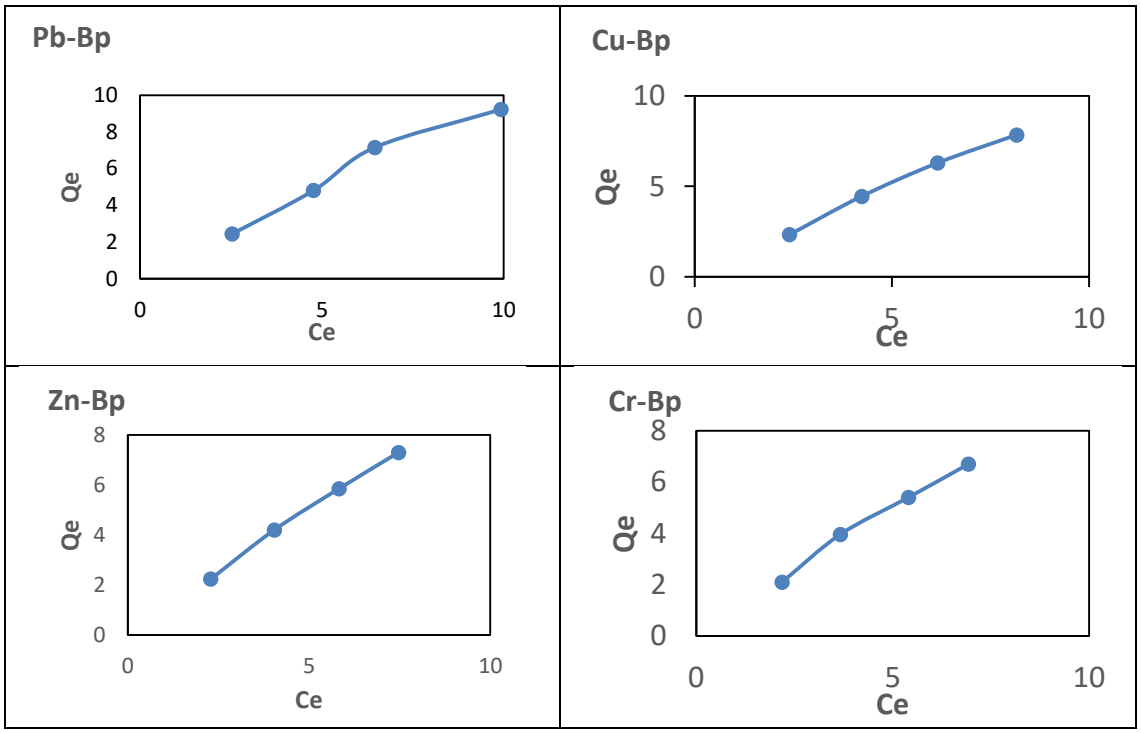

Figure 4.11: Freundlich plot for bio-sorption of lead, copper, zinc and chromium unto banana pith.

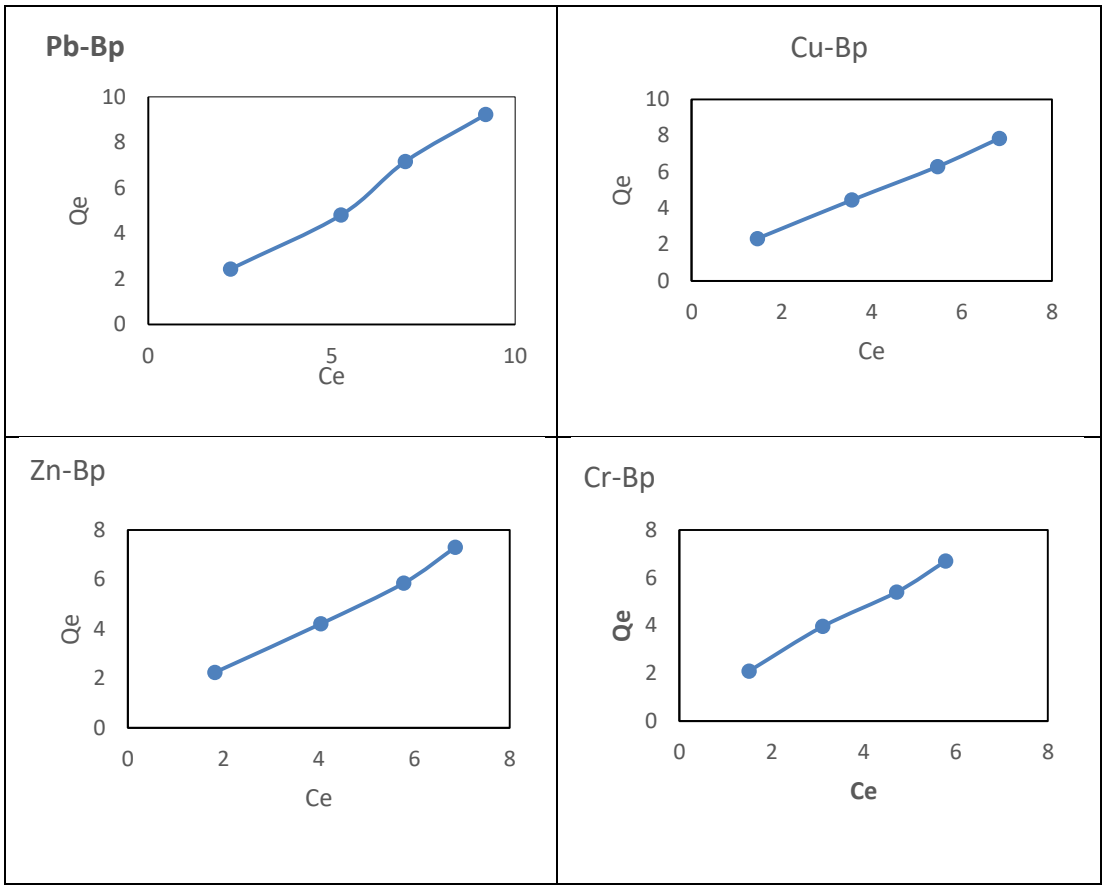

Figure 4.12: Langmuir plot for bio-sorption of lead, copper, zinc and chromium unto banana pith

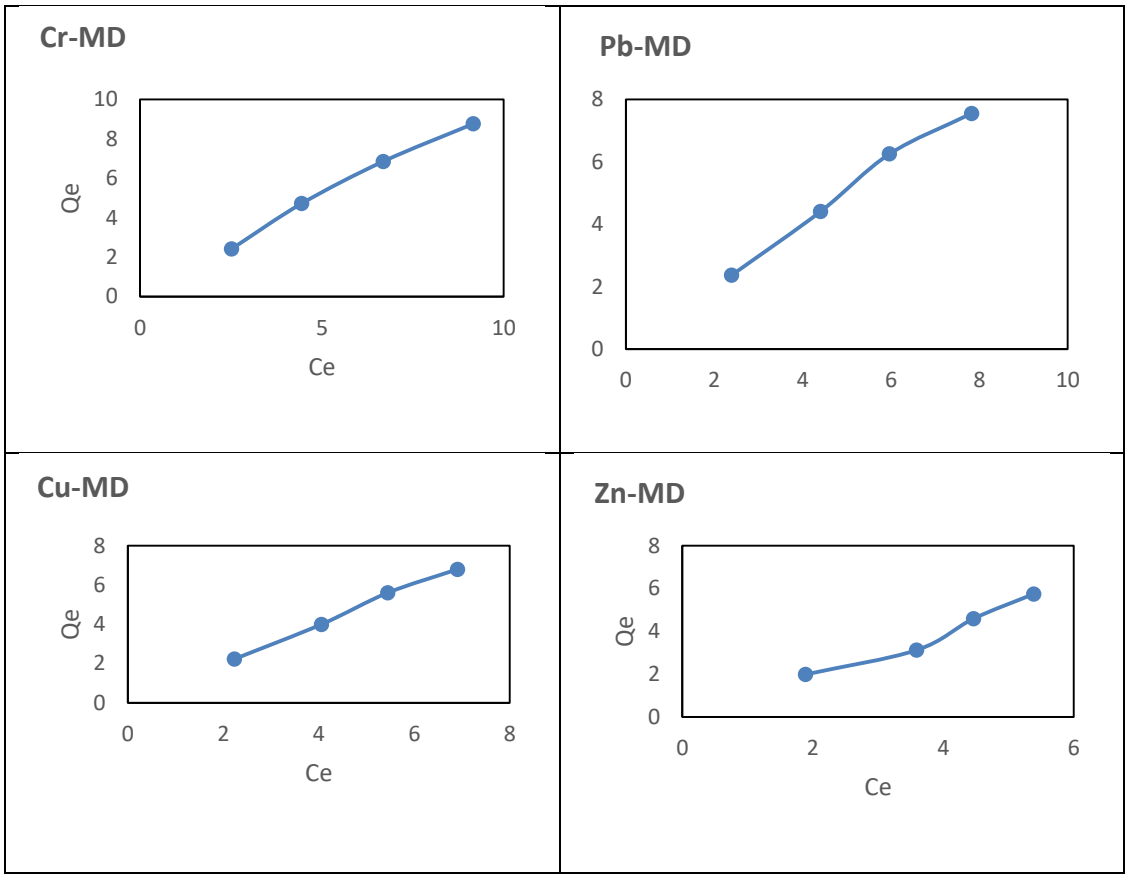

Figure 4.13: Freundlich plot for bio-sorption of chromium, lead, copper, and zinc unto Maerua Decumbent

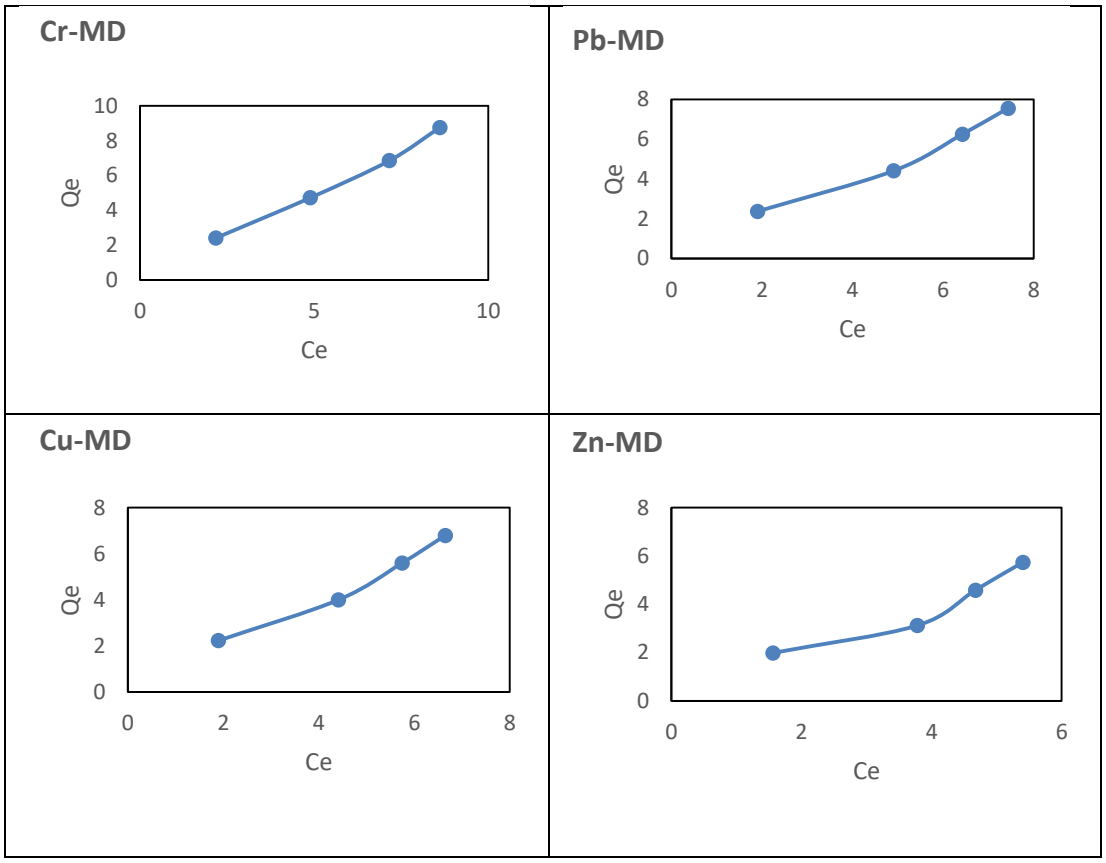

Figure 4.14: Langmuir plot for bio-sorption of chromium, lead, copper and zinc unto Maerua Decumbent

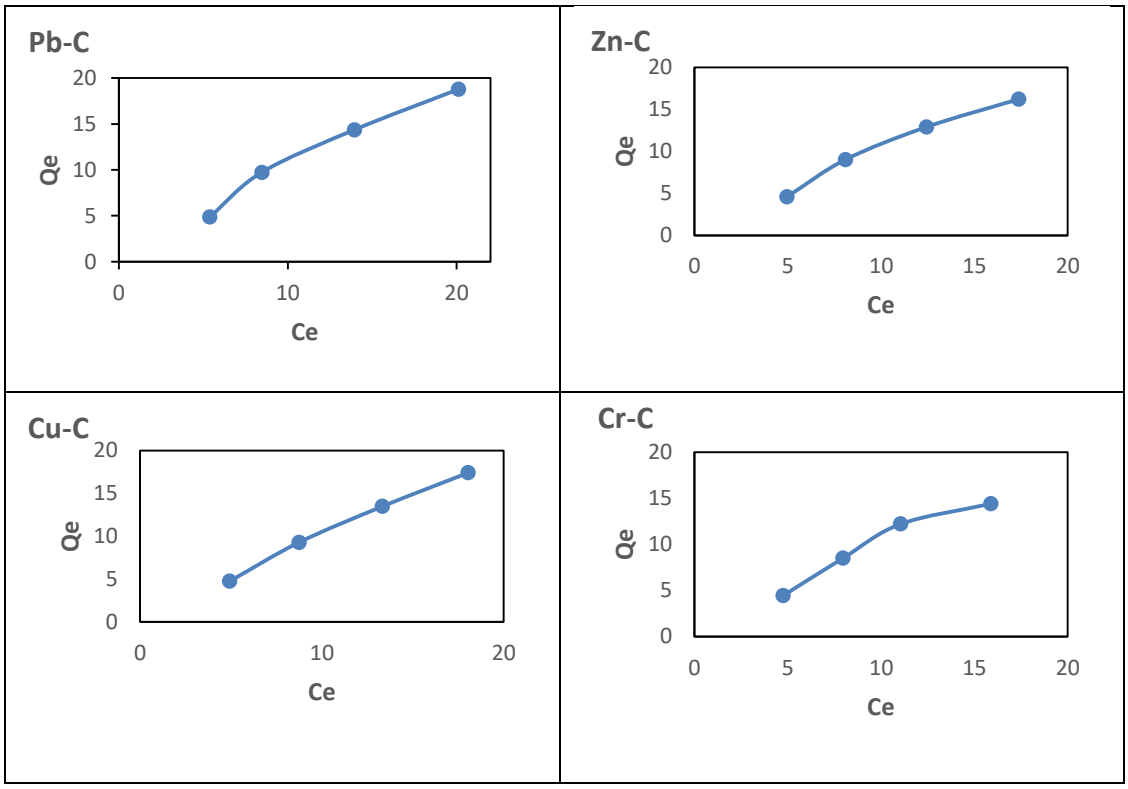

Figure 4.15: Freundlich plot for bio-sorption of lead, copper, zinc and chromium to Opuntia Spp.

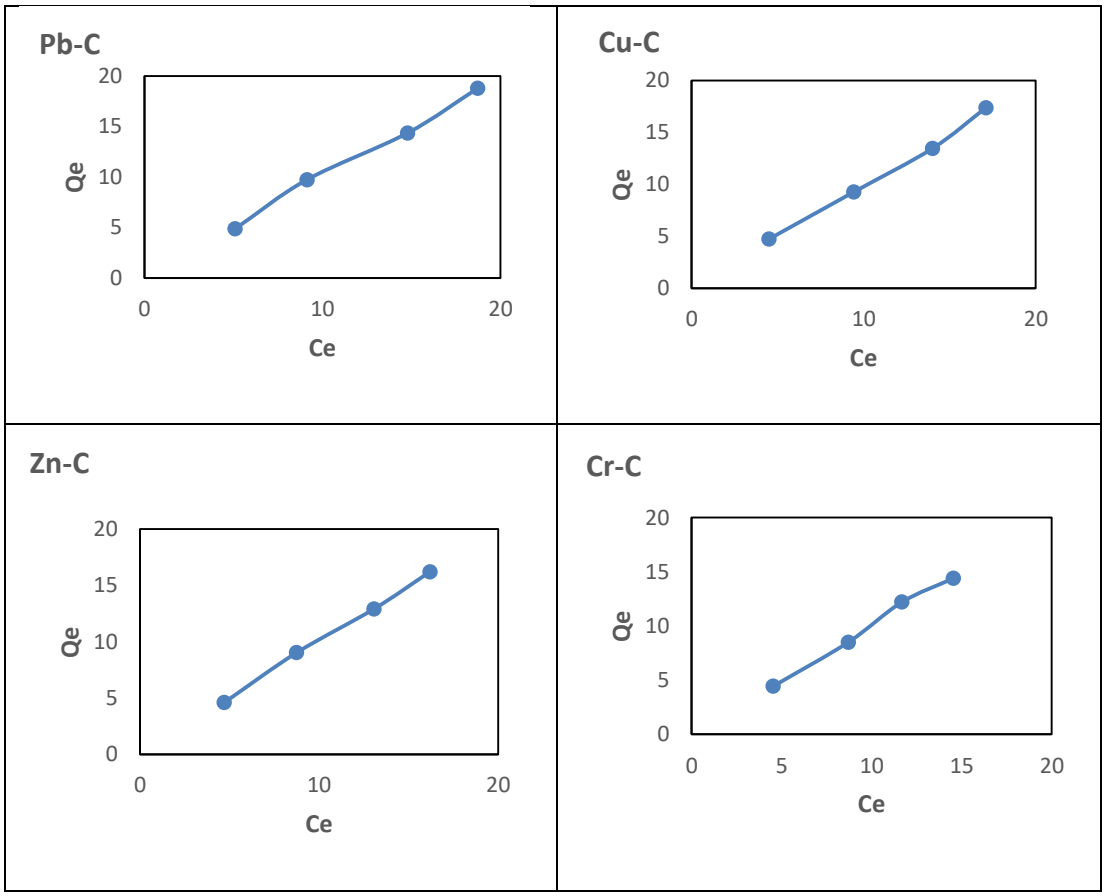

Figure 4.16: Langmuir plot for bio-sorption of lead, copper, zinc and chromium unto Opuntia Spp.

In view of the values of the linear regression coefficients, Langmuir model and Freundlich model fits well to the sorption data in the studied concentration range indicating single layer sorption on homogeneous material. The value of 1/n was found to range between 0 and 1, hence favourable bio-sorption conditions. The results were in agreement with those reported by (Magdy & Daifullah, 1988, Bhatti et al., 2007)

(f)Adsorption kinetics of banana pith, Maerua Decumbent and Opuntia Spp.

In order to investigate the mechanism of bio-sorption and its potential rate-controlling steps, which include the mass transfer and chemical reaction processes, kinetic models were exploited to test the experimental data. The data was processed and used in the linear regression to determine the kinetics model which provides best fit. For the validity of the order of the bio-sorption process two criteria were evaluated, the first based on the regression coefficient (R^2) and the second on the calculated q_e, which must approach the experimental q_e. (Li, et al., 2010)**.**

The Pseudo first and pseudo second plots for heavy metal removal using banana pith, Maerua Decumbent and Opuntia spp. are shown in Figure 4.17 to 4.22 and the calculated qe, K_1, K_2 and correlation coefficient (R^2) are presented in Table 4.4 to 4.6.

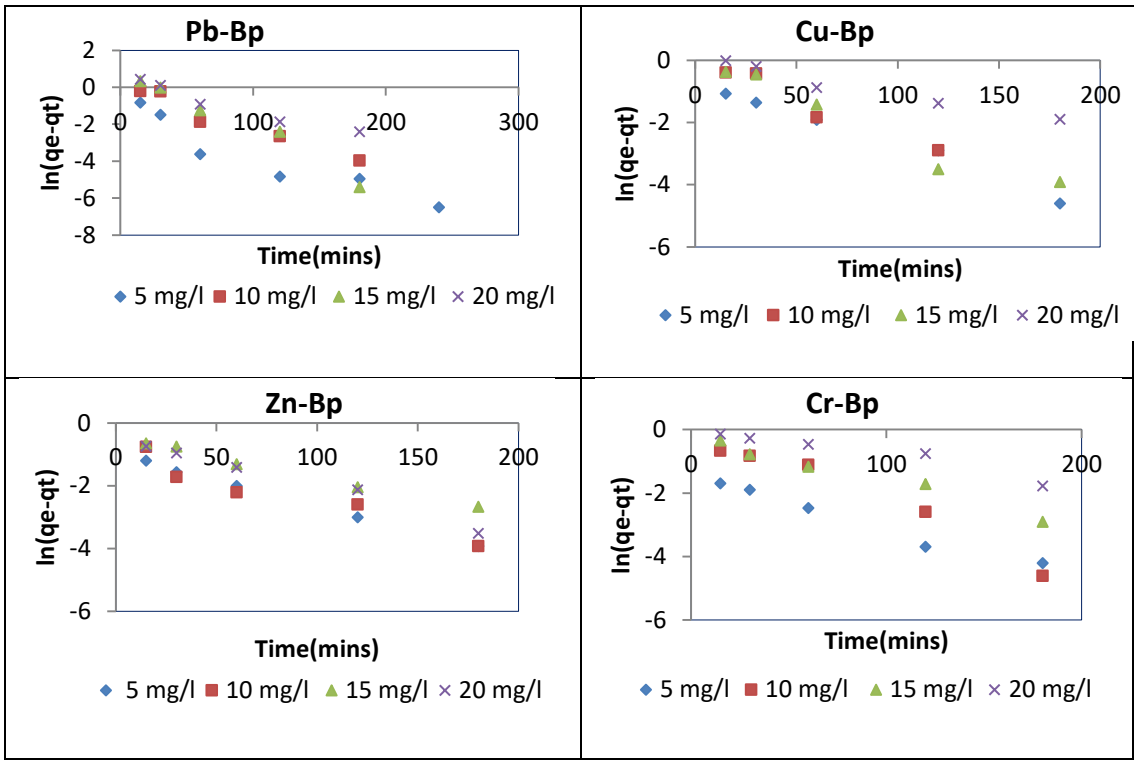

Figure 4.17: Pseudo first order kinetics for lead, copper, zinc and chromium unto banana pith

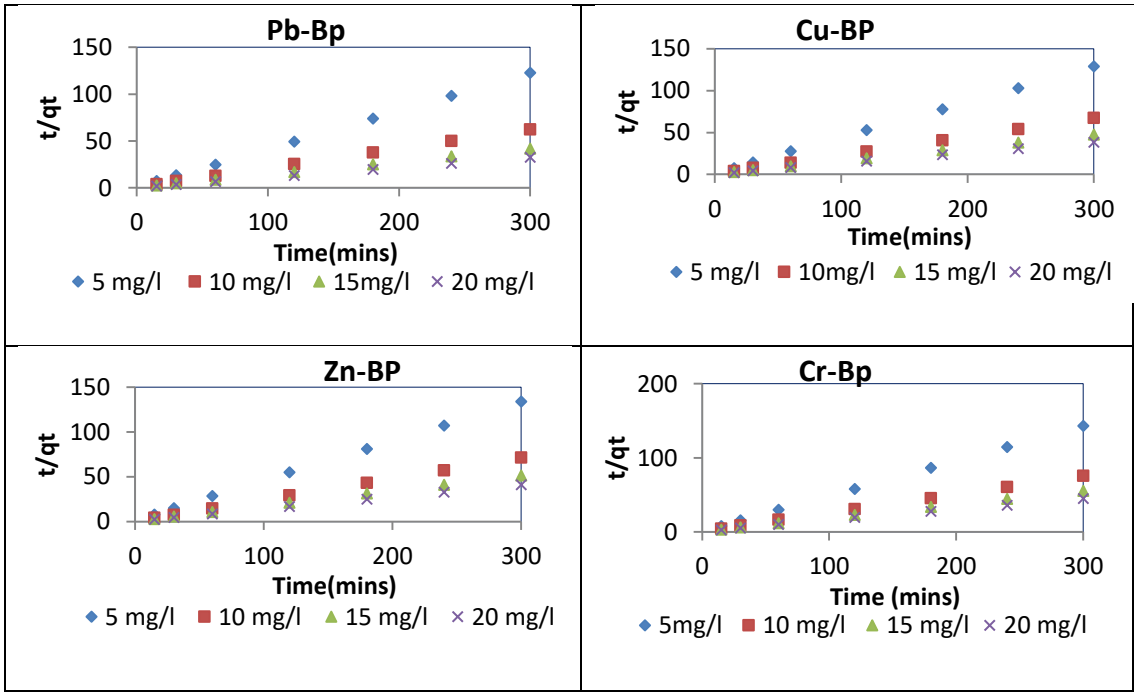

Figure 4.18: Pseudo second order kinetics for lead, copper, zinc and chromium unto banana pith

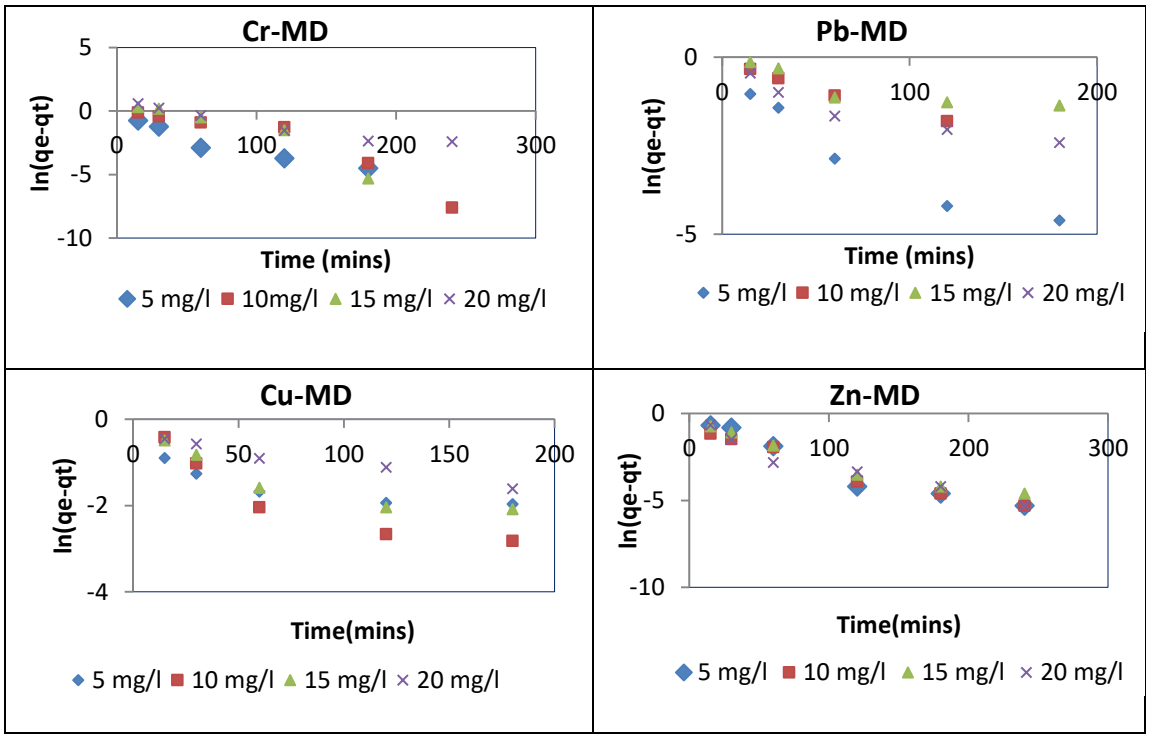

Figure 4.19: Pseudo first order kinetics for chromium, lead, copper and zinc unto Maerua Decumbent

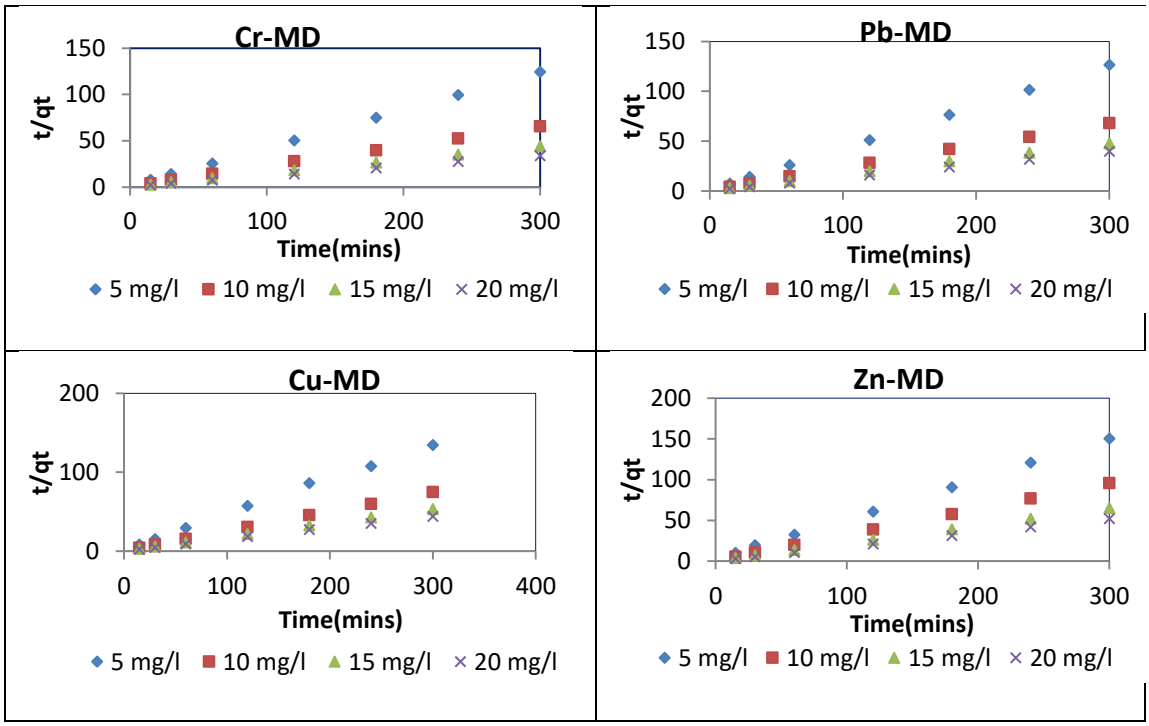

Figure 4.20: Pseudo first order kinetics for chromium, lead, copper and zinc unto Maerua Decumbent

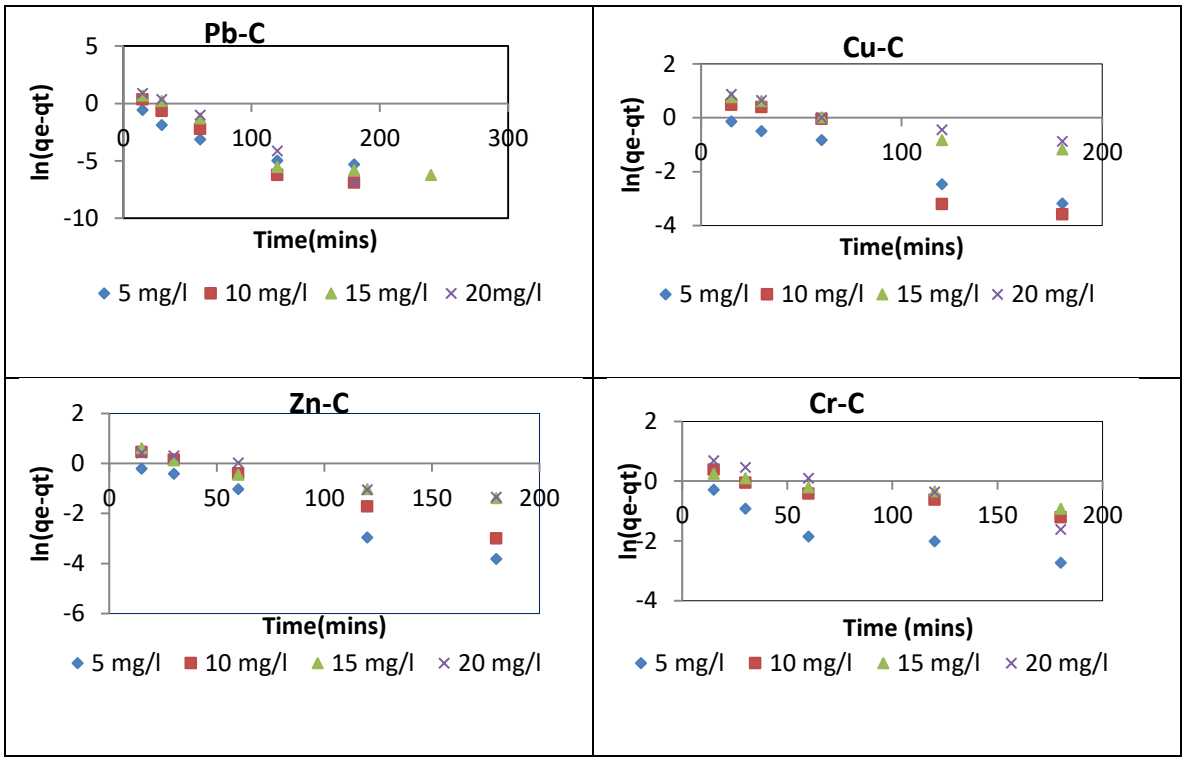

Figure 4.21: Pseudo first order kinetics for lead, copper, zinc and chromium unto Opuntia Spp.

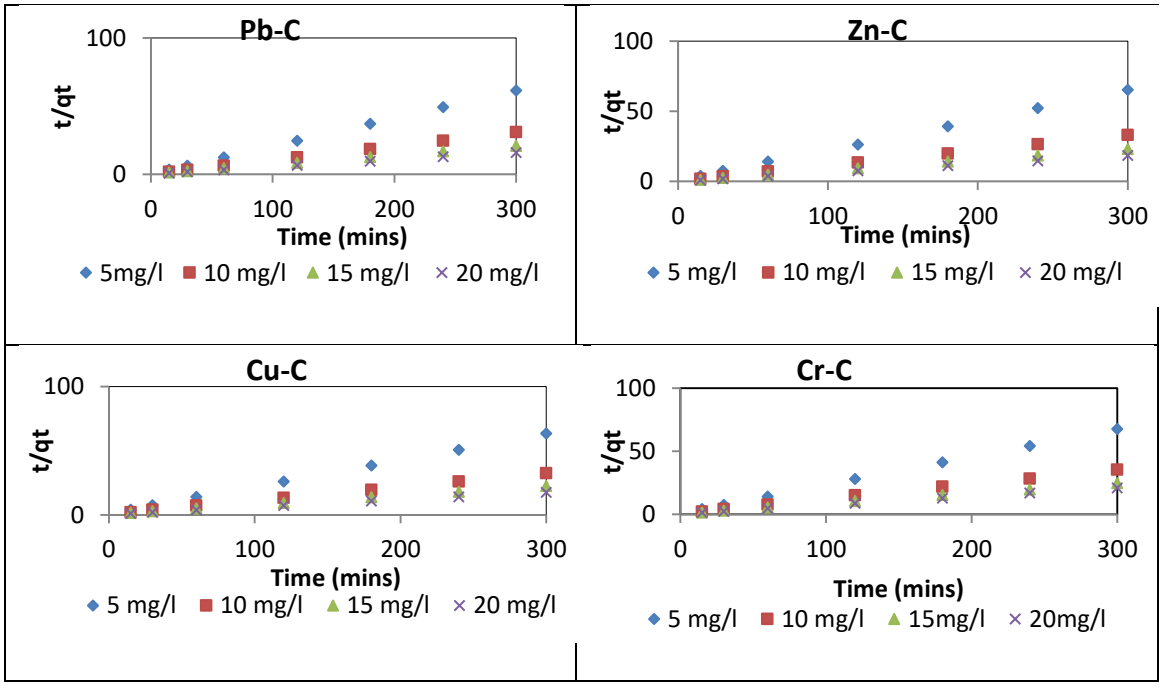

Figure 4.22: Pseudo second order kinetics for lead, copper, zinc and chromium unto Opuntia Spp.

Table 4.4: Kinetic parameters from pseudo first and pseudo second order bio-sorption of heavy metals on to banana pith.

		First order kinetics			Second order kinetics		
Heavy metal	$q_{e\ (exp)}$	R^2	$q_{e\ (cal)}$	K_1	R^2	$q_{e\ (cal)}$	K_2
lead							
5 mg/l	2.440	0.887	0.293	0.023	0.997	2.469	0.159
10 mg/l	4.807	0.954	1.085	0.023	0.999	4.885	0.049
15 mg/l	7.156	0.973	2.585	0.033	0.998	7.272	0.034
20 mg/l	9.220	0.948	1.616	0.017	0.999	9.346	0.028
Copper							
5 mg/l	2.330	0.986	0.502	0.021	0.999	2.363	0.106
10 mg/l	4.450	0.949	1.044	0.025	0.998	4.512	0.058
15 mg/l	6.300	0.944	0.997	0.024	0.998	6.365	0.059
20 mg/l	7.850	0.961	1.047	0.0114	0.998	7.936	0.032
Zinc							
5 mg/l	2.240	0.9982	0.360	0.0162	0.9999	2.267	0.121
10 mg/l	4.200	0.9182	0.399	0.0163	0.9999	4.228	0.115
15 mg/l	5.880	0.991	0.628	0.0125	0.9999	5.899	0.058
20 mg/l	7.300	0.9808	0.648	0.0162	0.9999	7.347	0.069
Chromium							
5 mg/l	2.095	0.9768	0.225	0.016	0.998	2.112	0.198
10 mg/l	3.960	0.9661	0.981	0.0239	0.999	4.021	0.060
15 mg/l	5.400	0.9758	0.801	0.0143	0.999	5.461	0.049
20 mg/l	6.700	0.9295	1.072	0.0092	0.999	6.803	0.025

Table 4.5: Kinetic parameters from pseudo first and pseudo second order bio-sorption of heavy metals on Maerua.

Heavy metal		First order kinetics			Second order kinetics		
	$q_{e\ (exp)}$	R^2	$q_{e\ (cal)}$	K_1	R^2	$q_{e\ (cal)}$	K_2
Chromium							
5 mg/l	2.413	0.908	0.448	0.022	0.999	2.445	0.117
10 mg/l	4.569	0.899	2.551	0.031	0.999	4.666	0.034
15 mg/l	6.800	0.905	3.467	0.032	0.999	6.959	0.024
20 mg/l	8.850	0.936	1.743	0.014	0.999	8.985	0.022
Lead							
5 mg/l	2.370	0.915	0.362	0.022	0.999	2.395	0.152
10 mg/l	4.410	0.992	0.842	0.014	0.999	4.470	0.043
15 mg/l	6.250	0.747	0.769	0.007	0.999	6.309	0.034
20 mg/l	7.550	0.877	0.531	0.011	0.999	7.593	0.067
Copper							
5 mg/l	2.230	0.785	0.347	0.006	0.999	2.257	0.068
10 mg/l	4.000	0.830	0.514	0.014	0.999	4.040	0.076
15 mg/l	5.600	0.817	0.532	0.009	0.999	5.640	0.060
20 mg/l	6.800	0.974	0.679	0.007	0.999	6.858	0.036
Zinc							
5 mg/l	1.99	0.927	0.579	0.022	0.999	2.042	0.074
10 mg/l	3.125	0.964	0.377	0.0194	0.999	3.153	0.131
15 mg/l	4.595	0.946	0.491	0.0181	0.999	4.632	0.096
20 mg/l	5.74	0.936	0.378	0.0186	0.999	5.770	0.134

Table 4.6: Kinetic parameters from pseudo first and pseudo second order bio-sorption of heavy metals on Opuntia Spp.

Heavy metal		First order kinetics			Second order kinetics		
	$q_{e\ (exp)}$	R^2	$q_{e\ (cal)}$	K_1	R^2	$q_{e\ (cal)}$	K_2
lead							
5 mg/l	4.879	0.890	0.401	0.028	0.999	4.904	0.161
10 mg/l	9.733	0.942	1.884	0.046	0.999	9.804	0.059
15 mg/l	14.359	0.868	1.838	0.034	0.999	14.492	0.031
20 mg/l	18.780	0.999	5.631	0.048	0.999	18.939	0.026
Copper							
5 mg/l	4.740	0.979	1.143	0.012	0.999	4.838	0.039
10 mg/l	9.280	0.917	3.026	0.028	0.999	9.569	0.017
15 mg/l	13.480	0.963	2.418	0.012	0.999	13.661	0.015
20 mg/l	17.400	0.948	2.418	0.010	0.999	17.544	0.0142
Zinc							
5 mg/l	4.590	0.981	1.226	0.023	0.999	4.673	0.045
10 mg/l	9.020	0.999	2.232	0.021	0.999	9.1743	0.023
15 mg/l	12.900	0.924	1.657	0.012	0.999	13.038	0.021
20 mg/l	16.200	0.962	1.853	0.012	0.999	16.367	0.018
Chromium							
5 mg/l	4.440	0.864	0.604	0.313	0.999	4.482	0.064
10 mg/l	8.500	0.925	1.351	0.008	0.999	8.621	0.020
15 mg/l	12.200	0.958	1.356	0.006	0.999	12.315	0.018
20 mg/l	14.400	0.963	2.507	0.013	0.999	14.619	0.014

The calculated q_e values for the pseudo second order for banana pith, Maerua decumbent and Opuntia Spp. were found to approach the experimental values and the correlation coefficient were close to 1, indicating a good ability of this model to describe the kinetics of the metal ion adsorption process.

This observation indicates that the rate –limiting steps in the bio-sorption of metallic ions to all the three bio-sorbents was chemisorption. Similar results were reported by (Reddy *et al.,* 2010) where they studied the removal of lead from aqueous solution using Moringa Oleifera.

4.2.2 Continuous flow

(a) Fixed bed column bio-sorption

The results of the performance of a fixed bed heavy metal bio-sorption were given in terms of maximum bed capacity, q_t (Eq.3.9), adsorbed metal percent, Y (Eq.3.11) and equilibrium metal uptake qe (Eq.3.12)

(i) Effects of depth to column performance

It was observed that the slope of the breakthrough curve decreased with increasing bed depth (Figure 4.23), which resulted in broadened mass transfer zone. Similar observation was made by (Song *et al.,* 2011).The area under breakthrough curve due to the effects of varying depths of adsorption are given in Figures 4.24 to 4.26 and the maximum bed capacity q_t, adsorbed metal per cent (Y), equilibrium metal uptake q_e and effluent volume ($V_{eff.}$) were determined as per equations 3.9, 3.11 and 3.12 and the results are given in Table 4.7

The results indicated that as the depth increased, exhaust time and effluent volume increased (Table 4.7)

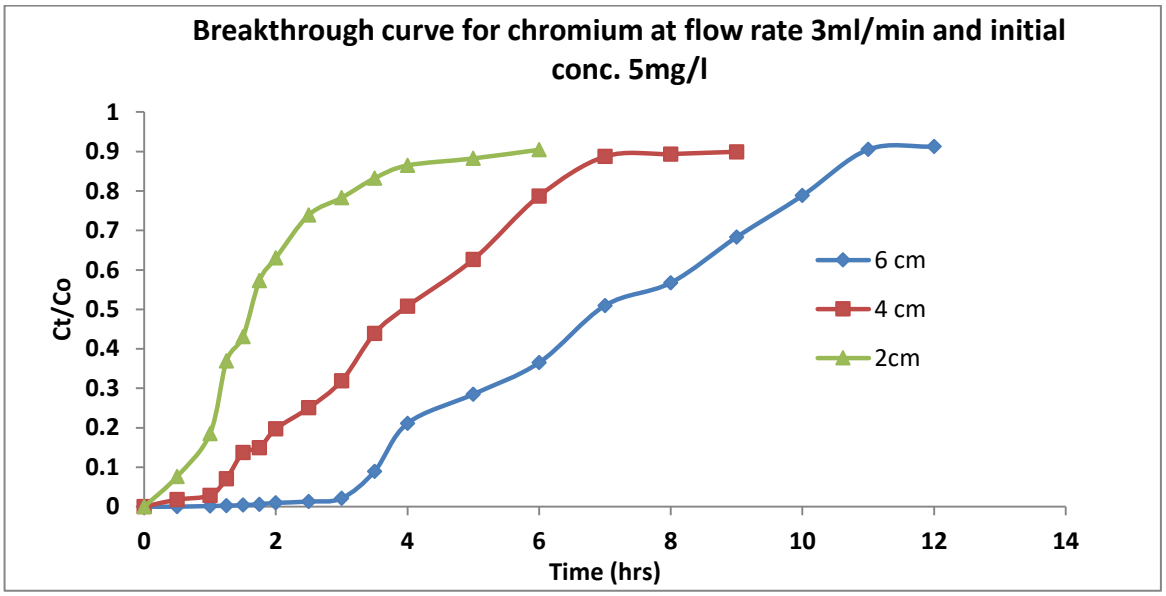

Figure 4.23: Breakthrough curve for chromium ions bio-sorption onto banana pith at different bed depths.

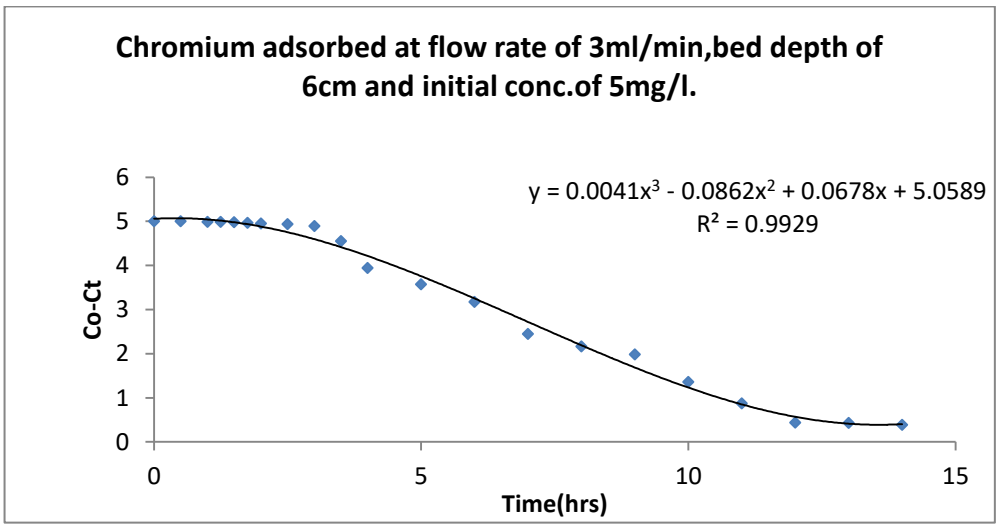

Figure 4.24: Plots of adsorbed chromium.

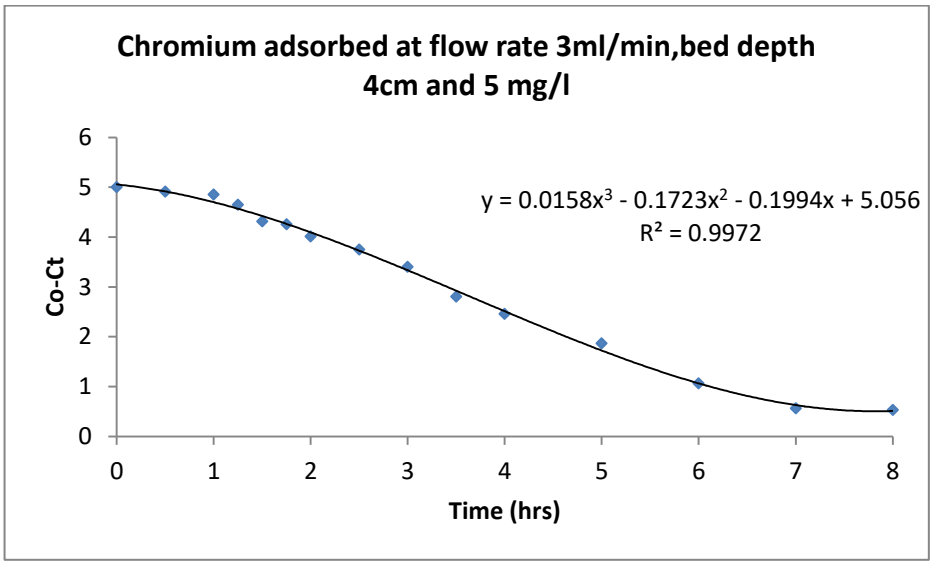

Figure 4.25: Plots of adsorbed chromium

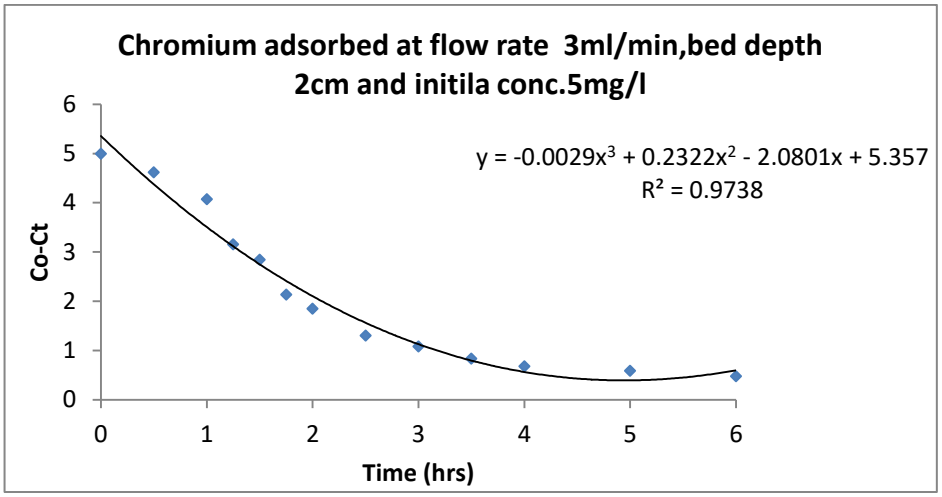

Figure 4.26: Plots of adsorbed chromium

Table 4.7: Bio-sorption parameters for Cr ions adsorption at different bed depths

Z(cm)	2	4	6
Q(ml/min)	3	3	3
Co (mg/l)	5	5	5
$T_{t(mins)}$	360	540	720
M_t (mg)	5.4	8.1	10.8
q_t (mg)	1.89	3.84	6.69
Mass of adsorbent (X) (g)	1.72	3.42	5.52
q_e(mg/g)	1.1	1.12	1.21
V_{eff}	1080	1620	2160
Y (%)	34.93	47.35	62

(ii) Effects of initial concentration to column performance

It was observed that decrease in concentration gave a later breakthrough curve (Figure 4.27). The breakthrough curves were sharper as influent concentration increased; indicating relatively smaller mass transfer zone and intra-particle diffusion controlled the sorption process. Bio-sorption of chromium varied, reducing as time increased. Shifting the breakthrough curve. For instance for flow rate of 5 and 10 ml/min the slope varied with time (Baral *et al*, 2009), reported similar behaviour in fixed bed column studies. The area under breakthrough curve due to the effects of varying initial concentration are given in Figures 4.24, 4.28 and 4.29 and the maximum bed capacity qt, adsorbed metal per cent (Y), equilibrium metal uptake qe and effluent volume were determined as per equations 3.9, 3.11 and 3.12 and the results are given in Table 4.8.

Higher treated volumes were achieved at low initial concentration and the uptake qe (mg/g) increased with increase in concentration. This was attributed to higher concentration gradient which causes the diffusion coefficient to increase, leading to faster transportation of metals ions. Similar behaviour was observed by (Long *et al.*, 2013).

As the initial influent concentration increased from 5-20 mg/l, the exhaust time decreased from 720 to 480 mins. The results indicate that higher initial influent concentration led to higher driving force for mass transfer; hence the adsorbent achieved saturation more quickly which resulted in a decrease of exhaust time and adsorption zone length according to (Baral *et al.*, 2009)

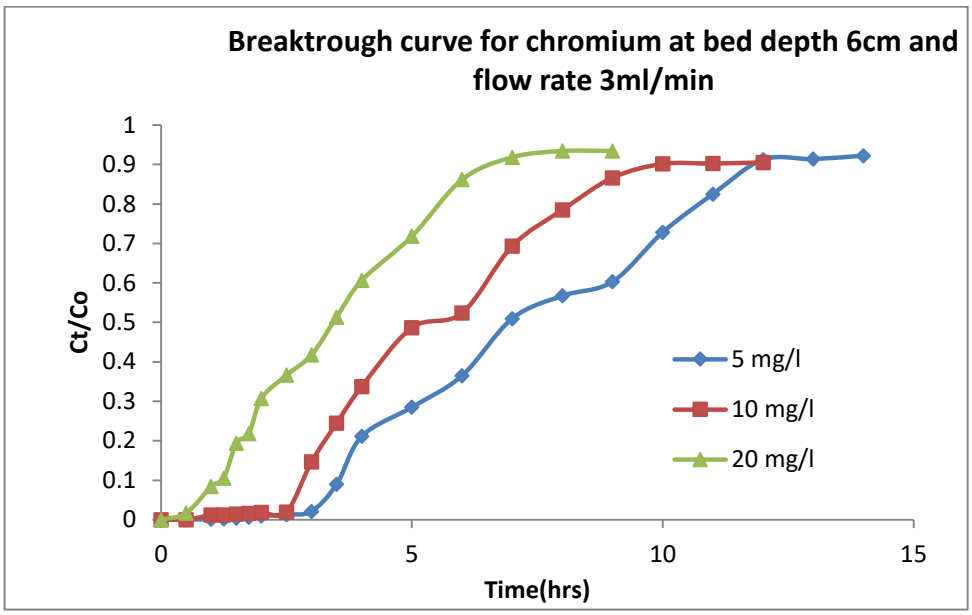

Figure 4.27: Breakthrough curve for chromium ions bio-sorption onto banana pith at different initial concentrations.

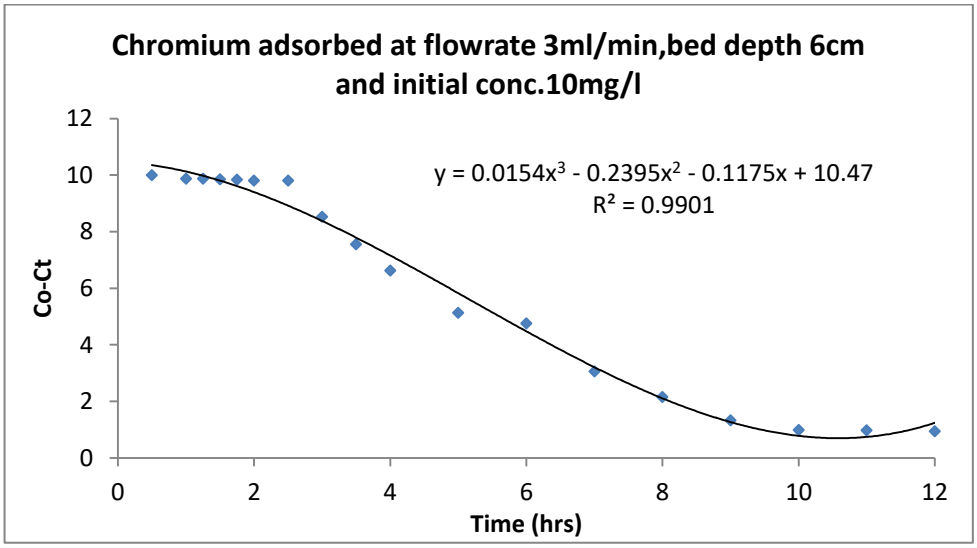

Figure 4.28: Plots of adsorbed chromium.

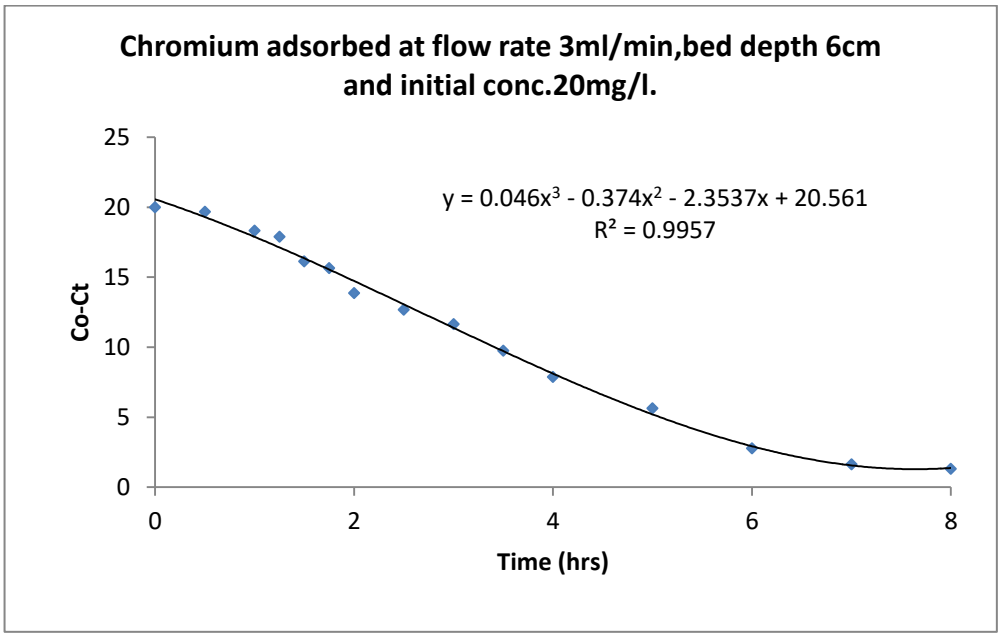

Figure 4.29: Plots of adsorbed chromium.

Table 4.8: Bio-sorption parameters for Cr ions adsorption at different concentrations

Co (mg/l)	5	10	20
Q(ml/min)	3	3	3
Z(cm)	6	6	6
$T_{t(mins)}$	720	600	480
M_t (mg)	10.8	18	28.8
q_t (mg)	6.7	10.35	13.04
Mass of adsorbent (X) (g)	5.52	5.52	5.52
q_e(mg/g)	1.21	1.87	2.36
V_{eff}	2160	1800	1440
Y(%)	62	57.5	45.28

(iii) Effects of flow rate to column performance

It was observed that as the flow rate increased, the slope increase. (Figure 4.30). The area under break through curve due to the effects of varying flow rate are given in Figures 4.25, 4.31 and 4.32 and the maximum bed capacity qt, adsorbed metal per cent (Y), equilibrium metal uptake qe and effluent volume were determined as per equations 3.9, 3.11 and 3.12 and the results are given in Table 4.9. As the flow rate increased from 3 to 7 ml/min the exhaust time decreased from 720 to 420 mins. At a

higher flow rate, the external film mass resistance at the surface of the adsorbent tends to decrease and the residence time decreases, hence the saturation time decreases and in turn gives the lower removal efficiency as reported by (Han et al., 2009b).It was also noted that the flow rate influenced the metal uptake. As the flow rate increased from 3 to 7 ml/min the qe reduced from 1.21 to 1.06 mg/g. The less time reduced the bonding capacity of the metal onto the adsorbent. Similar results were reported by (Aquoyo-Villarreal *et al*., 2011)

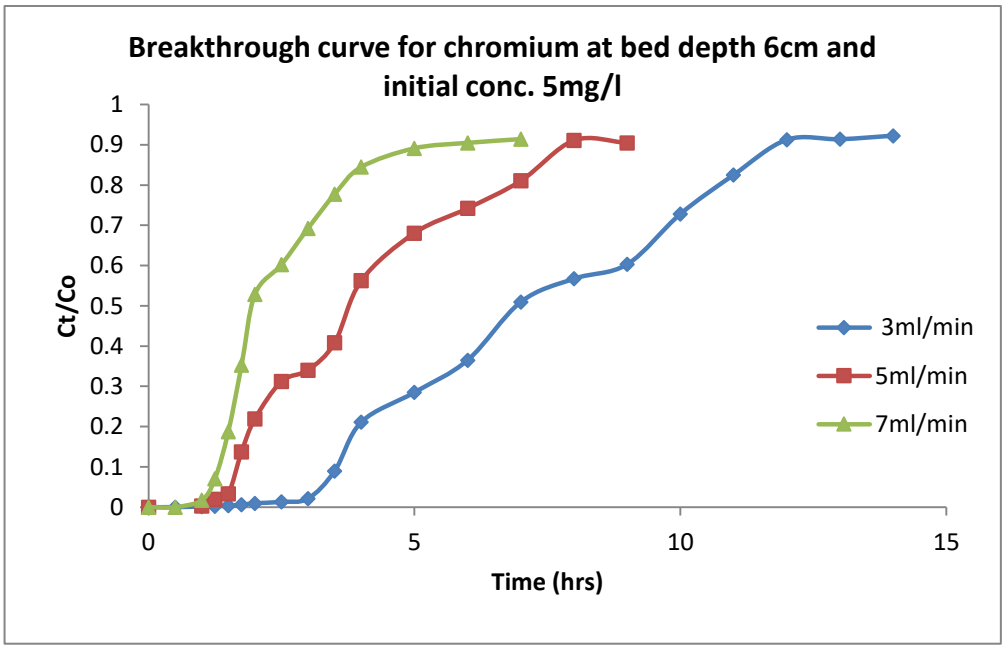

Figure 4.30: Breakthrough curve for chromium ions bio-sorption unto banana pith at different flow rates.

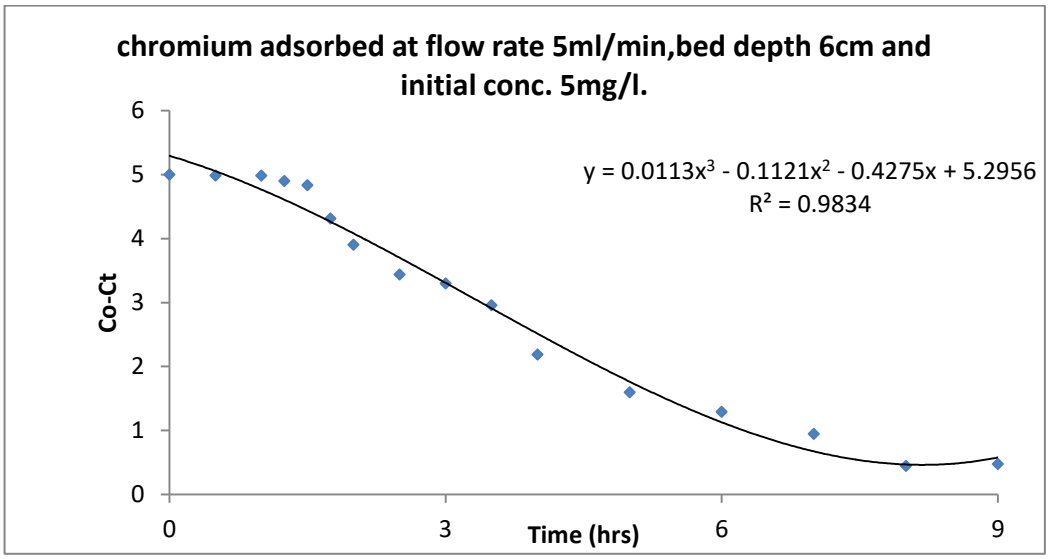

Figure 4.31: Plots of adsorbed chromium.

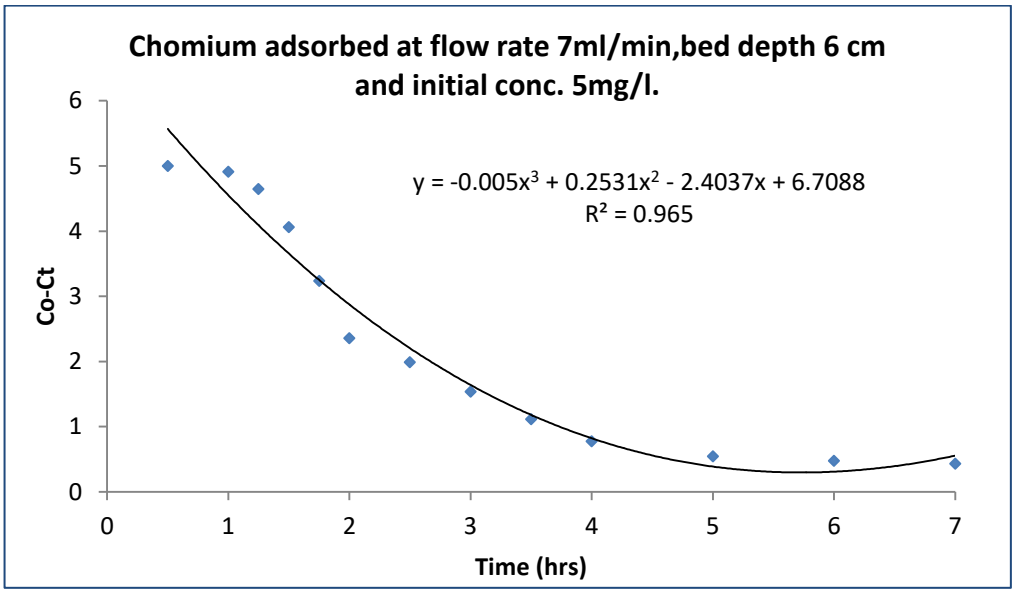

Figure 4.32: Plots of adsorbed chromium.

Table 4.9: Bio-sorption parameters for chromium ions adsorption at different flow rates.

Q(ml/min)	3	5	7
Co (mg/l)	5	5	5
Z(cm)	6	6	6
$T_{t(mins)}$	720	540	420
M_t (mg)	10.8	13.5	14.7
q_t (mg)	6.7	6.49	5.86
Mass of adsorbent (X) (g)	5.52	5.52	5.52
q_e(mg/g)	1.21	1.18	1.06
V_{eff}	2160	2700	2940
Y(%)	62	48.07	39.86

(b) Breakthrough curve modelling.

Three models were used to describe data through fixed bed according to (Naja & Volesky, 2006; Mohan & Sreelakshmi, 2008). The models used were namely, Thomas, Yoon Nelson and Adams-Bohart models. These kinetic models were implemented to explain the column dynamic process namely at the concentration parameters of 0.05<ct/co>0.90.

(i) Break through curve analysis using Adams-Bohart Model

Adams –Bohart equations 3.14 and 3.15 were used in the data analysis obtained by varying initial concentration, bed depths and flow rates. The results obtained from Adams-Bohart model plot, Figure 4.33 to 4.35 is recorded in Table 4.10. It was observed that the mass transfer coefficient (K_{AB}) increased with increase in initial concentration and flow rate but reduced with increase in bed depth. This implies that the reaction kinetics was influenced by external mass transfer. (Ahmad & Hameed ,

2010) reported a similar observation in their study of adsorption of azo dye onto granular activated carbon.

It was also noted that the sorption capacity, N_o, reduced with increase in the bed depth and flow rate but increased with increase in initial concentration. A similar trend was observed for sorption of chromium onto thermally activated weed, where by increasing the bed height, N_o decreased significantly. (Baral et al., 2009). The values of R^2 reveal the lack of applicability of the model (Table 4.10)

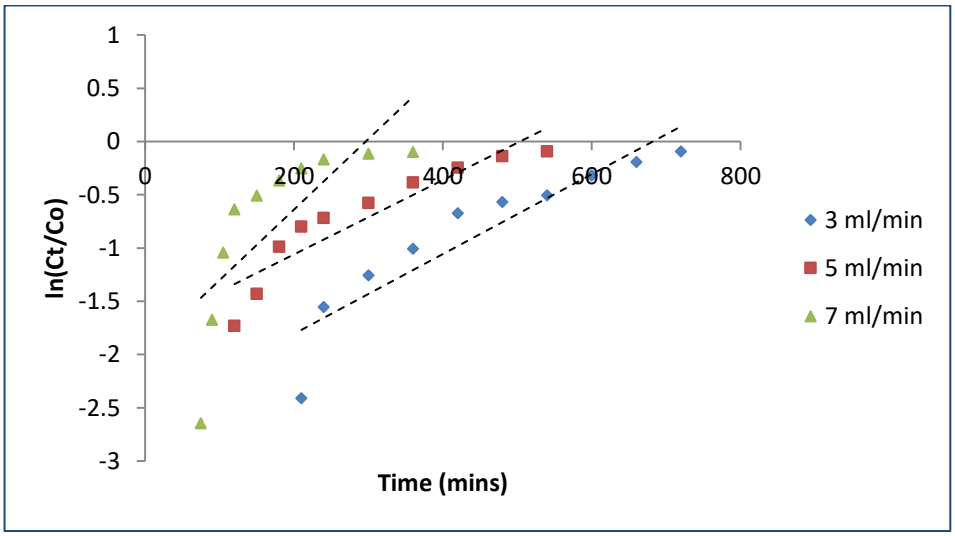

Figure 4.33: Linear regression analysis for breakthrough curve modelling by Adam-Bohart model at different initial concentration.

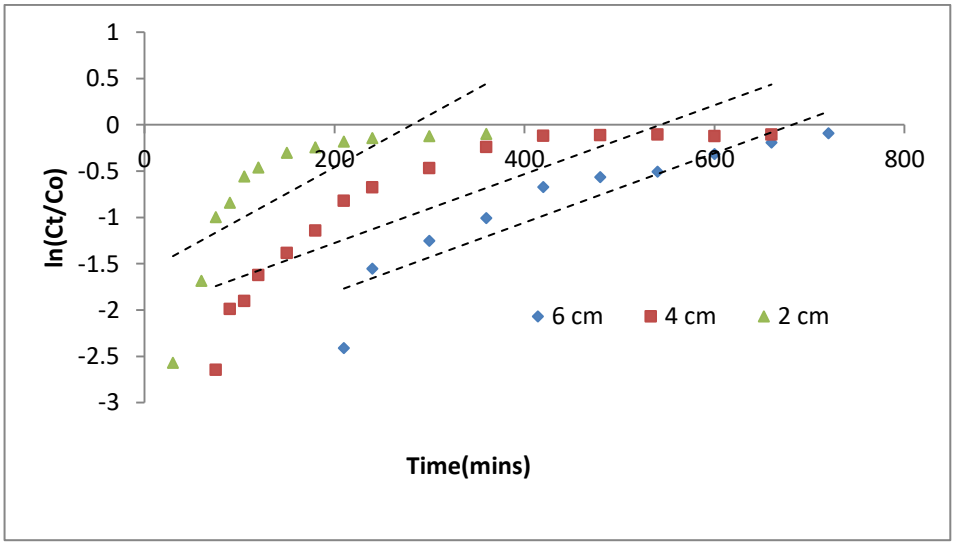

Figure 4.34: Linear regression analysis for breakthrough curve modelling by Adam-Bohart model at different bed depth.

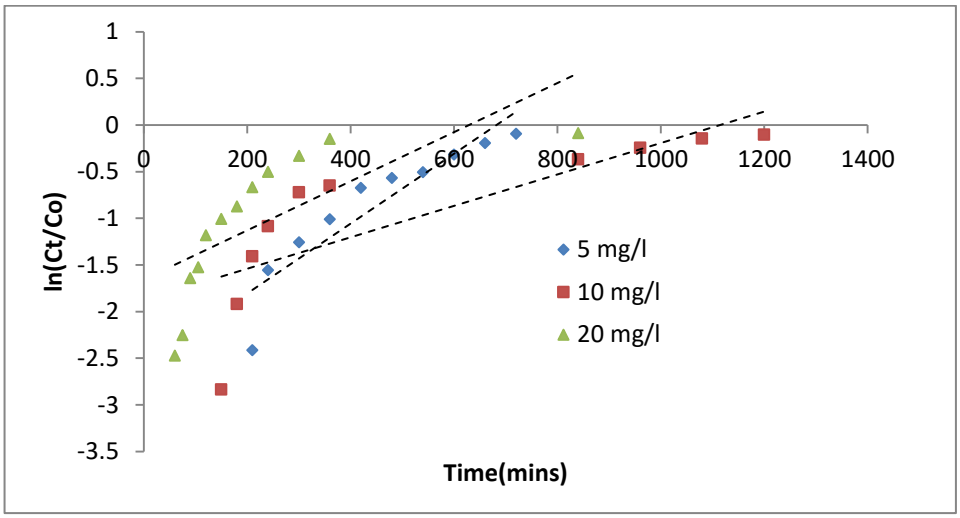

Figure 4.35: Linear regression analysis for breakthrough curve modelling by Adam-Bohart model at different initial concentration.

Table 4.10: Adams –Bohart parameters for chromium removal at different conditions using linear regression analysis

Q(cm3/min)	Z(cm)	Co (mg/l)	K_{AB} (l/min.mg)	No. (mg/l)	R^2
3	6	5	0.00074	977	0.851
3	4	5	0.00070	1159	0.762
3	2	5	0.00112	1203	0.570
3	6	5	0.00074	977	0.851
3	6	10	0.00017	3128	0.627
3	6	20	0.00013	3608	0.513
3	6	5	0.00074	977	0.85
5	6	5	0.00070	711	0.856
7	6	5	0.00132	421	0.573

(ii) Break through Curve analysis using the Thomas model

The experimental data were fitted with the linear form of the Thomas model, Eq.3.16 and 3.17. The constants K_{th} and q_e were calculated from the slope and intercepts of linear plot of ln (C_o/C_t -1) verse t(mins) under different operating conditions (Figure 4.36 to 4.38). The values were recorded in Table 4.11

It was observed that the adsorption capacity q_e (mg/g), increased with increase in depth and the corresponding values K_{TH} values decreased. This is because at higher bed heights, more reactive bed sites are available. As the concentration of metal increased qe increased and the corresponding K_{TH} decreased. This is because with increase in concentration, the driving force for adsorption increased.

From Table 4.11 it can be shown that the experimental adsorption capacities and the adsorption capacities determined using Thomas model were close an indication that the model can be used to describe the experimental data.

Overall regression coefficient R^2 determined by Thomas model demonstrated the absence of axial dispersion where the rate limiting step was not predominated by external and internal diffusion according to (Ahmad & Hameed , 2010).Similar results were reported by (Baral *et al.*, 2009) whereby Adsorption capacity of chromium unto activated weed increased with incease in initial concentration and depth.

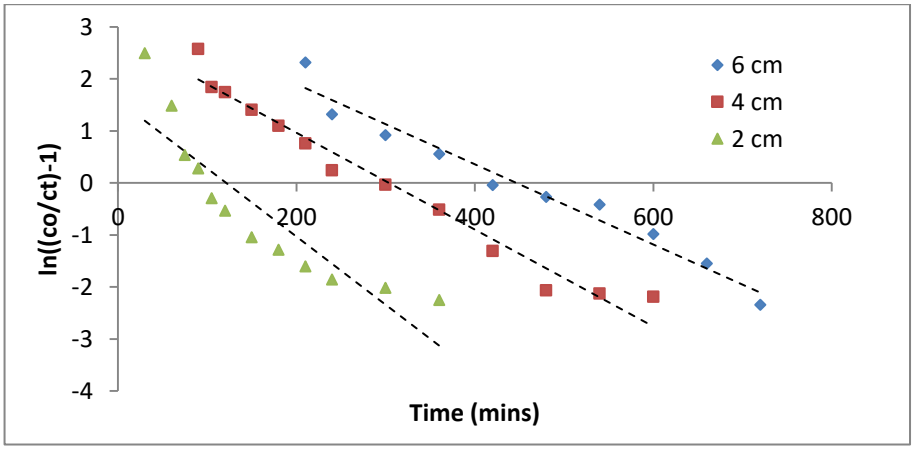

Figure 4.36: Linear regression analysis for breakthrough curve modelling by Thomas at different bed depth.

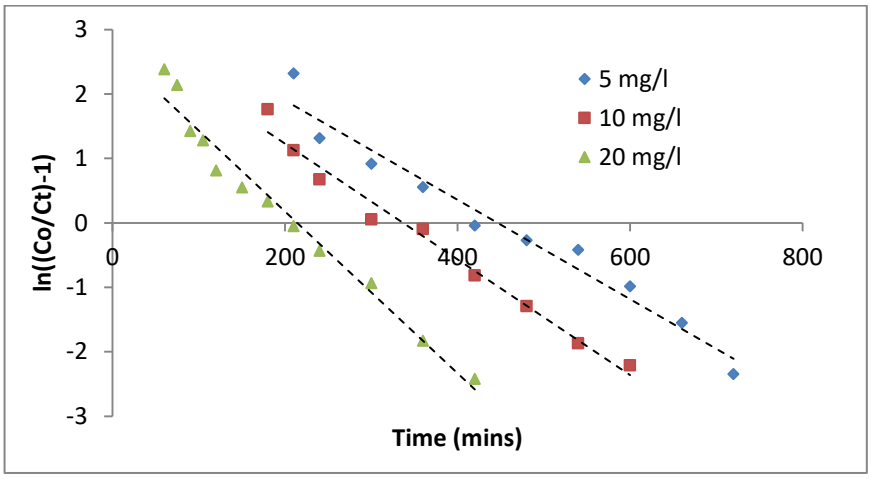

Figure 4.37: Linear regression analysis for breakthrough curve modelling by Thomas at different initial concentration.

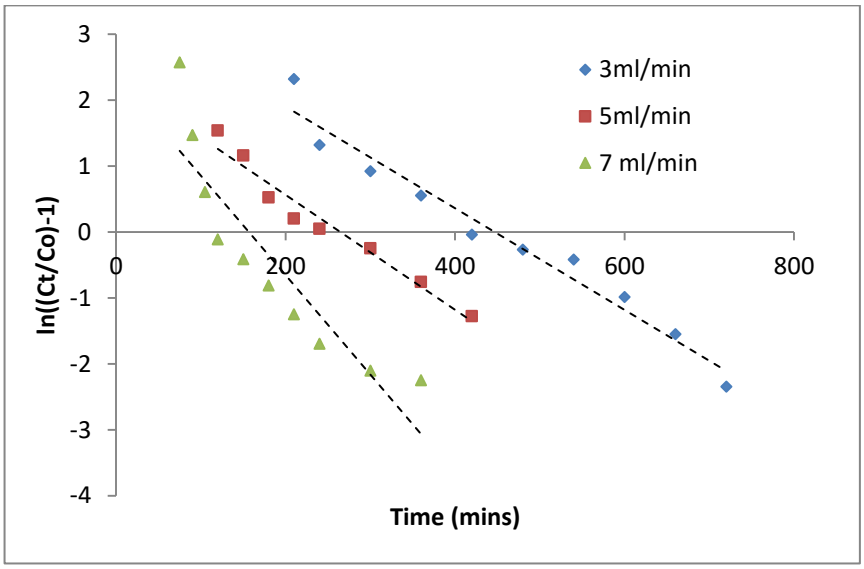

Figure 4.38: Linear regression analysis for breakthrough curve modelling by Thomas at different flow rates.

Table 4.11: Thomas model parameters for chromium removal at different conditions using linear regression analysis

Depth (cm)	Flow (Q) rate (ml/min)	Initial conc. (Co) (mg/l)	K_{th} (l/min.mg)	$qe_{(cal)}$ (mg/g)	R^2	$qe_{(exp)}$ (mg/g)
6	3.00	5.00	1.54	1.22	0.9637	1.21
4	3.00	5.00	2.00	1.13	0.9677	1.12
2	3.00	5.00	2.62	1.09	0.8081	1.10
6	3.00	10.00	0.90	1.82	0.9792	1.87
6	3.00	20.00	0.65	2.25	0.8081	2.36
6	3.00	5.00	1.54	1.22	0.9569	1.21
6	5.00	5.00	1.80	1.16	0.9569	1.18
6	7.00	5.00	3.00	0.99	0.8198	1.06

(iii) Break through Curve analysis using the Yoon-nelson model

The Yoon-Nelson model, Equation 3.18 and 3.19 were used for data fitting. The values of K_{YN} and τ were calculated from the linear plot of ln (Ct/(Co-Ct)) verses time(mins) at different flow rates, bed heights and initial concentration (Figure 4.39 to 4.41). The values of K_{YN} and τ for 50 % break through time (mins) are listed in Table 4.12.

It was observed that K_{YN} increased with decrease in depth and increase in flow rate, but reduced with increase in initial concentration. 50% break through time decreased with increase in flow rate, initial concentration and decrease in bed height. Similar results were reported by (Ahmad & Hameed , 2010). As the initial concentration increased the column got saturated faster as was reported by (Calero *et al*, 2009).The calculated half time were found to be close to the experimental half time (Table 4.12)

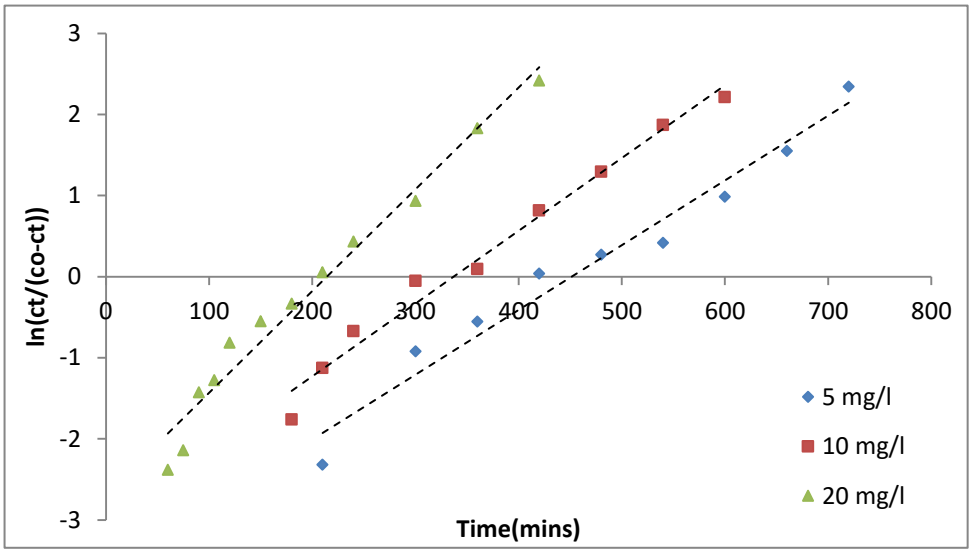

Figure 4.39: Linear regression analysis for breakthrough curve modelling by Yoon Nelson model at different initial concentration.

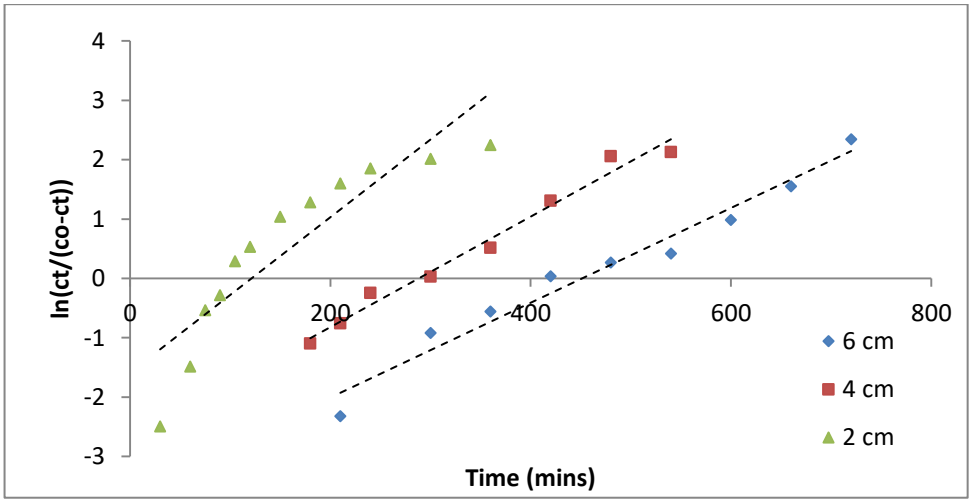

Figure 4.40: Linear regression analysis for breakthrough curve modelling by Yoon Nelson model at different bed depth.

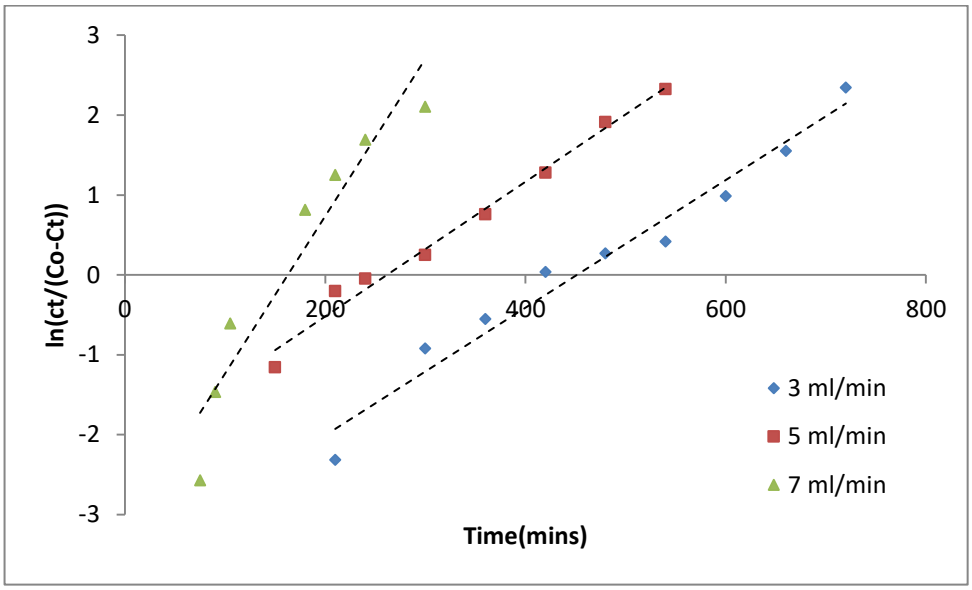

Figure 4.41: Linear regression analysis for breakthrough curve modelling by Yoon Nelson model at different flow rates

Table 4.12: Yoon-Nelson parameters for chromium removal at different conditions using linear regression analysis

Depth (cm)	Q (ml/mim)	Co (mg/l)	K_{YN} (mins-1)	τ_{cal}.(mins)	R^2	τ_{exp}.(mins)
6	3	5	0.008	450	0.9654	420
4	3	5	0.009	288	0.9803	300
2	3	5	0.013	121	0.8081	90
6	3	5	0.008	450	0.9654	420
6	3	10	0.009	336	0.981	360
6	3	20	0.013	214	0.9728	210
6	3	5	0.008	450	0.9654	420
6	5	5	0.008	262	0.9854	300
6	7	5	0.019	162	0.9073	161

It was therefore concluded that Thomas and Yoon Nelson models can be applied to predict the breakthrough curves, hence suitable for banana pith column design

To validate the Yoon Nelson model, the calculated values of K_{YN} and τ were used to regenerate the breakthrough curves for the different initial concentration. For this purpose, the Yoon-Nelson model equation was rearranged as follows

$$\frac{C_t}{C_o} = \frac{1}{1+e^{K_{YN}(\tau - t)}} \qquad (4.8)$$

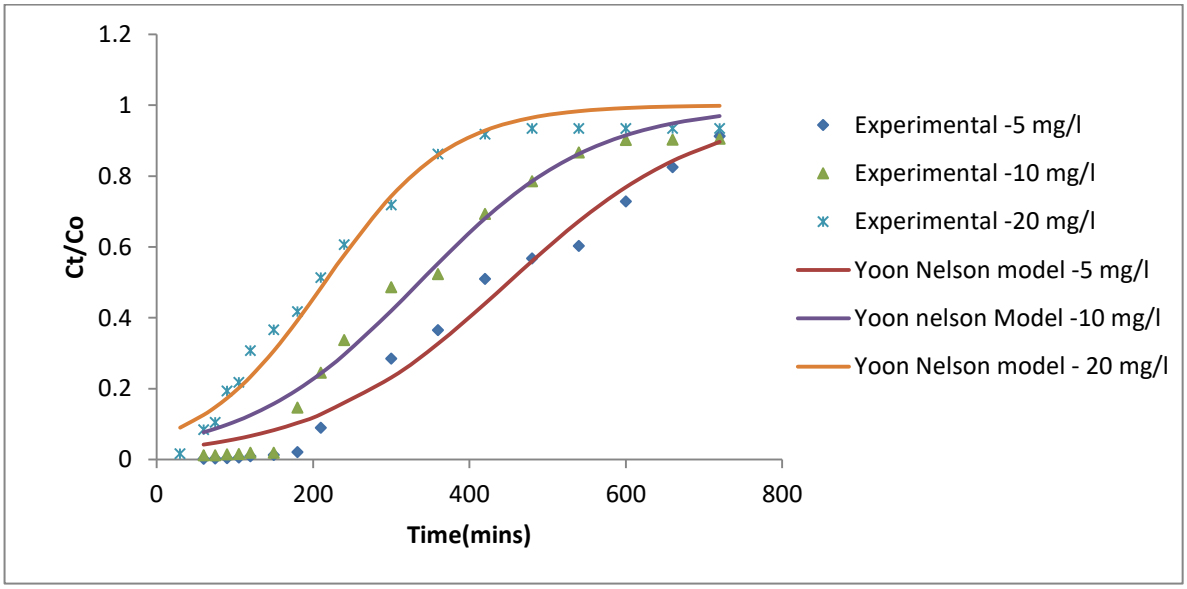

Figure 4.42: Comparison of experimental and Yoon-Nelson modelled breakthrough curves.

The breakthrough curves predicted based on Equation 4.8 is also shown in Figure 4.42(solid lines). There is a good agreement between experimental data and the model calculations.

4.3 Bio-coagulant Treatment of Surface Water (Nairobi River)

The performance of three plant coagulants namely Banana pith, Maerua Decumbent and Opuntia Spp. were investigated for removal of contaminants from polluted surface water (Nairobi River). The treatment using the bio-coagulants was monitored in terms of turbidity and heavy metal removal.

4.3.1. Quality of Nairobi river water.

The water samples for treatment were obtained along Nairobi River, at Ruai (SP) by-pass junction (Figure 3.3). The characteristic of the River water was determined and the results are shown in Table 4.13. The observed levels of contaminants in Nairobi River indicate that the River did not meet the quality requirement for a source of drinking water in Kenya (EMCR, 2006).

Table 4.13: Characteristic of raw Nairobi River water before treatment

Parameter	Mean Values	Allowable limits (KEBBS)s
Turbidity (NTU)	279	5
COD (mg/l)	160	-
Suspended solids (mg/l)	252	Nil
Nitrates (mg/l)	2662	10
Copper (mg/l)	0.149	0.1
Chromium (mg/l)	0.323	0.05
Iron (mg/l)	19.22	0.3
Zinc (mg/l)	0.63	5
Lead (mg/l)	0.194	0.05
Manganese (mg/l)	4.32	0.1

4.3.2 Performance of Banana pith (Bp), Maerua Decumbent (MD) and Opuntia Spp.(C) as coagulant for River water treatment.

(i) Turbidity removal

a) Effects of pH of solution on the removal of turbidity using the bio-coagulants.

The removal of turbidity was found to be greatest at acidic condition (Figure 4.43, 4.45 and 4.47). The significant effectiveness of banana pith, Maerua Decumbent and Opuntia Spp. coagulant at acidic pH may be attributed to the protonation of some of the functional groups such as amino and carboxyl resulting in high positive charge density that exerts strong electrostatic forces over negatively charged colloidal matter (Aparecido, Fernado, Claudinata, & Diego, 2015).

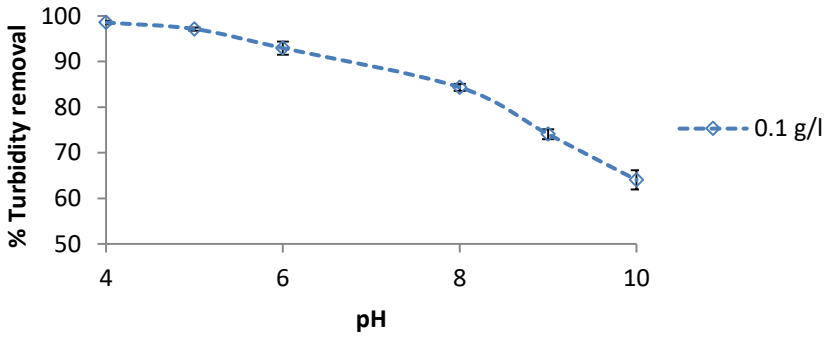

Figure 4.43: Effects of pH on turbidity removal using 0.1 g/l of banana pith at 30 minutes of settling.

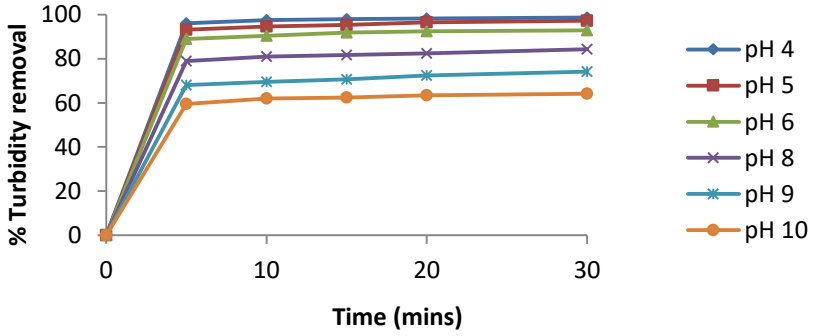

Figure 4.44: Effects of varied pH and settling time on turbidity removal using 0.1 g/l of banana pith

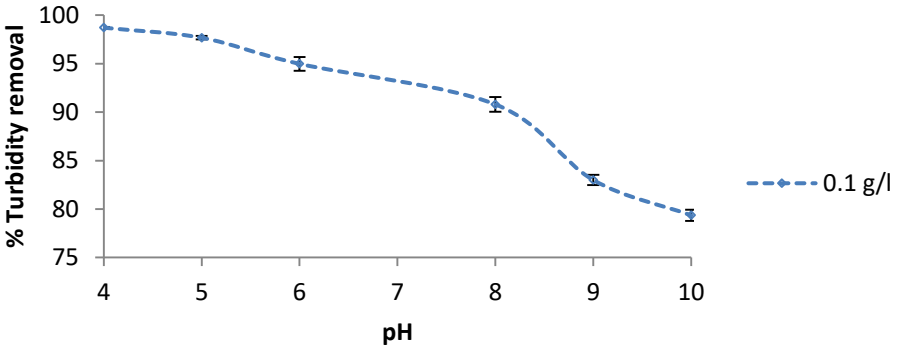

Figure 4.45: Effects of pH on turbidity removal using 0.1 g/l of Maerua Decumbent at 30 minutes of settling.

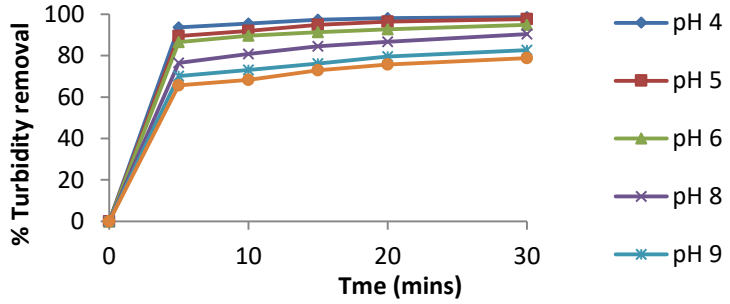

Figure 4.46: Effect of varied pH and settling time on turbidity removal using 0.1 g/l of Maerua Decumbent

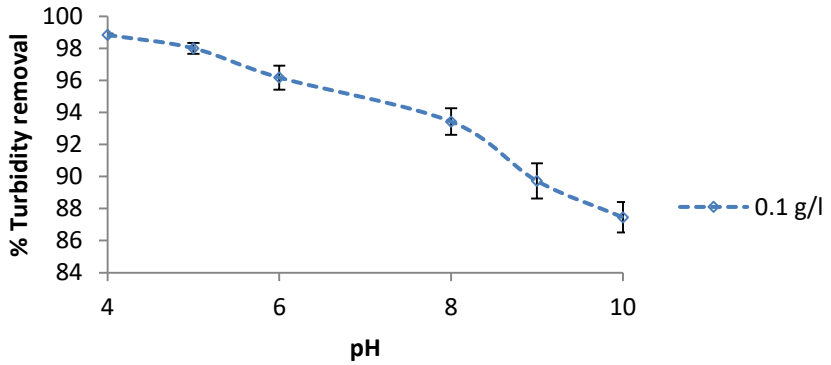

Figure 4.47: Effects of pH on turbidity removal using 0.1 g/l of Opuntia Spp. at 30 minutes of settling.

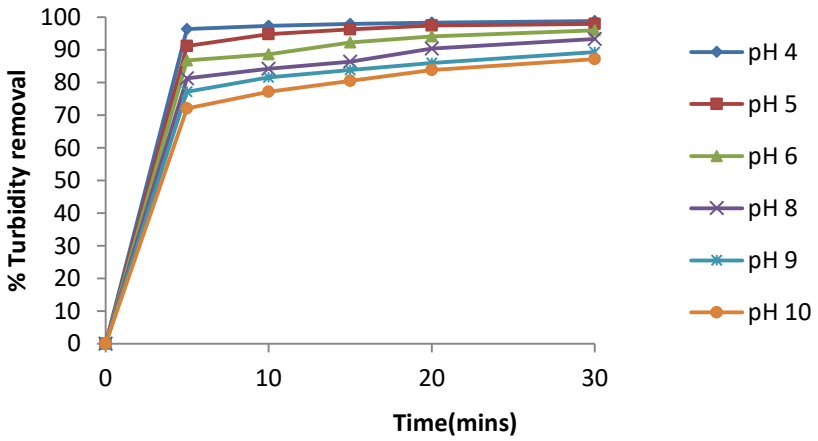

Figure 4.48: Effect of varied pH and settling time on turbidity removal using 0.1 g/l of Opuntia spp.

b) Effects of varied dosages of the coagulants on the removal of turbidity from River water

The maximum efficiency of suspended solids removal from the initial 270 NTU was obtained as over 98 % with 0.1 g/l of all of the three bio-coagulants. Significant treatment was observed between 0.1 g/l dosage and the other dosages according to the error bars. The lowest treatment was observed as 93, 91 and 94 % at a dosage of 1 g/l when using banana pith, Maerua Decumbent and Opuntia Spp. respectively (Figures 4.49, 4.51 and 4.53). Smaller coagulant dosages were marginally more effective than larger ones, which may be attributed to high charge density of the coagulant whereby lesser dosages are sufficient for destabilization of suspended particles (Ahmad, Sumathi, & Hameed, 2006; Ariffin *et al*., 2005) and larger one's cause interferences.

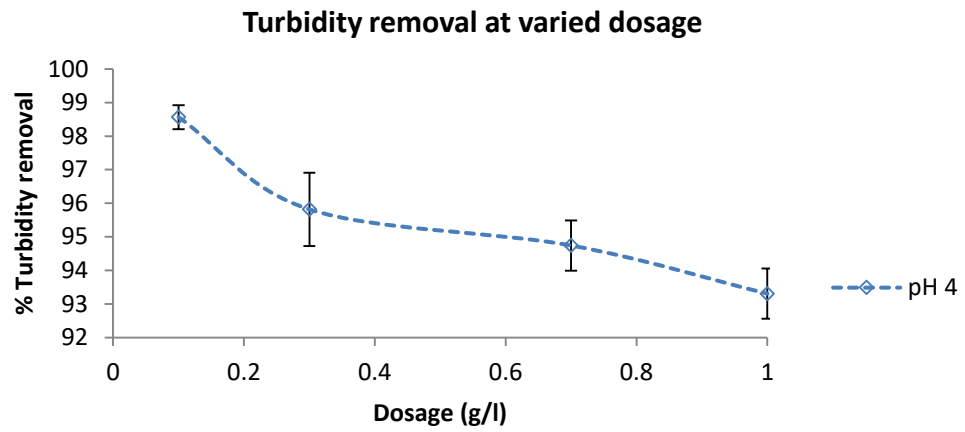

Figure 4.49: Effects of varied dosage at pH 4 to turbidity removal using banana pith at 30 minutes of settling.

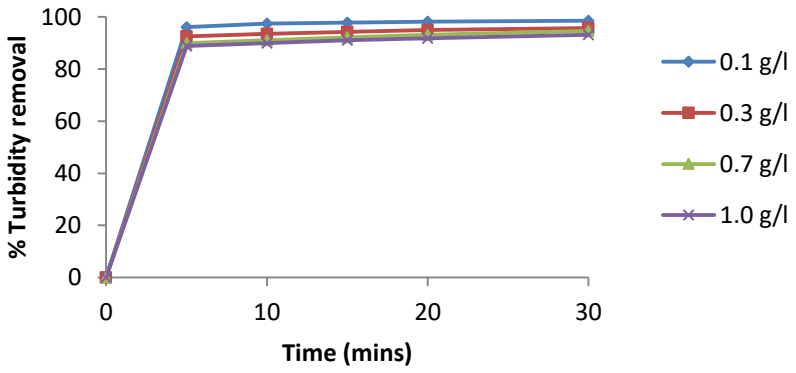

Figure 4.50: Effects of varied dosage and time on turbidity removal at pH 4 using banana pith.

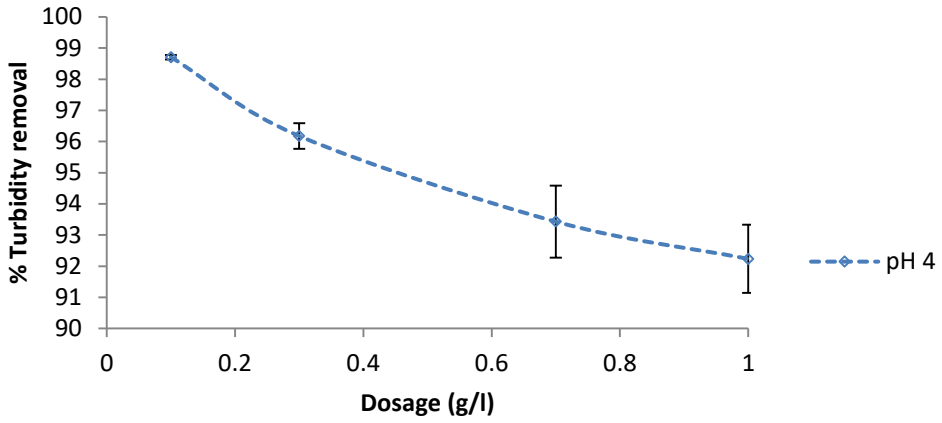

Figure 4.51: Effects of varied dosage at pH 4 to turbidity removal using Maerua Decumbent at 30 minutes of settling.

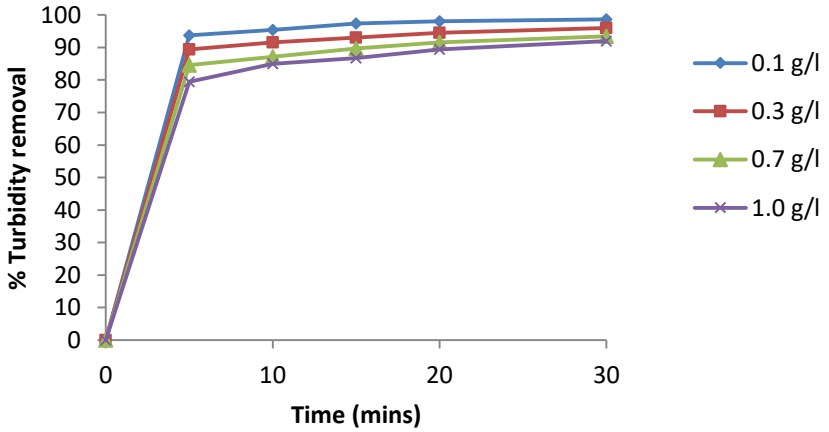

Figure 4.52: Effects of varied dosage and time on turbidity removal at pH 4 using Maerua Decumbent

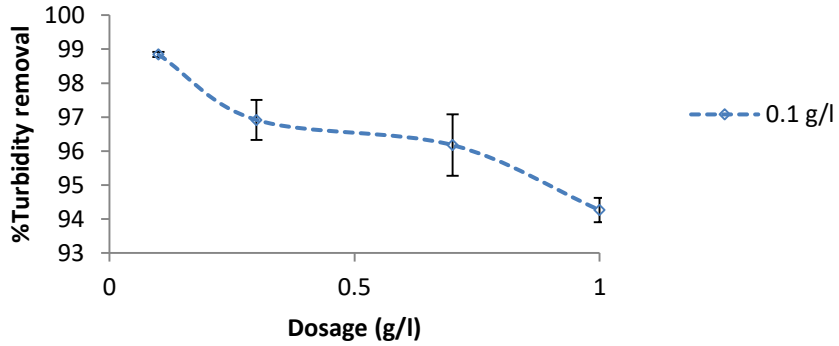

Figure 4.53. Effects of varied dosage at pH 4 to turbidity removal using Opuntia Spp. at 30 minutes of settling

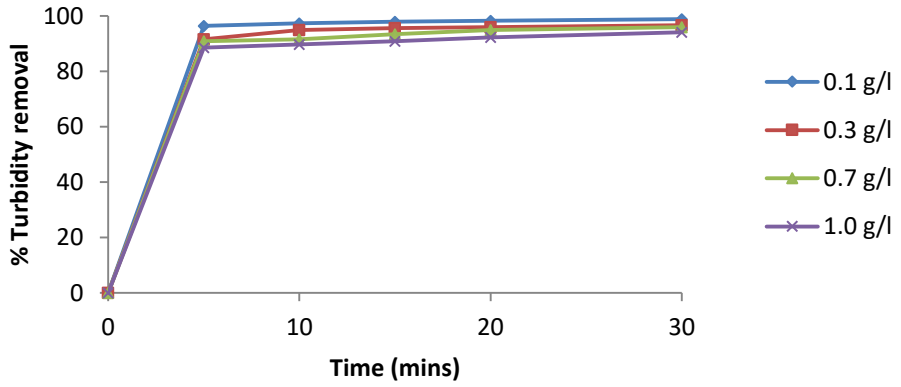

Figure 4.54: Effects of varied dosage and time on turbidity removal at pH 4 using Opuntia Spp.

c) Effects of settling time on the turbidity removal using Banana pith, Maerua decumbent and Opuntia Spp.as coagulant.

Turbidity removal efficiency increased rapidly to over 50% within 5 minutes of settling time for all pH (Figures 4.44, 4.46 and 4.48) and coagulant dosages (Figures 4.50, 4.52 and 4.54) and then gradually but relatively uniformly up to 30 minutes settling time. The initial rapid increase in efficiency reflects the fast settling of heavy

particles. The following gradual but uniform increase in efficiency represents continued flocculation that reduced the number colloidal particles (Yates et al., 2001).

d) Effects of size of particle in turbidity removal

Performances of various sizes of the coagulants were evaluated (Figure 4.55). It was established that the particle size 0.4 mm gave a better turbidity removal. The smaller the size of bio-coagulant particles the larger the amount of dissolved active compounds (Hendrawati *et al.*, 2015). Similar results were reported by (Muthuraman et al., 2013).They found that 0.4 mm size of a bio-coagulant was effective in removal of turbidity from water.

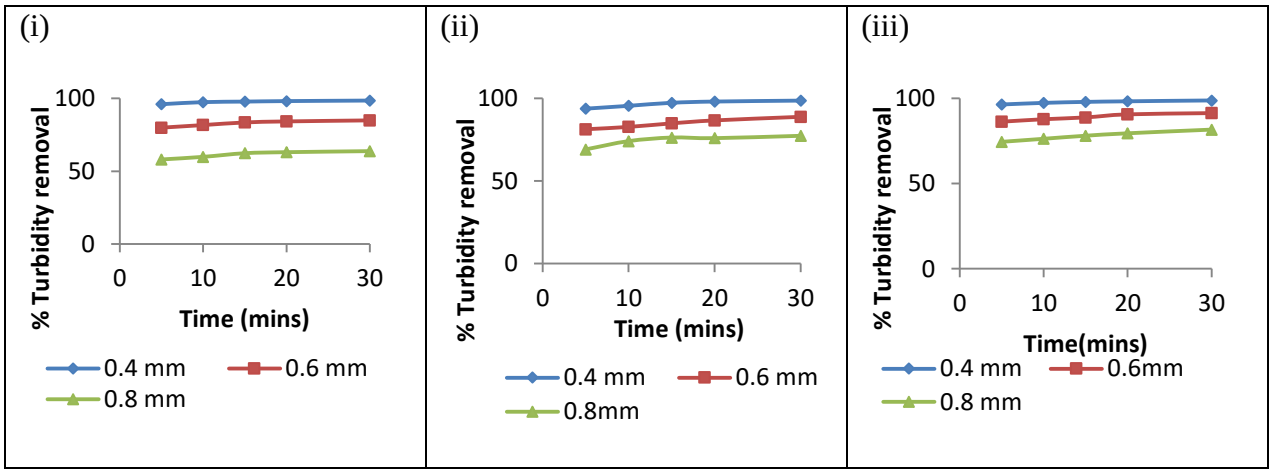

Figure 4.55: Effects of different particle size at pH 4 and 0.1 g/l dosage of Banana pith (i), Maerua Decumbent (ii) and Opuntia Spp. (iii)

(ii) Heavy metal removal

During the coagulation and flocculation process banana pith was able to remove upto 100 % of copper and lead, across all pH values and dosages. Chromium removal of 100 % was also achieved at acidic condition for all dosages and at alkaline conditions at banana pith dosage of above 0.7 g/l. The removal of iron ranged between 90-100 % across all the pH values and dosages. The removal of zinc and manganese increased with increase in dosage and pH. Highest zinc removal (98 %) and Manganese (99%) were achieved at pH 9 and banana pith dosage of 0.7 g/l (Figure 4.56).

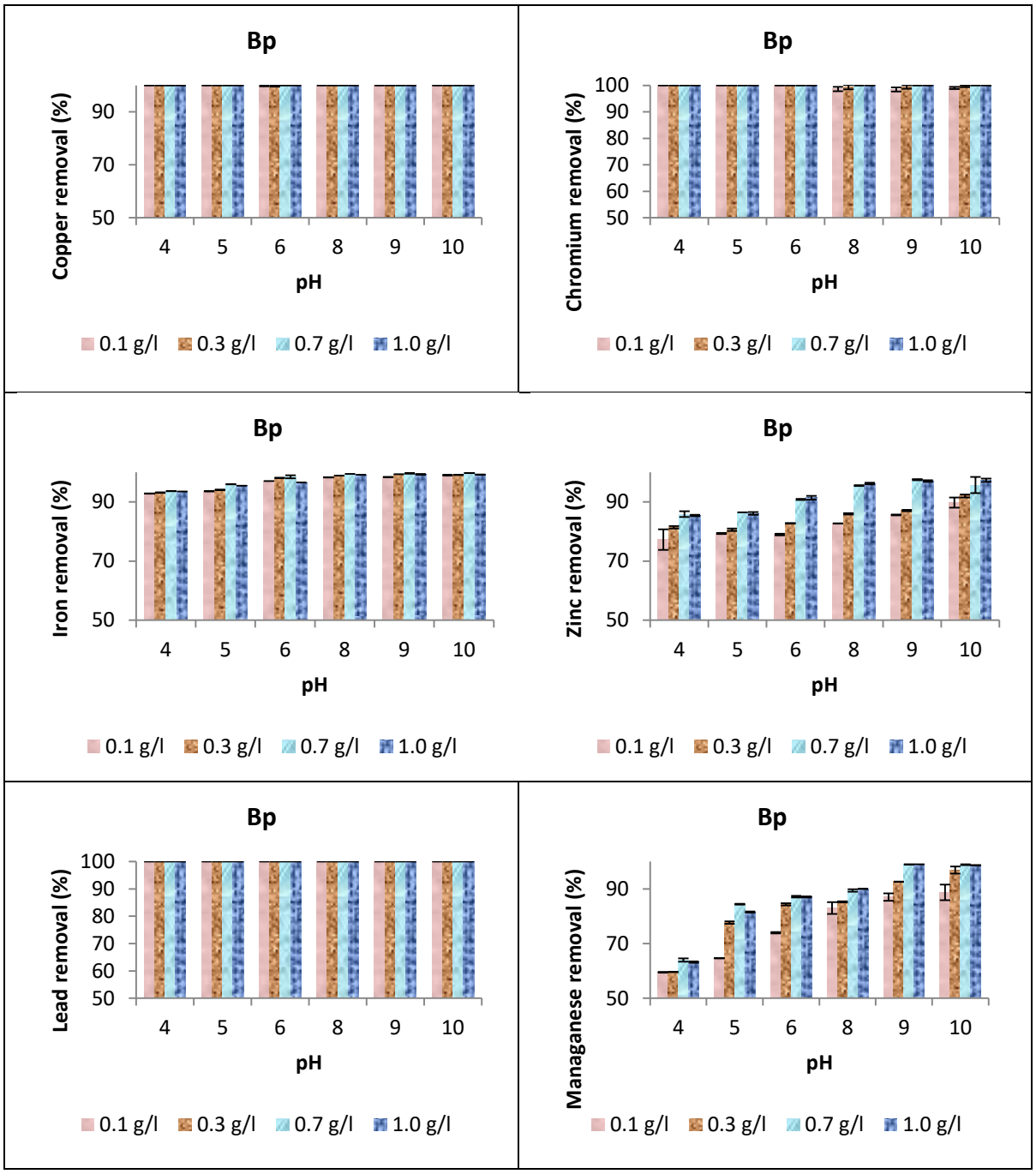

Figure 4.56: Heavy metal removal using banana pith as a coagulant at varied pH and dosage.

The use of Maerua Decumbent for River water treatment through coagulation and flocculation achieved over 90 % copper removal, 100% chromium and lead removal across all pH values. For the iron metal, 100% removal was achieved at alkaline conditions and over 90 % at acidic conditions. The removal of zinc varied between 50 and 90 % in acidic condition and between 90 and 100 % removal at alkaline conditions. The highest removal of manganese (97%) was achieved at pH 6. In the case of zinc and manganese the highest removals were achieved at 0.7 g/l dosages (Figure 4.57).

The use of Opuntia Spp. as a coagulant for River water treatment resulted in 100 % removal of lead metal across all the pH and dosages. The removal of copper ranged between 80-90% whereas for removal for chromium ranged from 90 to 100 % across all the pH and dosage value. The removal of zinc using Opuntia Spp. was found to range between 50-80 % for acidic condition and between 90-100 % for alkaline condition. The removal of manganese in acidic conditions ranged between 50-70% and 70-80% in alkaline conditions. For copper, zinc and manganese highest removal was achieved at 0.3 g/l of Opuntia Spp. (Figure 4.58)

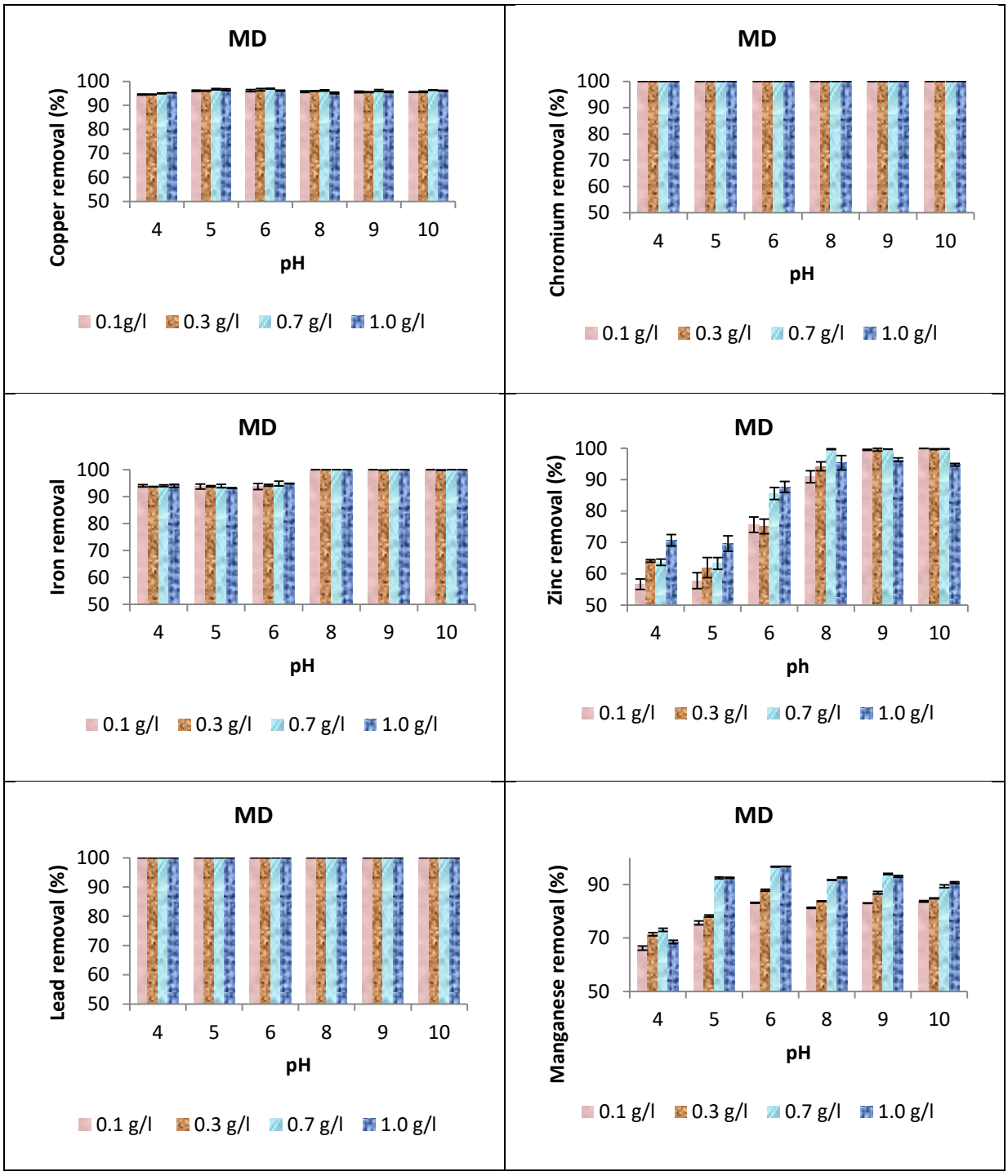

Figure 4.57: Heavy metal removal using Maerua Decumbent as a coagulant at varied pH and dosage.

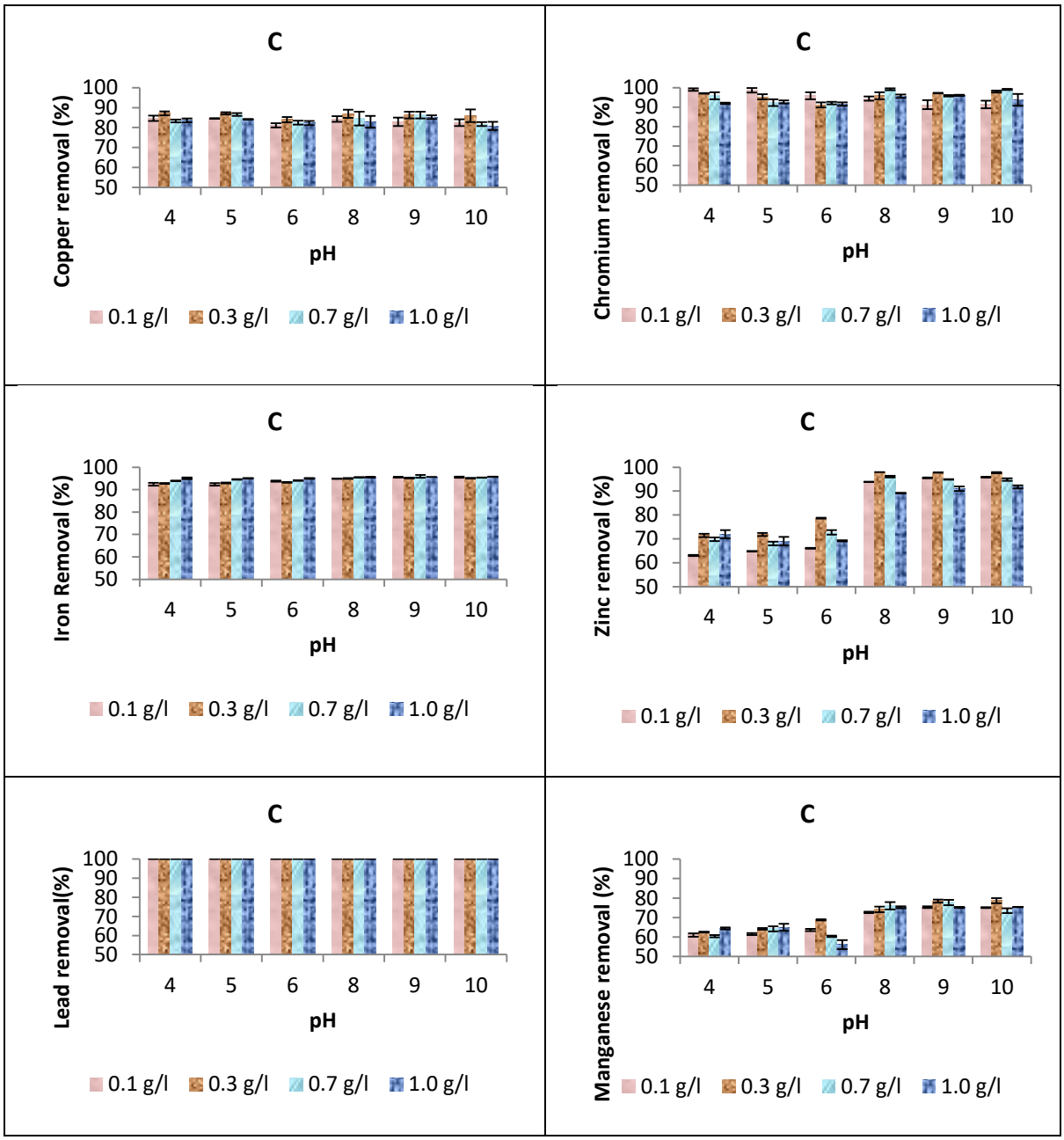

Figure 4.58: Heavy metal removal using Opuntia Spp. as a coagulant at varied pH and dosage

The removal of pollutants using coagulation-flocculation is a complex reaction process which can be brought about by one and/or any of the following mechanisms: Adsorption and charge neutralization, adsorption inter-particle bridging, or enmeshment in a precipitate (Duan & Gregory, 2003; Renault F. , Sancey, Badot, & Crini, 2009).

Banana pith, Maerua decumbent and Opuntia Spp. were found to contain functional groups such as carboxyl, hydroxyl, amino acids, aldehydes, phenols among others. The removal of heavy metal in the low pH is attributed to the fact that some of the functional groups bear negative surface charges under acidic conditions according to (Bustillos *et al*., 2013). While the removal of the heavy metal at higher pH is attributed to formation of the metal precipitate or enmeshment of the heavy metal by the precipitate especially at higher dosages according to (Fedala *et al.,* 2015; Miller et al., 2008)

The use of bio-coagulants for heavy metal removal was reported by Ravikumar & Sheeja, (2013) who found that Moringa Oliefera coagulant was able to remove 95% of copper, 93% of lead, 76 % of cadmium and 70% of chromium. Report by Ali H. G., (2017) indicated that a natural coagulant removed over 98% of lead and Shilpaa et al., (2012) found that a natural coagulant, Opuntia Ficus Indica removed over 65 % of nickel and chromium. Studies by Saidu.*et al*, (2006), found that Moringa Oleifera removal of lead, iron, and cadmium in the range of 70.86-89.4, 66.33-92.14, 44.95-47.73%, respectively whereas Vikashni et al., (2012), found that Moringa seeds removed 90, 80, 60, 50 and 50% of copper, lead, cadmium, zinc and chromium respectively.

4.3.3 Performance comparison between Natural coagulants and Aluminium sulphate.

The performance of the bio-coagulants including, banana pith, Maerua Decumbent and Opuntia Spp. were compared with that of aluminium sulphate. The comparison was carried out at the best turbidity removal dosage of 0.1 g/l and pH of 4 for the bio-coagulants and aluminium sulphate dosage of 0.1 g/l at pH 7. The results (Table 4.14) indicate that the results obtained from the natural coagulant were comparable to those obtained from the use of aluminium sulphate.

The three bio-coagulants were found to reduce turbidity, copper, chromium, zinc and lead to KEBBS standard levels. It was therefore concluded that the natural coagulants have potential in surface water treatment and are a viable alternative to conventional coagulant aluminium sulphate.

Table 4.14: Comparison of natural coagulants verses aluminium sulphate.

Parameter	Raw Water	Treated with Banana pith	Treated with Maerua	Treated with Opuntia Spp.	Treated with Alum	KEBBS Standards
Turbidity (NTU)	279	4.00	3.60	3.20	2.60	5
COD (mg/l)	160	73.00	67.00	54.00	43.00	-
Suspended solids (mg/l)	252	10.00	5.00	6.00	3.00	Nil
Nitrates (mg/l)	2662	299.9	325.00	315.00	305.00	10
Copper (mg/l)	0.149	ND	0.008	0.025	ND	0.1
Chromium (mg/l)	0.323	ND	ND	0.001	ND	0.05
Iron (mg/l)	19.22	1.37	1.21	1.559	2.84	0.3
Zinc (mg/l)	0.63	0.12	0.27	0.222	0.15	5
Lead (mg/l)	0.194	ND	ND	ND	ND	0.05
Manganese (mg/l)	4.32	1.74	1.42	1.64	1.87	0.1

4.3.4 Coagulation- flocculation kinetics using bio-coagulants

The experimental data obtained from laboratory test of Banana pith, Maerua Decumbent and Opuntia spp. as coagulant for River water treatment were fitted in the kinetic equations 2.26 and 2.27 The coagulation-flocculation functional parameter determined include, the k, coagulation rate constant of the α^{th} order, correlation coefficient R^2 the Brownian aggregation collision factor, K and coagulation half time $\tau_{\frac{1}{2}}$.

The order of coagulation -flocculation process α was taken as 2 according to (Fridklisberg, 1984; Hunter, 1993).

The particle distribution in the liquid suspension during coagulation-flocculation was evaluated using equation 2.36 and the results were analyzed through graphs at the least and highest half time for the various dosages of the Banana pith, Maerua Decumbent and Opuntia Spp.

4.3.4.1 Coagulation kinetics using Banana pith, Maerua Decumbent and Opuntia Spp. at varied dosages and pH values

To evaluate the kinetics followed by the use of natural coagulants in river water treatment, a plot of the first order kinetics and second order kinetics was carried out (Figure 4.59 to 4.62 for Banana pith, Figure 4.63 to 4.66 for Maerua Decumbent and Figures 4.67 to 4.70 for Opuntia Spp.). The graph results from the three bio-coagulants indicate that that the plot of ln (Co/Ct) against time did not pass through the origin and, therefore, was inconsistent with Eq. (2.26) for first order kinetics for all the pH and dosages studied. However, the plot of 1/ct against time was in agreement with Eq. (2.27). It was therefore concluded that the coagulation-flocculation process for treatment of River water using the natural coagulants can be described best by the second order equation.

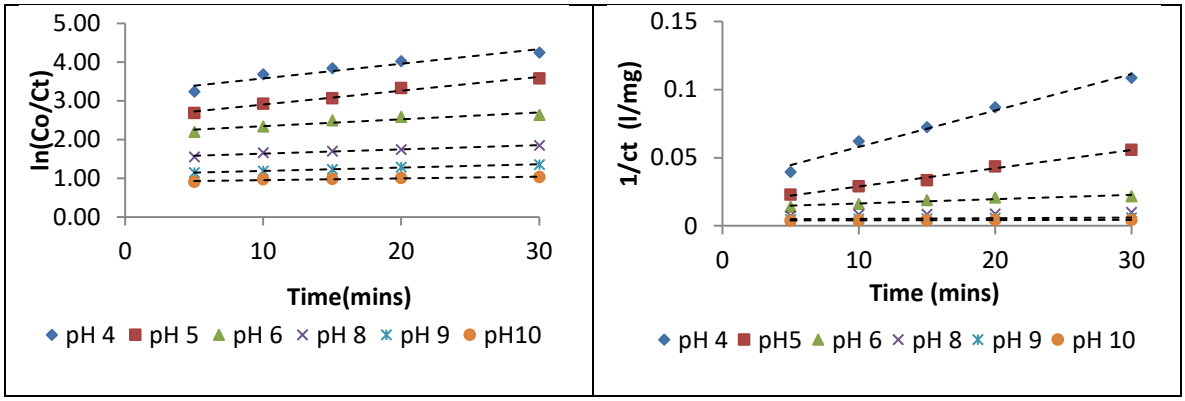

Figure 4.59: First and second order plots for banana pith dosage of 0.1 g/l at different initial pH of the River water.

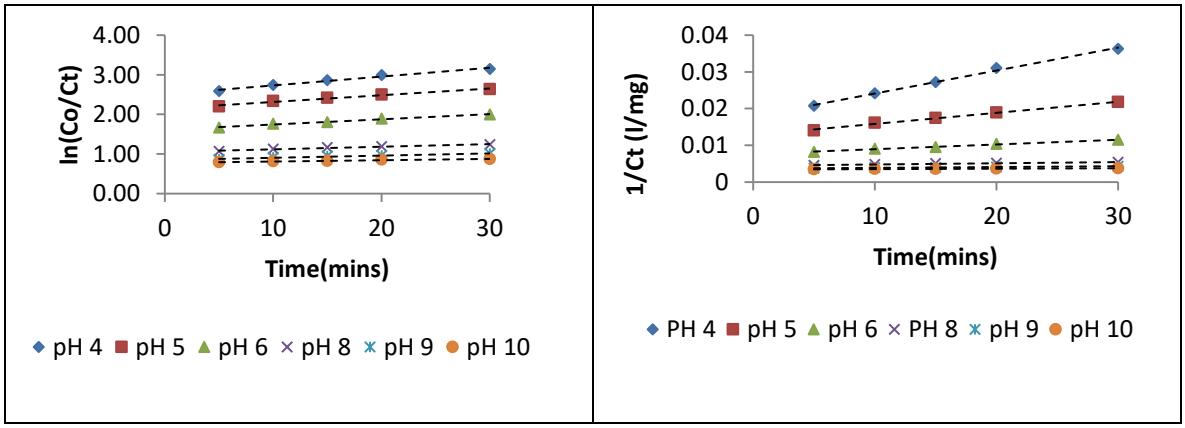

Figure 4.60: First and second order plots for banana pith dosage of 0.3 g/l at different initial pH of the River water.

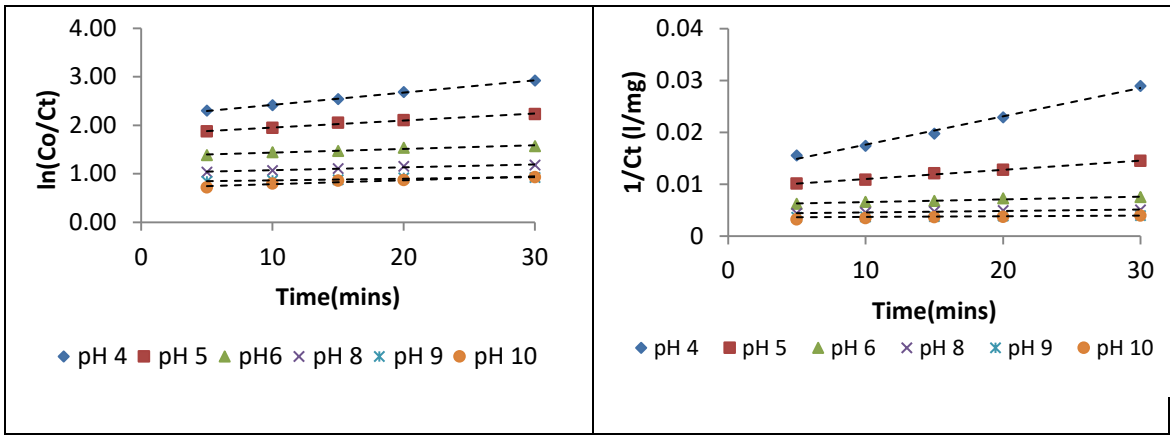

Figure 4.61: First and second order plots for banana pith dosage of 0.7 g/l at different initial pH of the River water.

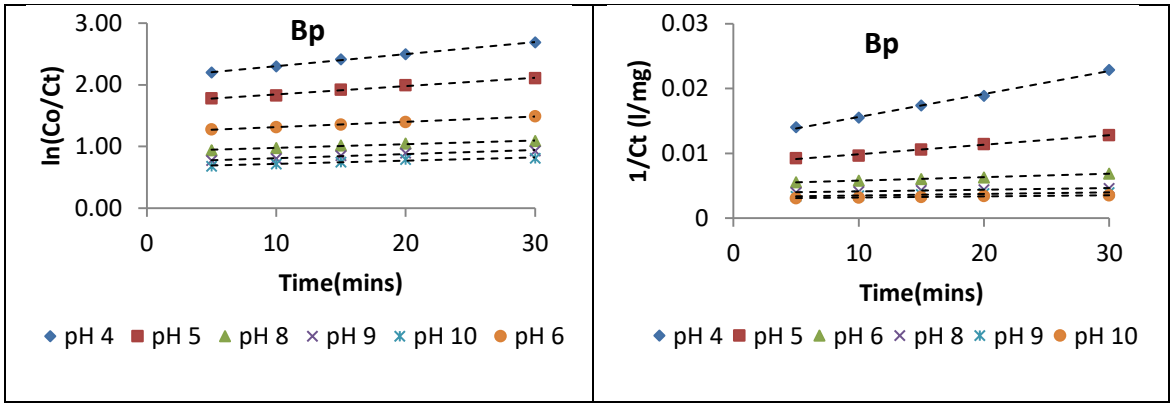

Figure 4.62: First and second order plots for banana pith dosage of 1.0 g/l at different initial pH of the River water.

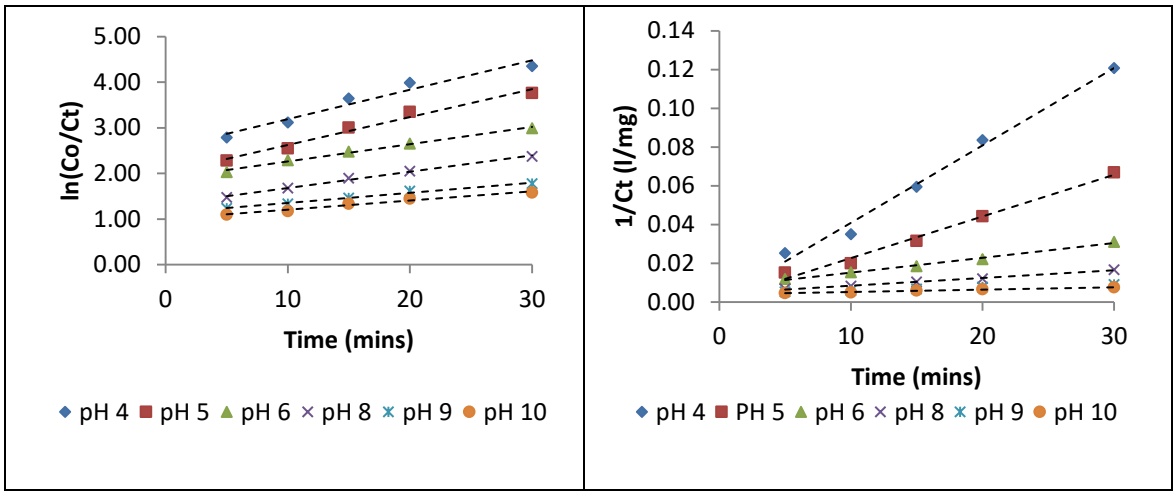

Figure 4.63: First and second order plots for Maerua Decumbent dosage of 0.1 g/l at different initial pH of the River water

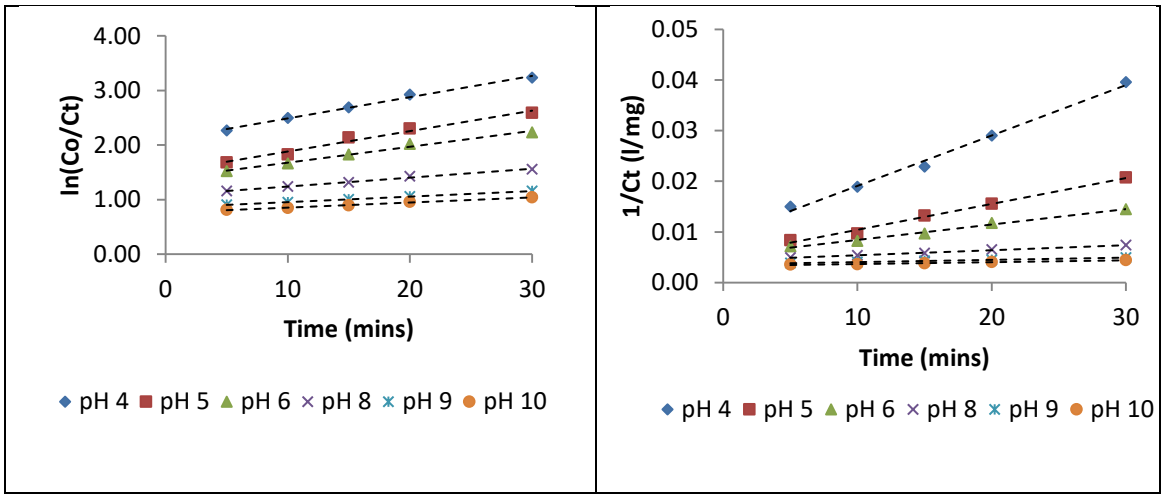

Figure 4.64: First and second order plots for Maerua Decumbent dosage of 0.3 g/l at different initial pH of the River water

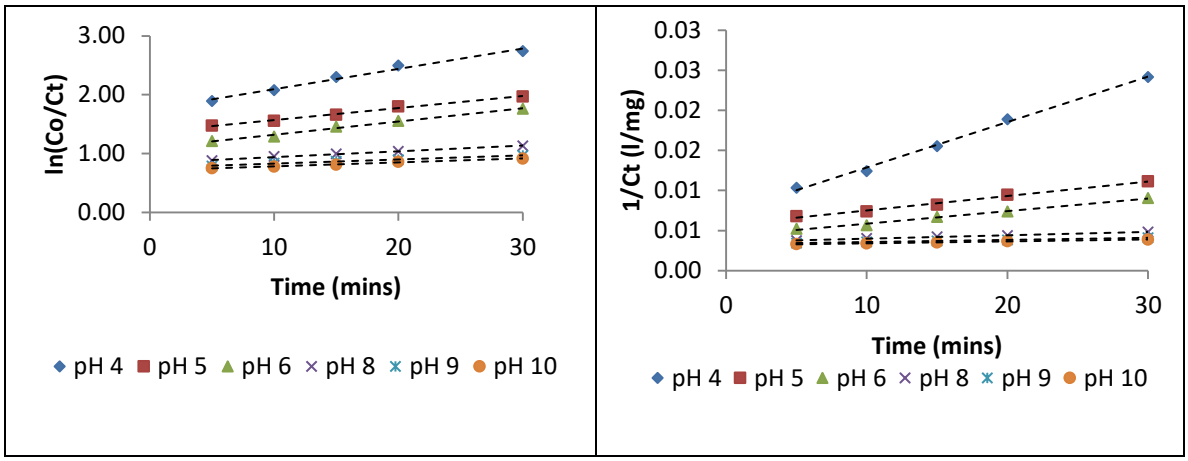

Figure 4.65: First and second order plots for Maerua Decumbent dosage of 0.7 g/l at different initial pH of the River water.

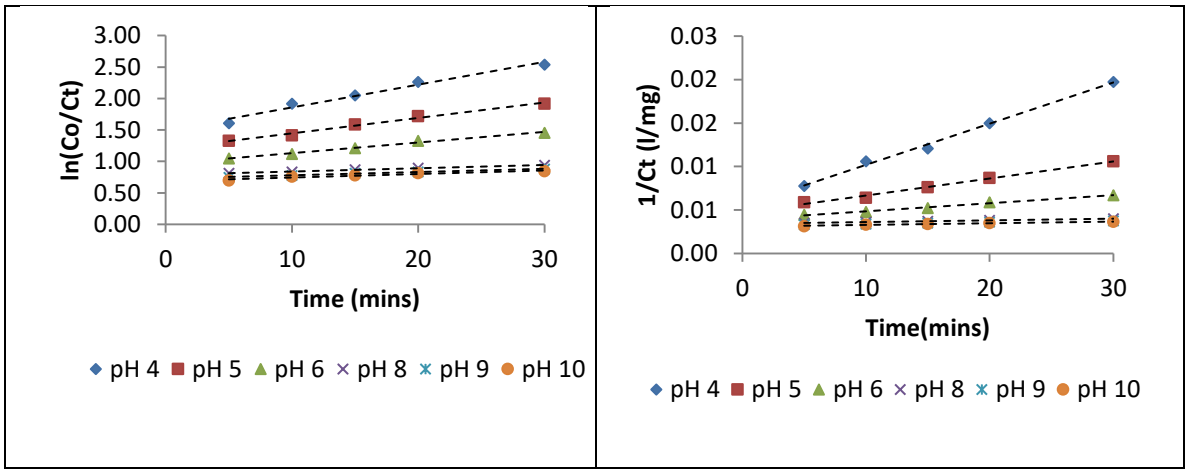

Figure 4.66: First and second order plots for Maerua Decumbent dosage of 1.0 g/l at different initial pH of the River water.

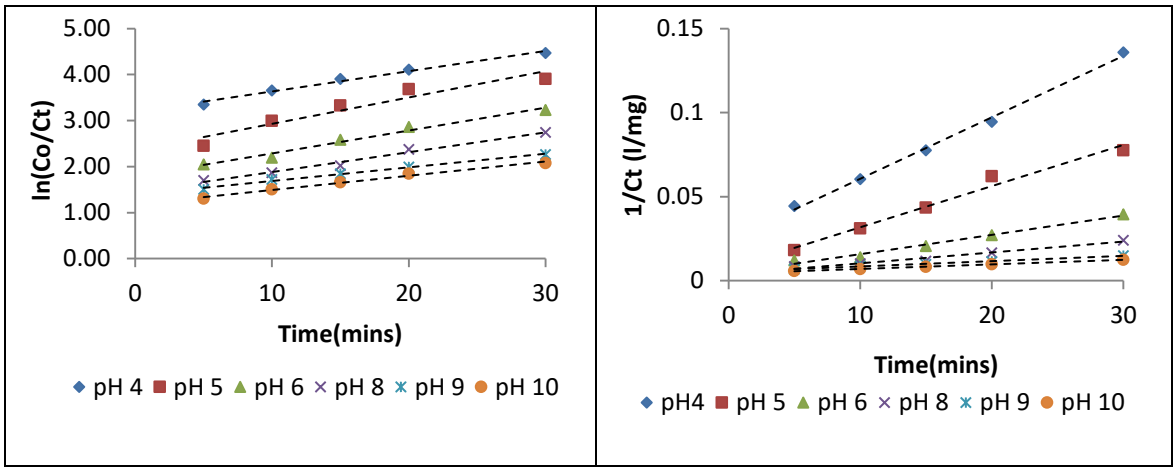

Figure 4.67: First and second order plots for Opuntia Spp. dosage of 0.1 g/l at different initial pH of the River water.

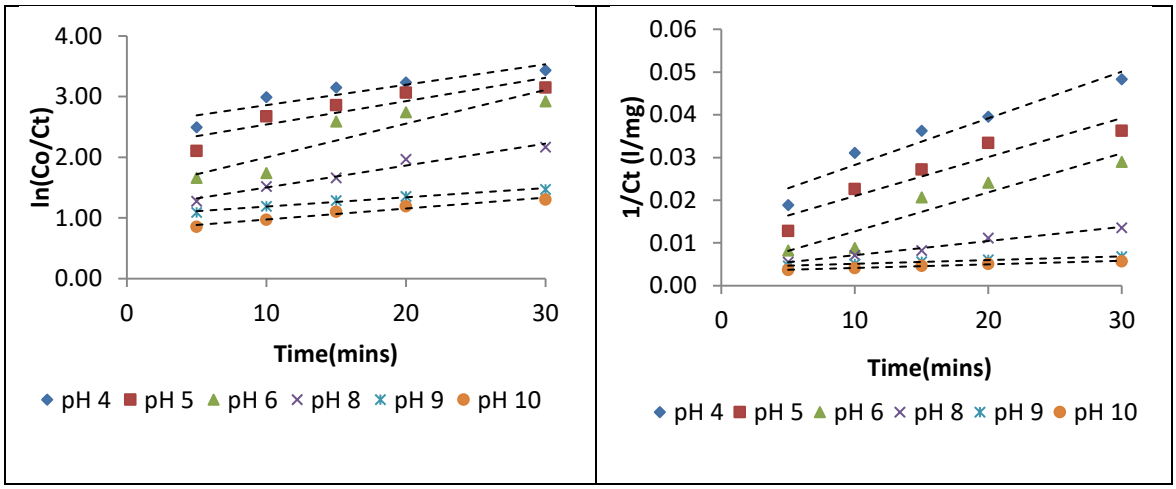

Figure 4.68: First and second order plots for Opuntia Spp. dosage of 0.3 g/l at different initial pH of the River water

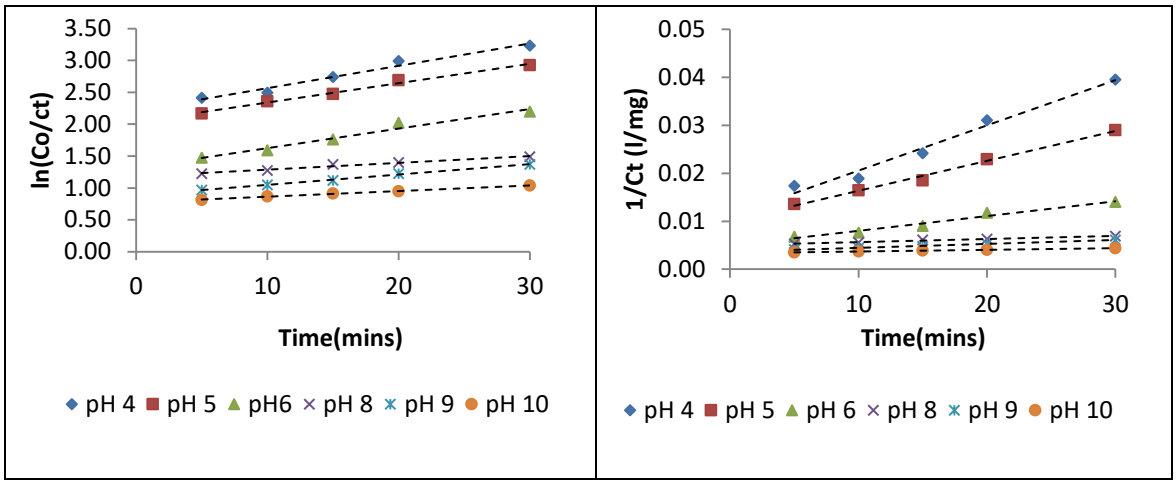

Figure 4.69: First and second order plots for Opuntia Spp. dosage of 0.7 g/l at different initial pH of the River water.

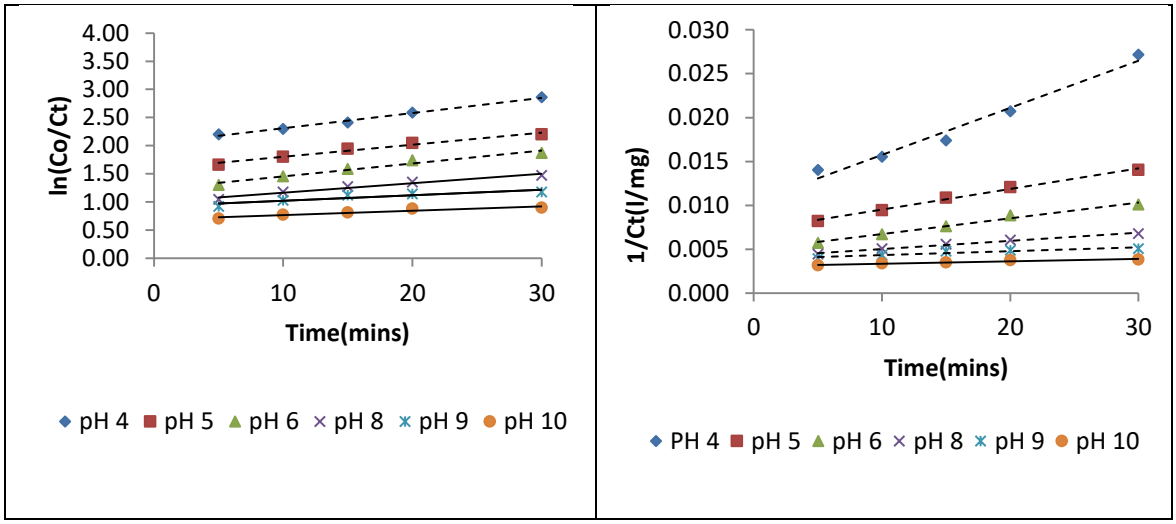

Figure 4.70: First and second order plots for Opuntia Spp. dosage of 1.0 g/l at different initial pH of the River water

The second order kinetics parameters of the coagulation/flocculation process were computed and recorded in Table 4.15, 4.16 and 4.17 for Banana pith, Maerua Decumbent and Opuntia spp. respectively. The R^2 and coagulation-flocculation rate constant *k* contained in the tables were determined from plots $1/c_t$ versus time. Low coagulation period was found to correspond to high coagulation rate constant, k = (0.5K) an indication of a relatively low repulsion and high coagulation period corresponded to low coagulation rate constant, k indicating high repulsion. The coagulation rate constant obtained from the three bio-coagulants varied with the pH of the solution. At the dosages of 0.1 g/l and pH 4 the values of coagulation time/ half-life, $\tau_{1/2}$ and coagulation rate constant, k were recorded as 1.15 mins and 0.0027 l/mg.min, 0.78 mins and 0.004 l/mg.min and 0.84 mins and 0.0037 l/mg.min for banana pith, Maerua Decumbent and Opuntia Spp. respectively. Whereas at dosages of 0.1 g/l and pH 10 the values of coagulation time and coagulation rate constant were recorded as 155.76 min and 0.00002 l/mg.min, 31.15 min and 0.0001 l/mg.min and 10.38 min and 0.0003 l/min for Banana pith, Maerua Decumbent and Opuntia Spp. Respectively (Table 4.15-4.17). The good performance of the bio-coagulants in acidic medium was attributed to existence of low repulsion and hence high attractive forces between the coagulant and the pollutant. Similar findings were reported by Menkiti and Onukwuli (2011). Increase of dosages of any of the three coagulants resulted in higher coagulation time values and low coagulation rate, consequently resulting to poor turbidity removal (Table 4.15 to 4.17). The values of R^2 were found to be equal or greater than 0.9. This result emphasizes its consistency with von Smoluchowski theory of coagulation (Babayemi, Onukwuli, & Menkiti, 2013).

Table 4.15: Functional parameters for banana pith at varied dosages and pH values

Parameters	pH					
	4	5	6	8	9	10
Dosage 0.1 g/l						
α	2	2	2	2	2	2
R^2	0.979	0.9903	0.9064	0.9781	0.9923	0.8723
k"(l/mg.min)	0.0027	0.0013	0.0003	0.00009	0.00005	0.00002
K(l/mg.min)	0.0054	0.0026	0.0006	0.00018	0.0001	0.00004
τ1/2 (mins)	1.156	2.396	10.384	34.614	62.305	155.763
Dosage 0.3g/l						
α	2	2	2	2	2	2
R^2	0.9951	0.9946	0.9903	0.9677	0.9698	0.9543
k" (l/mg.min)	0.0006	0.0003	0.0001	0.00003	0.00002	0.00002
K (l/mg.min)	0.0012	0.0006	0.0002	0.00006	0.00004	0.00004
τ1/2 (mins)	5.1921	10.3842	31.1526	103.842	155.763	155.76
Dosage 0.7 g/l						
α	2	2	2	2	2	2
R^2	0.9907	0.9952	0.9548	0.9452	0.953	0.9568
k''(l/mg.min)	0.0005	0.0002	0.00005	0.00003	0.00002	0.00002
K(l/mg.min)	0.001	0.0004	0.0001	0.00006	0.00004	0.00004
τ1/2 (mins)	6.2305	15.5763	62.3053	103.842	155.76	155.76
Dosage 1.0 g/l						
α	2	2	2	2	2	2
R^2	0.997	0.9917	0.9956	0.9834	0.9673	0.9563
K"(l/mg.min)	0.0004	0.0001	0.00005	0.00003	0.00002	0.00002
K (l/mg.min)	0.0008	0.0002	0.0001	0.00006	0.00004	0.00004
τ1/2 (mins)	7.7882	31.1526	62.3053	103.8422	155.763	155.763

Table 4.16: Functional parameters for Maerua Decumbent at varied dosages and pH values

Parameters	pH					
	4	5	6	8	9	10
Dosage 0.1 g/l						
α	2	2	2	2	2	2
R^2	0.9911	0.9863	0.9945	0.9941	0.9919	0.986
K"(l/mg.min)	0.004	0.0021	0.0008	0.0004	0.0002	0.0001
K(l/mg.min)	0.008	0.0042	0.0016	0.0008	0.0004	0.0002
τ1/2 (mins)	0.78	1.48	3.89	7.79	15.58	31.15
Dosage 0.3g/l						
α	2	2	2	2	2	2
R^2	0.9932	0.9911	0.9925	0.9941	0.9985	0.9912
k"(l/mg.min)	0.001	0.0005	0.0003	0.0001	0.00005	0.00004
K (l/mg.min)	0.002	0.001	0.0006	0.0002	0.0001	0.00008
τ1/2 (mins)	3.11	6.23	10.38	31.15	62.30	77.88
Dosage 0.7 g/l						
α	2	2	2	2	2	2
R^2	0.9961	0.9903	0.9912	0.9954	0.9947	0.991
k”(l/mg.min)	0.0006	0.0002	0.0002	0.00004	0.00003	0.00002
K(l/mg.min)	0.0012	0.0004	0.0004	0.00008	0.00006	0.00004
τ1/2 (mins)	5.19	15.58	15.58	77.88	103.84	155.76
Dosage 1.0 g/l						
α	2	2	2	2	2	2
R^2	0.995	0.992	0.9928	0.9962	0.9932	0.9441
K”(l/mg.min)	0.0005	0.0002	0.00009	0.00002	0.00002	0.00002
K (l/mg.min)	0.001	0.0004	0.00018	0.00004	0.00004	0.00004
τ1/2 (mins)	6.23	15.58	34.61	155.76	155.76	155.76

Table 4.17: Functional parameters for Opuntia Spp. at varied dosages and pH values

Parameters	pH					
	4	5	6	8	9	10
Dosage 0.1 g/l						
α	2	2	2	2	2	2
R^2	0.9965	0.9794	0.9828	0.9616	0.9956	0.9979
K"(l/mg.min)	0.0037	0.0024	0.0011	0.0006	0.0003	0.0003
K(l/mg.min)	0.0074	0.0048	0.0022	0.0012	0.0006	0.0006
τ1/2	0.84	1.29	2.83	5.19	10.38	10.38
Dosage 0.3g/l						
α	2	2	2	2	2	2
R^2	0.9331	0.881	0.8963	0.9789	0.9933	0.9635
k"(l/mg.min)	0.0011	0.0009	0.0009	0.0003	0.00009	0.00008
K(l/mg.min)	0.0022	0.0018	0.0018	0.0006	0.00018	0.00016
τ1/2 (mins)	2.83	3.46	3.46	10.38	34.61	38.94
Dosage 0.7 g/l						
α	2	2	2	2	2	2
R^2	0.9776	0.998	0.9736	0.805	0.995	0.9975
K(l/mg.min)	0.0009	0.0006	0.0003	0.00009	0.00008	0.00003
K(l/mg.min)	0.0018	0.0012	0.0006	0.00012	0.00016	0.00006
τ1/2 (mins)	3.46	5.19	10.38	34.61	38.94	103.84
Dosage 1.0 g/l						
α	2	2	2	2	2	2
R^2	0.9752	0.9934	0.9852	0.9882	0.8512	0.909
K”(l/mg.min)	0.0005	0.0002	0.0002	0.00006	0.00004	0.00003
K(l/mg.min)	0.001	0.0004	0.0004	0.00018	0.00008	0.00006
τ1/2 (mins)	6.23	15.58	15.58	51.92	77.88	103.84

Rate equations (Equation 4.1, 4.2 and 4.3) were developed for banana pith, Maerua Decumbent and Opuntia Spp. respectively at best dosage 0.1 g/l and best pH 4.

$$\frac{1}{C_t} = 0.0027t + 0.0312 \quad (4.1)$$

$$\frac{1}{C_t} = 0.004t + 0.001 \quad (4.2)$$

$$\frac{1}{C_t} = 0.0037t + 0.0241 \quad (4.3)$$

The rate equations were used to model the experimental data (Figure 4.71 to 4.73) for banana pith, Maerua Decumbent and Opuntia spp. respectively.

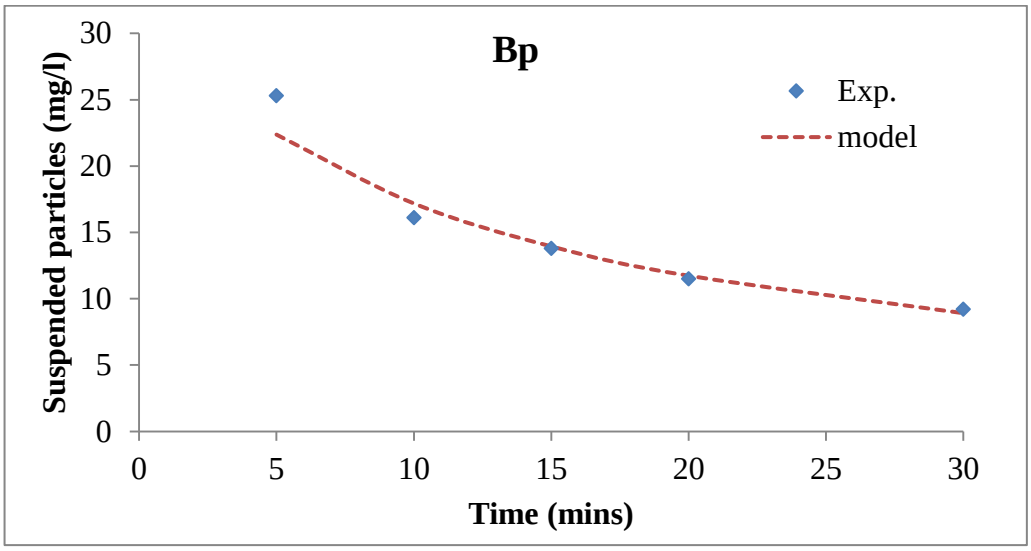

Figure 4.71: Experimental and Predicted variation of suspended particle concentration with time using banana pith.

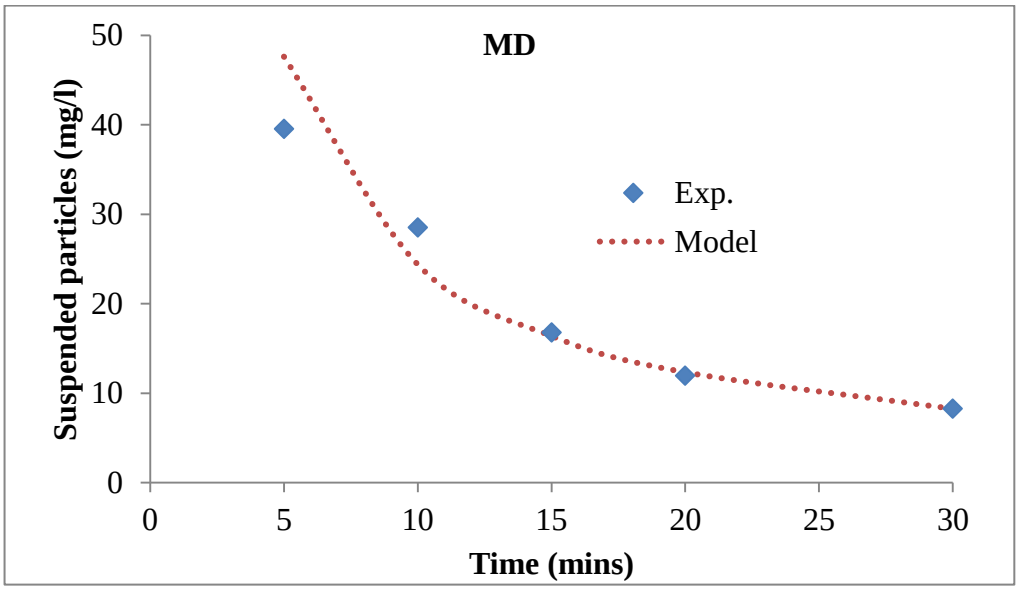

Figure 4.72: Experimental and Predicted variation of suspended particle concentration with time using Maerua Decumbent

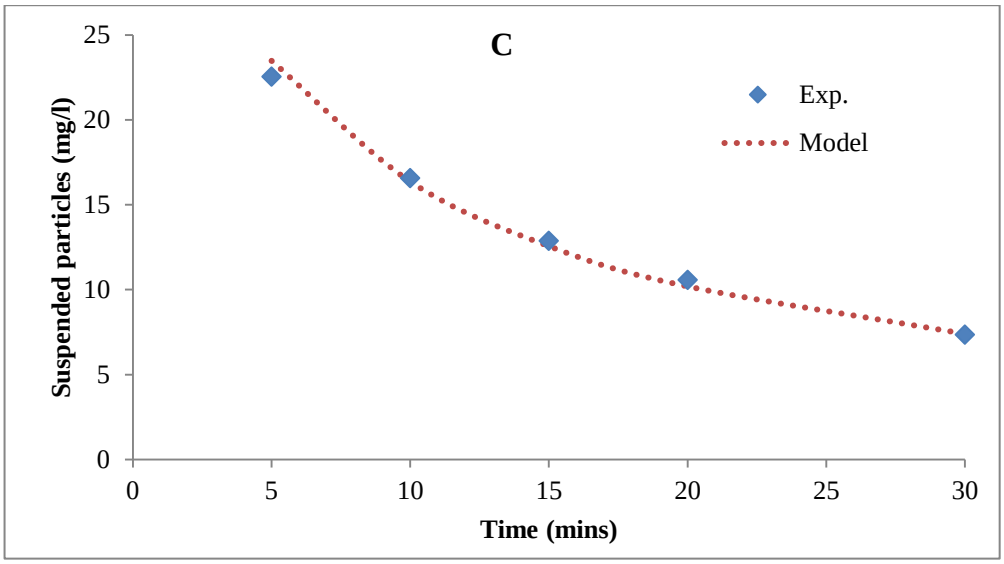

Figure 4.73: Experimental and Predicted variation of suspended particle concentration with time using Opuntia Spp.

4.3.4.2 Effects of time on suspended particle aggregation

To predict the time evolution of particles aggregates (singlets, doublets, triplet for m = 1, 2, 3 respectively), Equations (2.36) was applied using the value of k obtained from

equation (2.27). Figure 4.74 to 4. 97 show the response of equation (2.36) to different $\tau_{1/2}$ values obtained at pH 4 and pH 10 for the varied dosages of all of the three bio-coagulants.The number of primary particles (singlets) decreased rapidly (Figure 4.75, 4.77, 4.79, 4.81 for banana pith, Figure 4.83, 4.85, 4.87, 4.89 for Maerua Decumbent and 4.91, 4.93,4.95 and 4.97 for Opuntia Spp.) as the doublets and triplets increased (Duan & Gregory, 2003). The observation was attributed to formation of doublets and triplets from the quick aggregation of singlet's, to facilitate the flocculation process (Holthof *et al.,* 1996).The obtained curves are expected in coagulation-flocculation process where there is absence of excessive colloidal entrapment and high shear resistance. The dominant mechanism depicted in the graph is charge neutralization combined with low bridging. Figures 4.76, 4.78, 4.80, 4.82 for banana pith, Figures 4.84, 4.87, 4.88, 4.90 for Maerua Decumbent and Figures 4.92, 4.94,4.96 and 4.98 for Opuntia Spp. predicts the distribution of particles with time in favor of even destabilization regime, low entrapment profile and moderate bridging mechanism. Arguably, the shear resistance among the particles is relatively high, but not strong enough to operate outside peri-kinetics controlled process. The curve demonstrates the exclusion of sweeping phenomenon being in action. This is supported by high Half - periods. The high discrete nature of formation of doublets and triplets supports the existence of perceived energy barrier in view of the gentle trends of the graphs (Broide & Cohen, 1992)

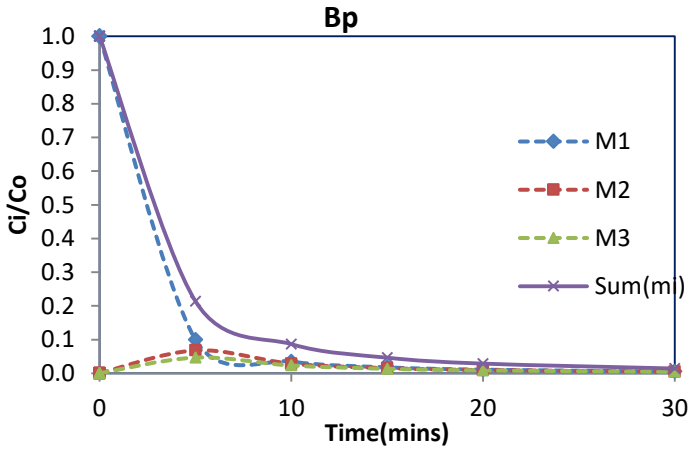

Figure 4.74: Particle size distribution plot for least half time of 1.16 mins, pH 4 and dosage of 0.1 g/l for banana pith.

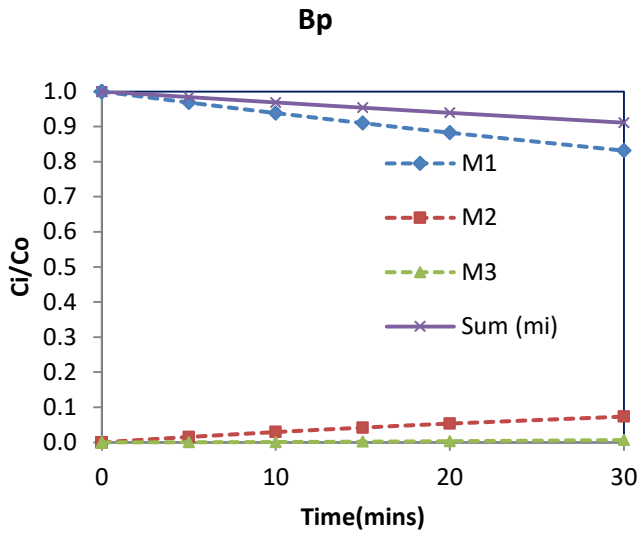

Figure 4.75: Particle size distribution plot for highest half time of 155.8 mins, pH 10 and dosage of 0.1 g/l for banana pith.

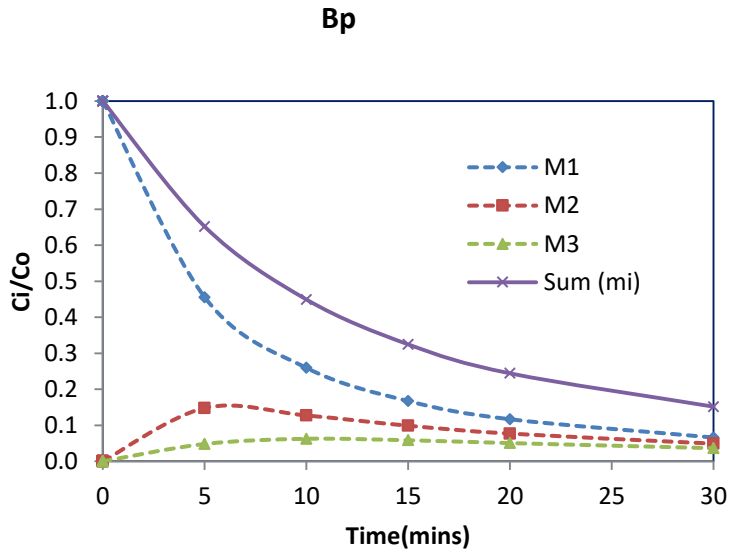

Figure 4.76: Particle size distribution plot for least half time of =5.19 mins, pH 4 and 0.3g/l for banana pith.

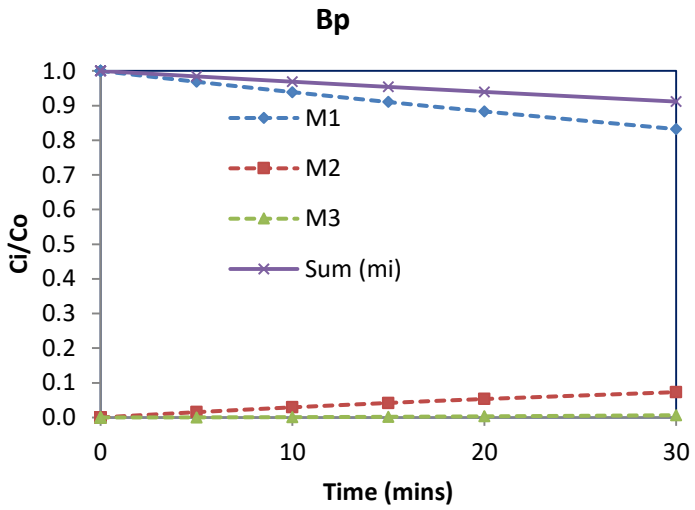

Figure 4.77: Particle size distribution plot for highest half time of 155.8mins, pH 10 and 0.3 g/l for banana pith.

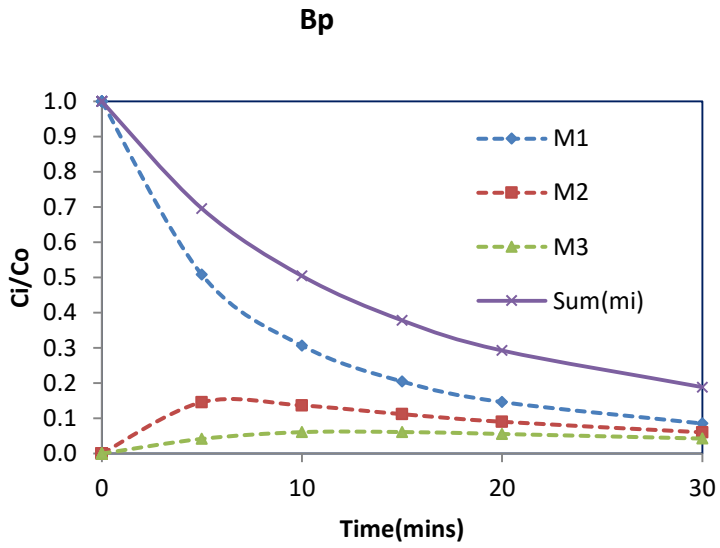

Figure 4.78: Particle size distribution plot for least half time of 1/2 =6.2 mins, pH 4 and 0.7 g/l for banana pith.

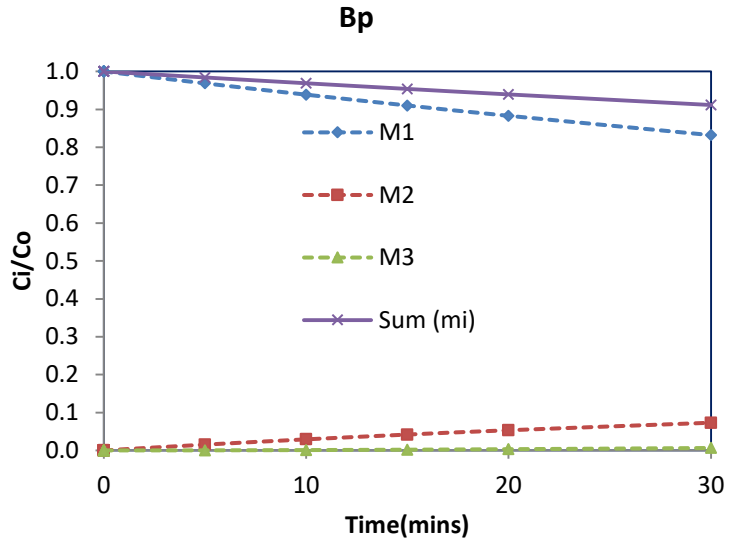

Figure 4.79: Particle size distribution plot for highest half time of =155.8 mins, pH 10 and 0.7g/l for banana pith.

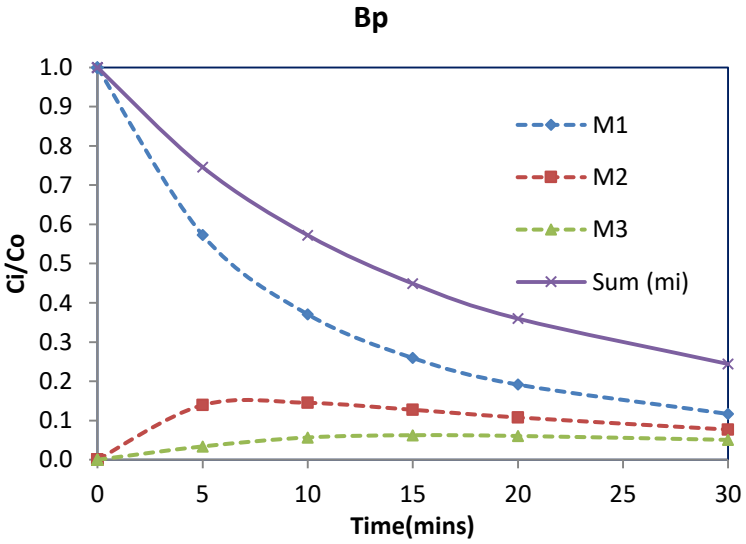

Figure 4.80: Particle size distribution plot for least half time of 7.78 mins, pH 4 and 1.0 g/l for banana pith.

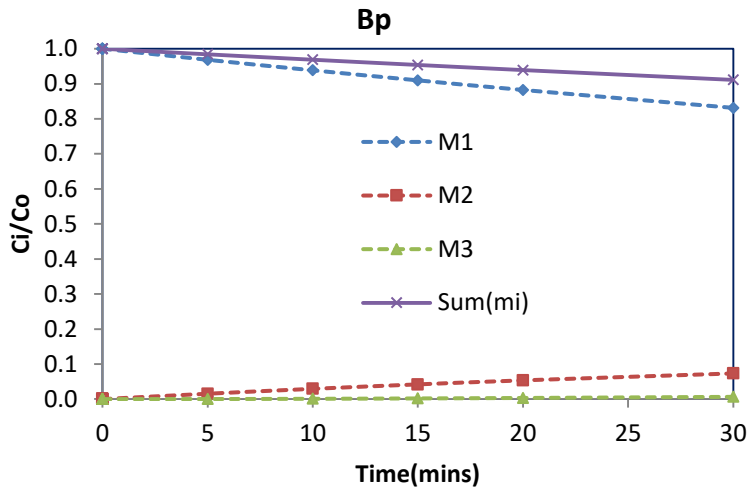

Figure 4.81: Particle size distribution plot for highest half time of 155.8 mins, pH 10 and 1.0g/l for banana pith.

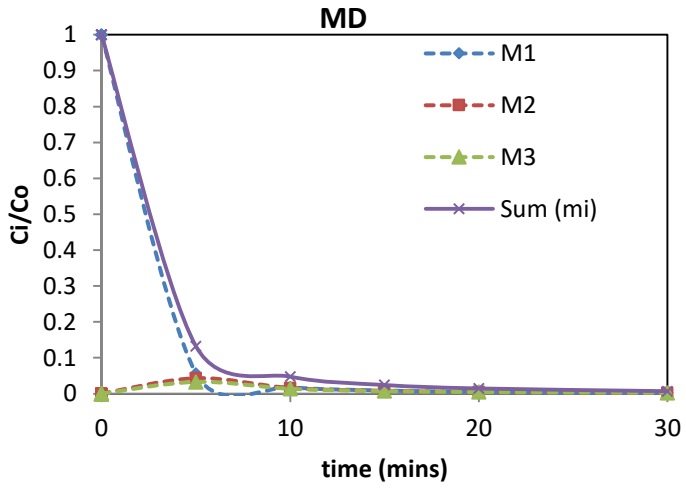

Figure 4.82: Particle size distribution plot for least half time of 0.78mins, pH 4 and 0.1g/l for Maerua Decumbent.

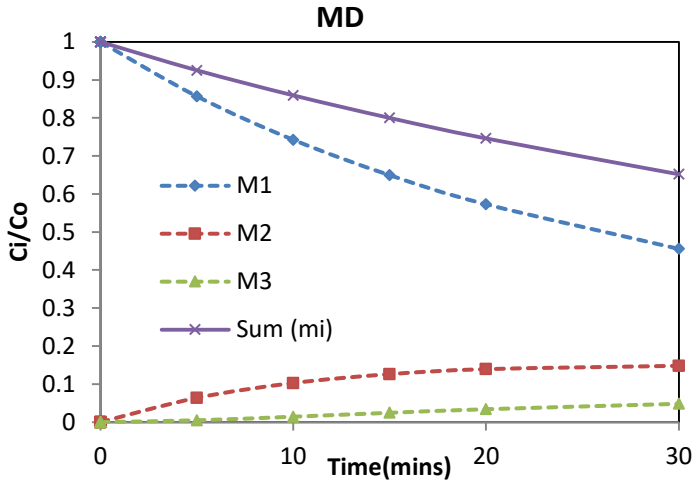

Figure 4.83: Particle size distribution plot for highest half time of 31.15 mins, pH 10 and 0.1 g/l for Maerua Decumbent.

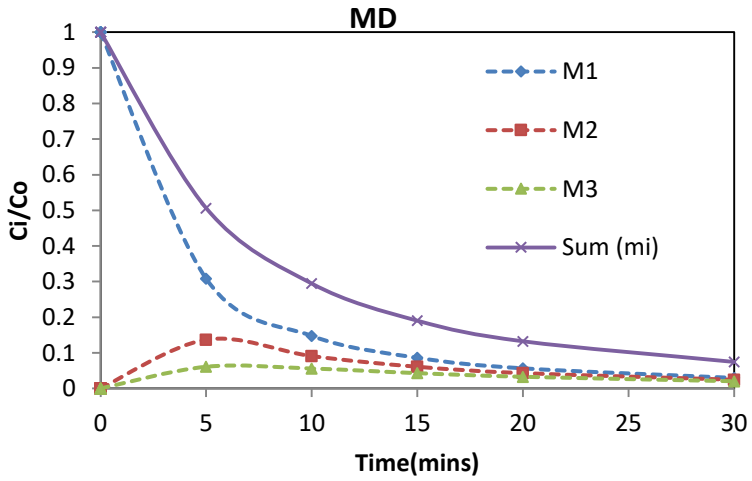

Figure 4.84: Particle size distribution plot for least half time of 3.12mins, pH 4 and 0.3g/l for Maerua Decumbent.

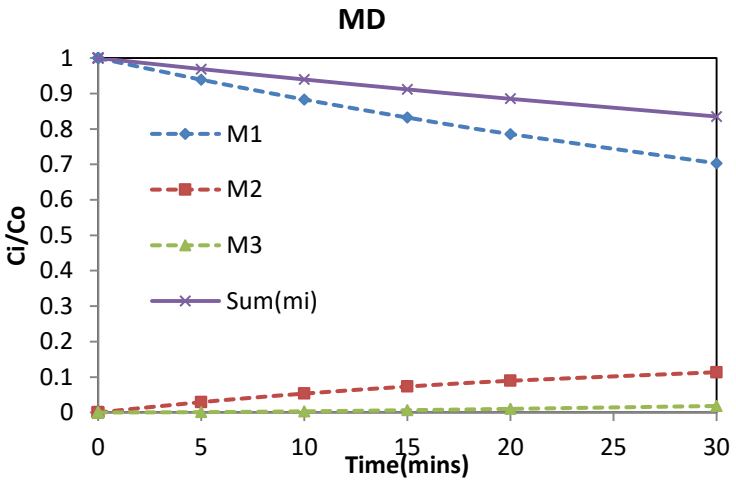

Figure 4.85: Particle size distribution plot for highest half time of 77.9 mins, pH 10 and 0.3 g/l for Maerua Decumbent

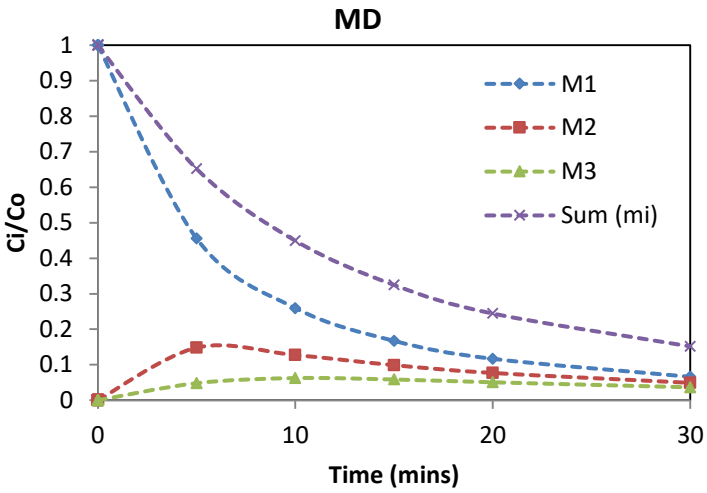

Figure 4.86: Particle size distribution plot for least half time of 5.19 mins, pH 4 and 0.7g/l for Maerua Decumbent

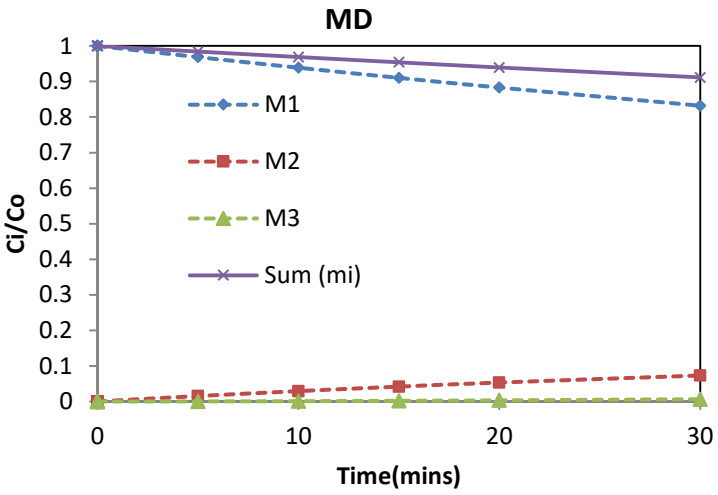

Figure 4.87: Particle size distribution plot for highest half time of 155.76mins, pH 10 and 0.7 g/l for Maerua Decumbent

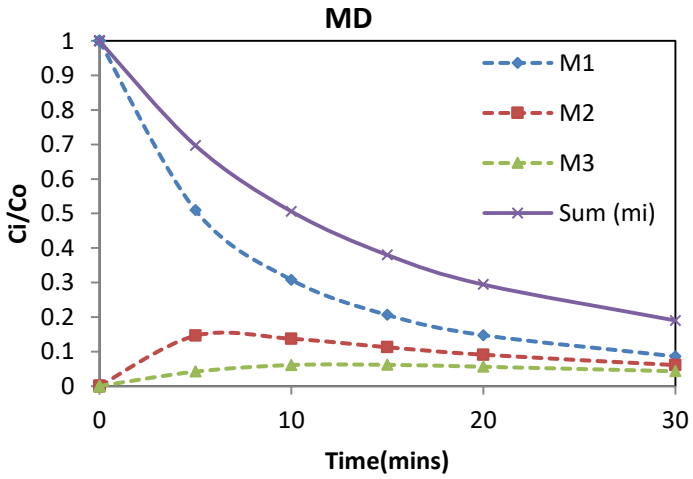

Figure 4.88: Particle size distribution plot for least half time of 6.23 mins, pH 4 and 1.0g/l for Maerua Decumbent

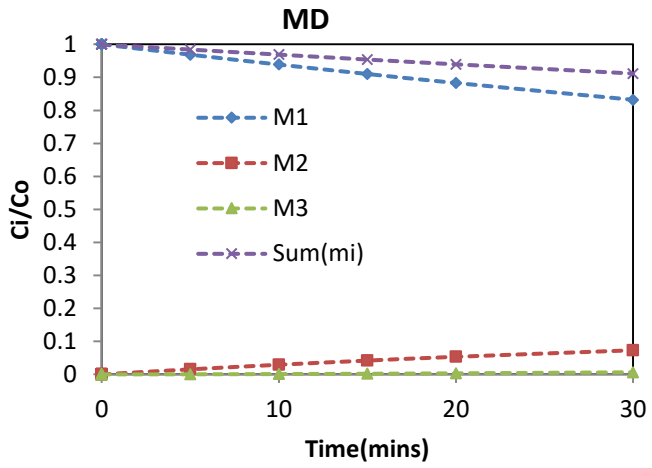

Figure 4.89: Particle size distribution plot for highest half time of 155.76 mins, pH 10 and 1.0 g/l for Maerua Decumbent

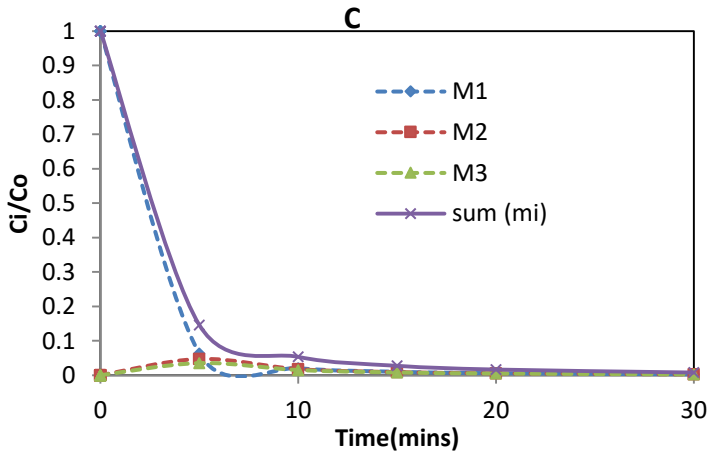

Figure 4.90: Particle size distribution plot for least half time of 0.84mins, pH 4 and 0.1g/l for Opuntia Spp.

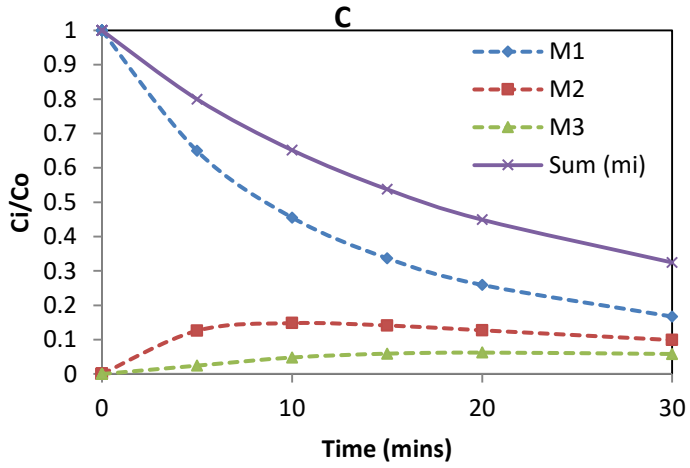

Figure 4.91: Particle size distribution plot for highest half time of 10.38mins, pH 10 and 0.1 g/l for Opuntia Spp.

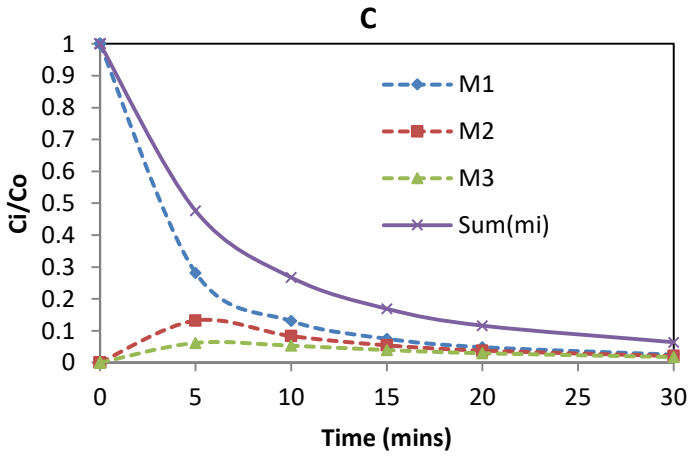

Figure 4.92: Particle size distribution plot for least half time of 2.83mins, pH 4 and 0.3 g/l for Opuntia Spp.

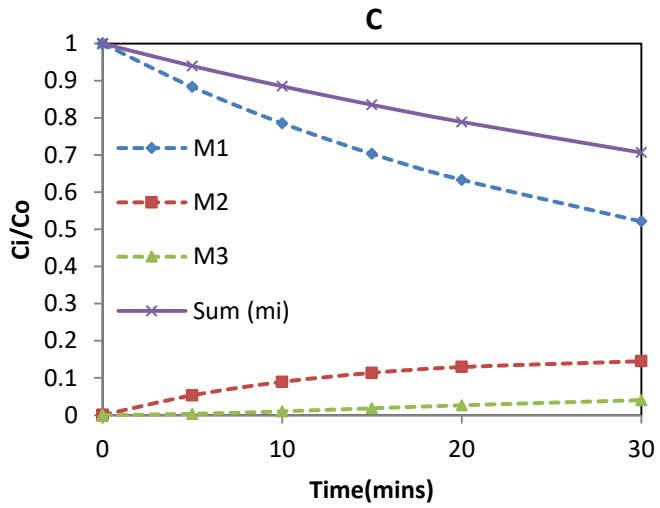

Figure 4.92: Particle size distribution plot for highest half time of 38.94 mins, pH 10 and 0.3 g/l for Opuntia Spp.

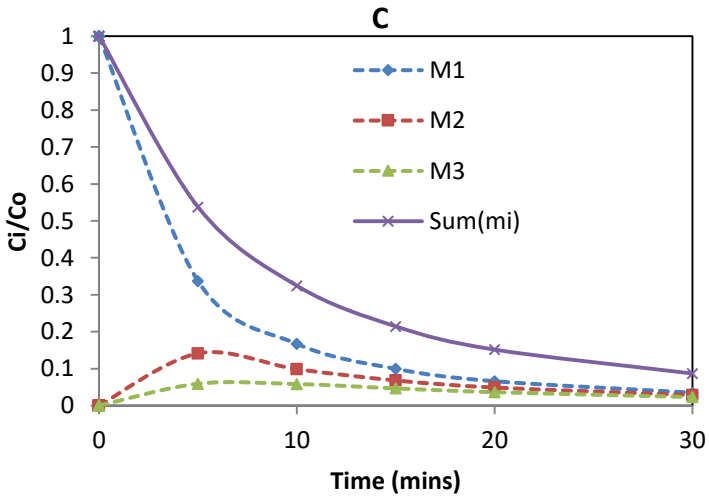

Figure 4.93: Particle size distribution plot for least half time of 3.46 mins, pH 4 and 0.7 g/l for Opuntia Spp.

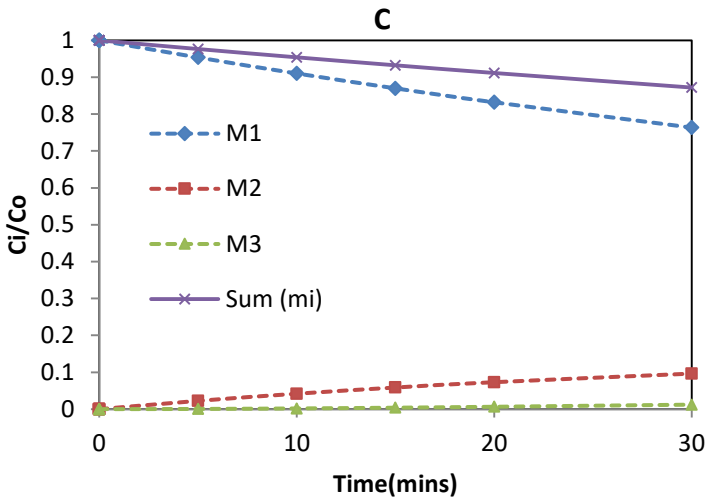

Figure 4.94: Particle size distribution plot for highest half time of 103.84 mins, pH 10 and 0.7 g/l for Opuntia Spp.

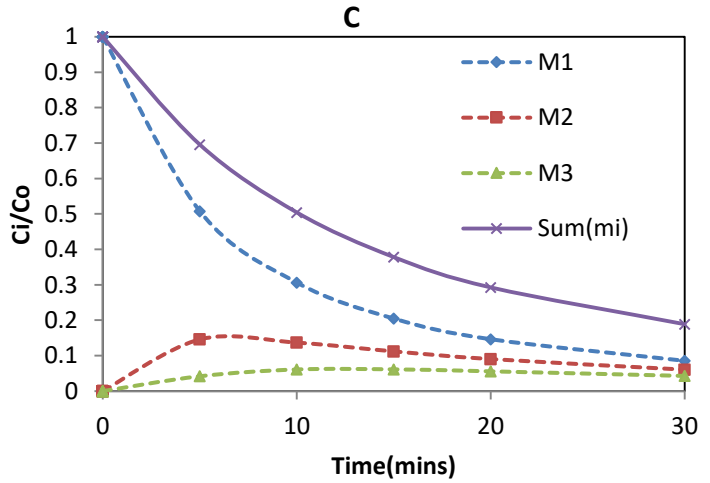

Figure 4.95: Particle size distribution plot for least half time of 6.2 mins, pH 4 and 1.0 g/l for Opuntia Spp.

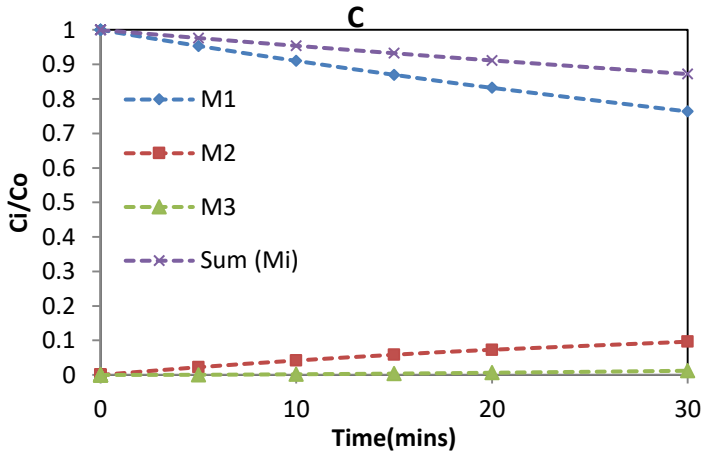

Figure 4.96: Particle size distribution plot for highest half time of 103.84 mins, pH 10 and 1.0 g/l for Opuntia Spp.

4.4 Bio-coagulant Treatment of paint wastewater

The quality of the wastewater effluent from the paint industry presented in Table 4.18 did not meet the Kenyan standards for effluent discharge into the environment with an exception of copper. No regulation was provided for turbidity (Water quality regulation, 2006). Reduction of the pollutant in the paint industry wastewater by coagulation-flocculation with aluminium sulphate and bio-coagulants was evaluated.

Table 4.18: Characteristics of paint wastewater

		Turbidity (NTU)	Concentration (mg/l)						
	pH		COD	Pb	Zn	Fe	Cr	Cd	Cu
Mean values of paint wastewater	8.0	2575	4480	4.19	3.17	42.90	3.24	ND	0.24
KEBSS	6.5-8.5	-	50	0.01	0.5	10.00	2.00	0.01	1.00

4.4.1 Efficacy of bio-coagulants and alum in paint wastewater treatment

The removal of turbidity and heavy metal using alum and Opuntia Spp. (C), alum and Banana pith (B) and alum and Maerua Decumbent (M) was evaluated to determine possible replacement of conventional alum with bio-coagulants. The optimum dosage for removal of turbidity using alum was found to be 1.0 g/l (Figure 4.98).

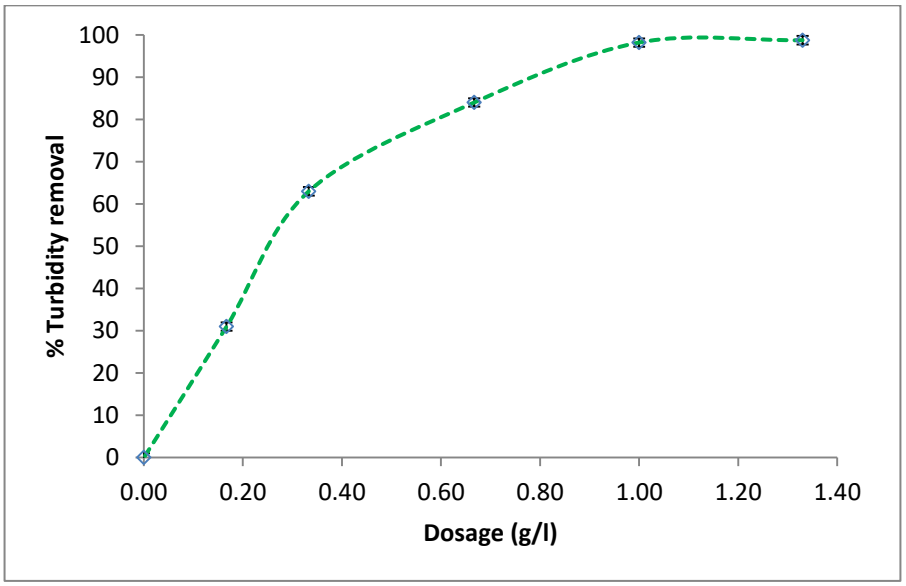

Figure 4.97: Effects of alum dosage on turbidity removal at pH 7.

(a) Turbidity removal from paint wastewater using alum and bio-coagulants

The removal of turbidity from paint wastewater was found to decrease with increase in pH when using alum and the bio-materials (Figure 4.99). Turbidity removal of above 90 % was recorded at 60:40 replacement of alum with Opuntia Spp. (C) and banana pith (B) and at 20:80 replacement of alum with Maerua Decumbent (M). With replacement of up to 80 % of alum with Opuntia Spp.(C) and Banana pith (B), turbidity removal from paint wastewater was reduced to <20%. However, the removal of turbidity was found to be above 80 % at pH 7 with 100 % when Maerua Decumbent bio-coagulant was used. It was therefore concluded that while Maerua Decumbent bio-coagulant can be used for paint wastewater to remove turbidity, it would be necessary to enhance the performance of Opuntia Spp. and Banana pith bio-coagulant with aluminium sulphate. The poor performance of the Opuntia Spp. and banana pith bio-coagulant in industrial paint wastewater treatment may be attributed to interferences

of their active ingredients by the paint chemicals which was not the case to Maerua Decumbent bio-coagulant.

The amount of sludge produced when only alum was used was higher compared to when alum was combined with the bio-coagulants. The sludge decreased with the increase in the amount of plant coagulant (Figure 4.100). Similar results were reported elsewhere, whereby sludge reduction of over 40% was recorded when bio-coagulants were used (Bahman R. , 2014), Nandini & Sheba, 2016)

The effect of coagulant to final pH of treated water was also studied. The use of the conventional chemical alum reduced the pH of the final effluent. This is expected because of the sulphuric acid produced when alum is added to water. When the alum was combined with the plant coagulants the pH varied as shown in Figure 4.101 achieving minimal pH change when only bio-coagulant were used. It was therefore concluded that the use of plant coagulant has minimal effects to the final pH of the treated effluent. Similar results were reported elsewhere (Joseane *et al*, 2013; Hayelon *et al.*, 2016).

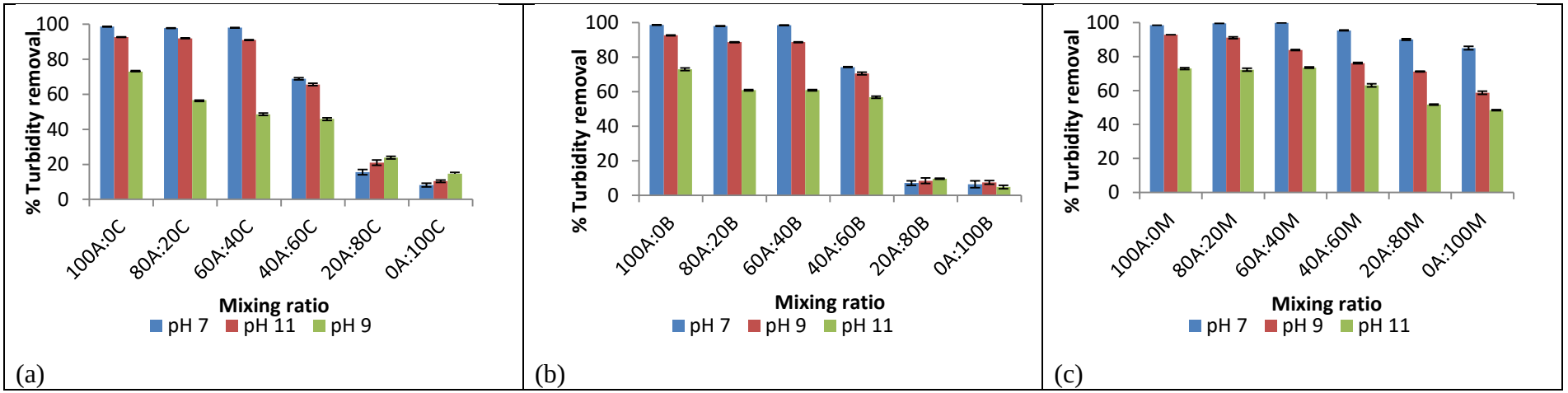

Figure 4.98: Effects of pH on the removal of turbidity using alum and (a) Opuntia Spp., (b) Banana pith and (c) Maerua Decumbent at varied pH

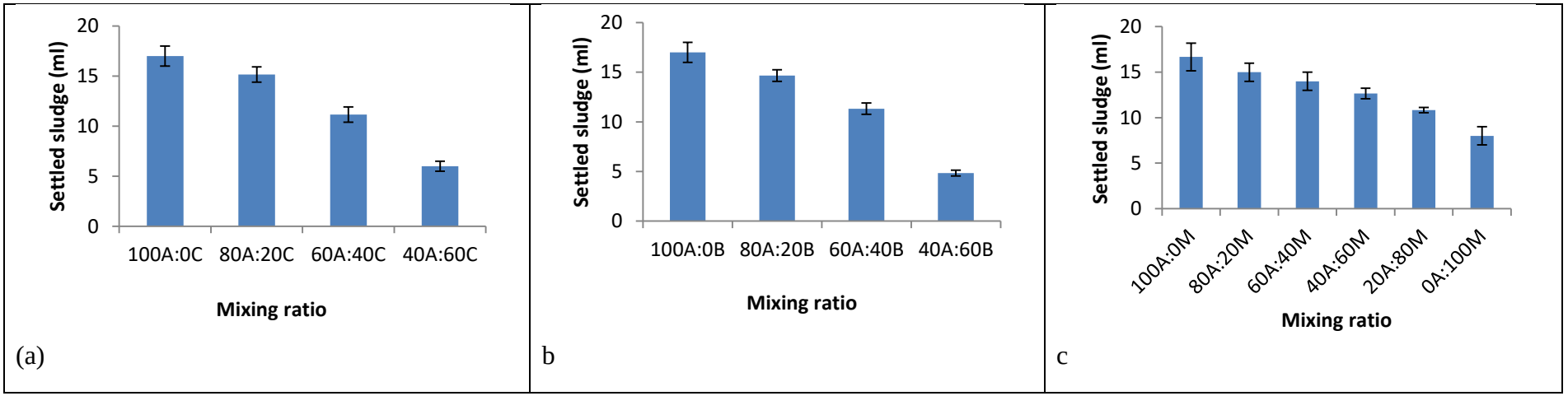

Figure 4.99: Effects on sludge production using alum and (a) Opuntia Spp., (b) Banana pith and (c) Maerua Decumbent at pH 7

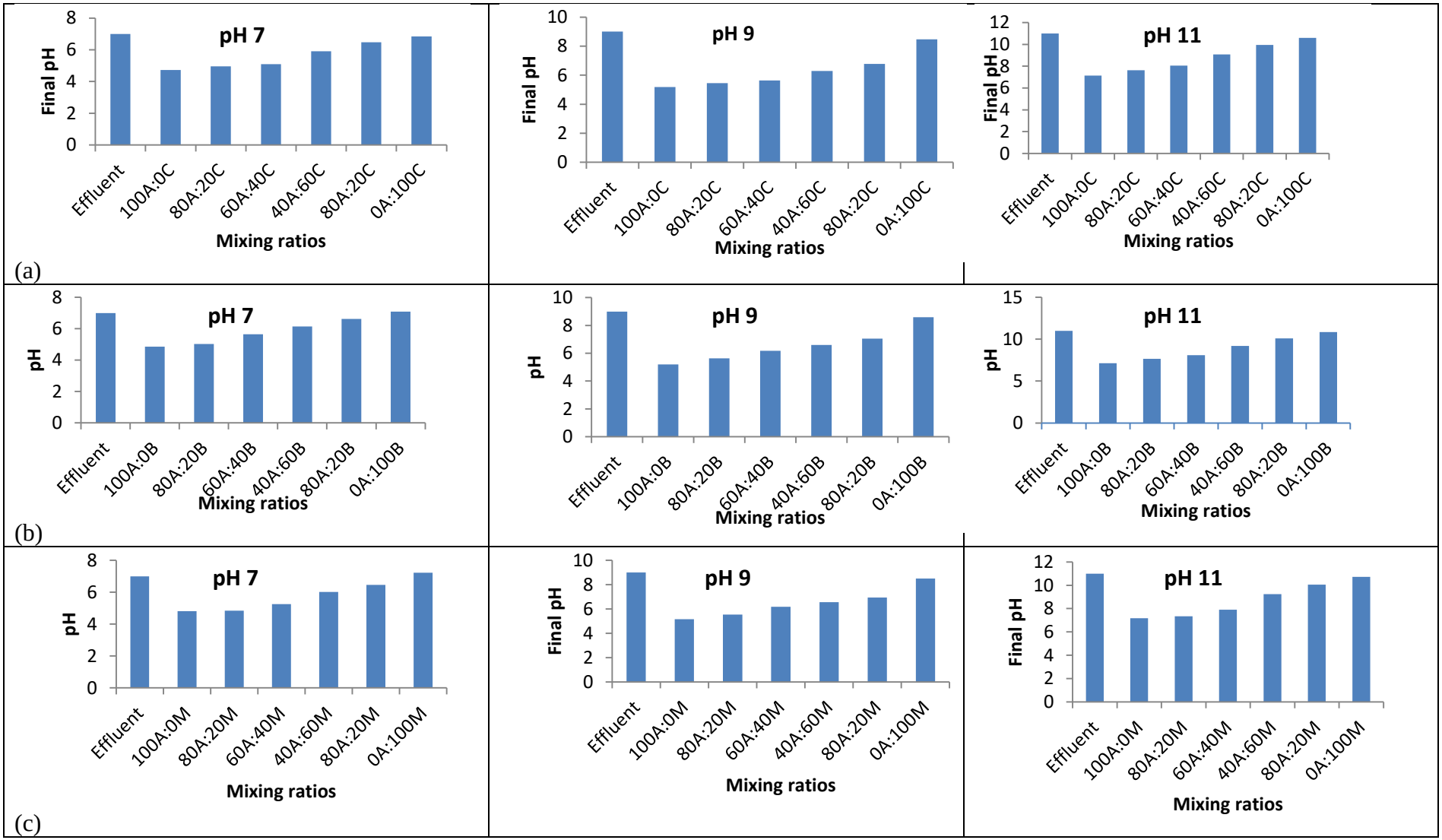

Figure 4.100: Effects of the use of alum and the bio-coagulants at varied pH

(b) Heavy metal removal from wastewater using alum and bio-coagulants

The removal of lead at pH 7 increased from 95% at zero alum replacement to about 97 and 98% at 40 replacements with Opuntia Spp. and banana pith respectively (Figure 4.102). At the same pH the highest lead metal removal. 99% was achieved at 100% replacement of alum by Maerua Decumbent. At pH 9 the highest removals were observed as 91, 94 and 98 % at 40% replacement of alum with Opuntia Spp., Banana pith and Maerua Decumbent respectively. Finally, at pH 11, lead removals were observed as 98, 96 and 92 % at 40% replacement of alum with Opuntia Spp., banana pith and Maerua Decumbent respectively.

An increase in chromium heavy metal removal was observed across all the pH value up to 40% aluminium replacement using all the three bio-coagulants. (Figure 4.103) For pH 7 chromium removal increased from 94 to 96, 97 and 98 % when 40, 20 and 40 % alum was replaced with Opuntia Spp., banana pith and Maerua decumbent respectively. Highest chromium removals at pH 9 were 86, 94 and 86 % when 40% alum was replaced with all the bio-coagulants whereas for pH 11, the removals were 98, 90 and 88% when 40% alum was replaced with all the bio-coagulants.

When Opuntia Spp. was used the highest removal (88 %) of zinc was found to occur at pH 7 by 40 % of alum replacement. For banana pith approximately 87% was achieved at pH 7 and 9 by 40 % of alum replacement while 87% removal was recorded for Maerua Decumbent by 20-60 % of alum replacement at pH 7 (Figure 4.104).

Approximately 90% of iron was removed when 40% of alum was replaced with Opuntia Spp. at pH 11 and Banana Pith at pH 7. At pH 7 and 9, 20-40% alum replacement with Maerua Decumbent achieved 86 % of iron metal removal (Figure 4.105)

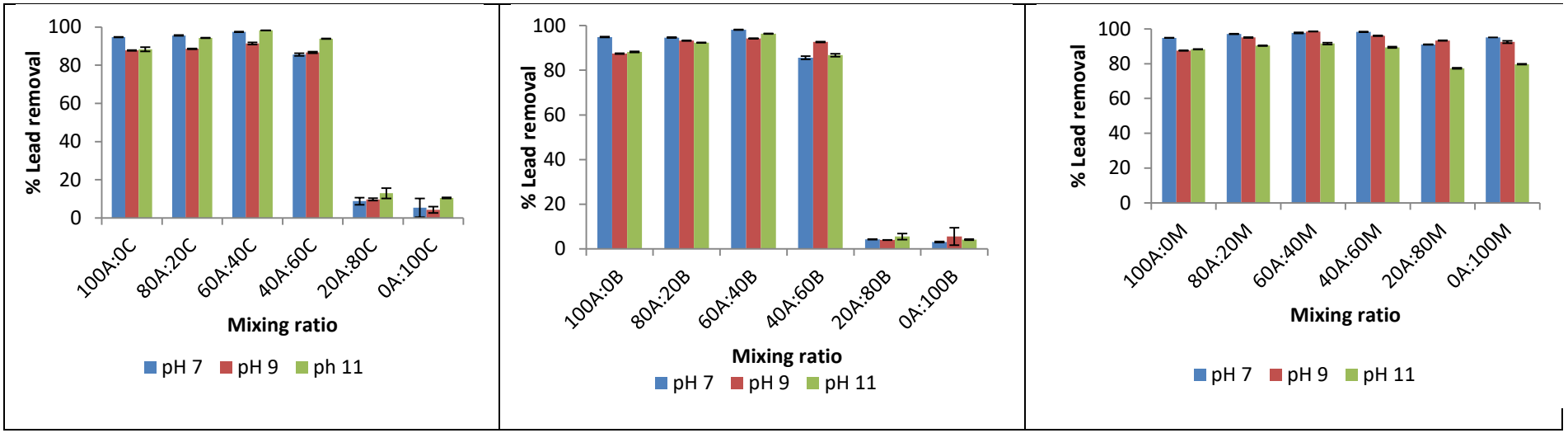

Figure 4.101: Removal of lead using Alum and bio-coagulants

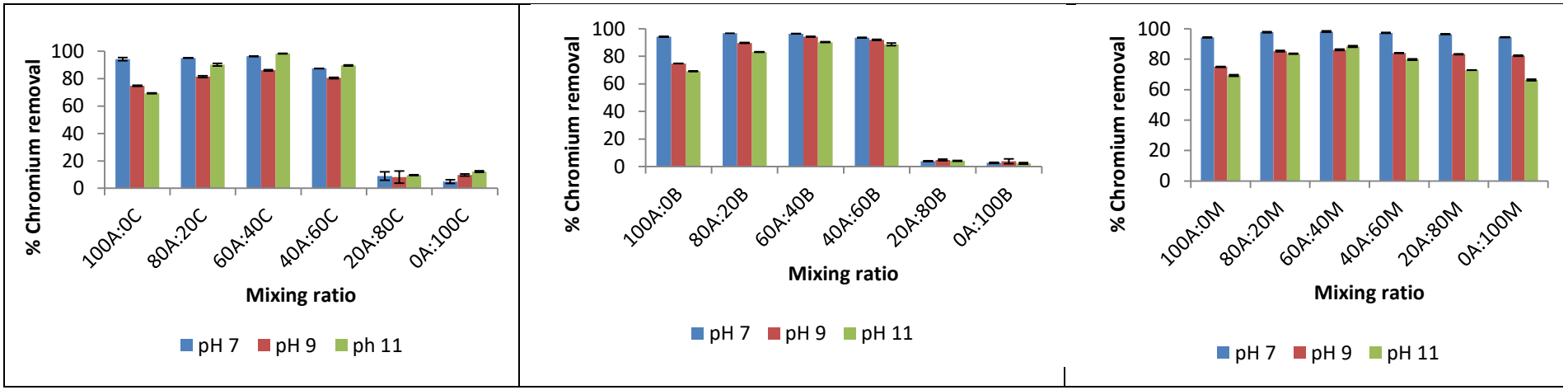

Figure 4.102: Removal of chromium using Alum and bio-coagulants

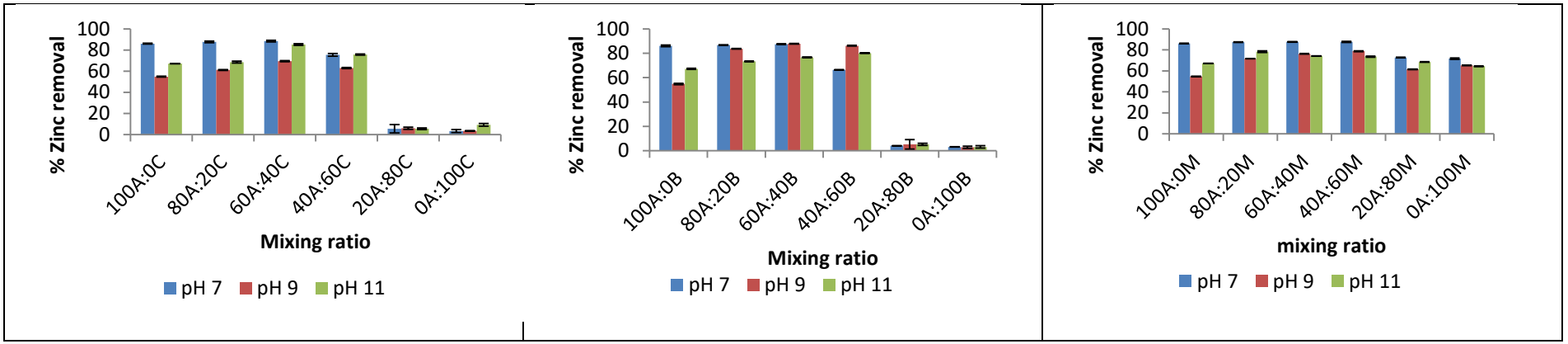

Figure 4.103: Removal of zinc using Alum and bio-coagulants

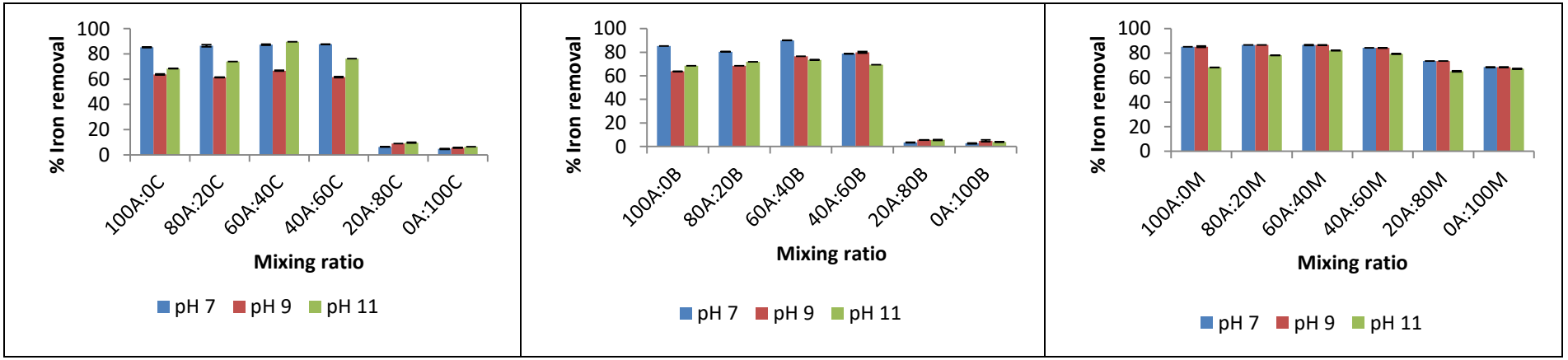

Figure 4.104: Removal of iron using Alum and bio-coagulants

4.4.2 Efficacy of Maerua Decumbent in paint wastewater

From section 4.4.1, it was established that Maerua Decumbent had the potential to treat paint wastewater. Further investigation was carried out to establish the effects of varied dosages and pH on its performance in paint wastewater treatment.

(a) Turbidity removal from paint wastewater using Maerua Decumbent

(i) Effect of varied pH on turbidity removal

Turbidity removal from paint wastewater was investigated at varied pH and constant dosage of 0.7 g/l (Figure 4.106). Turbidity removals of up to 85 % were observed at pH 5. However, the removal decreased as the pH increased indicating that low pH provided charged sites for colloidal particles (Aparecido *et al*., 2015). It was noted that use of Maerua Decumbent coagulant did not alter the final pH (Figure 4.107) of the treated water significantly as was also observed by (Joseane *et al.* 2013; Hayelon et al., 2016).

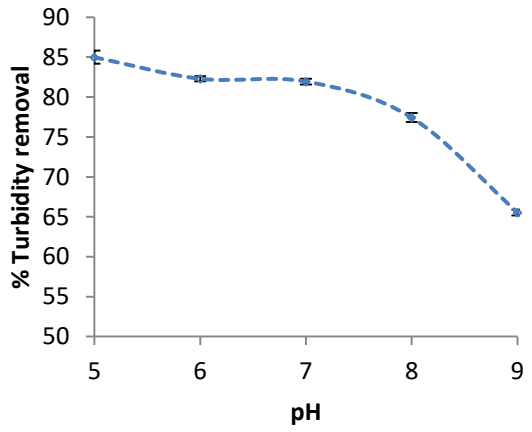

Figure 4.105: Effects of pH at 0.7g/l Maerua and 60 minutes settling time

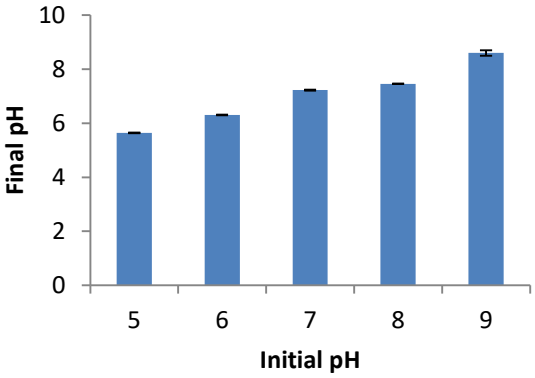

Figure 4.106: Effects of Maerua coagulant on final effluent pH at dosage of 0.7 g/l and 60 minutes settling

(ii) Effects of dosage and settling time on turbidity removal

Removal of turbidity using Maerua Decumbent was investigated at varied dosages and constant pH of 5 (Figure 4.108). Turbidity removal increased with increase in dosage up-to the dosage of 1.0 g/l beyond which there was no significant increase in removal. These findings are consistent with those reported by (Mishra & Malvika, 2005) on the flocculation of model textile wastewater with a food-grade polysaccharide. Above the optimum dosage, the trends showed a decrease in percentage removal attributed to particle stabilization due to some steric repulsion. (Tripathy & De, 2006) and (Aygun & Yilmaz, 2010) reported that flocculants forms an envelope on the suspended particles and causes them to remain in suspension; thus, removal efficiency decreases with increasing dosage beyond the optimum.

Maerua Decumbent achieved 95% turbidity removal in 60 minutes (Figure 4.109).

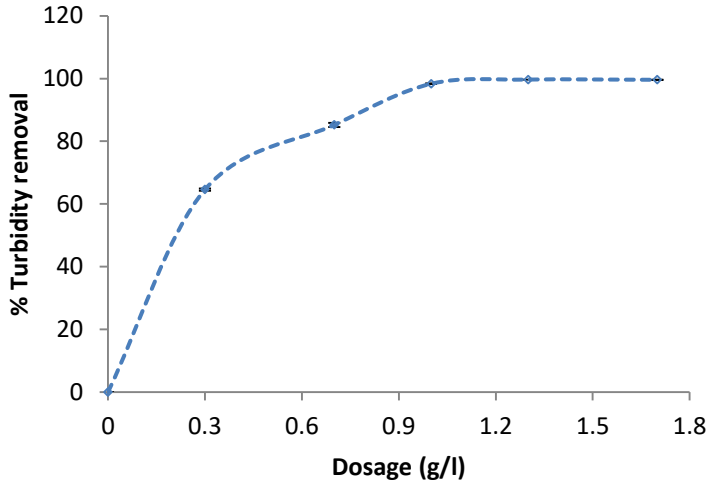

Figure 4.107: Effects of varied dosage at pH 5 and 60 minutes settling

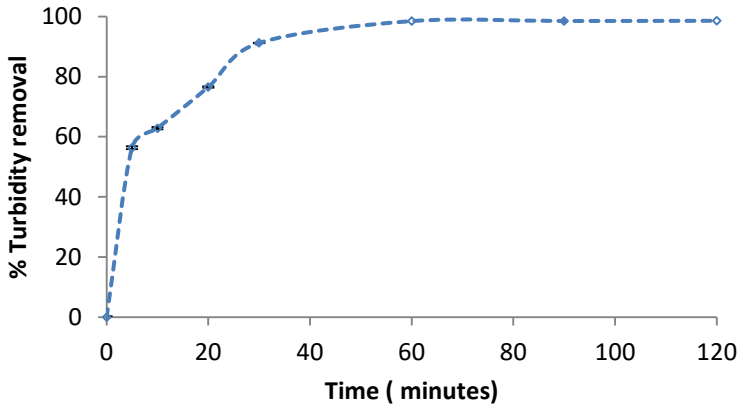

Figure 4.108 : Effects of settling time pH 5 and 1.0g/l of Maerua

(b)Heavy metal removal from paint wastewater using Maerua Decumbent

The removal of heavy metal from paint wastewater using Maerua Decumbent Coagulant was investigated at varied pH and dosages (Figure 4.110).

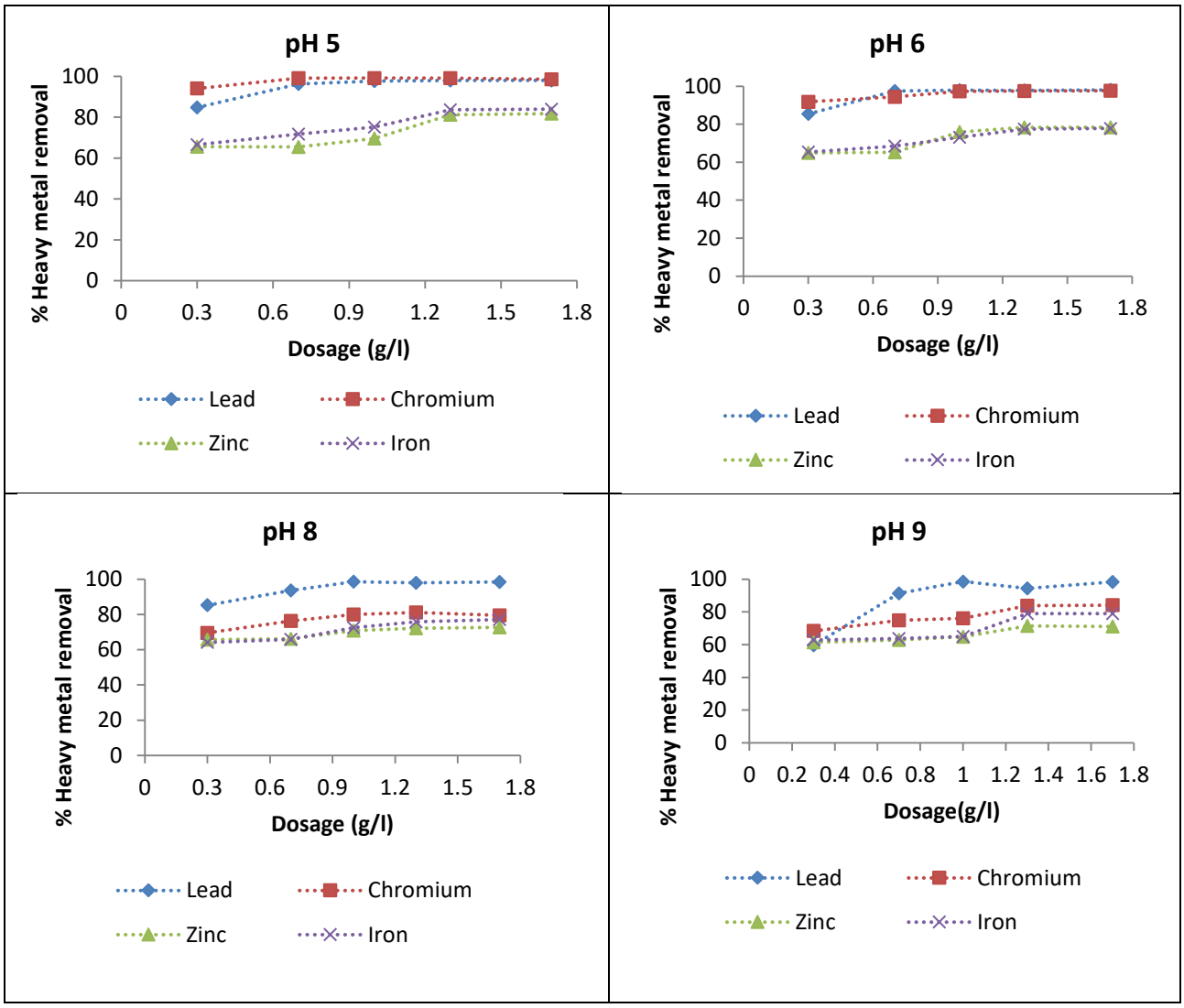

Figure 4.109: Heavy metal removal from paint wastewater using Maerua Decumbent at varied pH and dosages

Heavy metals removal varied from 60 and 65% for lead and chromium at dosage 0.3g/l, respectively at pH 9 to 100% at pH 5 and dosage 0.9 g/L, and from 60 and 65% for iron and copper, respectively to 80% at the same conditions. The optimum dosages for the various heavy metals varied. For example, at pH 5, over 99% removal of chromium and lead were achieved at dosages 0.7 g/l whereas the maximum removal of zinc and iron of 80% at dosages were achieved 1.3 g/l. Therefore, the required dosage would vary with the targeted heavy metal.

The result indicated that Maerua Decumbent coagulant had the potential to remove between 60 and 100% of heavy metals from paint wastewater. pH adjustment to the acidic range improved it effectiveness.

4.4.3 Efficacy of using Opuntia Spp. and Cement kiln dust (CKD) in paint wastewater treatment

Tests were carried out to evaluate the efficacy of improving the effectiveness of Opuntia Spp. using CKD, a waste by-product of cement production. CKD contains lime which when lime is added in water, it partly reacts with water carbonates to form calcium carbonate which is a coagulant. This precipitate removes pollutant either through enmeshment or adsorption (Lee et al., 2007). This section presents the evaluation of the potential use of bio-coagulants combined with lime from cement kiln dust, a waste by product of cement production.

(a) Characterisation of cement kiln dust

The cement kiln dust (CKD) was characterised and its content are as shown in Table 4.19. The amount of quick lime (CaO) from which lime (CaOH) was produced, was 65.4 %. Lime in slurry form was prepared from the (CKD) which was used as a coagulant.

Table 4.19: Characterisation of CKD

Compound	SiO_2	Al_2O_3	FeO_3	CaO	MgO	SO_3
Mean Value (%)	19.52	4.87	3.12	65.4	3.78	0.99
Compound	K_2O	Na_2O	TiO_2	Mn_2O_3	SrO	Cl
Mean Value (%)	0.86	0.35	0.22	0.17	1.9	0.069

(b) Removal of turbidity using different dosages of Opuntia Spp. and Cement kiln dust (CKD)

The removal of turbidity using varied dosages of lime were investigated. The results on turbidity removal using 0 to 1.0 g/l Opuntia Spp. with 4 - 10 ml of CKD are as shown in Figures 4.111 – 4.113. Increase in turbidity removal was observed as the dosage of Opuntia Spp. increased reaching the 99% at 0.3 g/l.

The highest removal of turbidity of about 90 % was recorded when 7 ml of CKD and 1.0 g/l of Opuntia Spp. were used (Figure 4.112). There was no significant removal noted between 0.7 and 1.0 g/l of Opuntia Spp. in this case. At 4 ml of CKD the highest removal of turbidity was 82 % at 1.0 g/l of Opuntia spp. (Figure 4.113). It was therefore established that the best combination for about 99 % of turbidity from paint wastewater, were Opuntia Spp. dosage range of 0.3-0.7 g/l and 10 ml of cement kiln dust.

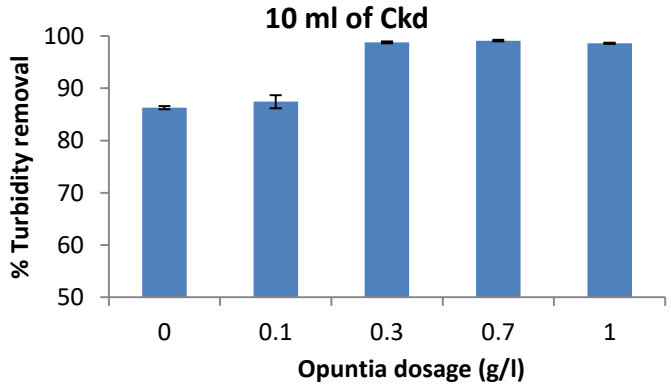

Figure 4.110: Removal of turbidity at varied dosages of Opuntia Spp. and constant amount of 10 ml CKD

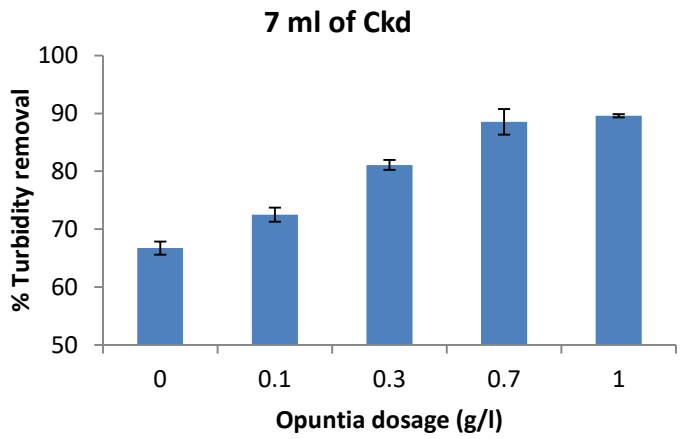

Figure 4.111: Removal of turbidity at varied dosages of Opuntia Spp. and constant amount of 7 CKD

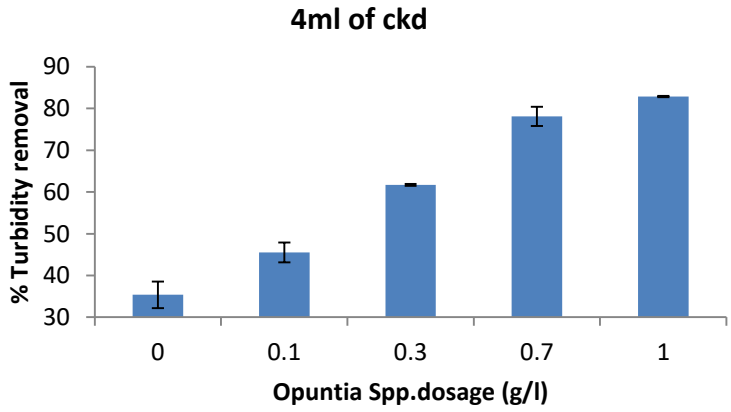

Figure 4.112: Removal of turbidity at varied dosages of Opuntia Spp. and constant amount of 4 ml CKD

(c) Removal of heavy metal using different dosages of Opuntia Spp. and cement kiln dust (CKD).

The removal of lead, chromium, zinc and iron were found to increase with increase in CKD dosage. The addition of Opuntia Spp. resulted into an increase in heavy metal removal. At the best performing CKD slurry dosage of 10 ml and 0 – 1.0 g/l Opuntia Spp. Dosage, lead removal varied from 41 to 99%, chromium 76 to 100%, zinc 66 to 99% and iron from 56 to 91 % (Figure 4.114). The use of Opuntia Spp. together with

CKD was found to enhance its performance. The use of lime for pollutant removal has been reported elsewhere (Pauline *et al.*, 2008).

Lime removes pollutant either through enmeshment or adsorption (Lee et al., 2007) in calcium carbonate precipitate (Environmantal protection agency (EPA), 2000). When bio-coagulant polymer is added it aids in gathering the remaining contaminants (through inter particle bridging/charge neutralization or bio-sorption) forming coarse floc which then settle down. (Salem *et al.*, 2015), reported that 10 g/l of cement kiln dust was able to eliminate heavy metal from sewage wastewater. Report by Esawy, 2014 indicates that CKD coagulant mixed with a polymer was effective in the removal of heavy metal from municipal wastewater.

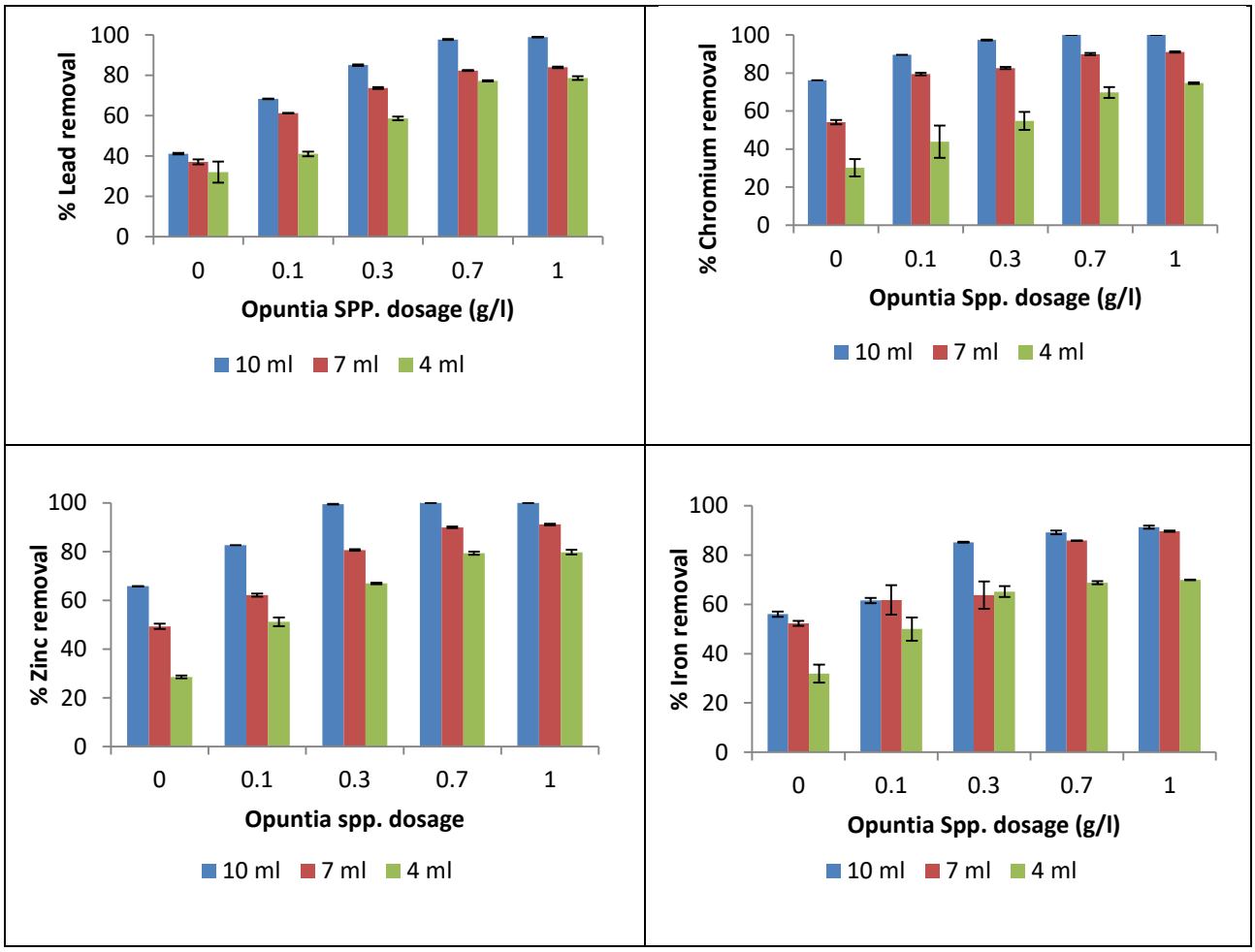

Figure 4.113: Heavy metal removal at varied dosages of Opuntia Spp. and cement kiln dust.

4.4.4 General Discussions of Bio-treatment of paint Industry Wastewater

The use of conventional coagulant, Aluminium sulphate in the treatment of paint wastewater achieved over 90 % of turbidity removal at the dosage of 1.0 g/l and pH 7. At the combination of 60:40 percent by weight of alum and Banana pith or Opuntia Spp. bio-coagulants and 60:20 percent of alum and Maerua decumbent a similar turbidity removal was achieved at pH 7. At 80 percentage replacement of alum by either banana pith or Opuntia Spp. the performance of the treatment deceased to less than 20 %. However, at 100% Maerua decumbent and pH 7, 80 % of turbidity removal was achieved. Further investigation of Performance of Maerua at varied pH and dosages revealed that over 98% of turbidity removal was achieved at Maerua dosage of 1.0 g/l and pH 5.

The removal of heavy metal was found to increase with the replacement of alum with the bio-coagulant, upto the combination ration of 60:40.at all the pH values with the highest amount occurring at pH 7. At pH 7 the highest amount of lead removed was 97, 98 and 98 %, chromium was 96,96 and 98%, zinc 88,87and 87% and iron 67,90 and 86% when alum was replaced with Opuntia Spp., Banana pith and Maerua decumbent respectively.

Further, CKD, a waste product from the cement industry combined with a Opuntia Spp. a bio--coagulant was found to be effective in turbidity removal. Over 99 % of turbidity and 85 % of all the heavy metals were removed at a combination of 10ml of ckd slurry with 0.3 g/l of Opuntia spp.

The use of the bio-coagulant alone or combined with conventional coagulant resulted in reduced sludge. And the effects to the final pH of the effluent decreased with addition of the bio-coagulants.

4.5 Optimization of coagulation-flocculation treatment of paint wastewater studies using response surface methodology

4.5.1 Introduction

The application of the Central Composite Design (CCD) in the treatment of paint wastewater through coagulation and flocculation was evaluated using the following materials:

1. Maerua Decumbent
2. Alum
3. Alum and banana pith and
4. Opuntia plus CKD

This section combines results obtained from laboratory experiments done according to the CCD design, with statistical analyses performed using Design Expert 10.0.

4.5.2 Optimization of paint wastewater treatment using Maerua Decumbent

4.5.2.1 Model Fitting

The effects Maerua dosage, pH and Settling time on removal of turbidity and COD and the effects of Maerua dosage and pH on removal of heavy metals through coagulation-flocculation process was analysed using response surface methodology (RSM). The central composite design (CCD) shown in Table 4.20 and 4.21 allowed the development of mathematical equations. Turbidity and COD removal was assessed as a function of dosage(A), pH(B) and settling time (C) which was calculated as the sum of a constant, three first order effects (terms A, B and C), three interactive effects (AB, AC and BC) and three second order effects (A^2, B^2 and C^2),whereas the assessment of heavy metal was done as a function of dosage(A) and pH(B), and calculated as the sum of a constant, two first order (A and B), one interactive (AB) and two second order effects(A^2 and B^2) according to equation 3.17. The results for fitted polynomial model equations for turbidity, COD and Heavy metals removals were determined (Table 4.22).

Table 4.20: CCD and Response results for study of three experimental variables for Maerua Decumbent coagulant.

	Coded			Actual			Removal (%)	
	A	B	C	A	B	C	Turbidity	COD
1	-1.000	1.000	-1.000	0.7	9	20	41.71	20.71
2	-1.682	0.000	0.000	0.495	7	40	70.24	54.78
3	-1.000	-1.000	1.000	0.7	5	60	84.00	77.73
4	0.000	0.000	0.000	1	7	40	89.10	63.14
5	1.682	0.000	0.000	1.505	7	40	87.35	29.85
6	1.000	-1.000	1.000	1.3	5	60	99.80	56.00
7	-1.000	1.000	1.000	0.7	9	60	58.63	33.85
8	0.000	0.000	0.000	1	7	40	91.20	66.50
9	1.000	-1.000	-1.000	1.3	5	20	71.62	30.21
10	1.000	1.000	1.000	1.3	9	60	67.62	23.66
11	0.000	0.000	0.000	1	7	40	93.30	62.10
12	0.000	0.000	1.682	1	7	73.64	77.17	65.84
13	-1.000	-1.000	-1.000	0.7	5	20	52.64	39.85
14	0.000	0.000	0.000	1	7	40	92.89	60.64
15	0.000	1.682	0.000	1	10.36	40	50.12	29.71
16	0.000	0.000	0.000	1	7	40	91.69	66.23
17	0.000	0.000	-1.682	1	7	6.364	27.17	12.78
18	0.000	0.000	0.000	1	7	40	88.90	53.60
19	1.000	1.000	-1.000	1.3	9	20	45.92	16.28
20	0.000	-1.682	0.000	1	3.636	40	89.10	68.26

A: Maerua Decumbent dosage (g/l), B: pH, C: Settling time (mins)

Table 4.21: CCD and Response results for study of two experimental variables for Maerua Decumbent coagulant.

	Coded		Actual		Removal (%)			
Run	A	B	A	B	lead	chromium	Zinc	Iron
1	0.000	0.000	1.00	7.00	99.68	96.05	71.46	64.41
2	0.000	0.000	1.00	7.00	97.91	93.67	72.62	67.61
3	0.000	0.000	1.00	7.00	99.83	95.49	74.93	69.31
4	-1.414	0.000	0.576	7.00	98.16	81.33	61.08	64.96
5	1.000	-1.000	1.30	5.00	98.18	99.19	79.78	83.45
6	-1.000	-1.000	0.70	5.00	95.5	99.1	65.35	71.23
7	0.000	0.000	1	7.00	98.92	94.21	68.24	67.12
8	-1.000	1.000	0.7	9.00	91.29	73.25	61.79	64.64
9	0.000	1.414	1	9.828	86.32	73.22	70.18	70.35
10	0.000	-1.414	1	4.172	89.26	99.99	80.25	85.92
11	1.000	1.000	1.3	9	94.64	84.66	70.92	78.13
12	0.000	0.000	1	7	99.84	97.64	73.66	62.68
13	1.414	0.000	1.424	7	100.00	99.89	75.58	85.81

A: Maerua Decumbent dosage (g/l), B: pH

Table 4.22: Model equations in terms of coded factors

Turbidity	= +91.18+5.62* A-11.70* B+13.34* C-2.70* AB+0.20* AC-2.61* BC-4.41* A^2-7.66*B^2-13.82* C^2
COD	= +62.20-6.44* A-12.75* B+12.70* C+2.09* AB-2.23* AC-5.39* BC-8.05* A^2 –5.70* B^2-9.12* C^2
Lead	= +99.24+1.08* A-1.49* B+0.17* AB+0.29* A^2-5.36* B^2
Chromium	= +95.41+4.72* A-9.78* B+2.83* AB-2.29* A^2-4.29* B^2
Zinc	= +72.18+5.51* A-3.33* B-1.32* AB-2.50* A^2+0.94* B^2
Iron	= +66.23+6.90* A-4.24* B+0.32* AB+3.98 * A^2+5.36* B2

4.5.2.2 Analysis of fitted model

Statistical parameters obtained from the ANOVA for the reduced model of the responses are given in Table 4.23. The models were found to be significant at (95%) confidence level by the Fisher's test with all p-values of regression ≤ 0.05. In addition, the models did not exhibit lack of fit (p>0.05) indicating insignificant lack of fit. The R^2 values for turbidity, COD, lead, chromium, zinc and iron removal by Maerua Decumbent coagulant were 0.9596, 0.9830, 0.9523, 0.9604, 0.9435 and 0.9607 respectively. The values of adjusted R^2 for turbidity, COD, lead, chromium, zinc and iron were 0.9232, 0.9677, 0.9183, 0.9320, 0.9022 and 0.9326 respectively. The values for adjusted R^2 were high indicating significance of the model (Ahmad, Ismail, & Bhatia, 2005; Khuri & Cornell, 1996). The difference between the adjusted and predicted R^2 obtained were ≤0.2, table 4.28 d confirming the accuracy of the model.
The significant (p<0.05) terms for turbidity removal were A, B, C, AB, BC, A^2, B^2, C^2 whereas for COD were A, B, C, BC, A^2, B^2, C^2. For the heavy metals the significant (p< 0.05) terms were A, B, B^2 for lead, A, B, AB, A^2, B^2 for chromium, A, B, A^2, for zinc and A, B, A^2, B^2 for iron (Table 4.23). Adequate precision was found to be higher than 4 for all the responses (Table 4.23).

Table 4.23: Anova analysis for turbidity, COD, leads chromium, zinc and iron using Maerua coagulant

Variable	Maerua Turbidity	COD	Lead	Chromium	Zinc	Iron
Significant terms	A, B, C, AB, BC, A^2, B^2, C^2	A, B, C, BC, A^2, B^2, C^2	A, B, B^2	A, B, AB, A^2, B^2	A,B,A^2	A,B,A^2,B^2
R2	0.9939	0.9593	0.9583	0.9671	0.9114	0.9367
Adj.R2	0.9885	0.9227	0.9285	0.9436	0.8481	0.8914
Pre.R2	0.9652	0.7789	0.7667	0.8133	0.7038	0.7320
Prob>F	< 0.0001	< 0.0001	0.0001	< 0.0001	0.0014	0.0005
Adequate Precision	45.262	16.537	18.229	18.364	13.472	11.79
Standard Deviation	2.24	5.63	1.20	2.34	2.34	2.78
Coefficient variance	3.05	12.09	1.25	2.56	3.28	3.86
PRESS	289.12	1726.38	56.88	217.17	127.9	299.17
Probability of Lack of fit	0.2444	0.2602	0.1262	0.1133	0.6332	0.4065

4.5.2.3 Diagnostic plots (Figure 4.115 to 4.117) for analysis of model developed by use of Maerua Decumbent for removal of turbidity, COD, Lead, chromium, zinc and iron.

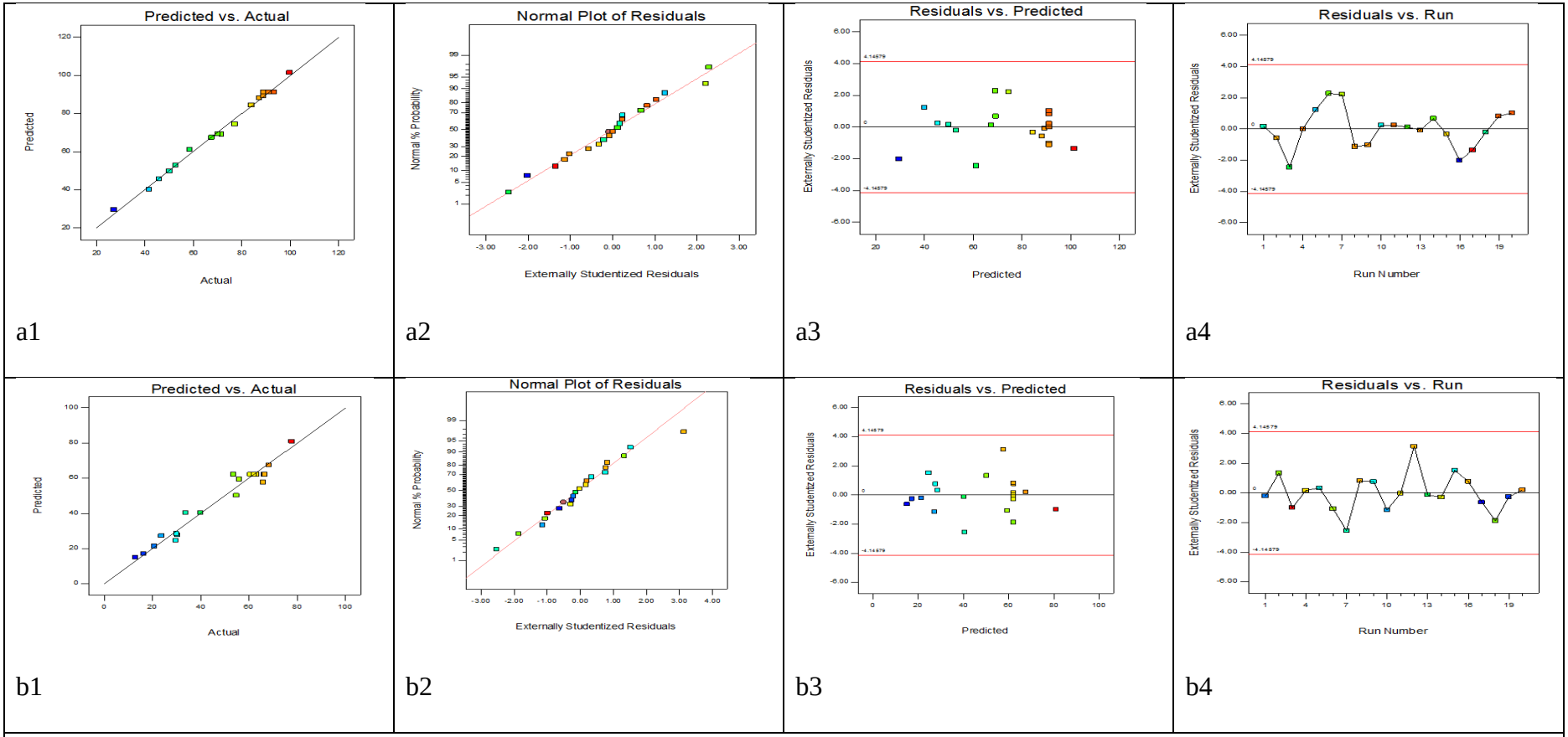

Figure 4.114: Design expert diagnostic plots for a (turbidity) and b (COD)

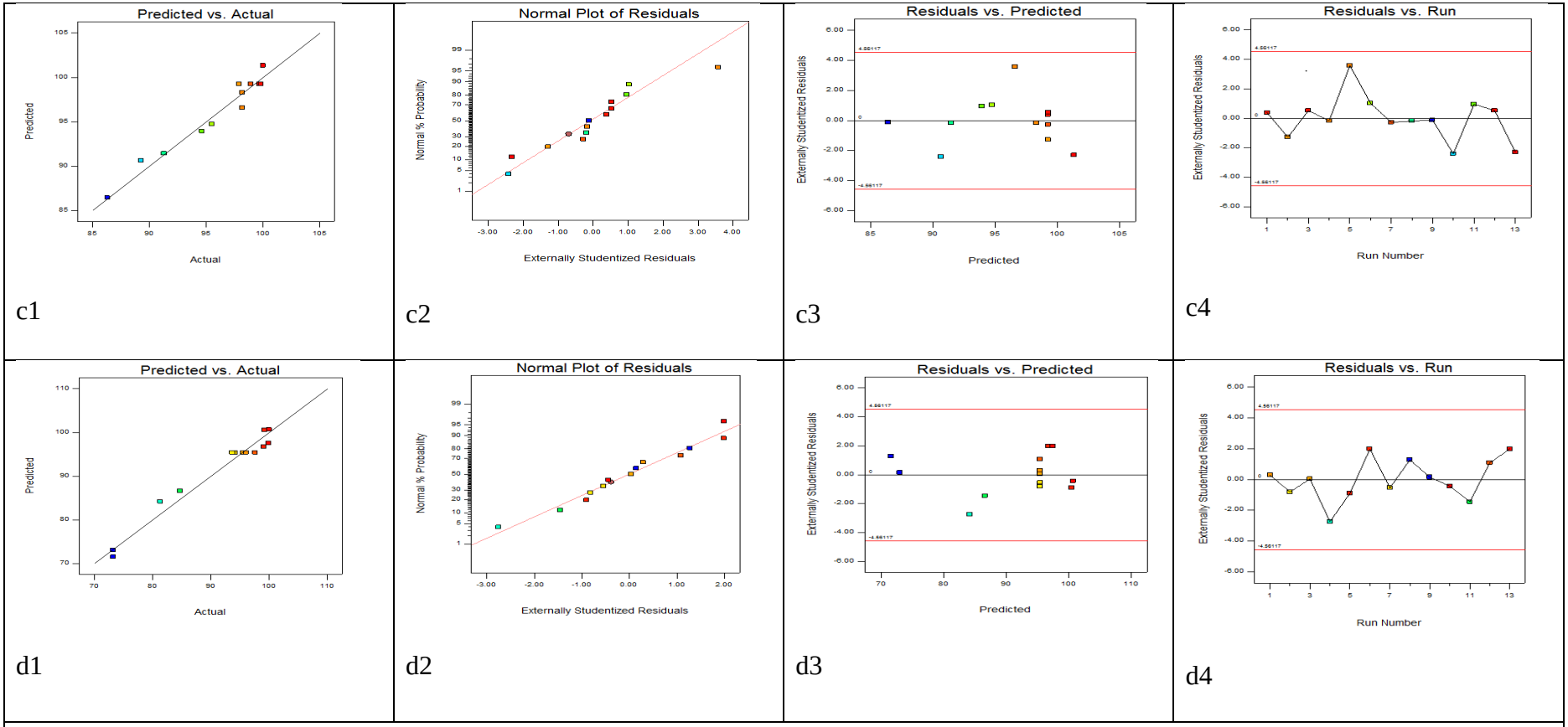

Figure 4.115: Design expert diagnostic plots for c (lead) and d (chromium)

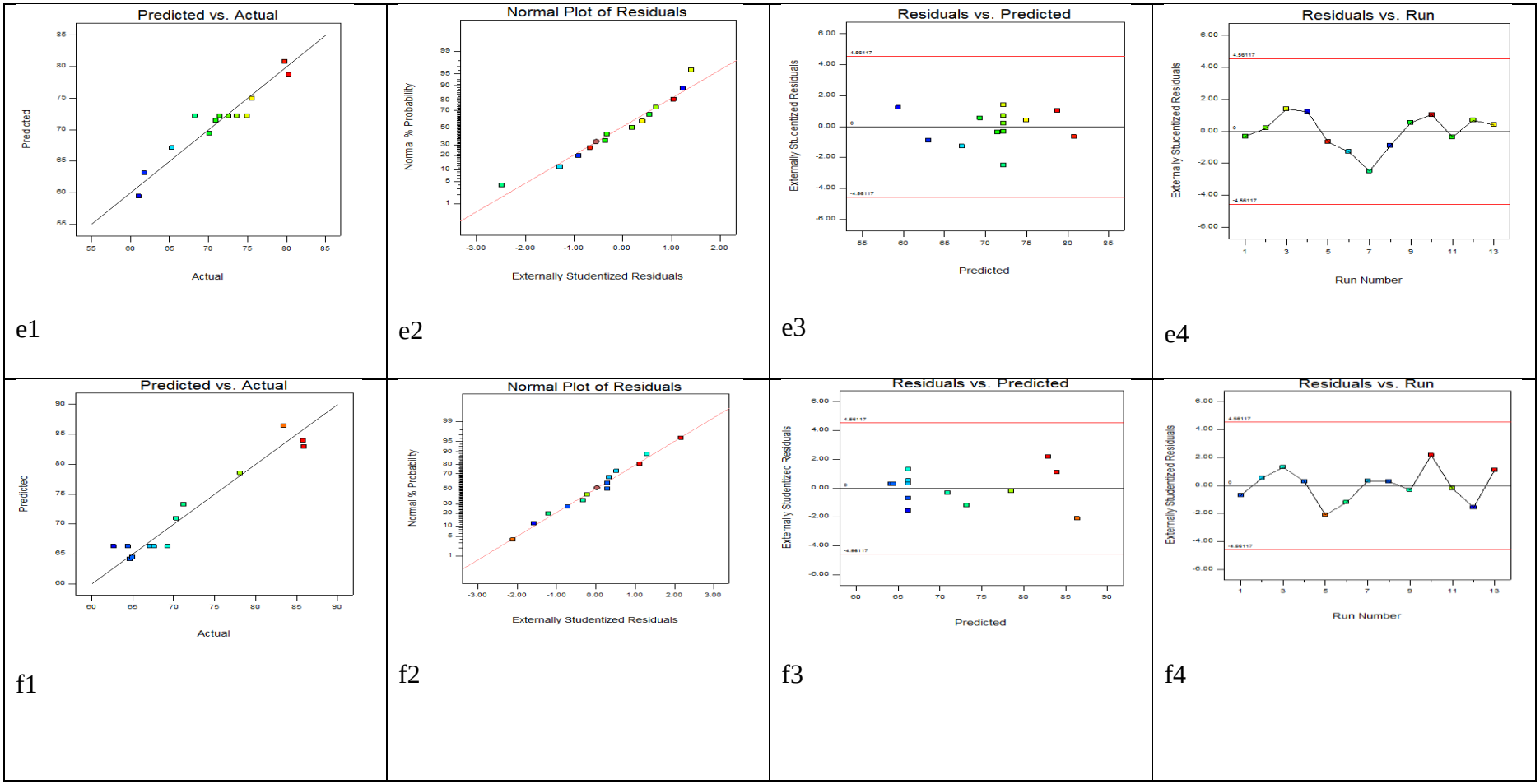

Figure 4.116: Design expert diagnostic plots for e (zinc) and f (iron)

The predicted versus actual plots for turbidity, COD, lead, chromium, zinc and iron shows that the models fitted well due to the fact that the data points are distributed randomly along the 45 degree line. The normal plot shows that the set of data used for this experiment is normally distributed because the pattern approximates a straight line. The data points for residual vs. Predicted are scattered randomly and for residuals versus experimental runs do not form a trend. All the data points in both plots are within the boundaries marked by the red line. Therefore, there are no outlier data.

4.5.2.4 Evaluation of process variables

From the 3D response surface and 2D contour plotting, turbidity removal of above 90 % was achieved when using Maerua at pH range of 5-7, dosage range of 0.85- 1.3 g/l and settling time in the range of 35-60 minutes (Figure 4.118). COD removal of above 60% was observed at pH range of 5-6, dosage range of 0.7-1g/l and settling time range of 40-60 minutes (Figure 4.119). For the heavy metals, over 95 % removal of lead was found at pH range of 6-7.5 and dosage range of 0.7-1.3 g/l, for chromium over 90% removal was found at pH range of 5-6 and dosage range of 0.9-1.3 g/l, and for zinc and iron 80% removal was observed at dosage range of 1.15-1.3 g/l and pH range of 5-6 (Figure 4.120 and 4.121).

Studies on the use of other natural coagulants for turbidity, COD and heavy metal were carried out by Som, Idris, & Hamid, 2007 , Tasneembano & Arjun, 2013 and Ravikumar and sheeja, 2013. Som, Idris, & Hamid, 2007 reported turbidty and COD removal of 99 and 92-97% respectively when Drgaon fruit was used as coagualnt; Tasneembano & Arjun, 2013 reported that Moringa Oliefera and Cicer arietinum removed 82 % of turbidity and 90 % of COD and Ravikumar and sheeja, 2013 reported 70-95% of heavy metal removal by Moringa Oliefera

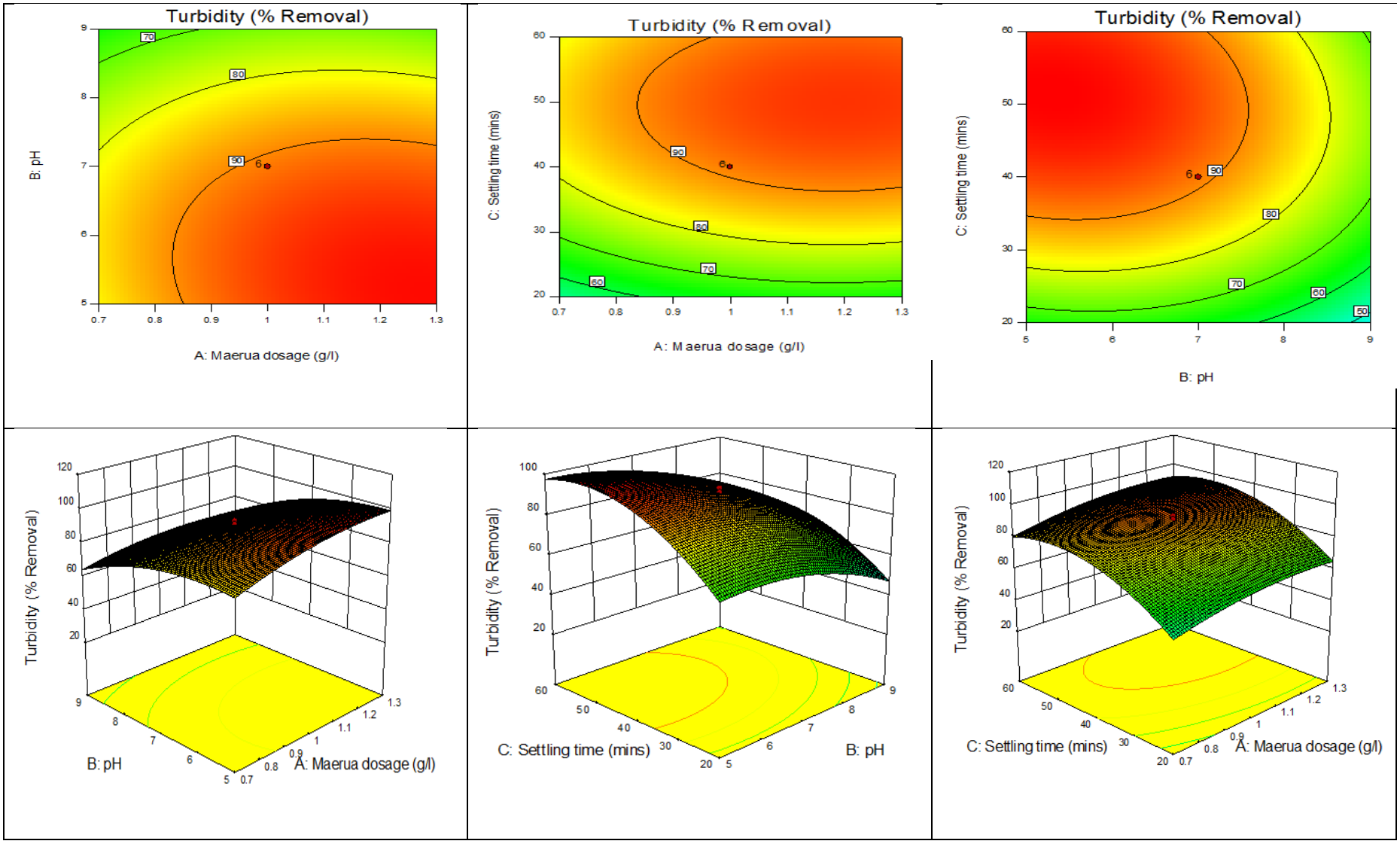

Figure 4.117: Contour and 3D plots for turbidity removal using Maerua Decumbent coagulant

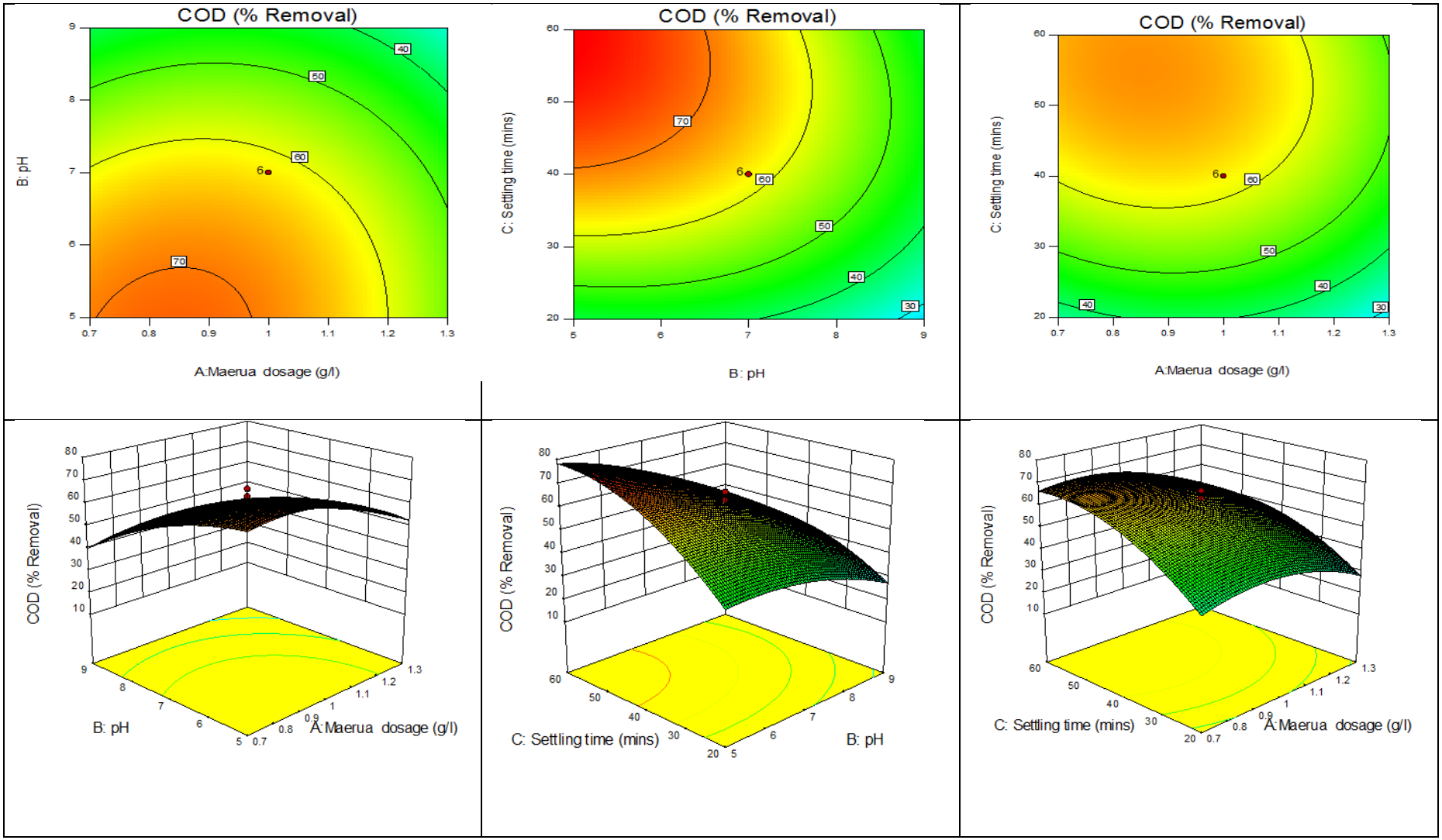

Figure 4.118: Contour and 3D plots for COD removal using Maerua Decumbent coagulant

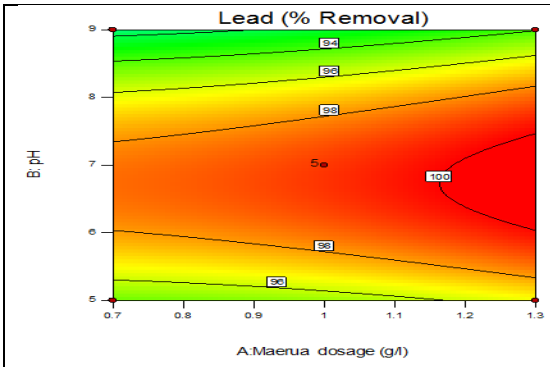

a1

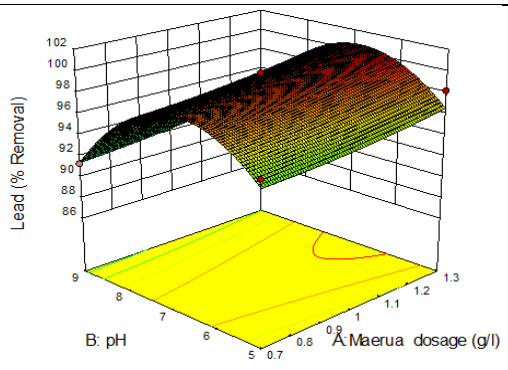

a2

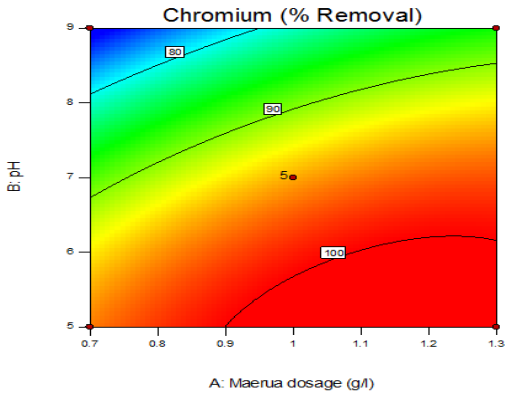

b1

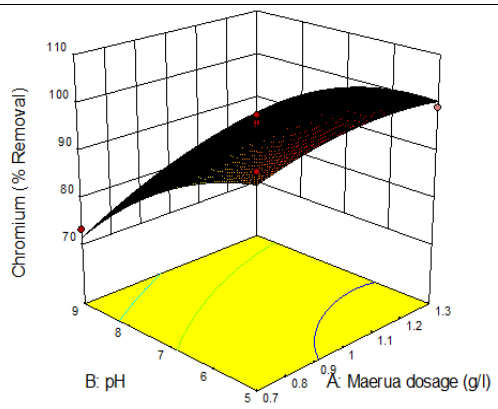

b2

Figure 4.119: Contour and 3D plots for a (lead) and b (chromium) removal using Maerua coagulant.

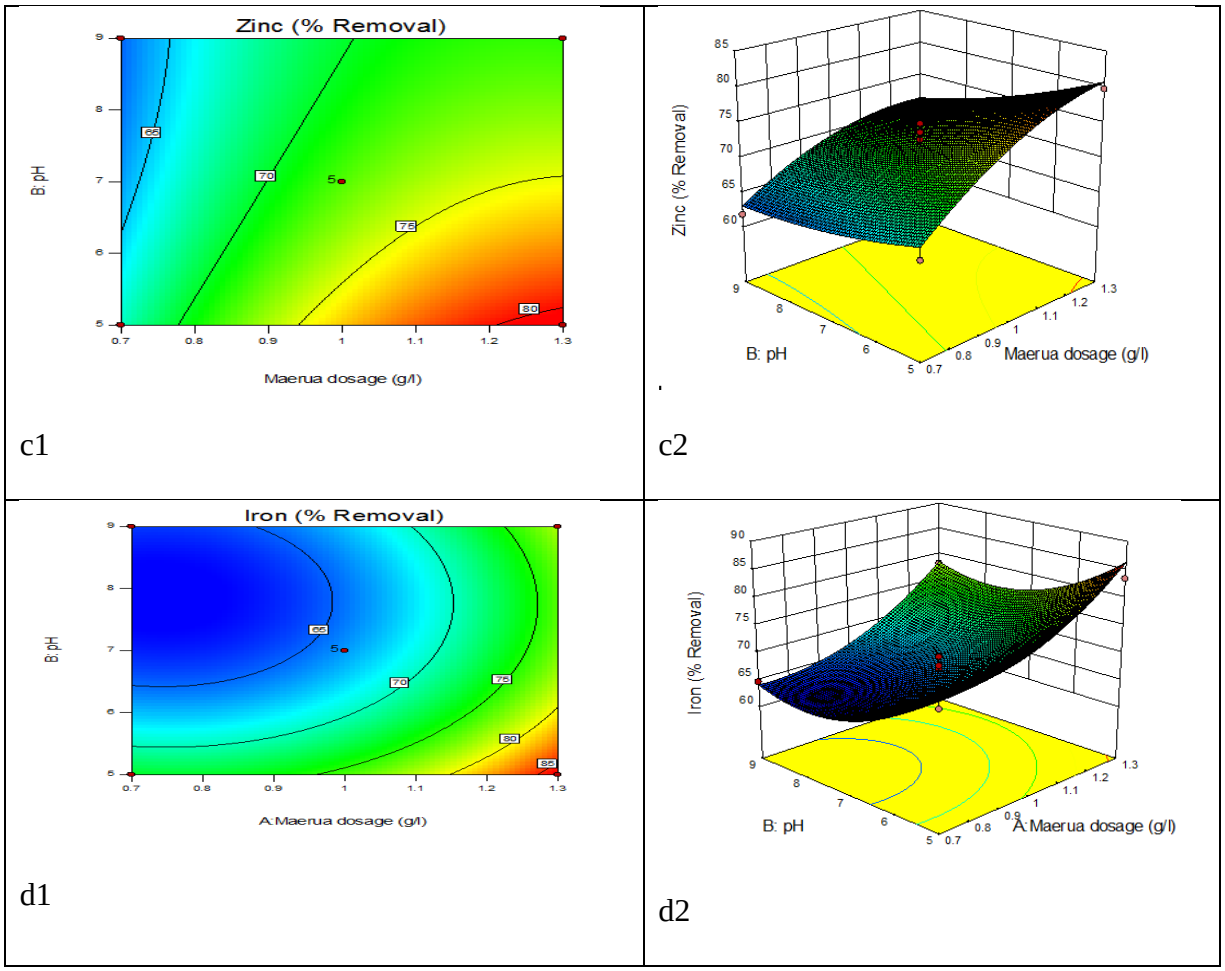

Figure 4.120: Contour and 3D plots for c (zinc) and d (iron) removal using Maerua coagulant

4.5.2.5 Design expert result and validation

Optimal conditions and optimization results are shown in Table 4.24. Results of laboratory experiments based on the predicted optimal conditions are also shown in Table 4.24.

Table 4.24: Numerical optimization and verification for turbidity, COD, lead, chromium, zinc and iron using Maerua

Response	Maerua dosage (g/l)	pH	Settling time (min)	Predicted value (% removal)	Experimental value (% removal)	Error (%)
Turbidity	1.0	5.56	52.31	99.97	99.24	0.73
COD	0.8	5.1	53.52	80.08	78.61	1.47
Lead	1.165	6.81	60	100	100	-
Chromium	1.028	5.78	60	100	99.97	0.03
Zinc	1.3	5.0	60	80.72	81.24	-0.52
Iron	1.3	5	60	86.384	85.61	0.77

4.5.2.6 Graphical multiple response optimization for turbidity, COD and heavy metal using Maerua Decumbent.

The turbidity and COD removal were two individual responses and their optimizations were achieved under different optimal conditions. The optimal turbidity removal might impact on the COD removal and vice versa. Therefore, a compromise between the optimum conditions for the two responses is desirable. By defining a desirability of 90 % turbidity removal and 70 % of COD removal, the optimal conditions can be visualized graphically by superimposing the contours for the two responses in an overlain plot as shown Figure 4.122. For the heavy metals a desirability of 95% for lead, 99% for chromium, 75 % for both zinc and iron, the optimal conditions can also be visualized graphically by superimposing the contours for the four responses in an overlain plot as shown in Figure 4.123.

Graphical optimization displays the area of feasible response values in the factor space. The area that satisfies the constraints is shade yellow, while the area that does not meet the criteria is gray. From the region shaded yellow shown in Figure 4.123, a compromise for 97.1% turbidity removal and 75.9% COD removal can be met at 0.945 g/l Maerua, pH 5.85 and settling time of 55.54 minutes whereas from Figure 4.124, a compromise of 98.37, 100, 78.25 and 78.31 % of lead, chromium, zinc and iron respectively were met at 1.2 g/l of Maerua and pH of 5.57 (Table 4.25).

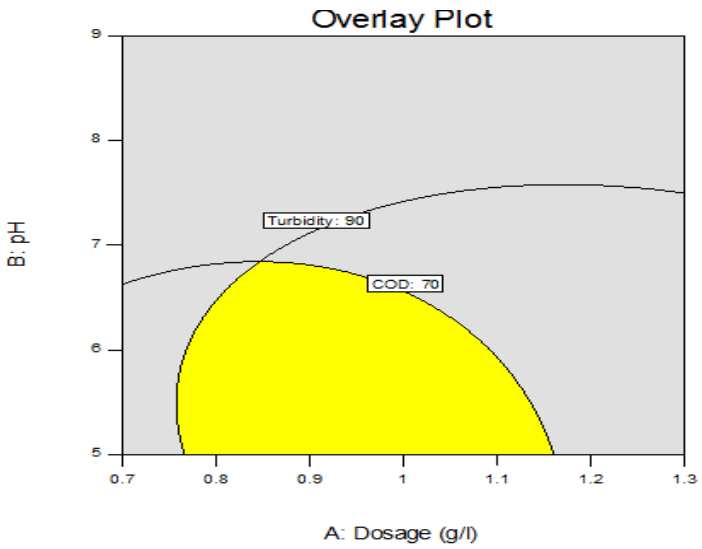

Figure 4.121: Design expert plot; overlay plot for optimal region for turbidity and COD using Maerua coagulant

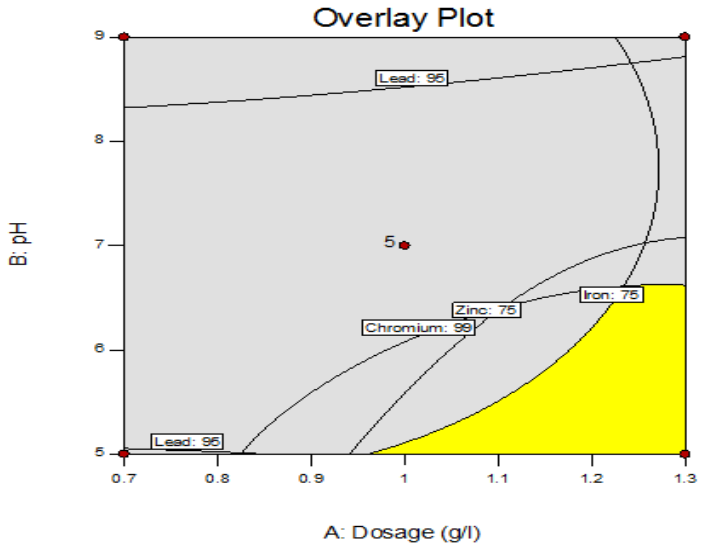

Figure 4.122: Design expert plot; overlay plot for optimal region for lead, chromium, zinc and iron using Maerua coagulant

Table 4.25: Predicted and verification results for multiple response analysis.

Optimized factors	Response	Predicted values (% removal)	Experimental values (% removal)	Error (%)
Maerua dosage 0.945g/l; pH 5.85, settling time 55.5 min	Turbidity	97.08	96.76	0.32
	COD	75.85	73.91	1.94
Maerua 1.2g/l	Lead	98.37	97.56	0.81
At pH 5.57	Chromium	100	99.27	0.73
	Zinc	78.25	75.41	2.84
	Iron	78.31	77.69	0.62

4.5.3 Optimization of paint wastewater treatment using alum

Treatment of paint wastewater using alum was optimized using RSM. The variables considered were alum dosage (g/l) (A), pH (B) and settling time (mins) (C) for turbidity and COD removal whereas for heavy metal removal the variables considered were alum dosage (A) and pH (B). The results of the CCD are in (Appendix Table C1 and C2). Regression model equations (Table 4.26) were developed from the CCD according to Equation 3.19 for the various responses.

Table 4.26: Model equations in terms of coded factors

Turbidity	= +69.08+22.21* A-9.08* B+7.73* C-1.44* AB+0.82* AC+2.38* BC -5.51 * A^2+1.62 * B^2-3.00* C^2
COD	= +41.09+17.20* A-7.07* B+5.58* C-3.99* AB+2.91* AC-0.14* BC-5.04 * A^2-0.75 * B^2 -2.87* C^2
Lead	= +82.50+18.58* A-0.57* B-4.28* AB-10.09* A^2+5.33* B^2
Chromium	= +74.37+13.32* A-8.55* B-4.57* AB-8.34* A^2+0.70* B^2
Zinc	=+54.17+11.60* A-3.82* B-5.69* AB-5.41* A^2+17.22* B^2
Iron	=+63.84+11.89* A-2.85* B-5.10* AB-4.76* A^2+10.52* B^2

(a) Analysis of variance

Analyse of variance (ANOVA) of the models obtained from CCD were found to be significant at (95%) confidence level by the Fisher's test with all p-values of regression ≤ 0.05 (Table 4.27). In addition, the models did not exhibit lack of fit ($p>0.05$)

indicating insignificant lack of fit. The R^2 values for turbidity, COD, lead, chromium, zinc and iron removal by alum coagulant were, 0.9774, 0.9467, 0.9634, 0.9866, 0.9509 and 0.9549 respectively. The values of adjusted R^2 for turbidity, COD, lead, chromium, zinc and iron were 0.9570, 0.8987, 0.9373, 0.9770, 0.9159 and 0.9226 respectively. The values for adjusted R^2 were also high indicating significance of the model (Khuri & Cornell, 1996, Ahmad *et al.,* 2005;).

It was also observed (Table 4.27) that the coefficient terms such dosage (A), pH (B), Settling time (C) were significant ($p<0.05$) in the removal of both turbidity and COD. This results compares well with the studies by (Ghafali *et al.,* 2008) and (Amirhossein & Sim, 2013) who found out that alum dosage and pH were significant in the removal of turbidity, COD, Color and TSS from a leachate and palm oil effluent.

Table 4.27: Anova analysis for turbidity, COD, leads chromium, zinc and iron using Alum coagulant

Variable	alum Turbidity	COD	Lead	Chromium	Zinc	iron
Significant terms	A, B, C, A^2, C^2	A, B, C, A^2	A, A^2, B^2	A, B, AB, A^2	A,A^2,B^2	A, AB, A^2, B^2
R2	0.9774	0.9467	0.9634	0.9866	0.9509	0.9549
Adj.R^2	0.9570	0.8987	0.9373	0.9770	0.9159	0.9226
Pre.R^2	0.8599	0.7032	0.8044	0.9475	0.8192	0.7483
Prob>F	< 0.0001	< 0.0001	< 0.0001	< 0.0001	0.0002	0.0001
Adequate Precision	25.825	17.681	20.962	35.636	18.65	19.25
Standard Deviation	4.65	5.71	4.57	2.24	5.29	3.97
Coefficient of variance	7.23	16.24	5.75	3.22	8.62	5.89
PRESS	1340.36	1815.75	783.44	138.26	722.95	615.63
Probability of Lack of fit	0.1122	0.2267	0.1673	0.4842	0.5443	0.1293

The square terms A^2 and C^2 were significant for turbidity removal and A^2 for COD removal. The significant ($p< 0.05$) terms for the heavy metal removal were A, A^2, B^2 for lead, A, B, AB, A^2 for chromium , A, A^2, B^2 for zinc and A, AB, A^2, B^2 for iron (Table 4.27).

The major conditions affecting alum coagulant in the removal of turbidity, COD, lead and zinc were the linear and quadratic, however for chromium and iron interactive effects between alum dosage and pH were found to affect its removal.
Adequate precision (AP) compares the range of the predicted values at the design points to the average prediction error. Ratios greater than 4 indicate adequate model discrimination (Mason, Gunst, & Hess, 2003). Adequate precision was found to be higher than 4 for all the responses (Table 4.27).

(b) Diagnostic plots using alum

The diagnostic plots (Appendix Figure C1) were found to follow the recommended trend (Statease, 2014), an indication that the regression models used for response measurement were significant and adequate.

(c) Evaluation of process variables

From the 3D response surface plots and the contour plots (Appendix Figure C2 and C3), over 90 % turbidity and over 60% COD were removed from paint wastewater using alum coagulant at a dosage range of 0.82-1 g/l, pH range of 7-8 and settling time range of 50-60 minutes. 100% of lead, 90% of chromium and 80% of zinc and iron were removed at alum dosage range of 0.7 -1.0 g/l and pH range of 7-7.5 (Appendix Figure C4).

(d) Optimization and model validation

Numerical optimization was employed and the desired maximum goal was set for each factor and responses. Optimal conditions and optimization results are shown in Table 4.28. Laboratory experiments were conducted based on the predicted optimal conditions and the results are shown in Table 4.28.

Table 4.28 : Numerical optimization and verification results for individual response using Alum coagulant

Response	Alum dosage (g/l)	pH	Settling time (mins)	Predicted value (% removal)	Experimental value (% removal)	Error
Turbidity	1.0	7.0	47.75	99.85	98.61	1.24
COD	1.0	7.0	55.73	68.57	66.22	2.35
Lead	0.89	7.0	60	99.42	96.16	3.26
Chromium	1.0	7.0	60	93.18	94.38	-1.2
Zinc	1.0	7.2	60	87.10	86.24	0.86
Iron	1.0	7.2	60	89.44	90.06	-0.62

(e). Graphical multiple response optimization for turbidity and COD using Alum

By defining a desirability of 90% turbidity removal and 60% of COD removal, the optimal conditions can be visualized graphically by superimposing the contours for the two responses in an overlain plot (Appendix Figure C5). For the heavy metal a desirability of 90% for both lead and chromium and 80% for zinc and iron, the optimal conditions can also be visualized graphically by superimposing the contours for the four responses in an overlain plot (Appendix Figure C6)

A compromise for 97.41% turbidity removal, and 65.38% COD removal was met at 0.95 g/l alum, pH 7.29 and settling time of 55.73 minutes and , a compromise of 99.49, 91.91, 83.45 and 86.35 % of lead, chromium, zinc and iron respectively were met at 0.925 g/l and pH of 7.10 (Appendix Table C3)

4.5.4 Optimization of paint wastewater treatment using Alum and banana pith as coagulants

The treatment of Paint wastewater using combined alum and banana pith was optimized using RSM. The variables alum dosage(g/l)(A), banana dosage(g/l)(B), pH(C) and settling time(mins)(D) were used in the CCD on removal of turbidity and COD whereas for the removal of heavy metals the variables used were alum dosage (A), banana dosage(B) and pH (C). The CCD design and results are shown in (Appendix Table D1 and D2). Second-order polynomial response model according to equation 3.19 was applied to reveal the interaction between four factors (alum dose, banana pith dose, pH and settling time) and two responses (turbidity and COD) and between three factors (alum dose, banana pith dose and pH and four responses (lead, chromium, zinc and iron) from which empirical relationship (Table 4.29) were obtained.

Table 4.29: Model Equations in terms of coded values

Turbidity	=+74.52+8.96 * A+5.62* B-10.09* C+13.60* D-4.28* AB-1.79* AC+2.80* AD +1.13 * BC-1.00* BD-1.02* CD-6.71* A^2-5.21* B^2+0.92 * C^2-7.63* D^2
COD	=+62.30+11.58* A+2.30* B-13.37* C+9.29 * D-4.84* AB-0.32* AC-0.18* AD +1.40* BC-0.45* BD+0.042 * CD-6.14* A^2-5.72* B^2-1.82* C^2-7.74* D^2
Lead	= +94.27+7.12* A+3.90* B-2.57* C-5.00* AB+0.48* AC-1.69* BC-2.67 * A^2 -2.53* B^2+0.59* C^2
Chromium	= +89.53+5.00* A+4.73* B-3.57* C-1.22* AB-1.09* AC+0.31* BC-1.32 * A^2 -2.77* B^2+2.15* C^2
Zinc	= +84.42+7.45* A+4.88* B-1.76* C-0.051* AB-7.71* AC-1.02* BC+0.050 * A^2-3.11* B^2-3.75 * C^2
Iron	= +74.37+4.56 * A+8.18* B-0.76* C-3.06* AB-0.87* AC-2.64* BC-4.30* A^2- 0.98* B^2 -0.58* C^2

(a) Analysis of variance

The models were found to be significant at (95%) confidence level by the Fisher's test with all p-values of regression ≤ 0.05 (Table 4.30). In addition, the models did not exhibit lack of fit ($p>0.05$) indicating insignificant lack of fit. The R^2 values for

turbidity, COD, lead, chromium, zinc and iron removal by alum and banana pith coagulant were, 0.9469, 0.9357, 0.8873, 0.9362, 0.9526 and 0.9367 respectively. The values of adjusted R^2 for turbidity, COD, lead, chromium, zinc and iron were 0.8973, 0.8757, 0.7859, 0.8789, 0.91and 0.8798 respectively. The values for adjusted R^2 were also high indicating significance of the model (Ahmad *et al.,* 2005; Khuri & Cornell, 1996). The difference between the adjusted and predicted R^2 obtained were ≤0.2, Table 4.30 confirming the accuracy of the model. The linear terms A, B, C, D, interactive term AB, square terms A^2, B^2 and D^2 were significant ($p<0.05$) in the removal of turbidity whereas for COD removal the significant terms were found to be the linear terms A, C, D; interactive terms AB and square terms A^2, B^2 and D^2. The significant terms ($p< 0.05$) for heavy metal removal were A, B, C, AB, A^2 and D^2 for lead, A, B, C B^2 and C^2 for chromium, A, B, AC, B^2 and C^2 for zinc and A, B, AB, BC and A^2 for iron (Table 4.30). Adequate precision was found to be higher than 4 for all the responses (Table 4.30)

Table 4.30: Anova analysis for turbidity, COD, lead chromium, zinc and iron using alum and banana pith coagulant

	Alum and Banana pith					
Variable	Turbidity	COD	Lead	Chromium	Zinc	iron
Significant terms	A,B,C,D, AB,A^2,B^2 ,D^2	A,C,D,AB,A^2,B^2, D^2	A, B, C, AB, A^2, B^2	A, B, C, B^2, C^2	A, B, AC, B^2, C^2	A, B, AB, BC, A2
R^2	0.9469	0.9357	0.8873	0.9362	0.9526	0.9367
Adj.R^2	0.8973	0.8757	0.7859	0.8789	0.9100	0.8798
Pre.R^2	0.7202	0.6796	0.6157	0.7330	0.7330	0.7075
Prob>F	<0.0001	<0.0001	<0.0011	<0.0001	<0.00001	<0.0001
Adequate Precision	16.43	15.44	9.354	14.643	19.24	15.167
Standard Deviation	7.02	7.69	4.23	2.69	3.10	3.30
Coefficient of variance	11.78	17.03	4.64	3.05	3.88	4.69
PRESS	3893.4	4423.7	610.29	303.45	540.39	503.54
Probability of Lack of fit	0.0745	0.1878	0.7887	0.6498	0.2404	0.4835

(b) Diagnostic plots using alum and banana pith coagulant

The diagnostic plots for turbidity, COD, lead, chromium, zinc and iron (Appendix Figure D1) were within the recommended trends hence models used for response measurement were significant and adequate.

(c) Evaluation of process variables

The 3D and contour plots (Appendix Figure D2) for removal of turbidity indicate that, over 90 % of turbidity was removed at alum dosage range of 0.7-0.8 g/l, banana pith dosage range of 0.3-0.6 g/l, pH range of 7-7.5 and settling time of 24-30 minutes. Over 70 % of COD (Appendix Figure D3) removal was recorded at alum dosage range of 0.55-0.8 g/l, banana pith dosage range of 0.25-0.58 g/l, pH range of 7-8 and settling time range of 18-30 minutes.The removal of heavy metal also varied with the variables, over 90% of lead and chromium (Appendix Figure D4 and D5) was observed at the alum dosage range of 0.55-0.8g/l, banana pith dosage range of 0.2-0.8 g/l and pH of 7-11. Zinc and iron removal of over 80 % (Appendix Figure D6 and D7) was achieved at alum dosage of 0.5-0.8 g/l, banana pith dosage range of 0.3-0.8 and pH range of 7-10.

(d) Optimization and model validation

Numerical optimization was employed and the desired maximum goal was set for each factor and responses. Optimal conditions and optimization results are shown in Table 4.31. Laboratory experiments were conducted based on the predicted optimal conditions and the results are shown in Table 4.31

Table 4.31: Numerical optimization and verification for turbidity, COD, lead, chromium, zinc and iron using alum and banana pith.

Response	Alum dosage (g/l)	Banana pith (g/l)	pH	Settling time (mins)	Predicted value (% removal)	Experimental value (% removal)	Error (%)
Turbidity	0.79	0.43	7.02	29.00	98.92	96.58	2.34
COD	0.71	0.32	7.19	25.00	80.67	79.25	1.42
Lead	0.69	0.53	7.45	30.00	99.97	99.99	-0.02
Chromium	0.78	0.45	7.09	30.00	100	100	-
Zinc	0.79	0.48	7.99	30.00	96.71	97.02	-0.31
Iron	0.66	0.60	7.00	30.00	84.71	86.42	-1.71

(e) Graphical multiple response optimization for turbidity, COD and heavy metal using alum and banana pith.

By defining a desirability of 90 % turbidity removal and 70 % of COD removal, the optimal conditions can be visualized graphically by superimposing the contours for the two responses in an overlain plot as shown (Appendix Figure D8). For the heavy metal a desirability of 95% for both lead and chromium, 85% for zinc and 70% for iron, the optimal conditions can also be visualized graphically by superimposing the contours for the four responses in an overlain plot as shown in (Appendix Figure D9).

A compromise for 92.79 % turbidity removal and 76.89 % COD removal was met at 0.63 g/l alum, 0.47 g/l banana pith pH 7.11 and settling time of 25.76 minutes whereas, a compromise of 99.74, 97.74, 88.79 and 76.09 % of lead, chromium, zinc and iron respectively were met at 0.68 g/l of alum, 0.4g/l of banana pith and pH of 7.00 (Appendix Table D3)

4.5.5 Optimization of paint wastewater treatment using Opuntia Spp. and CKD

The effects Opuntia Spp. dosage (A), CKD dosage (B) and Settling time (C) on removal of turbidity and COD and the effects of Opuntia Spp. dosage (A) and CKD dosage (B) on removal of heavy metals through coagulation-flocculation process was analysed using response surface methodology (RSM) (Appendix Table E1 and E 2)

The regression equations development from the CCD designs based on (Equation 3.17) for turbidity, COD, lead, chromium, zinc and iron are presented in Table 4.32

Table 4.32: Model equations in terms of coded factors

Turbidity	= +84.21+7.77*A+11.90*B+9.68*C-.98*AB+1.74*AC+0.94*BC-5.39*A2-1.79* B2-3.43* C2
COD	=+67.99+6.44*A+18.85*B+9.69*C-6.250E-003*AB-4.11*AC-2.80*BC-7.49*A2-8.03*B2-1.71*C2
Lead	=+91.68+11.08*A+10.52*B+0.63*AB-13.13A2-4.26B2
Chromium	= +85.88+6.52*A+16.49*B-3.57*AB-4.27*A2-2.63*B2
Zinc	= +81.13+12.00*A+7.49*B-4.33*AB-1.69*A2+5.60*B2
Iron	= +87.16+7.73*A+10.65*B+6.11AB-11.43*A2-4.08*B2

(a) Analysis of variance

Statistical parameters obtained from the ANOVA for the reduced model of the responses are given in Table 4.33. The models were found to be significant at (95%) confidence level by the Fisher's test with all p-values of regression ≤ 0.05. In addition, the models did not exhibit lack of fit ($p>0.05$) indicating insignificant lack of fit. The R^2 values for turbidity, COD, lead, chromium, zinc and iron removal by Opuntia Spp. and CKD coagulant were 0.9939, 0.9593, 0.9471, 0.9114 and 0.9184 respectively. The values of adjusted R^2 for turbidity, COD, lead, chromium, zinc and iron were 0.9885, 0.9227, 0.9093, 0.9436, 0.8481 and 0.8602 respectively. The values for adjusted R^2 were high indicating significance of the model. The difference between the adjusted and predicted R^2 obtained were ≤ 0.2 (Table 4.33), which confirmed the accuracy of the model.

The significant ($p<0.05$) terms for turbidity removal were A, B, C, A^2, C^2 whereas for COD were A, B, C, AC, A^2, B^2. For the heavy metals the significant ($p< 0.05$) terms were A, B, A^2 for lead, A, B, A^2 for chromium, A, B, B^2, for zinc and A, B, A^2, for iron (Table 4.33). Adequate precision was found to be higher than 4 (Table 4.33) for all the responses.

(b) Diagnostic plots using Opuntia Spp. and Cement Kiln Dust

Diagnostic plots for analysis of model developed by use of Opuntia Spp. and CKD for removal of turbidity, COD, lead, chromium, zinc and iron indicated that the models used to predict the responses were adequate and significant since the plots were within the recommended trends (Appendix E1).

(c) Evaluation of process variables

The 3D and contour plotting indicated, over 90 % of turbidity is removed at Opuntia Spp. dosage range of 0.3-0.6 g/l, CKD dosage range of 8.5-10 ml, and settling time of 20-30 minutes (Appendix Figure E2). Similarly, 70 % of COD (Appendix Figure E3) removal was recorded at Opuntia Spp. dosage range of 0.5-0.6 g/l, CKD dosage range of 8.5-10 ml and settling time range of 25-30 minutes.

Similar to turbidity and COD, the removal of heavy metal varied with coagulant dosage. Over 90 % of lead was observed at the Opuntia Spp. dosage range of 0.35-0.7g/l and CKD dosage range of 6.5-l0 ml, chromium, over 90 % removal was achieved at Opuntia spp. dosage range of 0.2-0.7 g/l and CKD dosage range of 8-10 ml. Over 90 % zinc removal was achieved at Opuntia Spp. dosage range of 0.5-0.7 g/l and CKD dosage range of 7-10 ml and iron removal of over 90 % was achieved at Opuntia Spp. dosage range of 0.2-0.7 g/l and CKD dosage range of 7.5-10 ml (Appendix Figure E4)

Table 4.33: Anova analysis for turbidity, COD, leads chromium, zinc and iron using Opuntia Spp. and CKD coagulant.

Variable	Opuntia and CKD Turbidity	COD	Lead	Chromium	Zinc	Iron
Significant terms	A,B,C,A^2 ,C^2	A,B,C,AC,A^2,B^2	A,B,A^2	A,B,A^2	A,B,B^2	A,B,A^2
R2	0.9596	0.9830	0.9471	0.9604	0.9435	0.9184
Adj.R2	0.9232	0.9677	0.9093	0.9320	0.9022	0.8602
Pre.R2	0.8278	0.9296	0.7526	0.8186	0.7028	0.6638
Prob>F	<0.0001	<0.0001	0.0002	<0.0001	<0.0001	0.0011
Adequate Precision	18.66	26.065	14.258	18.93	15.24	11.20
Standard Deviation	4.45	3.83	4.99	4.01	4.07	5.62
Coefficient of variance	5.78	6.81	6.16	4.91	4.87	7.24
PRESS	842	607.5	813.5	514.45	611.6	911.74
Probability of Lack of fit	0.600	0.614	0.3030	0.3256	0.1802	0.4334

(d) Optimization and model validation

Numerical optimization was employed and the desired maximum goal was set for each factor and responses. Optimal conditions and optimization results are shown in Table 4.34. Experiments to validate the optimization were conducted based on the predicted optimal conditions and the results are shown in Table 4.34.

Table 4.34: Numerical optimization and verification for turbidity, COD, lead, chromium, zinc and iron using Opuntia Spp. and CKD

Response	Opuntia Spp. dosage (g/l)	CKD (ml)	Settling time(min)	Predicted value (% removal)	Experimental value (% removal)	Error (%)
Turbidity	0.533	8.91	29.8	99.79	99.65	0.14
COD	0.523	9.46	22.9	80.97	80.21	0.76
Chromium	0.560	9.960	30	100	99.93	0.07
Zinc	0.7	9.87	30	99.6	98.56	1.04
Iron	0.601	10	30	97.92	97.25	0.67

(e) Graphical multiple response optimization for turbidity, COD and heavy metal using Opuntia Spp. and CKD

By defining a desirability of 90 % turbidity removal and 70 % of COD removal, the optimal conditions were visualized graphically by superimposing the contours for the two responses in an overlain plot as shown (Appendix Figure E5). For the heavy metals, a desirability of 90 % for both lead and chromium, 80 % for both zinc and iron was defined. The optimal conditions are depicted by superimposing the contours for the four responses in an overlain plot (Appendix Figure E6).

Graphical optimization displayed, a compromise for 93.44% turbidity removal, and 78.96% COD removal can be met at 0.52 g/l Opuntia Spp., CKD dosage of 9.32 ml and settling time of 20 minutes. whereas for heavy metal removal, a compromise removal of 98.0, 94.28, 88.87 and 93.53% of lead, chromium, zinc and iron respectively were met at 0.52 g/l of Opuntia Spp. and CKD of 8.45 ml (Appendix Table E3).

4.5.6 General discussion on use of RSM in optimization of pollutants removal from paint industry wastewater

Coagulation process was optimized using RSM. The relationship between coagulation-flocculation process responses: a) Turbidity and COD removals with variables (coagulant dosage, pH and settling time) and b) Lead, chromium, zinc and iron removals with variables (coagulant dosage and pH) were evaluated using CCD.

Quadratic models were found suitable to represent the correlation between experimental data and all responses because it had the lowest p value and highest coefficient of determination (R^2), adjusted R^2 and predicted R^2. The significant terms that majorly influenced the removal of the various pollutants were determined for the different coagulants.

The percent contributions of the various variables in the removal of the pollutants were determined based on the sum of square. When Maerua Decumbent was used as the coagulant, the linear terms that is Maerua dosage, pH and settling time were found to have the greatest contribution in turbidity and COD removal with a total contribution

of 54.25% (4.95 % Maerua dosage, 21.42% pH and 27.88% settling time) and 63.18% (7.17% Maerua dosage, 28.12% pH and 27.89% settling time) respectively. They were followed by quadratic terms with a total contribution 44.45% (3.21% Maerua dosage^2, 9.68% pH^2 and 31.56% settling time^2) and the least contribution from the interactive factors of 1.30% (0.67% dosage and pH, 0% (dosage and settling time) and 0.63% (pH and settling time). For the heavy metals that is lead, chromium, zinc and iron removal, the linear effects were 11.9, 82.74, 85.38, 62.86% respectively whereas the interactive effects were 0.05, 2.81, 1.81, 0.05% and quadratic effects were 88.06, 14.45, 12.81, 37.10% (Appendix Table F1). All the linear, quadratic and interactive terms had effects on the removal of the pollutants studied with an exception of interaction between dosage and settling time which had negligible effect on the removal of COD. When alum coagulant was used for removal of turbidity, COD, lead chromium and iron the linear terms played the greatest role with a total of 92.8, 88.21, 73.84, 77.82 and 53.72 % respectively, followed by quadratic terms with 6.48, 8.45, 24.2, 18.93 and 41.61% and finally the interactive effects with a total of 0.72, 0.72, 1.96, 3.25 and 4.67% (Appendix Table F2)

When alum was combined with banana pith the total contribution from the linear effects were 69.9, 70.42, 69.96, 78.57, 57.71 and 74.08% for turbidity, COD, lead, chromium, zinc and iron removal. The interactive effects were 3.82, 2.99, 15.89, 2.13, 24.77 and 8.42%. For quadratic effects the totals were 26.29, 26.58, 14.14, 19.30, 17.53 and 17.50% (Appendix Table F3). For Opuntia Spp. and CKD the linear effects were 84.56%, interactive 2.14% and quadratic 13.30% for turbidity removal and 77.21% linear, 2.28% interactive and 20.51% quadratic effects for COD removals. For lead, chromium zinc and iron the total linear effects were 58.45, 91.76, 83.64 and 54.14 % respectively whereas the interactive effects were 0.05, 1.86, 3.92 and 5.83% and quadratic effects were 41.50, 6.38, 12.44 and 40.03% (Appendix Table F4).

In order to figure out the mutual influence of factors on the responses, response surface and contour plots were used. From the analysis of 3D response surface and contour plots, the ranges of various variables were obtained, which were then used to determine the optimal conditions for the optimum responses.

The turbidity removal at optimum conditions for different coagulants were, 99.24% at Maerua dosage of 1.0 g/l, pH of 5.56 and settling time 52.31 mins, 98.61% at alum dosage of 1.0 g/l, pH 7 and settling time 47.8 mins, 96.58% at 0.79 g/l of alum, 0.43 g/l of banana pith, pH 7.02 and settling time of 29 minutes and 99.65% at 0.53 g/l of Opuntia Spp. and 8.91 ml of ckd and settling time of 29.8 minutes.

For COD the removals were 78.61% at Maerua dosage of 0.8 g/l, pH of 5.1 and settling time of 53.52 minutes, 66.22% at alum dosage of 1.0g/l, pH 7 and settling time of 55.7 mins, 79.25% at alum dosage of 0.71 g/l, 0.32 g/l of banana pith, pH of 7.2 and settling time of 25 minutes and 80.21% at Opuntia Spp. dosage of 0.52 g/l, 9.46 ml of ckd and settling time of 22.9 minutes.

Over 95% of turbidity was removed from the paint wastewater by the various coagulants. The combination of bio-coagulant with either alum or ckd reduced the settling time of treatment to approximately 30 minutes of treatment. This implies that heavier flocs are formed when such combinations are used resulting to faster settling as compared to when either alum or Maerua was used individually.

The removal of COD was not as good as that of turbidity. The highest removal of over 80% was achieved when Opuntia Spp. and CKD coagulant were used which did not satisfy the discharge limit (50 mg/l) hence in the case of COD removal the coagulation process should be used as a pre-treatment process.

At optimum conditions the removal of lead for different coagulants were 100% at 1.17 g/l of Maerua dosage and pH 6.81, 96.16% at 0.9 g/l of alum dosage and pH 7, 99.99% at 0.69 g/l of alum, 0.53 g/l of banana pith and pH 7.45, and 99.56% at 0.576 g/l of Opuntia Spp. and 9.48 ml of ckd. From the results it was found out that Maerua and both alum and banana coagulants were able to reduce lead in the effluent to the recommended level of 0.01 mg/l from 4.19 mg/l. For chromium the removal were 94.38% at 1.0 g/l of alum dosage and pH 7, 100% at 0.78 g/l of alum, 0.45 g/l of banana pith and pH 7.09, 99.97% at 1.03 g/l of Maerua dosage at pH 5.78 and 99.93% removal of chromium at 0.56 g/l of Opuntia Spp. and 9.96 ml of ckd. The recommended level of chromium to effluent discharge to the environment is 2 mg/l. All coagulants used in this study were able to remove chromium from paint wastewater to this

recommended level from 3.24 mg/l. Zinc removals were 81.24% at 1.3 g/l of Maerua dosage and pH 5.0, 86.24% at 1.0 g/l of alum dosage and pH 7.2, 97.02% at 0.79 g/l of alum, 0.48 g/l of banana pith and pH 7.99, and 98.56% at 0.7 g/l of Opuntia Spp. and 9.87ml of ckd.

The amount of zinc in the raw wastewater was 3.17 mg/l and the recommended level is 0.5 mg/l. Therefore all the coagulants with the exception of Maerua Decumbent were found to be effective in the removal of zinc from paint wastewater. Finally the removals of iron were 85.61% at1.3 g/l of Maerua dosage at pH 5, 90.06% at1.0 g/l of alum dosage at pH 7.2, 86.42% at 0.66 g/l of alum, 0.6 g/l of banana pith and pH of 7.00, and 97.92% at 0.6 g/l of Opuntia Spp. and 10 ml of ckd. The recommended level for iron in the final effluent to the environment is 10 mg/l., all the coagulants were able to reduce the amount of iron from 42.9 mg/l to less than 10 mg/l.

The experiments were conducted under optimum conditions to confirm the validity of the statistical experimental strategies. The obtained removal results of the experiments were close to those estimated by using response surface methodology. These validation experiments proved that the developed models could be considered to be accurate and reliable.

4.6 Evaluation of Sensitivity analysis for pollutant removal using Maerua Decumbent.

4.6.1 Sensitivity of dosage, pH and settling time on turbidity removal

The sensitivity equation for the dosage were obtained by differentiating equation (4.9) the model equations for turbidity in terms of actual terms with respect to dosage, pH and Settling time resulting to equation 4.10, 4.11 and 4.12 respectively, which was solved and the results are presented in Table 4.35.

Turbidity = +91.18+5.62* A-11.70* B+13.34* C-2.70* AB+0.20* AC-2.61* BC-4.41* A^2- 7.66*B^2-13.82* C^2

(4.9)

$$\frac{dT}{dA} = 5.62 - 2.7B + 0.2C - 8.82A$$

(4.10)

$$\frac{dT}{dB} = -11.7 - 2.7A - 2.61C - 15.32B$$

(4.11)

$$\frac{dT}{dC} = 13.34 + 0.2A - 2.61B - 27.64C$$

(4.12)

It should be noted that T represents turbidity; A represents dosage; B represents pH and C represents settling time.

Table 4.35: Turbidity sensitivity of process parameters

		B =7; C (mins) =40		
		dT/dA	dT/dB	dT/dC
Dosage, A (g/l)	0.5	20.44	-7.16	13.00
	0.7	14.44	-9.00	13.14
	1	5.62	-11.70	13.34
	1.3	-3.20	-14.40	13.54
	1.51	-9.20	-16.24	13.676
Dosage, A (g/l)=1.00, Setting time C,(mins)=40.00				
pH,	3.64	10.16	14.04	17.72
	5	8.32	3.62	15.95
	7	5.62	-11.70	13.34
	9	2.92	-27.02	10.73
	10.36	1.08	-37.44	8.96
Dosage, A (g/l)=1.00, pH, B =7.00				
Setting time, C(mins)	6.36	5.28	-7.31	59.78
	20	5.42	-9.09	40.98
	40	5.62	-11.7	13.34
	60	5.82	-14.31	-14.3
	73.64	5.956	-16.08	-33.09

Table 4.34 presents the effects of varying various process parameters and their sensitivity to turbidity removal. All the process parameters were found sensitive to turbidity removal. Most sensitive noted to be dosage followed by pH and then settling time.

4.6.2 Sensitivity of dosage, pH and settling time on COD removal

The sensitivity equation for the dosage were obtained by differentiating equation (4.13) the model equations for COD in terms of actual terms with respect to dosage, pH and Settling time resulting to equation 4.14, 4.15 and 4.16 respectively, which was solved and the results are presented in Table 4.36.

COD = +62.20-6.44* A-12.75* B+12.70* C+2.09* AB-2.23* AC-5.39* BC-

8.05* A2 –5.70* B2-9.12* C2

(4.13)

$$\frac{dCoD}{dA} = -6.44 + 2.09B - 2.23C - 16.1A$$

(4.14)

$$\frac{dCoD}{dB} = -12.75 + 2.09A - 5.39C - 11.4B$$

(4.15)

$$\frac{dCod}{dC} = 12.7 - 2.23A - 5.39B - 18.24C$$

(4.16)

Table 4.36: COD sensitivity of process parameters

pH, B =7.00, Setting time, C (mins) =40.00				
		dt/dA	dt/dB	dt/dC
Dosage, A (g/l)	0.5	20.61	-16.26	16.45
	0.7	9.66	-14.84	14.93
	1	-6.44	-12.75	12.7
	1.3	-22.54	-10.66	10.47
	1.51	-33.49	-9.24	8.95
Dosage, A (g/l)=1.00, Setting time C,(mins)=40.00				
pH,	3.64	-9.95	6.40	21.76
	5	-8.53	-1.35	18.09
	7	-6.44	-12.75	12.7
	9	-4.35	-24.15	7.31
	10.36	-2.93	-31.90	3.65
Dosage, A (g/l)=1.00, pH, B =7.00				
Setting time, C(mins)	6.36	-2.69	-3.69	43.34
	20	-4.21	-7.36	30.94
	40	-6.44	-12.75	12.7
	60	-8.67	-18.14	-5.54
	73.64	-10.18	-21.81	-17.94

The variation of dosage was found highly sensitive to COD removal (Table 4.36) Variation of pH and settling were also found to be sensitive on turbidity removal. The negative values of sensitivities mean that the turbidity removal decrease with the corresponding decrease in the values of the pH and settling time.

4.6.3 Sensitivity of dosage and pH on chromium removal

The sensitivity equation for the dosage were obtained by differentiating equation (4.17) the model equations for chromium in terms of actual terms with respect to dosage and pH resulting to equation 4.18 and 4.19 respectively, which was solved and the results are presented in Table 4.37.

Chromium = +95.41+4.72* A-9.78* B+2.83* AB-2.29* A2-4.29* B2

(4.17)

$$\frac{dCr}{dA} = 4.72 + 2.83B - 4.58A$$

(4.18)

$$\frac{dCr}{dB} = -9.78 + 2.83A - 8.58B$$

(4.19)

Table 4.37: Chromium sensitivity of process parameters

		pH,B =7.00	
		dCr/dA	dCr/dB
Dosage, A(g/l)	0.58	9.95	-13.01
	0.7	9.3	-12.61
	1	4.72	-9.78
	1.3	0.14	-6.95
	1.42	-0.51	-6.55
		Dosage =1.00g/l	
pH, B	4.17	1.49	0.01
	5	1.89	-1.2
	7	4.72	-9.78
	9	7.55	-18.36
	9.83	7.95	-19.57

4.6.4 Sensitivity of dosage and pH on lead removal

The sensitivity equation for the dosage were obtained by differentiating equation (4.20) the model equations for chromium in terms of actual terms with respect to dosage and pH resulting to equation 4.21 and 4.22 respectively, which was solved and the results are presented in Table 4.38.

Lead = +99.24+1.08* A-1.49* B+0.17* AB+0.29* A^2-5.36* B^2

(4.20)

$$\frac{dL}{dA} = 1.08 + 0.17B + 0.58A$$

(4.21)

$$\frac{dL}{dB} = -1.49 + 0.17A - 10.72B$$

(4.22)

Table 4.38: Turbidity sensitivity of process parameters

		pH =7.00			Dosage =1.0 g/l		
		dL/dA	dL/dB			dL/dA	dL/dA
Dosage, A(g/l)	0.58	0.42	-1.68	pH, B	4.17	0.89	10.75
	0.7	0.5	-1.66		5	0.91	9.23
	1	1.08	-1.49		7	1.08	-1.49
	1.3	1.66	-1.32		9	1.25	-12.21
	1.42	1.74	-1.29		9.83	1.27	-13.73

The variation of pH and dosage for both chromium and lead removal were found to be sensitive as depicted in Tables 4.37 and 4.38.

CHAPTER FIVE

CONCLUSSION AND RECOMMENDATIONS

5.1 CONCLUSIONS

This study evaluated the potential use of selected plant materials as coagulants and bio-sorbent in water and waste treatment. The study characterised the plant materials using proximate, elemental and functional group analysis and evaluated their removal of turbidity, COD, Pb, Cr, Cu and Zn from water. The following conclusions have been drawn from the study:

Characterisation of banana pith, Maerua Decumbent and Opuntia Spp. revealed that they comprised of polysaccharides, proteins and lipids with functional groups amino, carboxyl, sulfate, hydroxyl among others that play an important role in the removal of contaminants from polluted water.

Bio-sorption batch studies achieved maximum removal of Pb, Cr, Cu and Zn of 97.5, 82.8, 91.0 and 87.6%, respectively with 2 g/l Banana pith dose at pH 5; 94.2, 95.5, 83.4 and 79.0 % with 2 g/l of Maerua Decumbent dose at pH 5 and 97.6, 96.6, 93.0 and 91.4% with 1g/l Opuntia Spp. dose at pH 5. Langmuir and Freundlich isotherm models described the sorption data of the three-studied biomass, ($R^2 \approx 0.9$) with sorption kinetic data best described by the second order kinetic models suggesting that chemical sorption process could have been dominant. The experimental data was best described by Yoon Nelson model.

Using low dosages (0.1 g/L) of banana pith, Maerua Decumbent and Opuntia Spp. in an acidic environment over 98 % of turbidity was removed through coagulation – flocculation processes following second order kinetics. The removal of the heavy metal by the three bio-coagulants, Banana pith, Maerua Decumbent and Opuntia Spp., from the River water varied between 50% to 100% at different pH and dosage values. At optimal conditions established with response surface Methodology, Maerua decumbent removed 95, 70, 98, 99, 75 and 77 % of turbidity, COD, Pb, Cr, Zn and Fe which compared favorably with those of alum at optimal conditions, hence was concluded that Response surface methodology approach is an effective tool for modelling and optimization of coagulation-flocculation processes.

5.2 RECOMMENDATION

1. The performance test of the bio-coagulants and bio-sorbents were carried out using only one variety of the Musa Spp. (Musa Acuminata), Opuntia Spp. (Opuntia Monacantha) and Maerua Spp. (Maerua Decumbent) of the plant materials. The study recommends further research on the potential use of other varieties of the same species and the other parts of the plant (leaves, fruit)
2. The study recommends commercialization of Banana pith and Maerua Decumbent in water and wastewater treatment.

REFERENCES

Abbas, H., Dheyaa, W., & Ahmed, H. (2013). A comparative adsorption/biosorption for the removal of phenol and lead onto granular activated carbon and dried anaerobic sludge. *Desalination and water treatment, 51*(10-12), 2055-2067.

Ahalya, N., Ramachandra, T., & Kanamadi, R. (2003). Biosorption of Heavy metals. *Research journal of Chemistry and Environment, 7*(4), 71-79.

Ahmad, A., & Hameed , B. (2010). Fixed bed adsorption of reactive azo dye onto granular activated carbon prepared from waste. *Journal of hazardous Materials, 175*(1-3), 298-303.

Ahmad, A., Ismail, S., & Bhatia, S. (2005). Optimization of coagulation-flocculation process for palm oil mill effluent using response surface methodolgy. *Environtal Science & technology, 39*(8), 2828-2834.

Ahmad, A., Sumathi, S., & Hameed, B. (2006). Coagulation of residue oil mill effluent by chitosan,alum and PAC. *Chemical Engineering Journal, 118*(1), 99-105.

Ahmet , S., & Mustafa, T. (2008). Biosorption of Cd(II) from aqueous solution by red algae (Ceramium virgatum):Equilibrium,kinetics and thermodynamic studies. *Journal of hazardous Materials, 157*(2), 448-454.

Ajmal , M., Khan, A., Ahamd, S., & Ahmad, A. (1998). Role of saw dust in the removal of copper(II) from industrial wastes. *Water research, 32*(10), 3085-3091.

Alluri, H., Ronda, S., Settalluri, V., Bondili, J., Suryanarayana, V., & Venkateshwar, P. (2007). Biosorption:An eco-friendly alternative for heavy metal removal. *African Journal of Biotechnology, 6*(25), 2924-2931.

Amirhossein, M., & Sim, Y. (2013). Application of response surface methodology to optimize coagulation-flocculation treatment of anaerobically digetsed palm oil mill effluent using alum. *Desalination and water treatment, 51*(34), 6729-6935.

AOAC. (1999). *Official Methods of Analysis.* USA.

Aparecido, N., Fernado, R., Claudinata, A., & Diego, R. (2015). Assessment of the banana Pseudo stem as a low cost biosorbent for the removal of reactive blue 5G dye. *Environmental Technology, 36*(22), 2892-2902.

APHA. (1998). *Standards Methods For the Examination of Water and wastewater.* Washington DC: American PublicHealth Association.

Apiratikal, R., & Pavasant, P. (2008). Batch and column studies of biosorption of heavy metal by caulerpa lentillifera. *Bioresource Technology, 99*(8), 2766-2777.

Aquoyo-Villarreal, I., Bonilla-Petriciolet, A., Hernandez-montesmoran, M., & Reynel-Avila, H. (2011). Batch and column studies of Zn 2+ removal from aquoeus solution using chicken feathers as sorbents. *Chemical Engineering Journal, 167*(1), 67-76.

Ariffin, A., Shatat, R., Nik, N., & Mohd, O. (2005). Synthetic polyelectrolytes of varying charge densities but similar molar mass based on acrylamide and application on palm oil effluent treatment. *Desalination, 173*(3), 201-208.

Association, A. W. (1990). *Water Quality and treatment.fourthedition,.* New York: McGraw Hill.

Atalay, E., Gode, F., & Sharma, Y. (2010). Removal of selected toxic metals by a modified adsorbent,. *Practice periodical of hazardous toxic and radioactive waste management, 14*(2), 132-138.

Aygun, A., & Yilmaz, T. (2010). Improvement of coagualtion-floccualation process for treatment of detergent wastewater using coagualnt aids. *International Journal in Chemical Environmental Engineering, 1*(2), 98-101.

Azouaou, N., Sadaoui, Z., Djaafri, A., & Mokaddem, H. (2010). Adsorption of cadmium from aqueous solution onto untretaed coffeegrounds:Equilibrium,kinetics and thermodynamics. *Journal of Harzardous materials, 184*(1), 126-134.

Babayemi, K., Onukwuli, D., & Menkiti, M. (2013). Coag-flocculation kinetics of mucuna sloaneiseedfor phosphorus removal from wastewater. *American journal of analytical chemistry, 4*(12), 732-738.

Babu, B., & Gupta, S. (2008). Adsorption of Cr(VI) using activated neem leaves:Kinetic study. *14*(2), 85-92.

Bahman, R. (2014). Ttreatment of water turbidity and bacteria by using a coagulant extracted from Plantago ovata. *Water Resources and Industry, 6*(1), 36-50.

Bailey, S., Olin, T., Bicka, R., & Adrian, D. (1999). A review of potentially low-cost sorbents for heavy metals. *Water Research, 33*(11), 2469-2479.

Baral, S., Dan, N., Ramulu, T., Sahoo, S., Das, S., & Chaudhury, G. (2009). Removal of Cr(Iv)by thermally activated weed Salvinia cucullata in a fixed bed column. *Journal of Hazardous Materials, 161*(2), 1427-1435.

Bark, N., Abdennouri, M., Boussaoud, A., & Makhfouk, M. (2010). Bisorption charatceristics of cdnium(II) onto scolymus hispanicus L.as a low naturall biosorbent. *Desalination, 258*(1-3), 66-71.

Bezerra , M., Santelli, R., Oliveira, E., Villar, L., & Escaleira, L. (2008). Response surcae methodology (RSM) as a tool for optimization in analytical chemistry. *Talanta, 76*(5), 965-977.

Bhatti, H., Mumtaz, B., Hanif, M., & Nadeem , R. (2007). Removal of ions from acqueous solution using Moringa oleifera lam(horseradish tree) biomass. *Process biochem., 42*(4), 547-553.

Bratby, J. (2006). *Coagulants,in Coagualtion and flocculation in Water and Wastewater Treatment* (2nd ed.). London: IWA Publishing.

Broide, M., & Cohen, R. (1992). Measurement of cluster size distributions arising in salt-induced aggregation of polystyrenemicrospheres. *Journal of colloid and interface Science, 153*(2), 493-508.

Bustillos, L., Carpinteyro-Urban, S., & Departamento, C. (2013). Production and characterization of Opuntia ficus indica mucilage. *International Journal of Biotechnology Resources, 1*(3), 038-045.

Calero, M., Hernainz, F., Blazquez, G., Tenorio, G., & Martin-lara, M. (2009). Study of cr(III) biosorption in a fixed bed column. *Journal of Hazardous Materials, 171*(1), 886-893.

Chambers, J., Cleveland, W., Kleiner, B., & Turkey, P. (1993). *Graphical methods for data anlaysis.* New York: Chapman and Hall.

Chandrasekhar, S., & Pramada, P. (2006). Rice Husk as ad adsorbent for methylen blue-effects of ashing temperature. *Adsorption, 12*(1), 27-43.

Chaney , R., Malik , K., Li, Y., Brown, S., Brewer, E., & Angels, J. (1997). phytoremediation of soil metals. *8*(1), 279-284.

Chaudhuri , M., & Babu, R. (2005). Home water treatment by direct filtration with natural coagulant. *Journal of Water and Health., 3*(1), 27-30.

Check, J. (2005). *Characterilzation and removal of nom from raw waters in coastal environments.* Atlanta: Georgia Institute of Technology.

Chen, J., & Hao, O. (1998). Microbial chromium(VI) reduction. *Critic.Rev.Environ.Sci.Technol., 28*(1), 219-251.

Costa, F. (1995). Existence and uniqueness of density coserving solutions to the coagulation-fragmentation equation with strong fragmentation. *Journal of Mathematical Analysis & Applications, 192*(3), 892-914.

Crisafully, R., Milhome, M., Cavalcante, R., Selveira, E., Keukeleire, D., & Nascimento, R. (2008). Removal of some polycyclic aromatic hydrocarbons from petrochemical wastewater using low-cost adsorbents of natural origin. *Journal of bioresource Technology, 99*(10), 4515-4519.

Dan, N., Vimala, R., & Karthika, P. (2008). Biosorption of heavy metals-An overview. *Indian journal of Biotechnology, 7*(1), 159-169.

Dang, V., Doan, H., Dang, V., & Lobi, A. (2009). Equilibrium and kinetics of biosorptipon of cadmium ii and copper ii ions by wheat straw. *Bioresource technology, 100*(1), 211-219.

Davis, M. (2010). *Water and Wastewater Engineeering.* New York: McGraw - Hill.

Davis, T., Volesky, B., & Vieira, R. (2000). Sargassum seaweed as biosorbent for heavy metals. *Water Research, 34*(17), 4270-4278.

Debye, P. (1942). *Trans.AM.Electro-chem.Soc.*, 82:265.

Dempsey, B. (1984). CRC Critical Reviews in Environmental Control. *14*, 311.

Design expert Software. (2006). *Users guide,Technical manual,vesion 7.* Minneapolis,MN: Stat-ease Inc.,.

Diaz, N., Rincon, A., Escorihuela, N., Fernandez, E., Chacin, E., & Forster, C. (1999). *Process Biochemistry, 35*(3), 391-395.

Ding, Y., Jing, D., Gong, H., Zhou, L., & Yang , X. (2012). Biosorption of aquatic cadmium(II) by un modified rice straw. *Bioresource Technology, 114*(1), 20-25.

Duan, J., & Gregory, J. (2003). Coagulation by hydrolysing metal salts. *Advances in colloids and interface Science., 1*(1), 475-502.

Ehrl, L., Soos, M., Morbidelli, M., & Babler, M. (2009). Dependence of initial cluster aggregation kinetics on shear rate fro particles of different sizes under turbulence. *AICHE Journal, 55*(12), 3076-3087.

El Awady, M., & Sami, T. (1997). Removal of Heavy metal by Cement kiln dust. *Journal of Environmental Contamination and toxicology, 59*(1), 603-610.

EL Zayat, Mohamed, Sherien, E., & Salah, E. (2012). Treatment of various types of wastewater using cement kiln dust. *Proceeding of the 5th international perspetive on water resources and Environment 2012.* Marrakesh.: environment and water reosurce institute of the American Society of Civil Engineering.

El-Said, A., Badaway, N., & Garamon. (2010). Adsorption of Cadmium(II) and mercury(II) onto Natural adsorbents Rice Husk ash(RHA) from Aqueous Solutions:Study in Single and Binary System. *Journal of American Science, 6*(12), 400-409.

EMCR. (2006). *Environ.Management and Co-ord.Regulations.Standards for Effluent Discharge into Public sewers,water quality.*

Environmantal protection agency (EPA). (2000). *Wastewater technology fact sheet chemical precipitation.* Washington DC: National Service Center for Environmental Publications (NSCEP).

Esawy, K. (2014). Application of Cement kiln dust for chemically ehhanced primary treatment of municipal wastewater. *Desalination and water Treatment, 52*(27), 4698-4700.

Farinella, N., Matos, G., & Arruda, M. (2007). Grape bagasse as a potential biosorbent of metals in effluent. *Bioresource Technology, 98*(10), 1940-1946.

Farooq, U., Kozinski, J., Khan, M., & Athar M. (2010). Biosorption of heavy metal ions using wheat based biosrbents-a review of the recent literature. *Bioresource Technology, 101*(14), 5043-5053.

Fathi, H., Moghadam, M., Taremi, M., & Rahmani, M. (2011). Robust Parameters Design in Optimization of Textile Systems Using Response Surface and Dual Response surface methodologies,. *World applied sciences jpurnal,, 14*(7), 973-979.

Febrianto, J., Kosasih, A., Sunarso, J., Indraswati, N., & Ismadji, S. (2009). Equilibrium and kinetics and kinetics studies in adsorption of heavy metals using biosorbent:A summary of recent studies. *Journal of hazardous materials, 162*(2), 616-645.

Fedala, N., Lounici, H., Drouichec, N., Mameria, N., & Drouiche, M. (2015). Physical parameters affecting coagualtion of turbid waters with Opuntia ficus-indica cactus. *Ecol.Engineering, 77*(1), 33-36.

Francisco, W., Andre, G., Jefferson, P., Morsyleide, F., Denis, K., & Ronaldo, F. (2010). Green coconut shells applied as adsorbent for removal of toxic metal ions using fixed bed column technology. *Journal of Environmental Management, 91*(8), 1634-1640.

Fridklisberg, D. (1984). *A course in colloid chemistry.* Moscow,Russia: Mir Publishers.

Gadd, G. (2010). Metals,minerals and microbes:geomicrobiology and bioremediation. *Microbiology, 156*(3), 609-643.

Geng., Y. (2005). *Application of flocs analysis for coagulation optimization at the split lake water treatment plant.* Winnipeg,Manitoba.

Ghafali, S., Aziz, H., Isa, M., & Zinatizadeh, A. (2008). Appilcation of reponse surface methodology (RSM)to optimize coagulation-flocculation treatment of leachate using poly-aluminium chloride(PAC) and alum. *Journal of Hazardous Materials, 163*(2), 650-658.

Godt, J., Scheidig, F., Grosse-Siestrup, C., Esche, V., Brandenburg, P., Reich, A., . . . Panias, D. (2007). Copper and cadnium adsorption onpellets made from fired coal fly ash. *J.hazard Mater., 148*(3), 538-547.

GOK. (1993). *Government of kenya Development plan.* NAirobi.: Government Printers.

Gourdon, R., Bhande, S., Rus, E., & Sofer, S. (2006). Comptive bacteria from activated sludgearison of camium biosorption by gram positive and gram neg. *Biotechnology Letters, 12*(1), 839-842.

Grimm, A., Zanzi, R., Bjornbom, E., & Cukieman, A. (2008). Comparison of different types of biomass for copper biosorption. *Bioresource technology, 99*(7), 2559-2565.

Guo, B., Hong, L., & Jiang, H. (2003). Macroporous Poly(calciumacrylate-divinybenzene) bead-selective orthophosphate sorbent. *Industrial Enginnering Chemical Reseearch, 42*(1), 559-5565.

Gupta, V., Carrott, P., & Ribeiro, C. (2009). Low cost adss:orbent:growing approach to wastewater treatment-a review. *Critical reviewsin Environmnta Science and Technology, 39*(10), 783-842.

Habsahalwi, J., Musa, M., & Hamid, K. (2013). A Preliminary Studyof BananaStem Juice as a Plant basedcoagulant for treatment of spent coolant waste water. *Journal of Chemistry, 1*.

Hamdy, A. (2000). Biosorption of heavy metals by Marine algae. *Current microbiology, 41*(4), 232-238.

Han, R., Zhao, X., Xu , Y., Li, Y., & Wang, Y. (2009b). Characterization and properties of iron oxide-coated zeolite as adsorbent for removal of copper (II) from solution in a fixed bed column. *Chemcal Engineering Journal, 149*(1), 123-131.

Hart, E. (2001). *Optimizing oagulant onditions for the Worcester Water Filtration Plant.* JYP0201, Faculty of Worcester Polytechnique Institute.

Hayelon, D., Tessema, D., & Worku, B. (2016). Investigation of coagulation activity of cactus powder in water treatment. *Journal of applied chemisty, 1*(1), 1-9.

Hendrawati, Eti, R., Hefni, E., & Latifah, K. (2015). Characterisation of physico-chemical properties of Nano-sized moringa oleifera Seed powder and its application as Natural coagualnt in water purification process. *Journal of Environment and Eath Science, 5*(21), 19-26.

Ho, Y., & McKay, G. (1999). Pseudo-second order model for sorption process. *Process Biochem, 34*(5), 451-465.

Ho, Y., Ng, J., & Mckay, G. (2000). Kinetics of pollutant sorption by biosorbents:review. *Sep.Purif.Methods, 29*(2), 189-232.

Holtholf, H., Egelhaaf, S., Brokovec, M., Sharteh-Berger, P., & Sticher, H. (1996). Coagulation rate measurement of colloidal particles by simultaeneous and nynamic light Scatterring. *Journal of American Chemical Society, 12*(23), 5541-5549.

Horsfall, M., Abia, A., & Spiff, A. (2006). Kinetic studies on the adsoption of Cd2+,Cu2+and znzn 2+ ions from aquoeus solutions by cassava (Manihot sculenta cranz) tuber bark waste. *Journal of Bioresource Technology, 97*(2), 283-291.

Hu, C., Liu, H., Qu, J., Wang, D., & Ru, J. (2006). Coagulation behaviour of aluminium salts in eutrophic wter:significance of A113 species and pH control. *Environ mental Science and Technolology, 40*(1), 325-331.

Hunters, R. (1993). *An introduction to modern colloid science.* New york: Oxford University Press.

Ibarra, J., & Moliner, R. (1991). Coal characterisation using pyrolysis-FT-IR. *J.Anal.Appl.pyrolysis, 20*(1), 171-184.

Jiang , J., & Graham, J. (1998). Pre-polymerised inorganic coagulants and phosphorus removal by coagulation-a review. *Water SA,, 24*(3), 237-244.

Jiang, J. (2001). Development of coagulation theory and pre-polymerised coagulants for water treatment. *Separaion and purification methods, 30*(1), 127-141.

Jiang-Ping, W., Yong-Zhen, C., Xue-Wu, G., & Han-Qing, Y. (2007). Optimization of coagulation-flocculation process for a papaer-recyling wastewater treatment using response surface methodology. *Colloids and Surfaces A:Physicochem.Eng.Aspects, 302*(1), 204-210.

Johnson, P., Watson, M., Brown , J., & Jefcoat, I. (2002). Peanuthull pellets as a single sorbent for the capture of Cu(II) from wastewater. *Journal of Waste Management, 22*(5), 471-480.

Joseane, D., Guilherme, F., Ricardo, F., & Rosangela, B. (2013). Coagulants and Natural polymers:Perspectives for the treatment of water. *Plascic and polymer Technology, 2*(3), 55-62.

Karthikeyan, S., Balasubramanian, R., & Iyer, C. (2007). Evaluation of Marine algae Ulva Fasciata and Sargassum Spp. for the biosorption of Cu(II) from aqueous solutions. *Biores.Technol., 98*(2), 452-455.

Khuri, A., & Cornell, J. (1996). *Response Surfaces,design and Analyses,2nd ed.* New York: Wiley and Sons.

Korbathi, B., & Tanyolac, A. (2008). Electrochemical treatment of simulated textile wastewater with industrial componentsand levafix blue CA reactive dye:Optimization through response surface methodology. *Journalof hazardous Materials, 151*(2), 422-431.

Kratochvil, D., & Volesky, B. (1998). Advances in the biosorption of heavy metals. *Trends in Biotechnology, 16*(7), 291-300.

Kumar, Y., King, P., & Prasad, V. (2006). Removal of copper from acqueosu solution using Ulva Fasciata Sp.A marine algae. *J.Hazard Mater., 137*(1), 367-373.

Kwaambwa, H., & Maikokera, R. (2007). A fluorescent specrtoscopic study of a coagulating protein extracted from moringa oleifera seeds. *Colloids and surfaces B: Biointerfaces, 60*(1), 213-220.

Larous, S., Meniai, A., & Lehocine, M. (2005). Experimental study of the removal of copper from aqueous solution by adsorption using sawdsut. *Desalination, 185*(1-3), 483-490.

Lawrence, K., Wang, J., Stephen, T., & Yung-Tse, H. (2010). *Handbook of environmental engineering,environmntal bioengineering.* London: Springer New York Dordrecht Heidelberg.

Lee, M., Paik, I., Kim, I., Kang, H., & Lee, S. (2007). Remediation of heavy metal contaminated ground water originated from abandoned mine using limeand calciumcarbonate. *Journal ofHazardous Materials, 144*(1), 208-214.

Lenz, G. F., Zara, R. F., & Thomazini, M. H. (2011). Study of the effeiciency of natural polymer extracted mandacaru cactus as caogulation and flocculation aids for water treatment. *Symposium on sustainable sytstems.* Toledo.

Letterman, R. (1999). *Water and Treatment. A Handbook of community water Supplies* (5 th ed.). The American Water Works Association, Inc. McGraw-Hill Book company.

Li, X., Zheng, W., Wang, D., Yang , Q., Cao, J., Yue, X., . . . Zeng, G. (2010). Removal of Pb (II) from aqueosu solutions by adsorption onto modified areca waste:Kinetic and thermodynamic studies. *Desalination, 258*(1), 148-153.

Liyang, I. (1988). *Effects of surface chemistry on kinetics of coagualtion of submicron iron oxide particles in water.* California: Pasedena:W.M. Keck Laboratory of ENvironmental Engineering Science, Division of Engineering and apllied Science.

Loderio, P., Herreo, R., & SastredeVicentes, M. (2006). The use of protonated Sargassum muticum as biosorbent for cadnium removal in a fixed bed column. *Journal of Hazard Materials, 137*(1), 244-253.

Lucas, S., & Cocero, M. (2004). Adsorption isotherms for Ethyllacetate and Furfural on activated carbon from Suoercritical Carbon Dioxide. *Fluid Phase Equilibria, 219*(1), 171-179.

Mackie, A., Boilard, S., Walsh, M., & Lake, C. (2010). physiochemical characterization of cement kiln dust for potential use in acidic wasteater treatment. *Journal of hazardous materials, 173*((1)), 283-291.

Magdy, Y., & Daifullah, A. (1988). Adsorption of a basic dye from aqueous solutions onto sugar -industry -mud in two modes of operations. *Waste manage., 18*(4), 219-226.

Mahajeri, S., Aziz, H., Zahed, M., Moahajeri, L., Bashir, M., Aziz, S., . . . Isa, M. (2011). Mutlipleresponses analysis and modelling of fenton process treatment of high strength Landfill leachate. *Water science and Technology, 64*(8), 1652-1660.

Manohar, D., Krishnan, K., & Anirudhan, T. (2002). Removal of Mercury (II) fro aqueous solutions and Chor-alkali industryusing 2-mercaptoberzimidazole-clay. *Water Res.,, 36*(1), 1609-1619.

Mason, R., Gunst, R., & Hess, J. (2003). *Statistical Design and Analysis of experiments,Eighth Applicationsto Engineering and Science* (2nd ed.). New York: Wiley.

Mathialagan, T., & Viraraghavan, T. (2009). Biosorption of pentachlorophenol from aqueous solutions by fungal biomass. *Bioresource technology, 100*(2), 549-558.

Mattoli, I., Cangi, F., Maidecchi, A., Ghiara, C., Ragazzi, E., Tubaro, M., . . . Traldi, P. (2006). Metabolomic finger printing of plant extracts. *J.Mass Spectrometry, 41*(12), 1534-1545.

Mavura, W., Chemelil, M., Saenyi, W., & Mavura, H. (2008). Investigation of chemical and biochemical properties of Maerua Subcordata extract: a local water clarification agent. *Bull.Chem.Soc.Ethiop., 22*(1), 143-148.

Mearkin, P. (1991). Fractal aggregates in geophysics. *Rev.Geo-Physics, 29*(1), 317-331.

Menkiti, M., & Onukwuli, O. (2011). Coagulation-flocculation studies of afzella bella coagulant in coal effluent using single and simulated angle nephelometry. *Journal of Mineral Material Characterization Engineering, 10*(2), 279-298.

Metcalf and Eddy, Inc. (1991). *Wastewater Engineering: Treatment, Disposal and Reuse.* USA: McGraw Hill.

Miller, S., Fugate, E., Craver, V., Smith, J., & Zimmerman, J. (2008). Toward undestanding the efficicacy and mechanism of Opuntia Spp. as a natural coagulant for potential application in water treatment. *Environmental Science and Technology, 42*(1), 4274-4279.

Mishra, A., & Malvika, B. (2005). Floccu;ation behaviour of model textile wastewater treated with a food grade polysaccharide . *Journal of Hazardous Materials, 118*(1-3), 213-217.

Mohammad, M., Parisa, R., Atefeh, A., & Ali, R. (2011). Kinetics and equilibrium studies on biosorption of cadmium,lead and nickel ions from aqueous solutions by intact and chemically modified brown algae. *Journal of Hazardous materials., 185*(1), 401-407.

Mohd, A., Lim, S., Zainura, N., & Zaini, U. (2008). Removal of boron from industrial wastewater by Chemical precipitation Using Chitosan. *Journal of Chemical and natural Resources Engineering, 4*(1), 1-11.

Montgomery, D. (1997). *Design and anlysis of experiments* (4th ed.). Hoboken,New Jersey: John Wiley and sons,inc.

Montgomery, D. (2001). *Design and Analysis of Experiment* (5th ed.). New York: Wiley.

Montgomery, D. (2008). *Design and analysis of Experiments* (7th ed.). New york: John Wiley and sons,Inc.

Montgomery, D. (2009). *Design and analysisi of experiments* (7th ed.). Hoboken: John Wiley and sons Ltd.

Moussas, P., & Zouboulis, A. (2008). A study on the properties and coagulation behaviour of modified inorganic polymeric coagualnt-polyferric silicate sulphate. *Seperation and Purification Technology, 63*(2), 475-483.

Muhammad, S., Muhammad, T., Muhammad, M., Syed, W., & Muhammad, Z. (2015). Potato Starch as a coaugulant for dye removal from textile wastewater. *Water, Air and Soil pollution, 226*(8), 1-11.

Muthuraman, G., Sasikala, S., & Prakash, N. (2013). Proteins from natural coagulant for potential application of turbidity removal in water. *International journal of Engineering and Innovative Technology (IJEIT), 3*(1), 278-283.

Muyubi, S. A., & Kuofu, C. A. (1995). Coagulation of low turbid surface water with moringa Oliefera seeds. *International Journal of Environmental studies, 46*(1), 263-273.

Mwachiro, E., Gachanja, A., & Mayabi, A. O. (2004). Development of Low Cost Water Purification System:Use of Moringa Oliefera and Maerua decumbent. *2nd Regional Microbiology conference*, (pp. 84-92).

Myers, R., Mongomery, D., & Anderson-cook, C. (2009). *Response surface methodology. Process and product optimization using designed experiments* (3rd ed.). Hoboken,New Jersey: John Wiley and sons,Inc.

Naja, G., & Volesky, B. (2006). Behaviour of mass transfer zone in a biosorption column. *Environmental Science and Technology, 40*(12), 3996-4003.

Nandini, M., & Sheba, C. (2016). Emanating trends in the Usage of Bio-coagulants in portable water treatment :A review. *International journal of Engineering and Technology, 3*(1), 970-974.

Nasernejad, B., Zadeh, T., Pour , B., Bygi, M., & Zamani, A. (2005). Comparison for Biosorption modeling of heavy metals (Cr(III), cu(II), zn(II) adsorption from wastewater by carrot residue. *Journal of process Biochemistry, 40*(3), 1319-1322.

Nieboer, E., & Richardson, D. (1980). The replacement of the nondescript term 'heavy metals' by a biologically and chemically singficant classification of metal ions. *Environmental polluition series B,Chemical and physical, 1*(1), 3-26.

Nor AzimahBinti, A., Mohd, A., & Zanura, Z. (2013). Optimization of the performance of chitisan for the Nickel from Wastewater. *World Applied Sciences Journal, 25*(7), 1118-1124.

Nriagu, J. (1996). A history of global metal pollution,. *Science, 272*(5259), 223-224.

Nwabanne, J., & Igbokwe , P. (2012). Mechanism of copper(II) removal from aqeous solutions using activated carbon prepared from different agricultuural materials. *International journal of multidispilnary Sciences and Engineering, 3*(7), 46-52.

Odegaard, H., Fettig, J., & Ratnaweera, H. (1990). *Coagulation with prepolymerized metal salts.In chemical and wastewater treatment.* Berlin: Springer,Heidelberg.

Okolo, B., Menkiti, M., & Nnaji, P. (2014). The performance of ofra seed extract in removal of suspended particles from brewery effluent by coa-flocculation process. *Journal of Applied Science and Technology, 4*(34), 4791-4806.

Olago, D. O., & Akech. (2002). Pollution Assessment in Nairobi River Basin. *Journal of Earth Sciences, 30*(4), 957-969.

Onyancha, D., Mavura, W., Ngila, J., Ongoma, P., & Chacha, J. (2008). Studies of Chromium removal from tannery wastewaters by algae biosorbents,Spirogyra condensata and Rhizochlomium Heiroglyphicium. *Journal of hazardous Materials, 158*(2), 605-614.

Otieno. (1995). Role of industries in sustaining water quality. *Proceedings of 21st WEDC conference* . Kampala: F.A.O.

Ozturk, A. (2007). Removal of nickel from aqueous solution by the bacterium Bacillus thuringiensis. *Journal of Hazard Materials, 147*(1), 518-523.

Pauline, D., Padmanabhan, G., Kurt, N., Stephen, R., Leah, T., & Jason, K. (2008). Enhanced removal of heavy metals in primarytreatment using coagulation and flocculation. *Water Environment Research, 80*(5), 472-479.

Peavy , H., Rowe, D., & Tchobanoglous, G. (1985). *Environmental Engineering.* Singapore: Mc Graw- Hill.

Raghuwanshi, P., Mandloi, M., Sharma, A., Malviya, H., & Chaudhari, S. (2001). Improving filtrate quality using agrobased materials as coagulant aid. *Water Quality Research Journal of Canada, 37*(4), 745-756.

Rani, M., Hemapriya, j., & Kannan, V. (2009). Comparative assessment of heavy metal removal by immobilized and dead bacterial cells: a biosorption approach. *Africa jpurnal of science and technology, 4*(2), 77-83.

Rashidi, F., Sarabi, R., Ghasemib, Z., & Seif, A. (2010). Kinetic ,Equilibrium and thermodynamic studies for the removal of lead(II) and copper (II)ions from aqueous solution by nanaocrystalline TiO2,. *Super lattices and microsturctures, 48*(6), 577-591.

Ravikumar, K., & Sheeja, A. (2013). Heavy metal removal from water using Moringa Oliefera seed Coagulant and Double filtration. *International journal of scientific and Engineering Research, 4*(5), 10-13.

Razmovski, R., & Sciban, M. (2008). Biosorption of Cr(II) and Cu(II) by waste tea fungal biomass. *Ecological Engineering, 34*(2), 179-186.

Reddy, D., Harinatha, Y., Seshaiah , K., & Reddy , A. (2010). Biosorption of P(II) from aqueous solutions using chemically modified Moringa oliefera tree leaves. *Chemical Engineering Journal, 162*(2), 626-634.

Renault, F., Sancey, B., & Badot, M. W. (2009). Chitosan for caogulation/flocculation proc.ess-an eco-friendly approach. *European Polymer Journal, 45*(5), 1337-1348.

Rico, T. E., Santos, F. M., Reis, E. M., Silva, F. F., & Zonett, P. C. (2010). Treatment of tannery wastewater using seeds of Moringa Oliefera. *Agro Magazine Environment, 4*(1), 96-101.

Romera, F., Gonzalex, F., Ballester, A., Blazquez, M., & Munoz, J. (2006). Biosorption with algae: a statistical review. *Critucal Reviews in Biotechnology, 26*(4), 223-235.

Saenz, C., Sepulveda, E., & Matsuhiro, B. (2004). Opuntia Spp. mucilage's: a functional component with industrial pespectives. *Journal of Arid Environment, 57*(3), 275-290.

Saficoban, C., & Yilmaz, M. (2010). modellingeffects of processing Factors on the changes in colour Parametersof cooked Meatballs UsingResponse Surface methodology. *World applied SciencesJournals, 9*(1), 14-22.

Saidu, S. I., Henry, E. I., Persson, I., Masamba, W. L., & Kayambazinthu, D. (2006). pH Dependenceof sorption of Cd(+2),Zn(+2),Cu(+2) andCr(+3),on Crude Water and SodiumChloride extracts of Moringa Stenopetala and Moringa Oliefera. *African Journal of Biotechnology., 5*(23), 2397-2401.

Salamatinia , B., Bhatia, S., & Abdullah, A. (2011). Response Surface Methodology Based Modelling of Temperature Variation in an Ultrasonic-Assisteed Biodiesel Production Process. *World Apllied Sciences Journal, 12*(9), 1549-1557.

Salem, W., Sayed, W., Hawawy, S., & Elamary, R. (2015). Physicochemical and microbiological characteirization of cement kiln dust for potential reuse in wastewater treatment. *Ecotoxicology and eEnvironmantal Safety, 119*(1), 155-161.

Se-Kwon Kim. (2015). *Marine Biotechnology*. New york: Sprinker Dordrecht Heidelberg london.

Senesi, N., D'Orazio, V., & Ricca, G. (2003). Humic acids in the first generation of Eurosoils. *Geoderma, 116*(3), 325-344.

Shahin, G., HAmidi, A., Mohamed, H., & Ali, A. (2009). Application of response surface methodology(RSM) to optimize coagulation-flocculation treatment of leachate using Poly-aluminium chloride(PAC) and alum. *Journal of Hazardous Materials, 163*(2), 650-656.

Sharker, M., & Acharya, P. (2006). Use of the fly ash for the removal of phenol and its analogues from contaminated water. *Waste Management, 26*(6), 559-570.

Shilpaa, B., Akanksha, K., & Girish, P. (2012). Evaluation of cactus and hyacinth bean peels as natural coagulants. *International journal, 3*(3), 187-191.

Shruthi, L., Jagadish, K., & Shrikantaswamy, S. (2016). Photocatalytic Degradation and Removal of Heavy metals in Pharmaceutical waste by Selenium Doped ZnO Nano Composite Semi-conductor. *Journal of Research, 2*(05), 47-54.

Singh, K., Singh, A., & Hasan, S. (2006). Low cost bio-sorbent wheat bran for the removal of cadmium from wastewater:kinetics and equilibrium studies. *Biores.Technol., 97*(8), 994-1001.

Skoog, D., & Leary, J. (1992). *Principles of instrumental Analysis* (4th ed.). Florida: Saunders College Publishing,Orlando.

Song, J., Zou, W., Bian, Y., Su, F., & Han, R. (2011). Adsorption characteristics of mehylene blue by peasant husk in batch and column modes. *Desalination, 265*(1), 119-125.

Srivastava, S., & Goyal, P. (2010). *Novel Biomaterials:decontamination of toxic metals from wastewater.* Berlin: Springer-Verlag.

Statease, I. (2014). *Stat-ease handbook for experiments (online).* Available :www.statease.com.

Steppan, D., Werner, I., & Yeater, R. (1998). Essential regression and experimental design for chemist Engineers. *http://IIgeocities.corn/Silicon Valley/Network/1032/CGpagel.Html.*

Stumm, W., & O'Melia, C. (1968). Stoichiometry of coagualtion. *Journal of American water works Association, 60*(5), 514-539.

Surkannen, K. (1987). *Lignins:Occurance,formation,structure and reaction.* Washington: University of Washington,Seattle.

Taha, N. (2003). *Treatment of municipal Wastewater and sludge Using Cement kiln dust.* Master thesis, The American University in Cairo, Egypt.

Talaro, K. (2002). *Foundations in microbiology fourth edition.* OHIO,USA: McGraw-Hill College.

Tatsi, A., Zouboulis, A., Matis, K., & Samaras, P. (2003). Coagulation-flocculation pretreatment of sanitary landfill leachates. *Chemosphere, 53*(7), 737-744.

Thomas, D., Judd, S., & Fawcett, N. (1999). Flocculation modelling:A review. *Water resources, 33*(1), 1579-1592.

Trinh, T., & Kang, L. (2011). Response surface methodological approach to optimize the coagulation-flocculation process in drinking water treatment. *Chemical Engineering Research and design, 89*(7), 1126-1135.

Upendra, K., & Manas, B. (2006). Fixed bed column study for Cd(II) removal from wasteater using treated rice husk. *Journal of hazardous materials, 129*(1), 253-259.

Uysal, M., & Ar., I. (2007). Removal of Cr (VI) from industrial wastewaters by adsorption:part I:Determination of optimum conditions. *Journal of Hazardous Materials, 149*(2), 482-491.

Vijayaraghavan, G., Sivakumar, T., & Vimal Kumar, A. (2011). Application of plant based coagulants for wastewater treatment. *International Journal of advanced Engineering Research and Studies, 1*(1), 88-92.

Vijayaraghavan, K., & Yun, Y. (2008). Bacterial biosorbents and biosorption. *Biotechnology Advances, 26*(3), 266-291.

Vikashni, N., Matakite, M., Kanayathu, K., & Subramanium, S. (2012). Water Purification Using Moringa Olieferaand Other Locally Available Seeds in Fiji For Heavy Metal Removal. *International Journal of Applied Science and Technology., 2*(5), 125-129.

Volesky, B. (2003). *Sorption and Biosorption.* Quebec: BV-Sorbex, Inc., St.Lambert.

Volesky, B. (2007). Biosorption and me. *Water research, 41*(18), 4017-4029.

Von Smoluchowski, M. (1917). Versucheiner Mathematischen Theorie der Koagulations kinetic Kolloider Lousungen. *Z.Phys.chem., 92*(1), 129-168.

Wandiga, S. O., Odipo, R. W., & Jonnalagada, S. B. (1995). Water Pollution-Effects of industrial and Sewage effluent disharged on the quality of Nairobi River Water. *Kenya Journal of sciences, 17*(2), 95-110.

Wang , J., & Chen , C. (2009). Biosorbents for heavy metals removal and their future. *Biotechnology Advances, 27*(2), 195-226.

Wang , J., Chen, Y., Wang, Y., Yuan, S., & Yu, H. (2011). Optimization of the coagulation flocculation process for pulp mill wastewater treatment using combination of uniform design and response surface methodology. *Water Research, 45*(1), 5633-5640.

Wankasi, D., Horsfall, M., & Spiff, A. (2006). Sorption kinetics of Pb 2+ and cu 2+ ions from acqueous solution by nipa palm shhot biomass. *Journal of biotechnology, 9*(5), 587-592.

Wardzynska, R., & Beata, Z. (2016). Computer simulation of the coagualtion of suspended solids-The appicability of the muller -Smoulchowski theory. *Journal of environmantal Science, 44*(1), 197-203.

Weber, W., & Morris, J. (1963). Kinetics of Adsorption on carbon solution. *Journal Sanitary Engeering Division Proceedings. American Society of Civil Engineers, 89*(2), 31-59.

WHO. (2001). *Environmental Health Criteria 221: Zinc.* Geneva: WHO.

WHO. (2004). *Guidelines for drinking water quality.* Geneva: Wolrd Health Organisation.

WHO. (2004). *Guidelines for Drinking water Quality.* Geneva: WHO.

WHO. (2011). *Guidelines for Drinking water Quality.* Geneva: World Health Organization.

Yates, P., Yan, Y., Jamson, G., & Biggs, S. (2001). Heteroaggragation of particle system:Aggregation mechanism and aggregate structure determination. *6th World congress of chemical Engineering* (pp. 1-10). Australia: Melbourne.

Yoon, Y., & Nelson, J. (1984). Application of Gas adsorption kinetics.A theoretical model for respirator cartridge service time. *American Industrial Hygiene Association Journal, 45*(1), 405-516.

Zhang, J., Zhang, F., Luo, Y., & Yang, H. (2006). A preliminary study on cactus as a coagulant in water treatment. *Process Biochemistry, 41*(3), 730-733.

Zouboulis, A., Loukido, M., & Matis K. (2004). Biosorption of toxic metals from aqueous solutions by bacteria strains isolatedfrom metal -polluted soils. *Process Biochem., 39*(8), 909-916.

Appendix A

Table A.1: Effects of contact time on removal of heavy metal using banana pith dose of 0.2g/100 ml, initial heavy metal conc. of 5 mg/l, pH of 5 and shaking speed of 250 rpm

Time(mins)	Final mean heavy metal concentration (mg/l)			
	Lead	Copper	Zinc	Chromium
15	0.986	1.024	1.124	1.182
30	0.563	0.854	0.942	1.114
60	0.165	0.635	0.793	0.983
120	0.128	0.451	0.621	0.865
180	0.126	0.322	0.514	0.845
240	0.115	0.343	0.521	0.812
300	0.112	0.350	0.523	0.811

Table A.2: Isotherm Freundlich and Langmuir data obtained for biosorption of heavy metal using banana pith.

Metal conc.(mg/l)	Qe	Ce	log qe	loq ce	ce/qe
Lead					
5	2.441	0.115	0.3874	-0.9393	0.0471
10	4.807	0.386	0.6819	-0.4134	0.0803
15	7.156	0.688	0.8547	-0.1624	0.0961
20	9.221	1.562	0.9647	0.1931	0.1692
Copper					
5	2.332	0.341	0.3674	-0.4685	0.1459
10	4.453	1.102	0.6484	0.0414	0.2472
15	6.314	2.414	0.7993	0.3802	0.3809
20	7.852	4.321	0.8949	0.6335	0.5478
Zinc					
5	2.241	0.522	0.3502	-0.2843	0.2321
10	4.222	1.621	0.6232	0.2041	0.3809
15	5.853	3.315	0.7671	0.5185	0.5641
20	7.315	5.405	0.8633	0.7324	0.7397
Chromium					
5	2.095	0.813	0.3212	-0.0915	0.3866
10	3.963	2.084	0.5977	0.3181	0.5252
15	5.410	4.204	0.7324	0.6232	0.7778
20	6.723	6.616	0.8261	0.8195	0.9851

Table A.3: Kinetic data for biosorption of heavy metal using banana pith

	Lead		**Copper**		**Zinc**		**Chromium**	
Time (mins)	ln(qe-qt)	t/qt	ln(qe-qt)	t/qt	ln(qe-qt)	t/qt	ln(qe-qt)	t/qt
Initial heavy metal concentration -5 mg/l								
15	-0.8278	7.4738	-1.0729	7.5453	-1.1973	7.7399	-1.6874	7.8534
30	-1.4894	13.5226	-1.3587	14.4718	-1.5606	14.7783	-1.8971	15.4242
60	-3.6268	24.8201	-1.9139	27.4914	-2.0025	28.5035	-2.4651	29.8507
120	-4.8283	49.2611	-2.9004	52.7472	-2.9957	54.7945	-3.6889	57.9710
180	-4.9618	73.8613	-4.6051	77.5862	-3.9120	81.0811	-4.1997	86.5385
240	-6.5023	98.2599	-	103.0042	-	107.1428	-	114.5585
300	-	122.7495	-	128.7554	-	133.9286	-	143.1981
Initial heavy metal concentration -10 mg/l								
15	-0.2052	3.7570	-0.3930	3.9735	-0.7550	4.0214	-0.6636	4.3541
30	-0.2294	7.4776	-0.4231	7.9051	-1.7148	7.4627	-0.8210	8.5227
60	-1.8702	12.8952	-1.8326	13.9860	-2.2073	14.6699	-1.1087	16.5289
120	-2.6593	25.3325	-2.9004	27.3037	-2.590	29.0909	-2.5903	30.8880
180	-3.9633	37.5939	-	40.8163	-3.9120	43.0622	-4.6052	45.5696
240	-	49.9272	-	53.9326	-	57.1428	-	60.6060
300	-	62.4089	-	67.4157	-	71.4286	-	75.7576
Initial heavy metal concentration -15 mg/l								
15	0.32792	2.6005	-0.3711	2.6738	-0.6444	2.8169	-0.3355	3.2017
30	-0.0171	4.8599	-0.4541	5.2957	-0.7444	5.5813	-0.7765	6.0729
60	-1.2431	8.7368	-1.4272	9.9010	-1.3093	10.7527	-1.1712	11.7878
120	-2.4135	16.9815	-3.5066	19.1387	-2.0402	20.9790	-1.7148	22.9885
180	-5.4037	25.1695	-3.9120	28.6624	-2.6593	31.1418	-2.9004	33.6763
240	-	33.5383	-	38.0952	-	41.0256	-	44.4444
300	-	41.9229	-	47.6190	-	51.2820	-	55.5555
Initial heavy metal concentration -20 mg/l								
15	0.4357	1.9547	-0.0101	2.1866	-0.7340	2.1994	-0.1335	2.5751
30	0.0977	3.6957	-0.1984	4.2674	-0.9545	4.3384	-0.2679	5.0547
60	-0.9096	6.8048	-0.8795	8.0699	-1.4065	8.5046	-0.4620	9.8846
120	-1.8643	13.2377	-1.3863	15.7895	-2.1203	16.7130	-0.7550	19.2616
180	-2.4079	19.7152	-1.8971	23.3766	-3.5066	24.7593	-1.7720	27.5651
240	-	26.0304	-	30.5732	-	32.8767	-	35.8209
300	-	32.5379	-	38.2165	-	41.0959	-	44.7761

Table A.4: Effects of contact time on removal of heavy metal using Maerua Decumbent dose of 0.2g/100 ml Initial heavy metal conc. of 5 mg/l, pH of 5 and shaking speed of 250 rpm

Time(mins)	Final mean heavy metal concentration (mg/l)			
	Lead	Copper	Zinc	Chromium
15	0.972	1.362	2.044	1.135
30	0.741	1.111	1.925	0.763
60	0.374	0.916	1.324	0.285
120	0.293	0.833	1.053	0.223
180	0.280	0.824	1.042	0.197
240	0.262	0.541	1.036	0.175
300	0.260	0.541	1.024	0.175

Table A.5: Isotherm Freundlich and Langmuir data obtained for biosorption of heavy metal using Maerua Decumbent.

Metal conc.(mg/l)	Ce	Qe	log Ce	loq qe	ce/qe
Lead					
5	0.26	2.37	-0.5850	0.3747	0.1097
10	1.18	4.41	0.0719	0.6444	0.2676
15	2.52	6.25	0.3979	0.7959	0.4032
20	4.91	7.55	0.6902	0.8780	0.6490
Copper					
5	0.54	2.23	-0.2676	0.3483	0.2421
10	2.02	4.01	0.3010	0.6021	0.5037
15	3.83	5.61	0.5798	0.7482	0.6786
20	6.44	6.82	0.8062	0.8325	0.9412
Zinc					
5	1.03	1.99	0.0128	0.2978	0.5189
10	3.76	3.12	0.5752	0.4941	1.2051
15	5.83	4.58	0.7657	0.6613	1.2715
20	8.52	5.74	0.9304	0.7589	1.4843
Chromium					
5	0.17	2.41	-0.7569	0.3824	0.0725
10	0.56	4.72	-0.2495	0.6738	0.1193
15	1.30	6.85	0.1139	0.8357	0.1898
20	2.48	8.76	0.3944	0.9425	0.2831

Table A.6: Kinetic data for bio-sorption of heavy metal using Maerua Decumbent.

	Lead		**Copper**		**Zinc**		**Chromium**	
Time (mins)	ln(qe-qt)	t/qt	ln(qe-qt)	t/qt	ln(qe-qt)	t/qt	ln(qe-qt)	t/qt
Initial heavy metal concentration -5 mg/l								
15	-1.0356	7.4442	-0.8915	8.2417	-0.6733	10.1351	-0.7339	7.7619
30	-1.4271	14.0845	-1.2552	15.4241	-0.7985	19.4805	-1.2242	14.1609
60	-2.8647	25.9403	-1.6713	29.3829	-1.8839	32.6442	-2.9004	25.4507
120	-4.1997	50.9554	-1.9310	57.5540	-4.1998	60.7595	-3.7297	50.2407
180	-4.6052	76.2712	-1.9661	86.1244	-4.6052	90.9091	-4.5099	74.9532
240	-	101.2658	-	107.6233	-5.2983	120.9068	-	99.4818
300	-	126.5823	-	134.5292	-	150.7538	-	124.3523
Initial heavy metal concentration -10 mg/l								
15	-0.3285	4.0650	-0.4155	4.4910	-1.1552	5.3381	-0.1065	4.0872
30	-0.5978	7.7720	-1.0216	8.2417	-1.4697	10.3627	-0.4170	7.6726
60	-1.0788	14.7420	-2.0402	15.5039	-1.9310	20.1342	-0.9063	14.4058
120	-1.8018	28.2685	-2.6593	30.5343	-3.9120	38.6473	-1.2765	27.9720
180	-1.9310	42.2039	-2.8134	45.6853	-4.6052	57.7849	-4.1044	39.5387
240	-	54.4217	-	60.0012	-5.2983	76.9231	-7.6009	52.5336
300	-	68.0272	-	75.0315	-	96	-	65.6598
Initial heavy metal concentration -15 mg/l								
15	-0.1450	2.7855	-0.4861	3.0090	-0.7236	3.6496	0.3111	2.7599
30	-0.3147	5.4348	-0.8210	5.8139	-1.0788	7.0505	0.1781	5.3524
60	-1.1379	10.1189	-1.5847	11.1214	-1.8325	13.5287	-0.5025	9.6852
120	-1.2729	20.1005	-2.0402	21.9378	-3.5065	26.2869	-1.5141	18.2371
180	-1.3665	30.0250	-2.0794	32.8767	-4.1997	39.3013	-5.2983	26.4901
240	-	38.4124	-	42.8571	-4.6051	52.3446	-	35.2941
300	-	48.1347	-	53.5714	-	65.2883	-	44.1176
Initial heavy metal concentration -20 mg/l								
15	-0.4463	2.1707	-0.4463	2.4351	-0.6539	2.8708	0.5794	2.1231
30	-0.9943	4.1783	-0.5710	4.8115	-1.4916	5.4348	0.2390	3.9578
60	-1.661	8.1522	-0.9039	9.3823	-2.8134	10.5541	-0.3425	7.3710
120	-2.040	16.1725	-1.1087	18.5471	-3.3524	21.0157	-1.5371	13.8969
180	-2.4079	24.1287	-1.6094	27.2727	-4.1997	31.4136	-2.3539	20.5596
240	-	31.7881	-	35.2941	-5.2983	41.8118	-2.4079	27.3972
300	-	39.7351	-	44.1176	-	52.2193	-	33.8983

Table A.7: Effects of contact time on removal of heavy metal using Opuntia Spp. dose of 0.1g/100 ml Initial heavy metal conc. of 5 mg/l, pH of 5 and shaking speed of 250 rpm

Time(mins)	Final mean heavy metal concentration (mg/l)			
	Lead	Copper	Zinc	Chromium
15	0.690	1.131	1.222	1.312
30	0.275	0.874	1.073	0.958
60	0.165	0.698	0.769	0.718
120	0.128	0.345	0.462	0.694
180	0.126	0.302	0.432	0.625
240	0.121	0.262	0.413	0.563
300	0.121	0.261	0.412	0.562

Table A.8: Isotherm Freundlich and Langmuir data obtained for biosorption of heavy metal using Opuntia Spp.

Metal conc.(mg/l)	Ce	qe	log qe	log ce	ce/qe
Lead					
5	0.12	4.88	0.6883	-0.9172	0.0248
10	0.27	9.73	0.9882	-0.5735	0.0274
15	0.64	14.36	1.1571	-0.1931	0.0446
20	1.22	18.78	1.2737	0.0864	0.0649
Copper					
5	0.26	4.74	0.6758	-0.5850	0.0548
10	0.72	9.28	0.9675	-0.1427	0.0776
15	1.52	13.48	1.1297	0.1818	0.1127
20	2.61	17.4	1.2405	0.4150	0.1494
Zinc					
5	0.41	4.59	0.6618	-0.3872	0.0893
10	0.98	9.02	0.9552	-0.0088	0.1086
15	2.1	12.9	1.1106	0.3222	0.1628
20	3.8	16.2	1.2095	0.5798	0.2345
Chromium					
5	0.56	4.44	0.6474	-0.2518	0.1261
10	1.5	8.5	0.9294	0.1760	0.1765
15	2.8	12.2	1.0863	0.4471	0.2295
20	5.6	14.4	1.1584	0.7482	0.3889

Table A.9: Kinetic data for bio-sorption of heavy metal using Opuntia Spp..

	Lead		**Copper**		**Zinc**		**Chromium**	
Time (mins)	ln(qe-qt)	t/qt	ln(qe-qt)	t/qt	ln(qe-qt)	t/qt	ln(qe-qt)	t/qt
Initial heavy metal concentration -5 mg/l								
15	-0.5644	3.4800	-0.1393	3.8759	-0.2107	3.9682	-0.2877	4.0650
30	-1.8708	6.3492	-0.4878	7.2709	-0.4155	7.6335	-0.9213	7.4221
60	-3.119	12.4100	-0.8255	13.9470	-1.0244	14.1810	-1.8452	14.0121
120	-4.9618	24.6305	-2.4651	25.7787	-2.9565	26.4433	-2.0099	27.8681
180	-5.2983	36.9306	-3.1701	38.3142	-3.8167	39.4045	-2.7334	41.1428
240	-	49.1904	-	50.6329	-	52.2875	-	54.0541
300	-	61.4880	-	63.2911	-	65.3594		67.5676
Initial heavy metal concentration -10 mg/l								
15	0.3527	1.8050	0.4824	1.9582	0.4574	2.0161	0.3853	2.1337
30	-0.6578	3.2556	0.3988	3.8511	0.1570	3.8216	-0.0513	3.9735
60	-2.2164	6.2344	-0.0408	7.2115	-0.4005	7.1856	-0.4155	7.6531
120	-6.2146	12.3317	-3.1942	12.9884	-1.7148	13.5747	-0.6162	15.0754
180	-6.9077	18.4957	-3.5756	19.4552	-2.9957	20.0669	-1.2040	21.9512
240	-	24.6584	-	25.8621	-	26.6075	-	28.2353
300	-	30.8230	-	32.3276		33.2594		35.2941
Initial heavy metal concentration -15 mg/l								
15	0.6926	1.2136	0.7654	1.3239	0.6152	1.3575	0.2469	1.3736
30	0.2013	2.2838	0.6259	2.5839	0.1222	2.5488	0.1044	2.7051
60	-1.2909	4.2601	0.0198	4.8154	-0.4463	4.8939	-0.1985	5.2724
120	-5.5215	8.3594	-0.8209	9.2024	-1.0216	9.5694	-0.3425	10.4439
180	-5.8091	12.5383	-1.1712	13.6674	-1.3862	14.2292	-0.9163	15.2542
240	-6.2146	16.7166	-	17.8041	-	18.6046	-	19.6721
300		20.8928		22.2552		23.2558		24.5902
Initial heavy metal concentration -20 mg/l								
15	0.8919	0.9179	0.8671	0.9987	0.4253	1.0225	0.6931	1.2097
30	0.3436	1.7271	0.6523	1.9380	0.3075	2.0216	0.4700	2.3437
60	-1.0272	3.2569	0.0100	3.6608	0.0198	3.9526	0.0953	4.5113
120	-4.1352	6.3952	-0.4463	7.1600	-1.0498	7.5710	-0.3567	8.7591
180	-6.9078	9.5852	-0.8675	10.6007	-1.3471	11.2923	-1.6094	12.6760
240		12.7796	-	13.7931	-	14.8148	-	16.6667
300		15.9744		17.2414		18.5185		20.8333

Table A.10: Performance of banana pith column at a depth of 6 cm, initial concentration of 5 mg/l and flow rate of 3 ml/min.

Time (hrs)	Mean values of C_t	C_t/C_o	C_o-C_t
0	0	0	5
0.500	0	0	5
1.00	0.0083	0.0017	4.9917
1.25	0.0124	0.0025	4.9876
1.5	0.0193	0.0038	4.9807
1.75	0.0298	0.0059	4.9702
2.00	0.0483	0.0096	4.9517
2.50	0.0648	0.0129	4.9352
3.00	0.1066	0.0213	4.8934
3.50	0.4486	0.0897	4.5513
4.00	1.0561	0.2112	3.9439
5.00	1.4256	0.2851	3.5744
6.00	1.8254	0.3651	3.1746
7.00	2.5481	0.5096	2.4519
8.00	2.8365	0.5673	2.1635
9.00	3.0154	0.6031	1.9846
10.00	3.6412	0.7282	1.3588
11.00	4.1256	0.8251	0.8744
12.00	4.5623	0.9125	0.4377
13.00	4.5686	0.9137	0.4314
14.00	4.6123	0.9225	0.3877

Appendix B

Figure B.1: Jar test for banana pith bio-coagulant in River water treatment

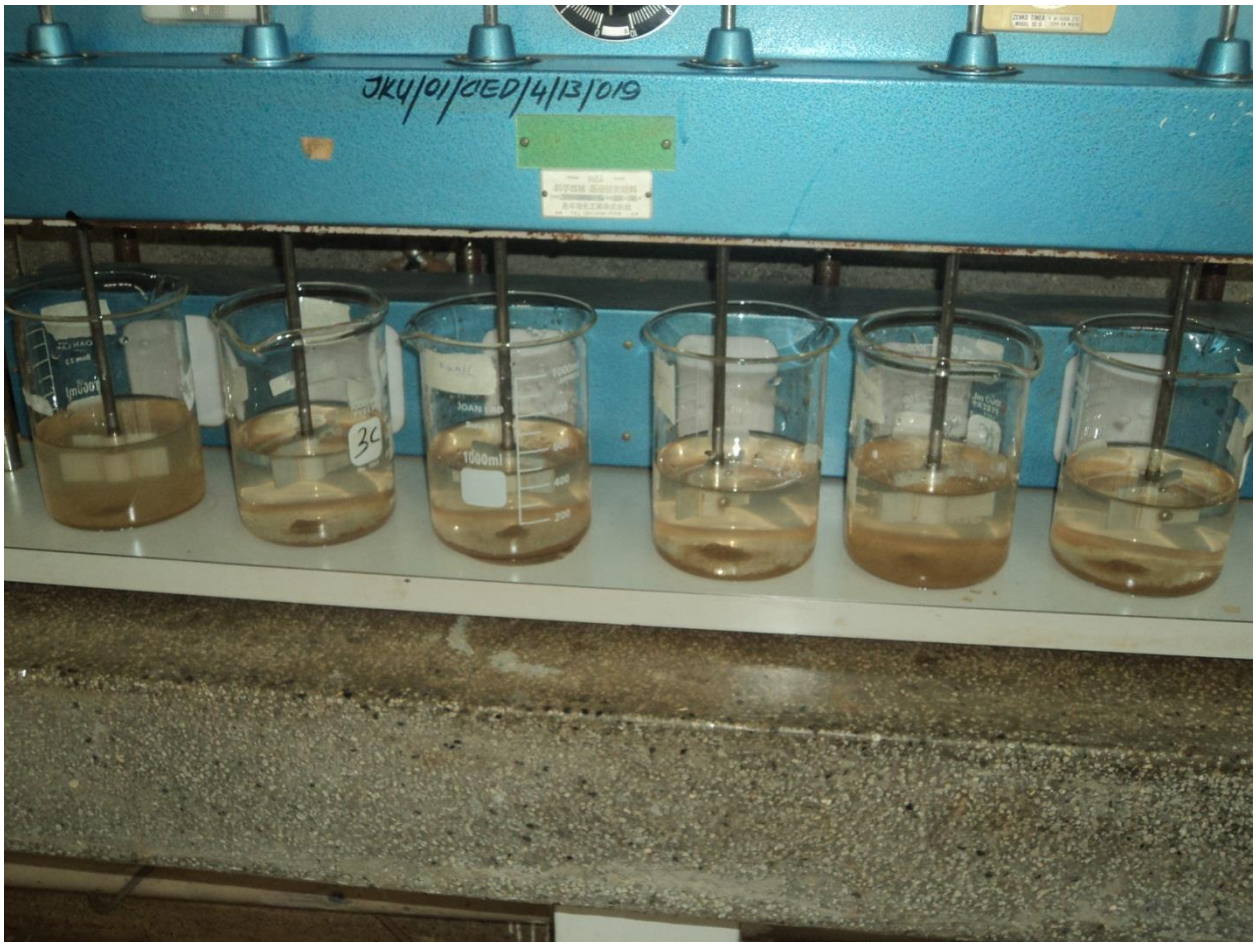

Figure B.2: Jar test for Maerua Decumbent bio-coagulant in River water treatment

Figure B.3: Jar test for Opuntia Spp. bio-coagulant in River water treatment

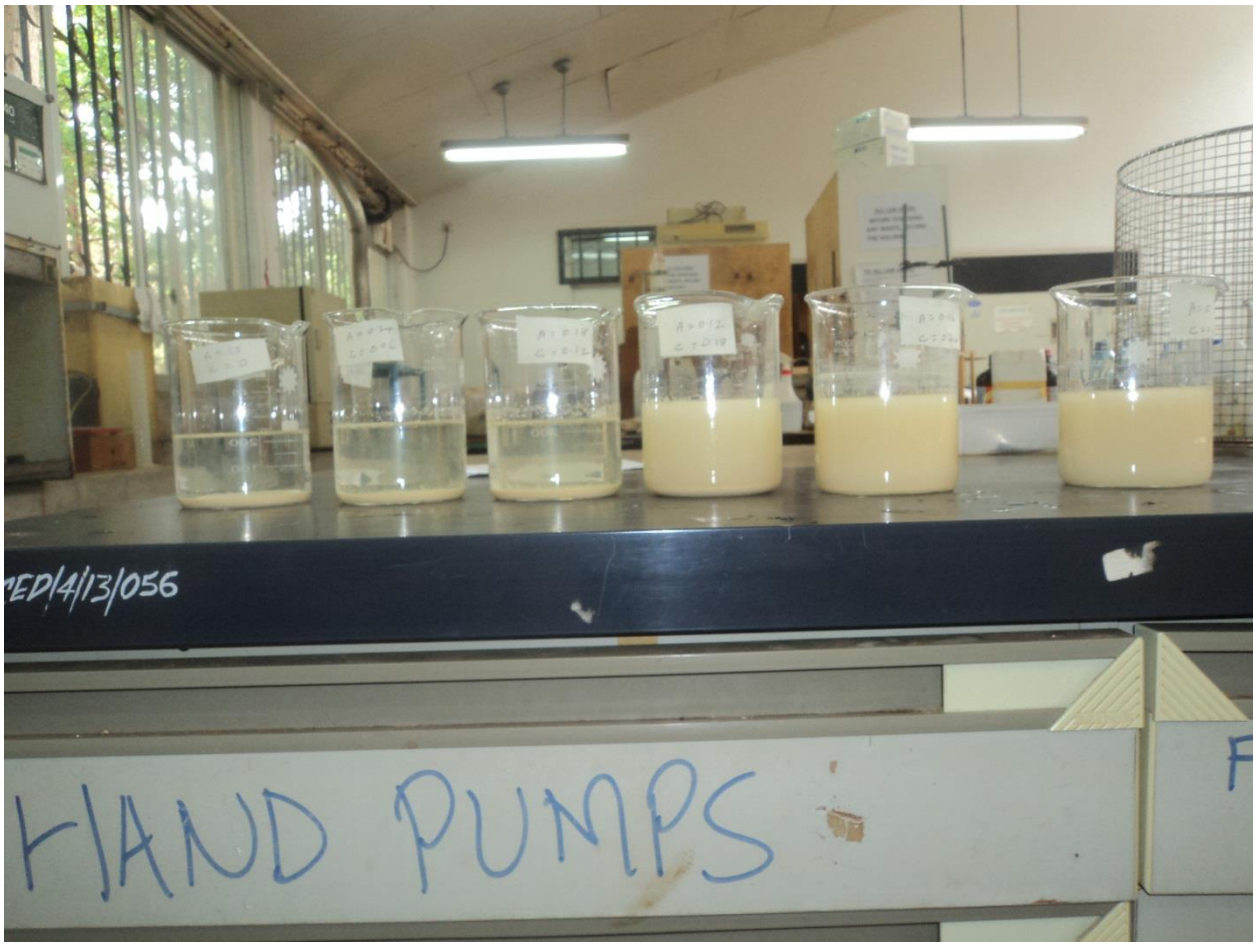

Figure B.4: Jar test for alum and Opuntia Spp. coagulants in industrial (paint) wastewater treatment

Figure B.5: Jar test for alum and Banana pith coagulants in industrial (paint) wastewater treatment

Figure B.6: Jar test for alum and Maerua Decumbent coagulants in industrial (paint) wastewater treatment

Appendix C: Optimization using alum only

Table C1: CCD and Response results for study of three experimental variables for alum coagulant.

Run	Actual			Coded			Responses (% Removal)	
	A	B	C	A	B	C	Turbidity	COD
1	0.26	7	20	-1.000	-1.000	-1.000	45.96	10.97
2	0.26	11	20	-1.000	1.000	-1.000	21.25	7.36
3	0.0087	9	40	-1.682	0.000	0.000	13.4	5.14
4	1	11	60	1.000	1.000	1.000	78.96	45.71
5	0.26	7	60	-1.000	-1.000	1.000	52.96	16.48
6	0.63	12.36	40	0.000	1.682	0.000	63.58	30.21
7	0.26	11	60	-1.000	1.000	1.000	41.94	9.32
8	0.63	9	73.6	0.000	0.000	1.682	75.69	48.32
9	1.25	9	40	1.682	0.000	0.000	97.77	56.62
10	0.63	9	40	0.000	0.000	0.000	68.61	35.01
11	0.63	9	40	0.000	0.000	0.000	65.01	37.4
12	1	7	20	1.000	-1.000	-1.000	85.46	51.71
13	0.63	9	40	0.000	0.000	0.000	65.88	38.41
14	1	7	60	1.000	-1.000	1.000	99.92	65.85
15	0.63	9	40	0.000	0.000	0.000	69.28	42.31
16	1	11	20	1.000	1.000	-1.000	59.17	29.14
17	0.63	9	6.36	0.000	0.000	-1.682	49.71	25.71
18	0.63	5.64	40	0.000	-1.682	0.000	87.94	55.85
19	0.63	9	40	0.000	0.000	0.000	73.14	45.71
20	0.63	9	40	0.000	0.000	0.000	71.86	46.3

A: Alum dosage (g/l); B: pH; C: Settling time (minutes)

Table C2: CCD and Response results for study of two experimental variables for alum coagulant.

	Actual		Coded		Responses (% Removal)			
Run	A	B	A	B	Lead	Chromium	Zinc	Iron
1	0.63	6.17	0.000	-1.414	98.51	88.02	96.25	90.83
2	0.63	9	0.000	0.000	84.01	75.96	45.36	60.68
3	0.63	9	0.000	0.000	86.23	72.97	53.87	63.63
4	1	7	1.000	-1.000	95.08	94.35	86.06	85.23
5	0.63	9	0.000	0.000	77.06	71.18	59.63	67.61
6	0.63	9	0.000	0.000	83.16	75.12	54.14	65.41
7	1.153	9	1.414	0.000	93.87	74.36	59.06	76.51
8	0.63	9	0.000	0.000	82.04	76.62	57.86	61.89
9	0.107	9	-1.414	0.000	34.92	39.73	32.14	36.68
10	0.26	7	-1.000	-1.000	53.88	56.39	48.2	55.63
11	0.63	11.83	0.000	1.414	91.96	62.27	85.47	83.45
12	1	11	1.000	1.000	88.86	69.19	67.91	68.85
13	0.26	11	-1.000	1.000	64.8	49.53	51.91	59.64

A: Alum dosage (g/l); B: pH

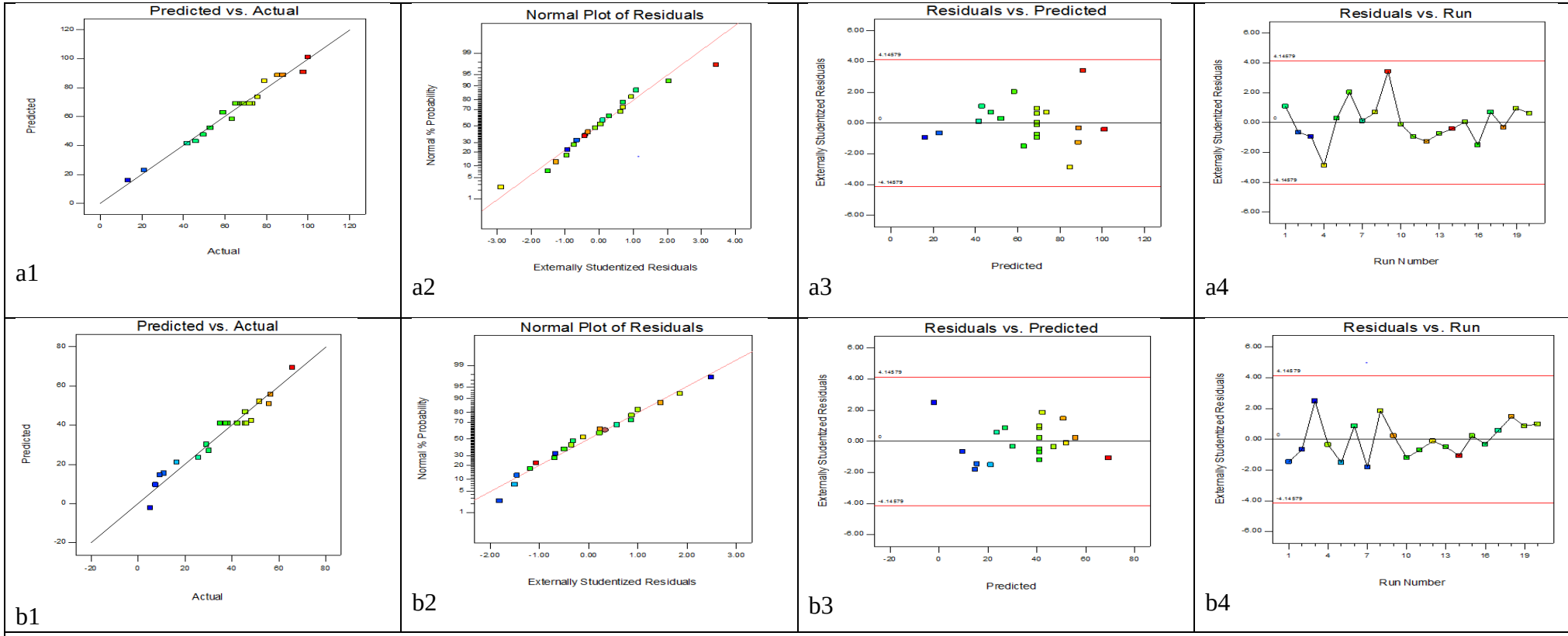

Figure C1(i): Design expert diagnostic plots for a (turbidity), and b (COD)

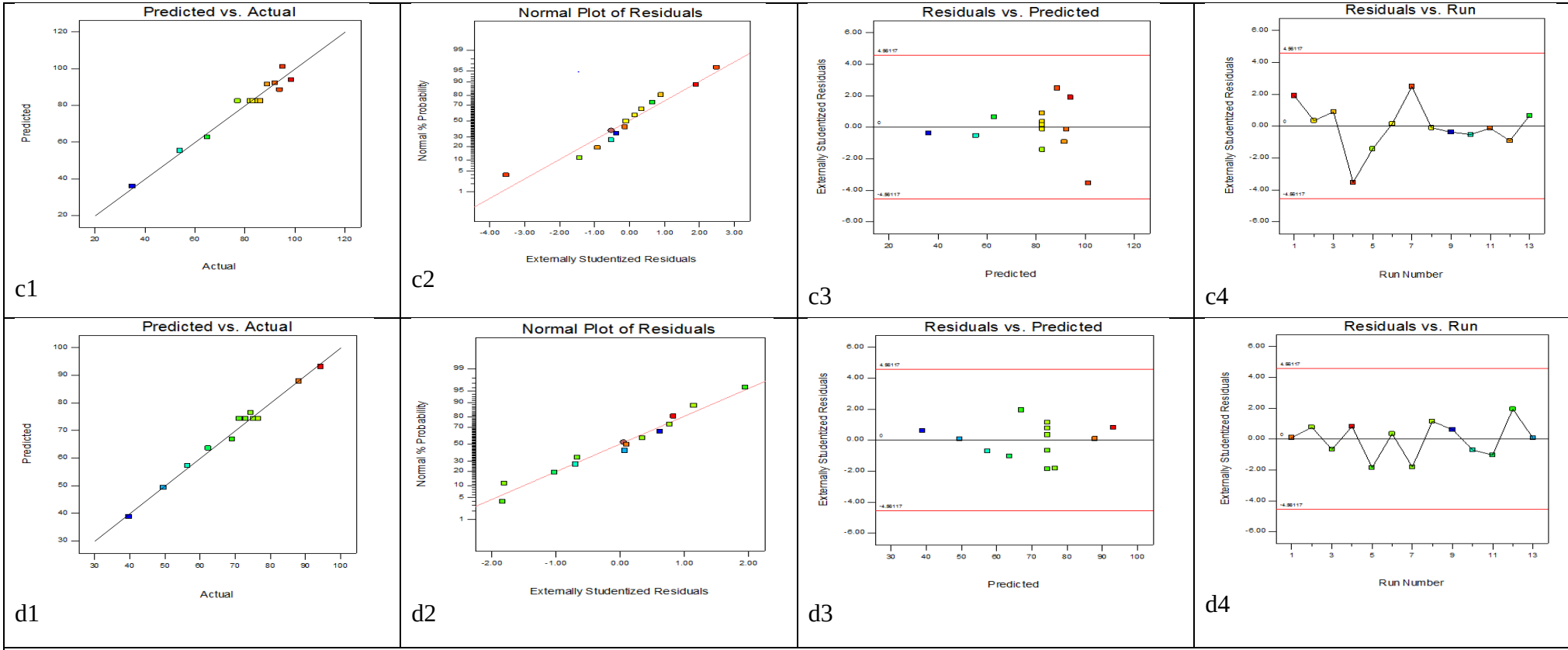

Figure C1(ii): Design expert diagnostic plots for c (lead) and d (chromium),

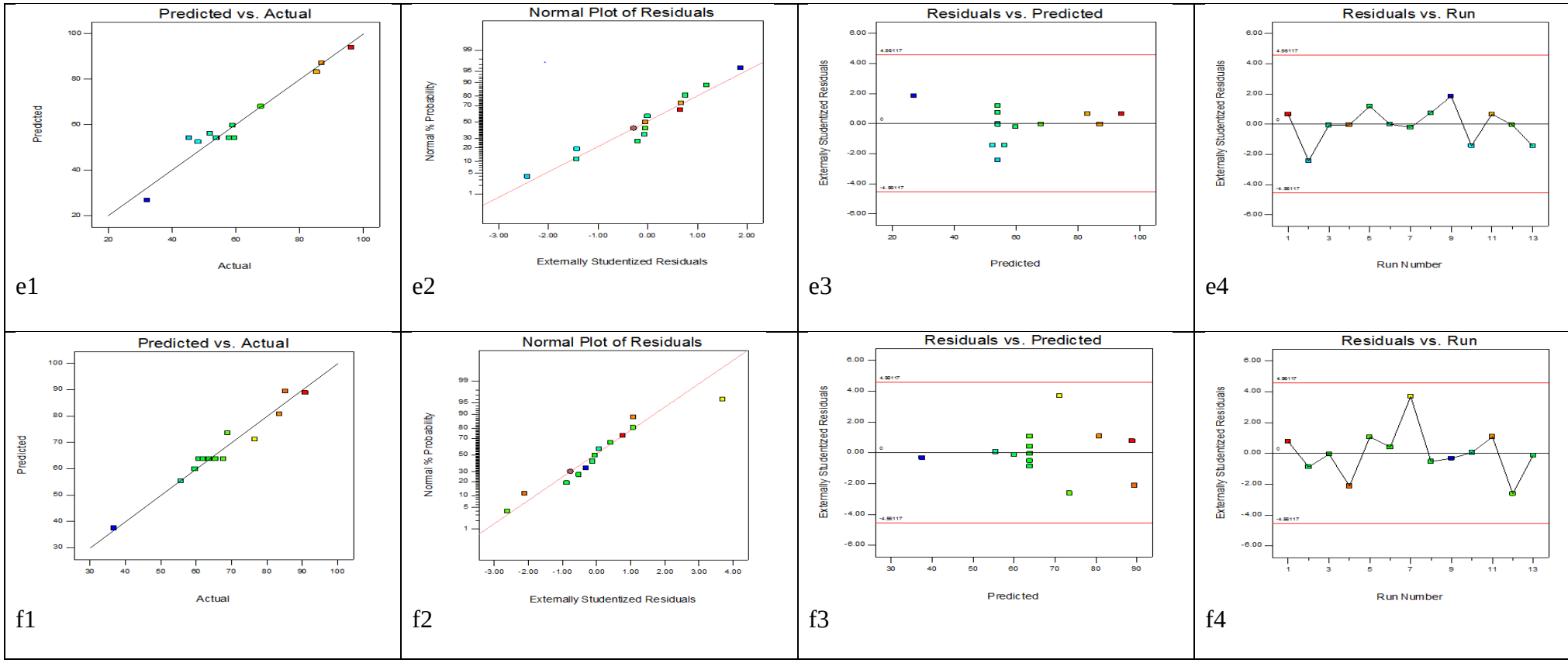

Figure C1 (iii): Design expert diagnostic plots for e (zinc) and f (iron)

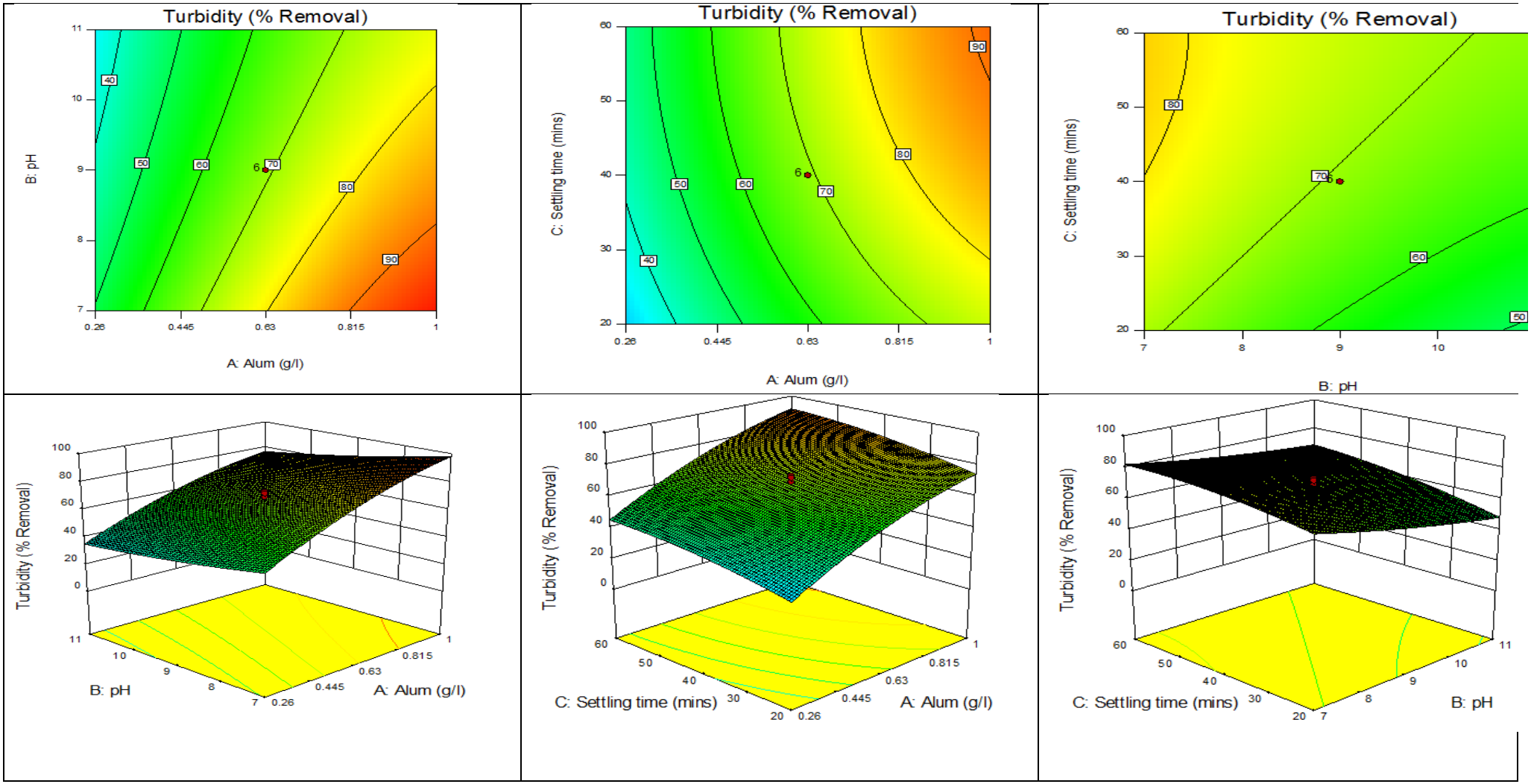

Figure C2: Contour and 3D plots for turbidity removal using Alum

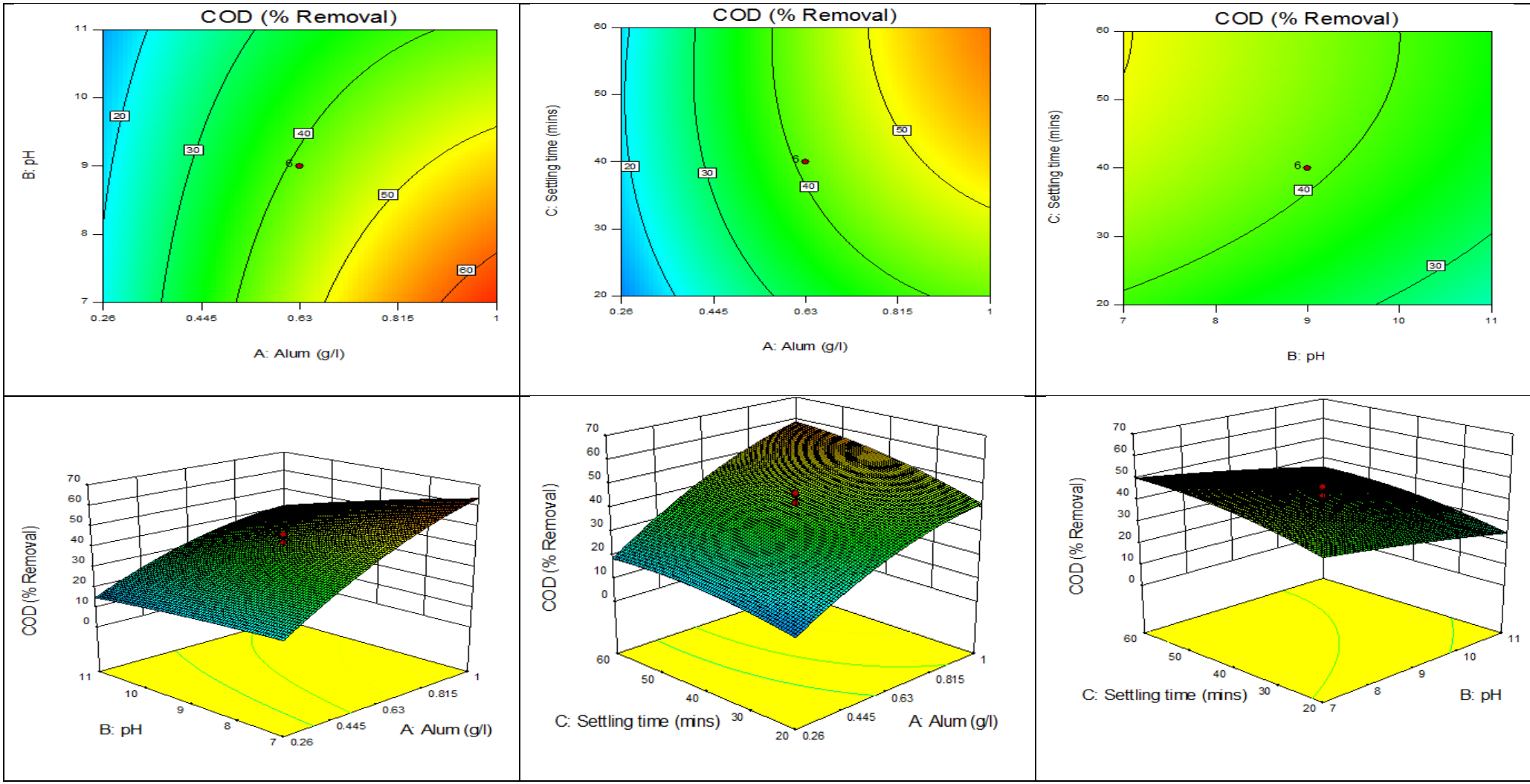

Figure C3: Contour and 3D plots for COD removal using Alum

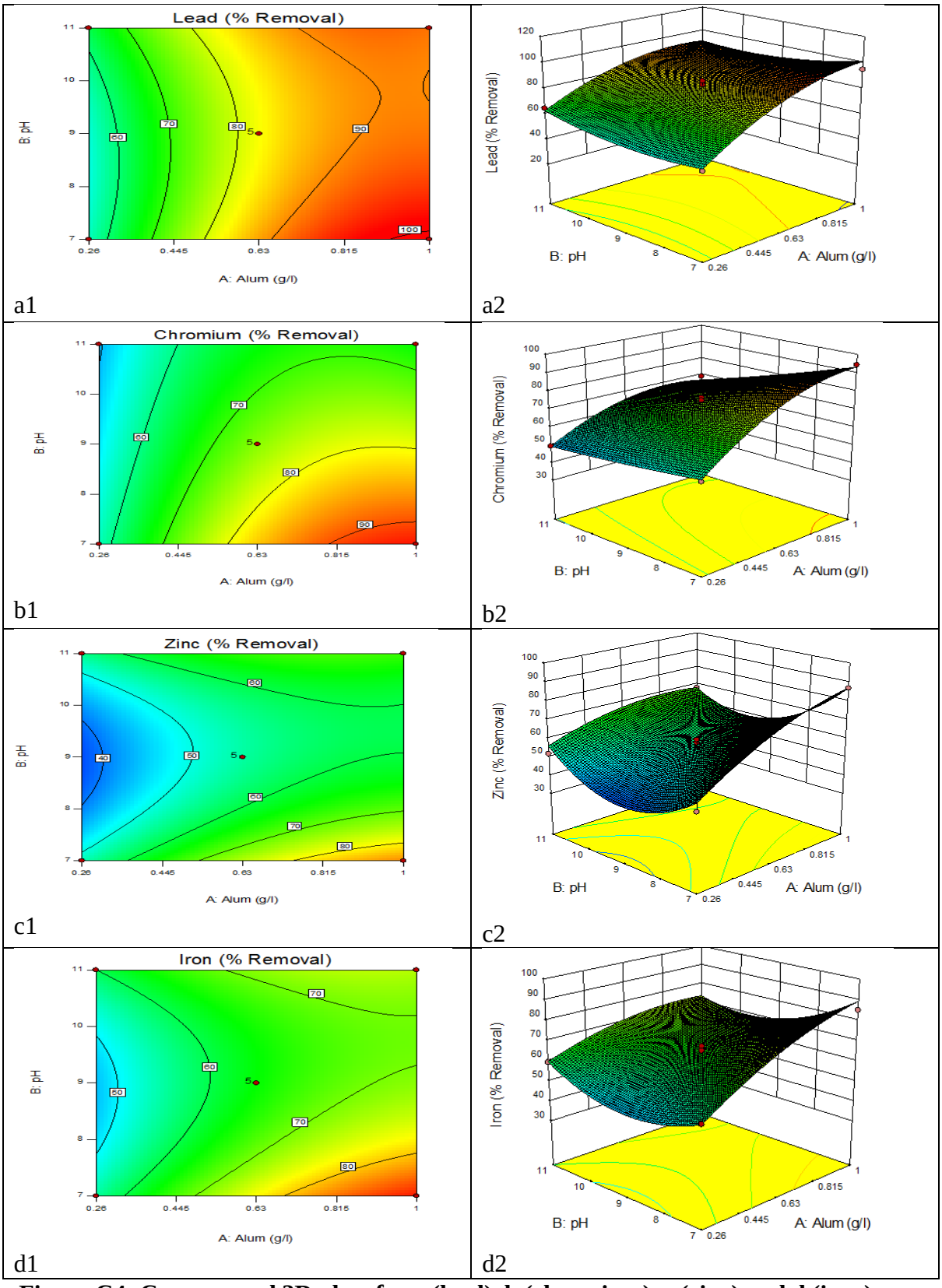

Figure C4: Contour and 3D plots for a (lead), b (chromium), c (zinc) and d (iron) removal using Alum

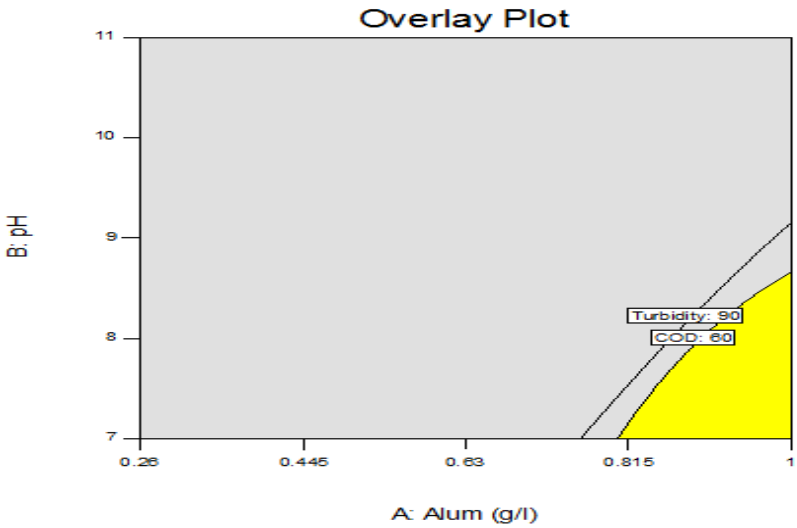

Figure C5: Design expert plot; overlay plot for optimal region for turbidity and COD using alum coagulant

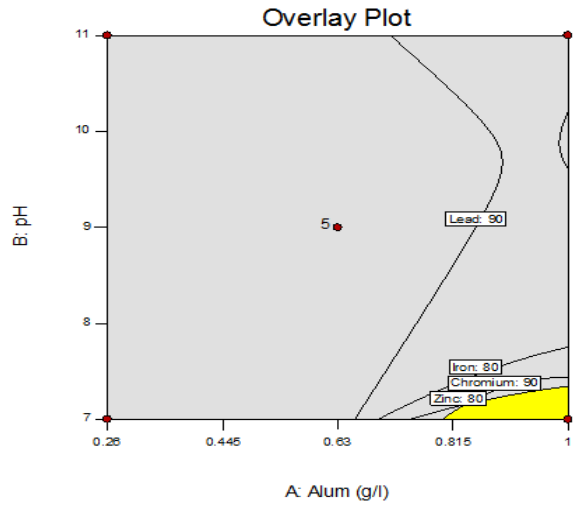

Figure C6: Design expert plot; overlay plot for optimal region for lead, chromium, Zinc and iron using alum coagulant

Table C3: Predicted and verification results for multiple response analysis.

Optimized factors	Response	Predicted (% removal) values	Experimental (% removal) values	Error
Alum 0.95g/l; pH 7.3 at settling time 55.73 minutes	Turbidity	97.41	94.71	3.0
	COD	65.38	61.35	4.03
Alum 0.925g/l; pH 7.10 at Full settling of 60 minutes.	Lead	99.49	99.14	0.35
	Chromium	91.91	88.25	3.66
	Zinc	83.45	79.54	3.91
	Iron	86.35	87.41	-1.06

Appendix D: Optimization using Alum and Banana pith

Table D1: CCD and Response results for study of four experimental variables for alum and banana pith coagulant.

	Actual				Coded				Responses (% removal)	
Run	A	B	C	D	A	B	C	D	Turbidity	COD
1	0.6	0.4	5	20	0.000	0.000	-2.000	0.000	98.23	79.95
2	0.8	0.2	7	30	1.000	-1.000	-1.000	1.000	98.68	76.56
3	0.6	0.4	9	20	0.000	0.000	0.000	0.000	68.26	58.57
4	0.4	0.2	7	10	-1.000	-1.000	-1.000	-1.000	39.58	28
5	0.6	0.4	9	20	0.000	0.000	0.000	0.000	78.98	66.35
6	0.6	0.4	9	40	0.000	0.000	0.000	2.000	80.96	60.21
7	0.6	0.4	9	0	0.000	0.000	0.000	-2.000	8.01	2.64
8	1	0.4	9	20	2.000	0.000	0.000	0.000	71.53	68.69
9	0.8	0.2	11	10	1.000	-1.000	1.000	-1.000	34.34	32.16
10	0.6	0.4	9	20	0.000	0.000	0.000	0.000	70.93	68.14
11	0.4	0.6	11	10	-1.000	1.000	1.000	-1.000	36.69	17.35
12	0.8	0.2	7	10	1.000	-1.000	-1.000	-1.000	59.21	66.36
13	0.8	0.6	7	10	1.000	1.000	-1.000	-1.000	56.32	51.26
14	0.4	0.6	11	30	-1.000	1.000	1.000	1.000	56.79	29.35
15	0.4	0.2	11	10	-1.000	-1.000	1.000	-1.000	22.69	5.43
16	0.8	0.6	11	30	1.000	1.000	1.000	1.000	63.45	43.65
17	0.2	0.4	9	20	-2.000	0.000	0.000	0.000	24.83	6.96
18	0.4	0.2	11	30	-1.000	-1.000	1.000	1.000	42.17	18.56
19	0.6	0.4	9	20	0.000	0.000	0.000	0.000	75.1	67.65
20	0.6	0.4	13	20	0.000	0.000	2.000	0.000	59.15	30.25
21	0.6	0	9	20	0.000	-2.000	0.000	0.000	38.08	28.41
22	0.6	0.8	9	20	0.000	2.000	0.000	0.000	70.25	50.62
23	0.4	0.2	7	30	-1.000	-1.000	-1.000	1.000	52.97	50.71
24	0.8	0.6	11	10	1.000	1.000	1.000	-1.000	46.83	25.98
25	0.8	0.2	11	30	1.000	-1.000	1.000	1.000	60.24	43.56
26	0.4	0.6	7	10	-1.000	1.000	-1.000	-1.000	59.31	46.36
27	0.6	0.4	9	20	0.000	0.000	0.000	0.000	77.6	56.61
28	0.6	0.4	9	20	0.000	0.000	0.000	0.000	76.25	56.45
29	0.4	0.6	7	30	-1.000	1.000	-1.000	1.000	74.16	53.82
30	0.8	0.6	7	30	1.000	1.000	-1.000	1.000	86.96	64.42

A: Alum dosage (g/l); B: Banana pith dosage (g/l); C: pH and D: settling time(mins)

Table D2: CCD and Response results for study of three experimental variables for alum and banana pith coagulant.

	Actual			Coded			Responses (% removal)			
Run	A	B	C	A	B	C	Lead	Chromium	Zinc	Iron
1	0.6	0.4	9	0.000	0.000	0.000	93.34	93.64	82.54	73.44
2	0.4	0.2	11	-1.000	-1.000	1.000	69.36	76.03	70.85	53.32
3	0.6	0.736	9	0.000	1.682	0.000	96.11	88.31	86.12	86.41
4	0.6	0.4	9	0.000	0.000	0.000	95.31	87.64	85.36	72.26
5	0.6	0.4	9	0.000	0.000	0.000	91.23	85.24	80.36	74.21
6	0.6	0.4	9	0.000	0.000	0.000	98.87	91.26	84.21	69.82
7	0.4	0.6	7	-1.000	1.000	-1.000	86.21	93.44	66.06	78.15
8	0.4	0.2	7	-1.000	-1.000	-1.000	75.13	79.69	56.81	48.82
9	0.94	0.4	9	1.682	0.000	0.000	99.22	94.23	97.18	69.65
10	0.8	0.2	7	1.000	-1.000	-1.000	94.58	96.63	86.6	80.45
11	0.6	0.4	9	0.000	0.000	0.000	99.73	89.32	86.14	77.35
12	0.6	0.4	5.64	0.000	0.000	-1.682	99.61	100	80.85	72.48
13	0.6	0.4	9	0.000	0.000	0.000	86.53	90.45	87.36	78.67
14	0.6	0.064	9	0.000	-1.682	0.000	81.51	72.76	68.21	59.37
15	0.8	0.2	11	1.000	-1.000	1.000	92.38	82.99	73.41	71.74
16	0.8	0.6	11	1.000	1.000	1.000	89.35	93.11	78.66	73.25
17	0.26	0.4	9	-1.682	0.000	0.000	77.62	75.02	75.02	57.35
18	0.4	0.6	11	-1.000	1.000	1.000	86.25	88.42	80.1	69.34
19	0.6	0.4	12.36	0.000	0.000	1.682	95.69	88.87	69.85	75.56
20	0.8	0.6	7	1.000	1.000	-1.000	99.96	99.88	99.54	82.78

A: Alum dosage (g/l); B: Banana dosage (g/l); C. pH

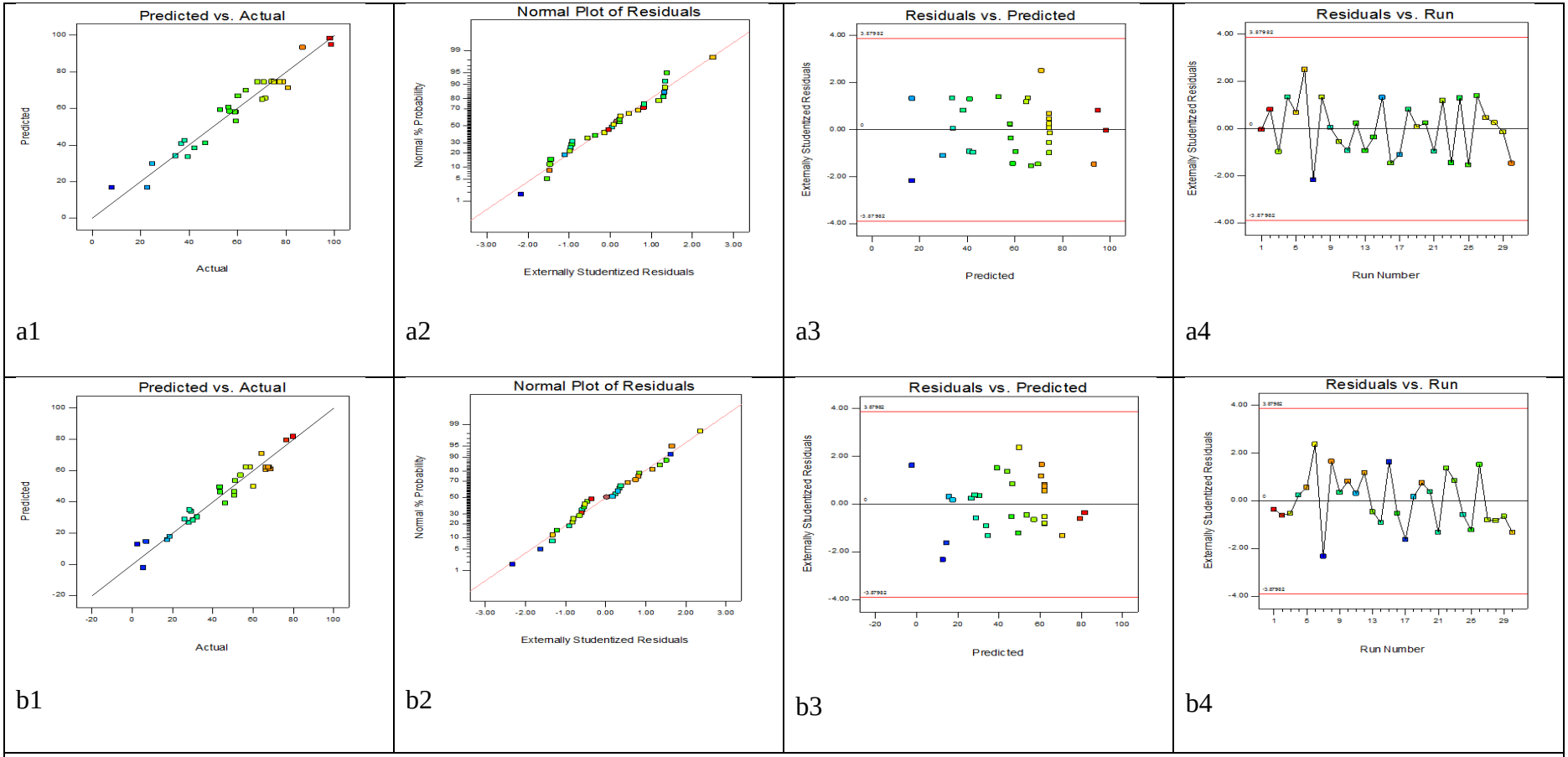

Figure D1(i): Design expert diagnostic plots for a (turbidity) and b (COD)

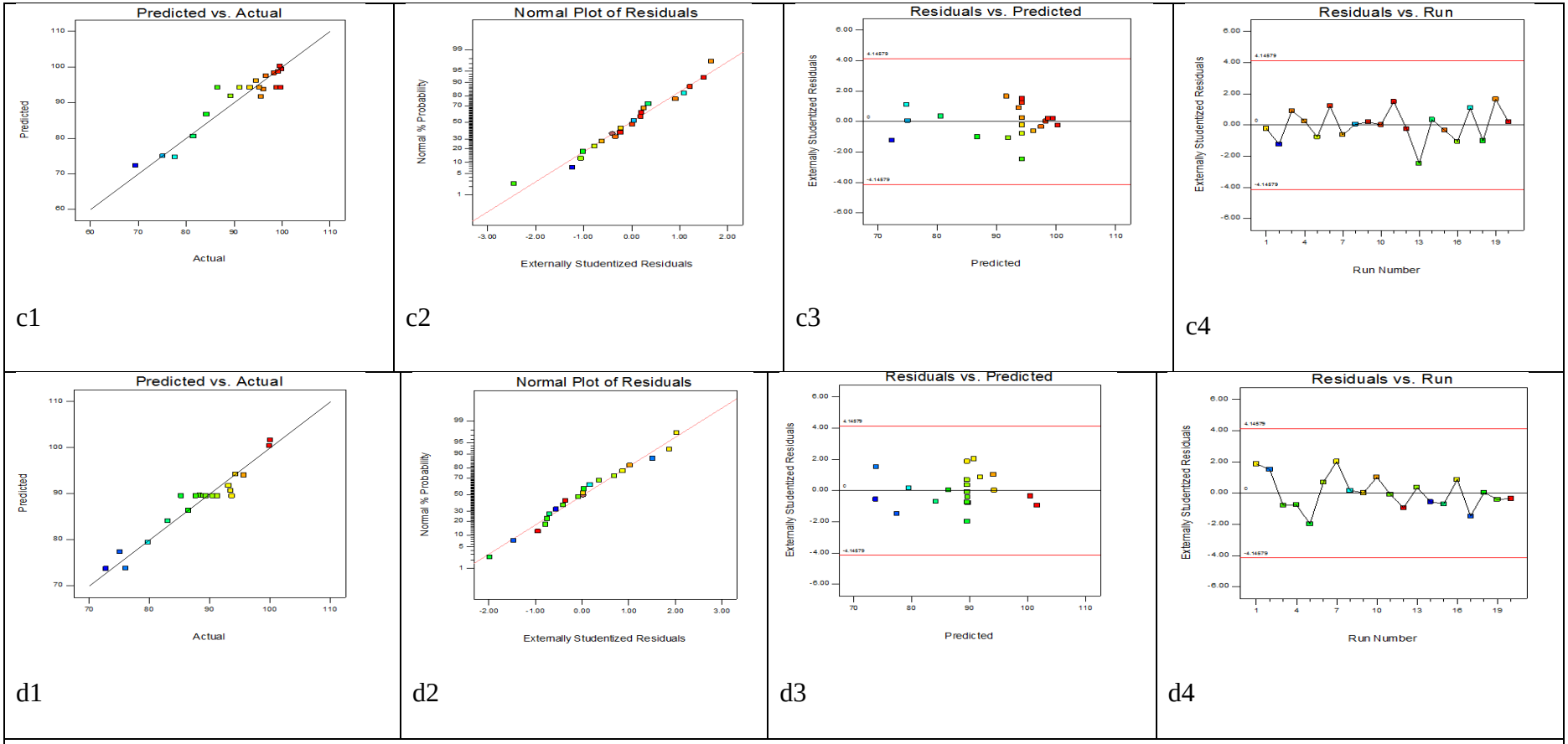

Figure D1 (ii): Design expert diagnostic plots for c (lead) and d (chromium).

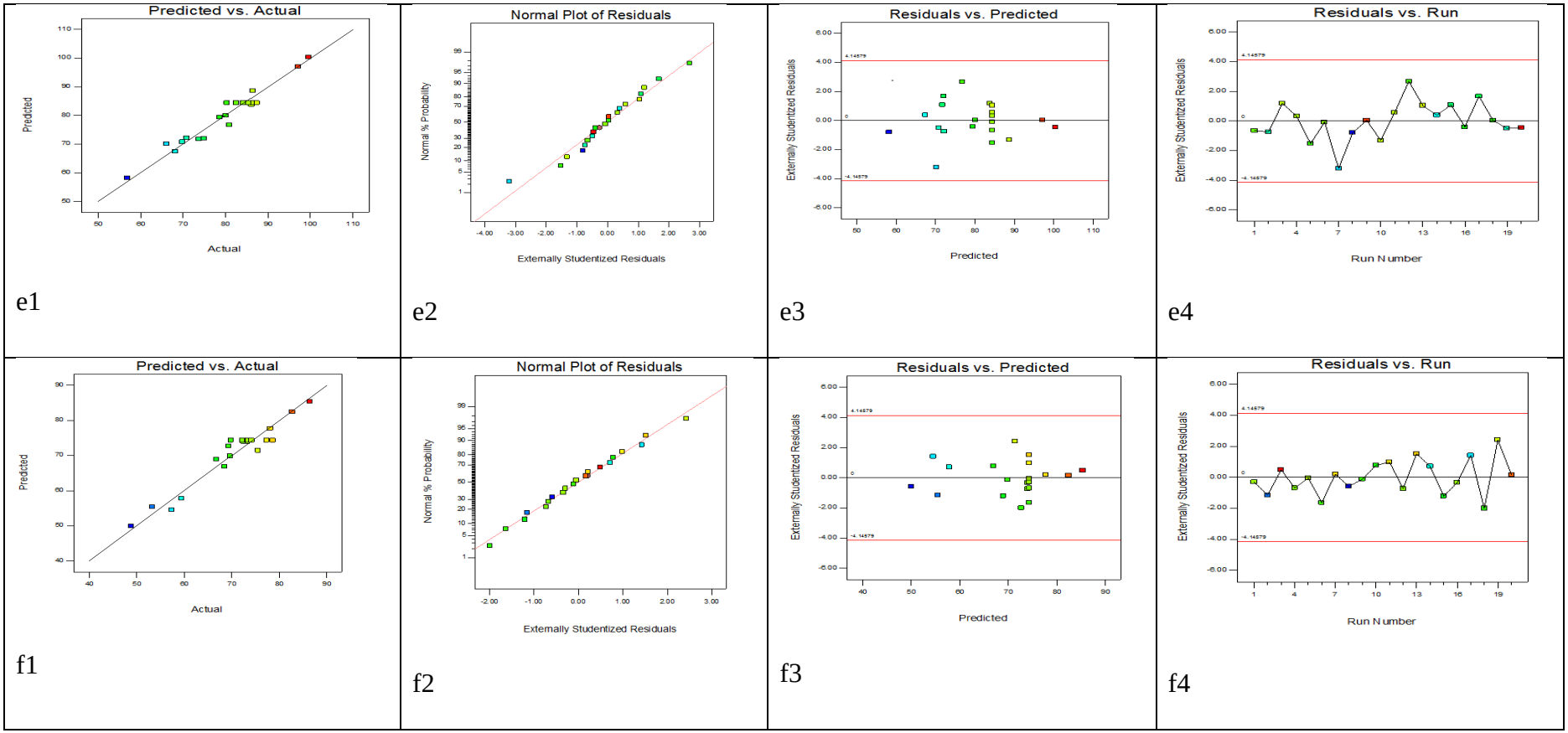

Figure D1 (iii): Design expert diagnostic plots for e (zinc) and f (iron)

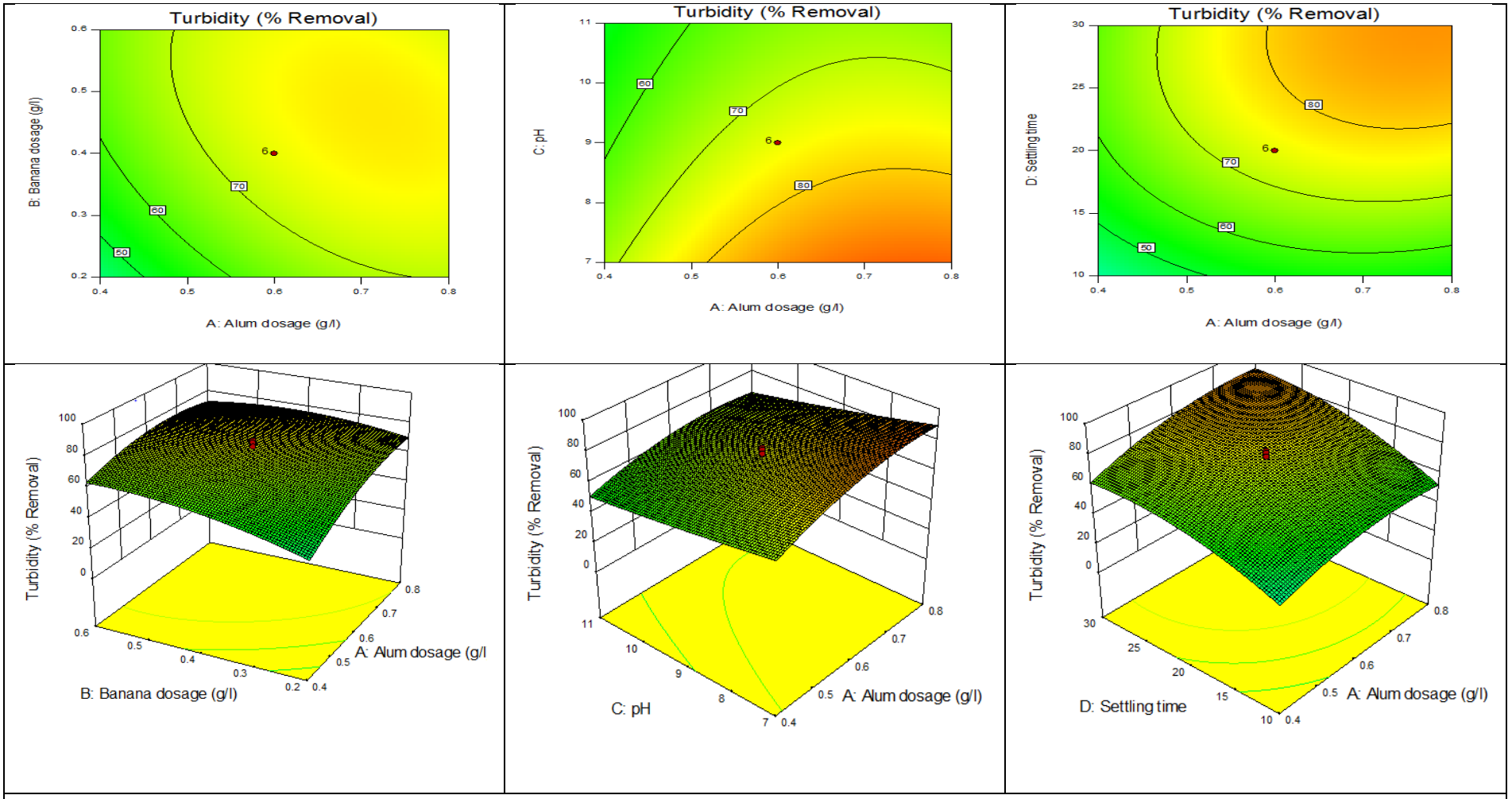

Figure D2(i): Contour and 3D plots for turbidity removal using alum and banana coagulant

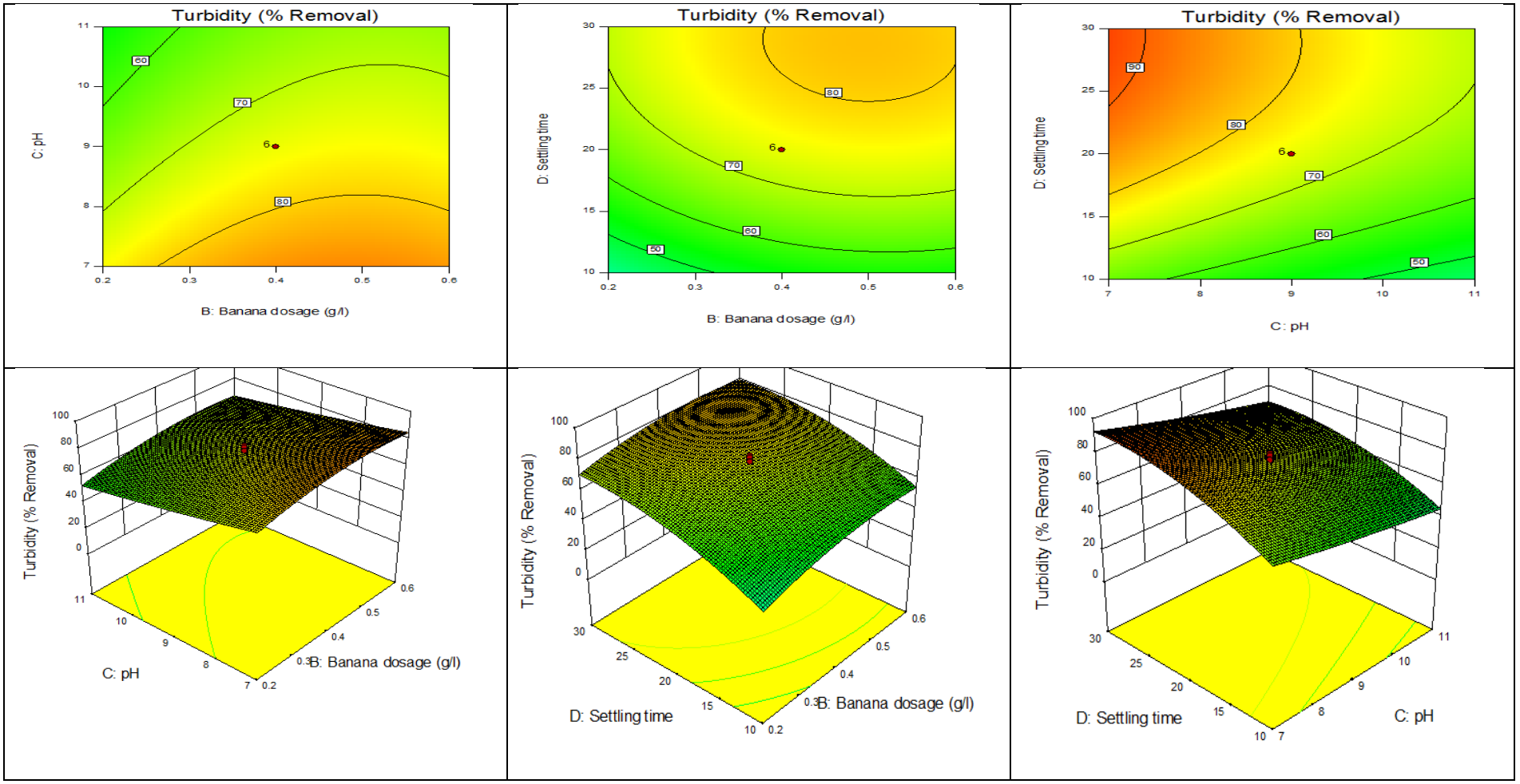

Figure D2: Contour and 3D plots for turbidity removal using alum and banana coagulant

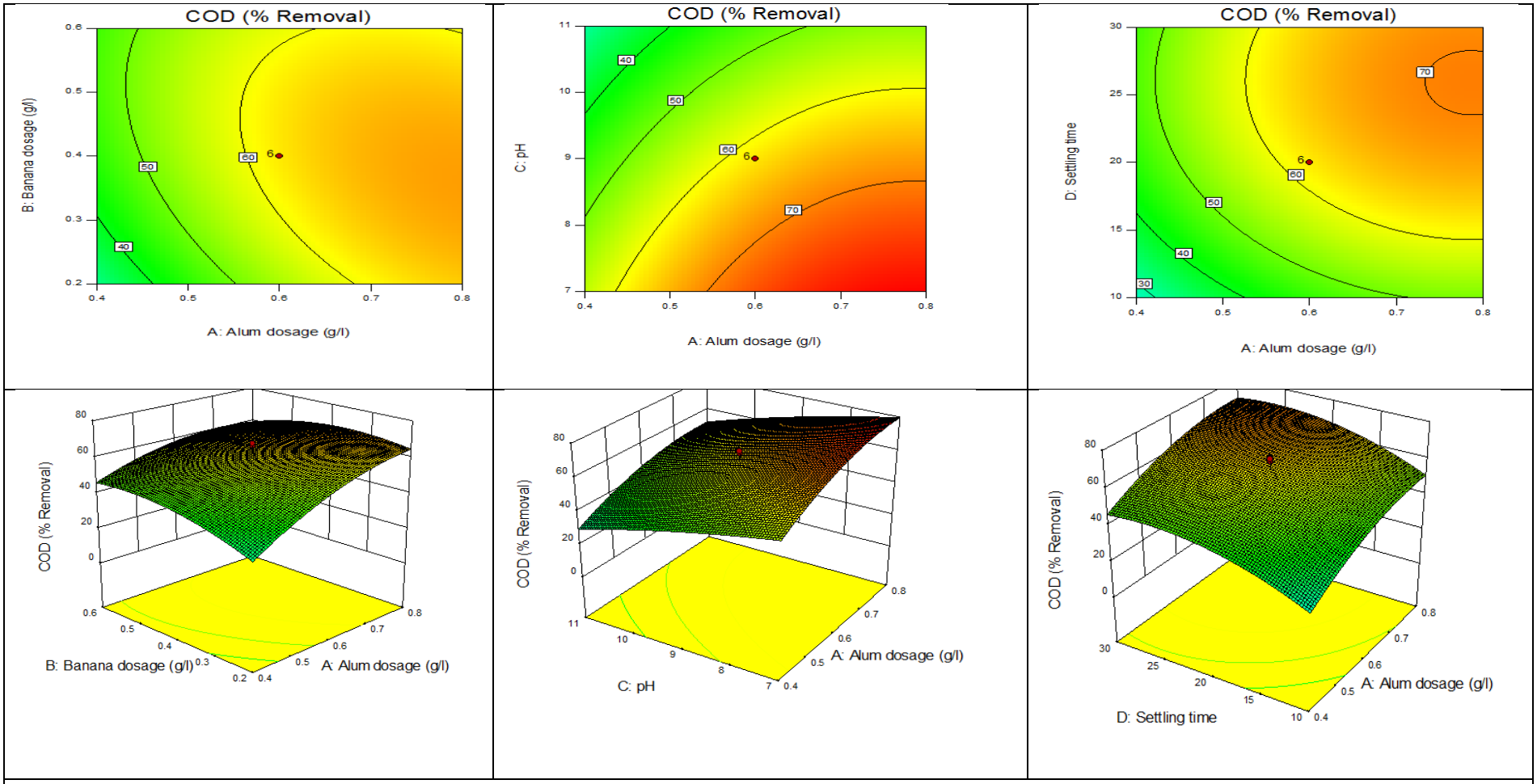

Figure D3(i): Contour and 3D plots for COD removal using alum and banana pith coagulant

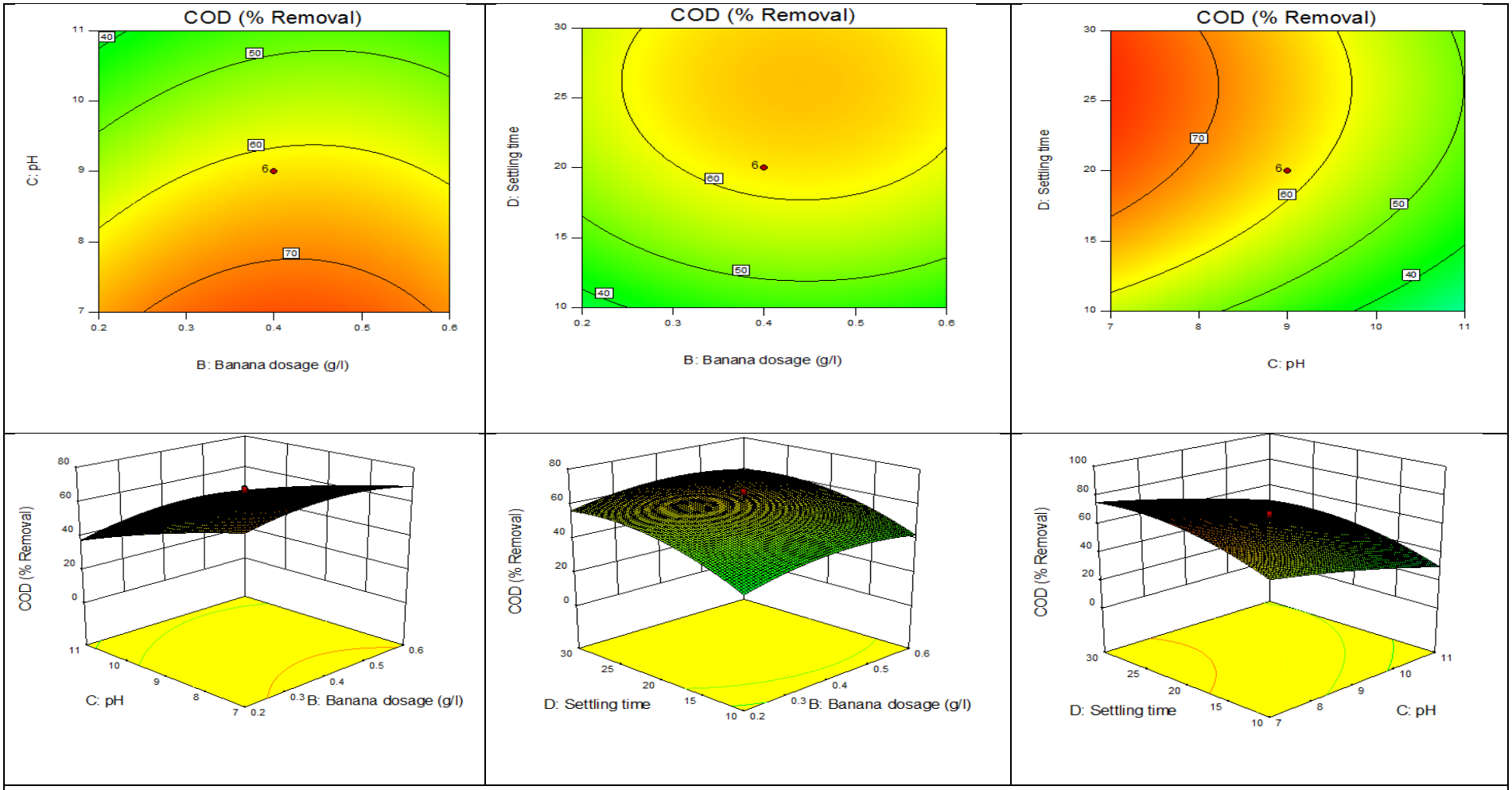

Figure D3(ii): Contour and 3D plots for COD removal using alum and banana pith coagulant

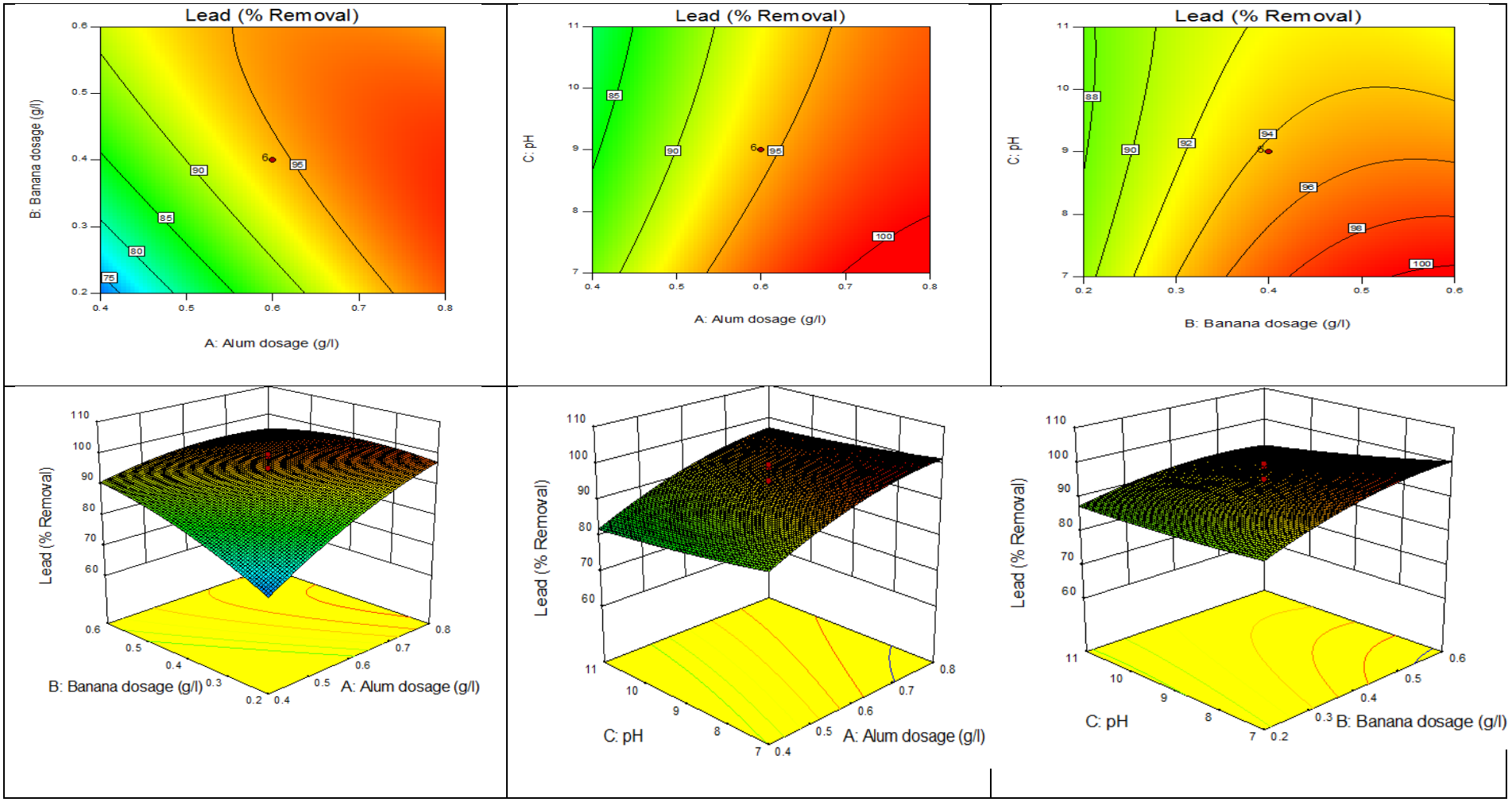

Figure D4: Contour and 3D plots for lead removal using alum and banana pith coagulant

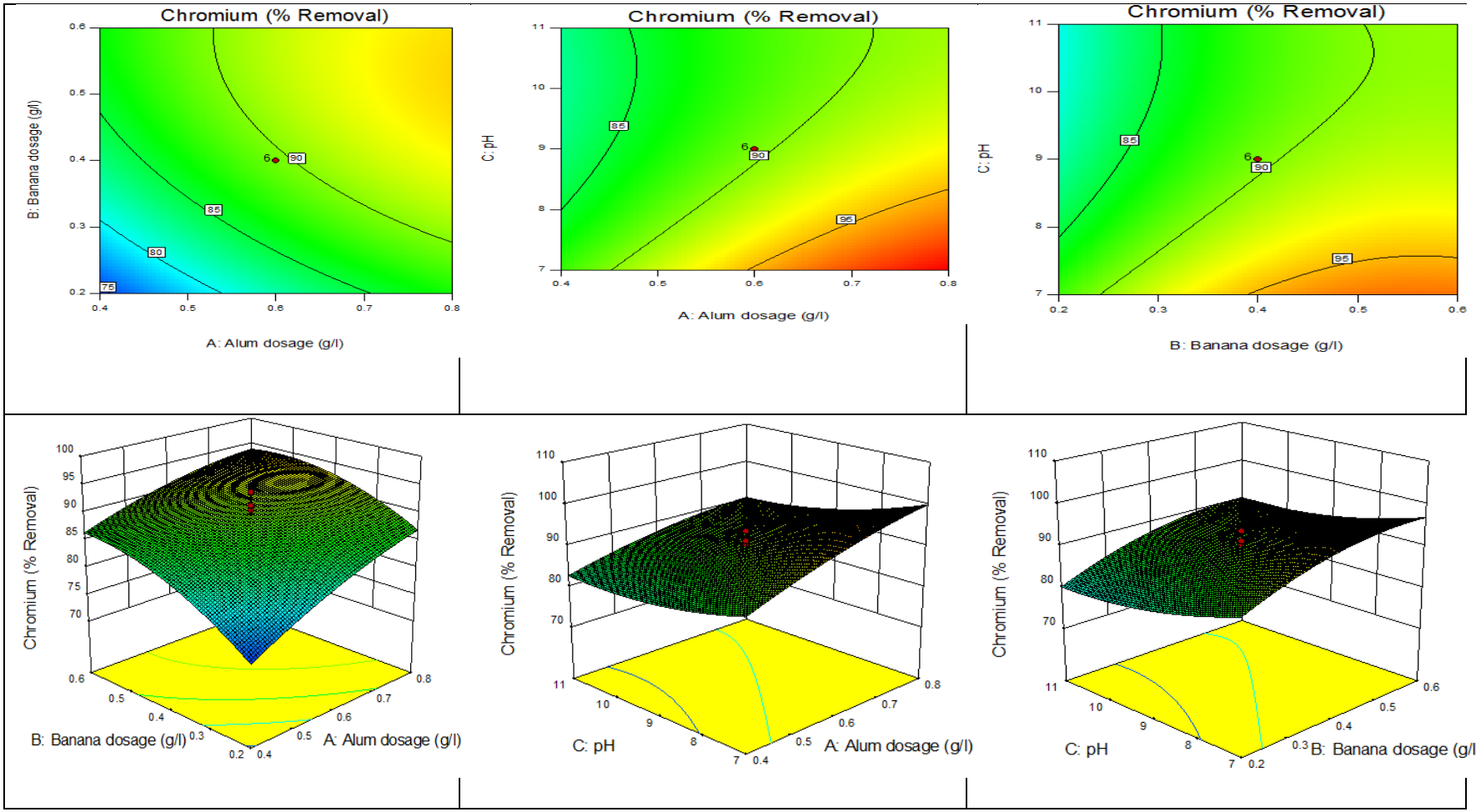

Figure D5: Contour and 3D plots for chromium removal using alum and banana pith coagulant

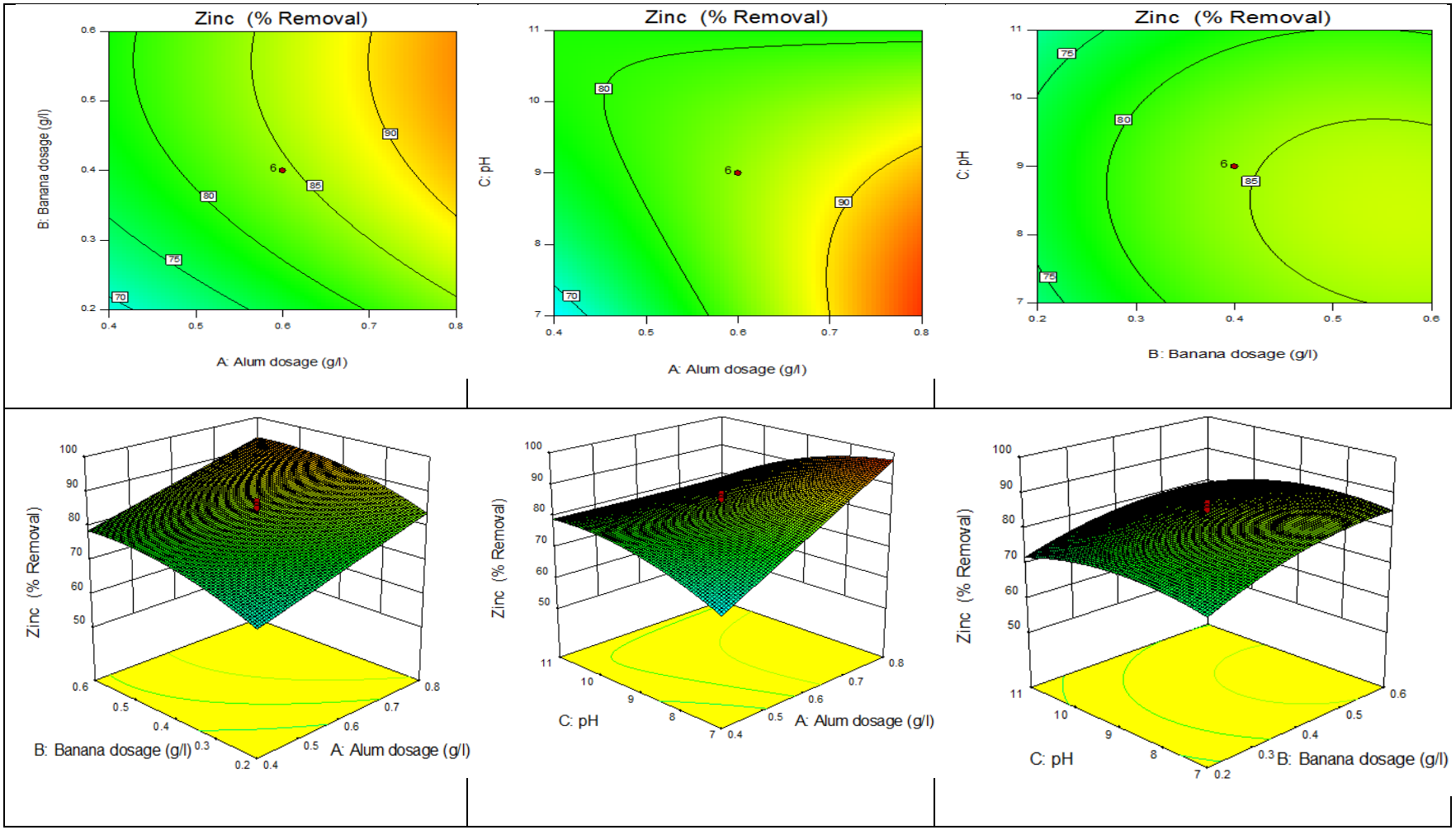

Figure D6: Contour and 3D plots for zinc removal using alum and banana pith coagulant

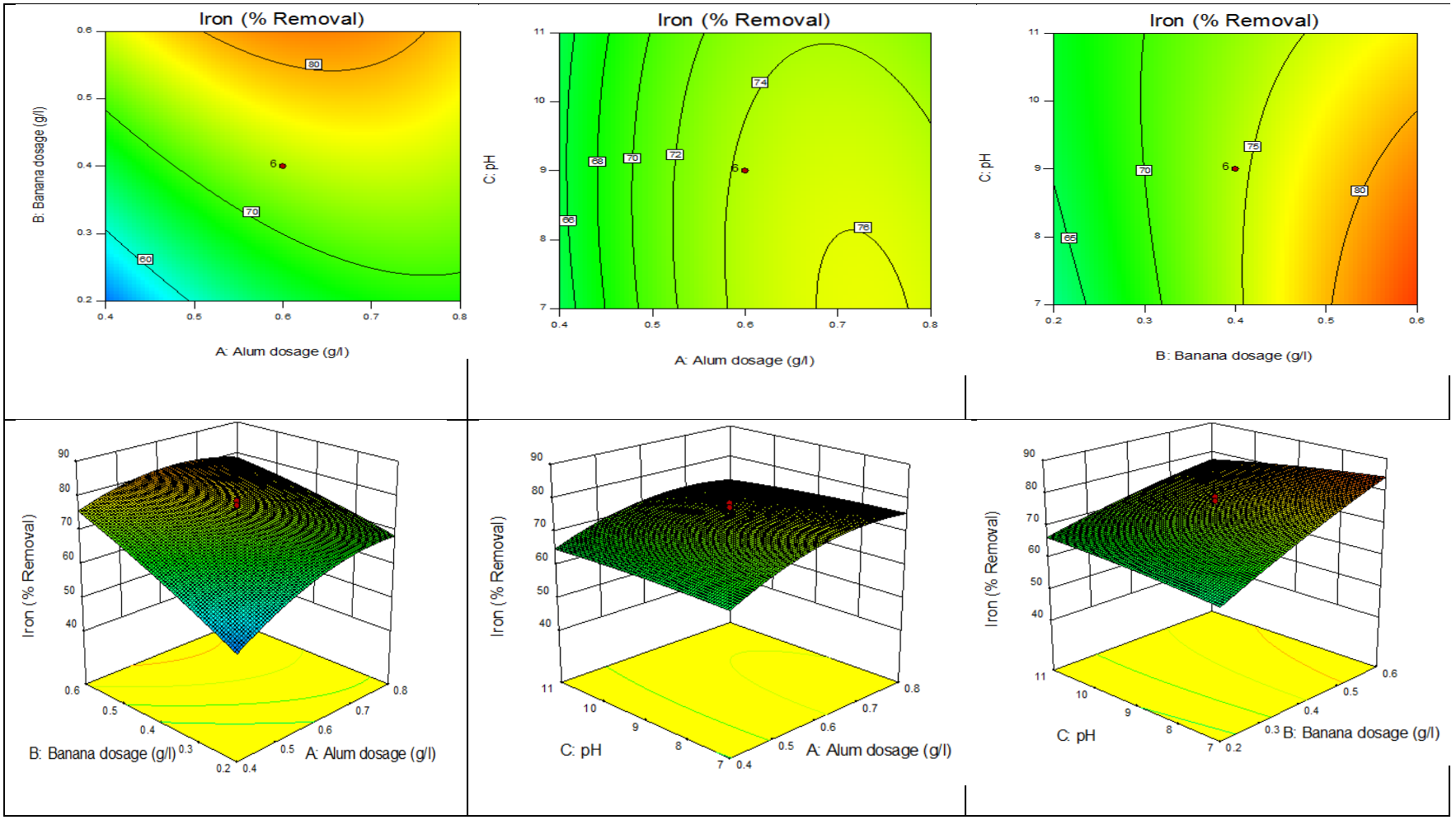

Figure D7: Contour and 3D plots for iron removal using alum and banana pith coagulant.

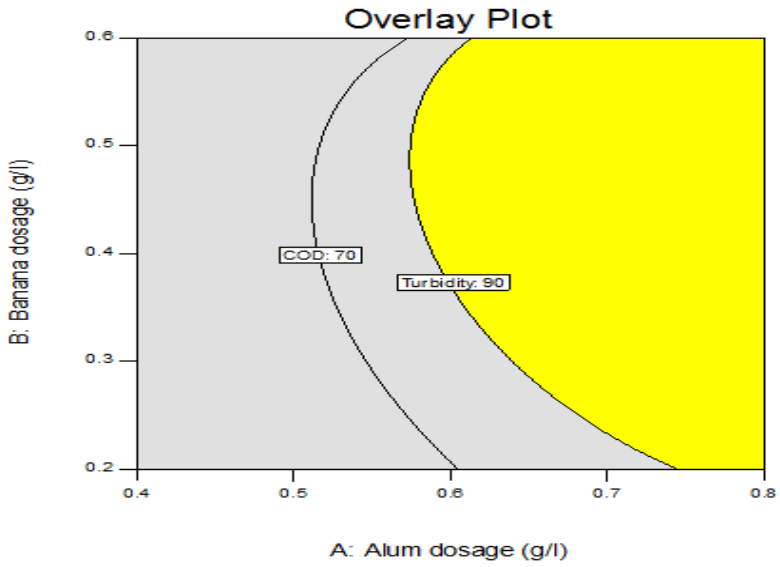

Figure D8: Design expert plot; overlay plot for optimal region for turbidity and COD using alum and banana pith coagulant

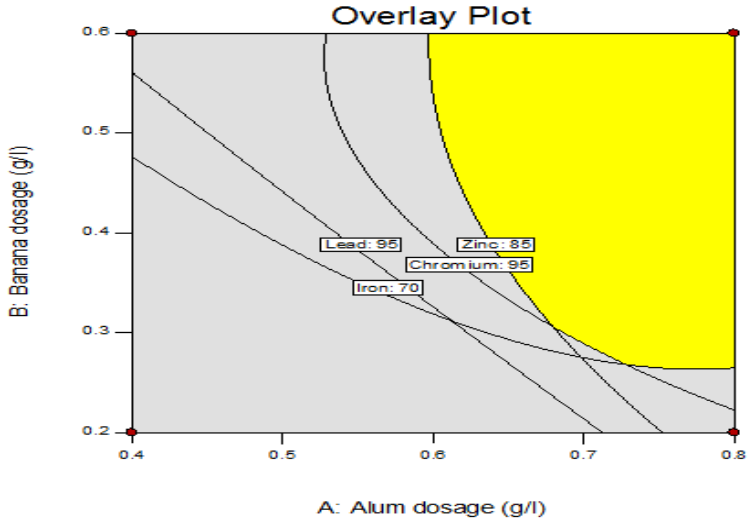

Figure D9: Design expert plot; overlay plot for optimal region for lead, chromium, zinc and iron using alum and banana pith coagulant

Table D3: Predicted and verification results for multiple response analysis.

Optimized factors	Response	Predicted values	Experimental values	Error
Alum 0.63g/l; Banana 0.47g/l at pH 7.11 and settling time 25.76 minutes	Turbidity	92.79	91.47	1.32
	COD	76.89	73.84	3.05
Alum 0.68g/l ; Banana pith0.4 g/l at pH 7	Lead	99.74	99.21	0.53
	Chromium	97.57	96.98	0.59
	Zinc	88.79	86.53	2.26
	Iron	76.09	76.51	-0.42

Appendix E: Optimization using Opuntia Spp. and CKD.

Table E1: CCD and Response results for study of three experimental variables for Opuntia Spp. and CKD coagulant.

Run	Actual			Coded			Response (% removal)	
	A	B	C	A	B	C	Turbidity	COD
1	0.029	7	20	-1.682	0.000	0.000	56.83	32.21
2	0.7	4	10	1.000	-1.000	-1.000	62.83	30.12
3	0.45	7	20	0.000	0.000	0.000	78.43	67.2
4	0.45	7	36.82	0.000	0.000	1.682	95.47	80.86
5	0.7	10	10	1.000	1.000	-1.000	81.46	74.65
6	0.2	4	30	-1.000	-1.000	1.000	54.26	42.29
7	0.87	7	20	1.682	0.000	0.000	81.3	59.12
8	0.7	10	30	1.000	1.000	1.000	99.75	76.58
9	0.45	12.04	20	0.000	1.682	0.000	99.18	76.14
10	0.45	7	3.182	0.000	0.000	-1.682	53.77	43.17
11	0.45	7	20	0.000	0.000	0.000	88.37	63.36
12	0.45	7	20	0.000	0.000	0.000	79.78	71.28
13	0.45	7	20	0.000	0.000	0.000	82.18	73.52
14	0.2	10	10	-1.000	1.000	-1.000	72.08	54.28
15	0.45	1.95	20	0.000	-1.682	0.000	59.36	12.14
16	0.45	7	20	0.000	0.000	0.000	86.83	63.71
17	0.2	10	30	-1.000	1.000	1.000	88.56	75.63
18	0.2	4	10	-1.000	-1.000	-1.000	46.68	12.71
19	0.45	7	20	0.000	0.000	0.000	89.63	69.26
20	0.7	4	30	1.000	-1.000	1.000	78.11	46.25

A: Opuntia spp. dosage (g/l) B: CKD dosage (ml) C: Settling time (mins)

Table E2: CCD and Response results for study of two experimental variables for Opuntia Spp. and CKD coagulant.

Run	Actual		Coded		Responses (% Removal)			
	A	B	A	B	Lead	Chromium	Zinc	Iron
1	0.45	2.76	0.000	-1.414	63.12	59.58	84.95	63.25
2	0.2	10	-1.000	1.000	75.5	97	89.12	65.98
3	0.803	7	1.414	0.000	79.25	87.79	98.01	80.08
4	0.45	7	0.000	0.000	92.84	86.67	77.83	91.01
5	0.45	7	0.000	0.000	97.75	80.09	85.67	82.66
6	0.45	11.24	0.000	1.414	97.14	100	99.99	99.25
7	0.2	4	-1.000	-1.000	58.71	52.48	61.14	61.04
8	0.45	7	0.000	0.000	88.18	85.33	80.12	88.28
9	0.7	10	1.000	1.000	97.2	100	100	89.97
10	0.45	7	0.000	0.000	86.74	87.76	79.32	80.49
11	0.7	4	1.000	-1.000	77.91	69.77	89.34	66.61
12	0.45	7	0.000	0.000	92.91	89.54	82.69	93.35
13	0.096	7	-1.414	0.000	45.52	65.23	57.77	53.02

A: Opuntia spp. dosage (g/l) B: CKD dosage (ml)

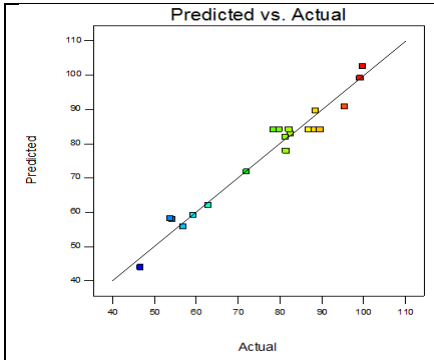

a1

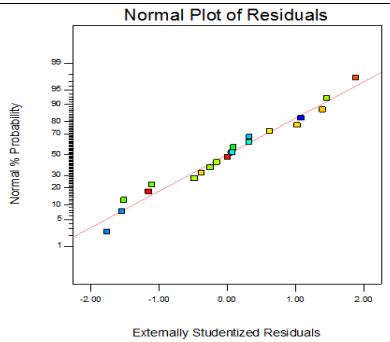

a2

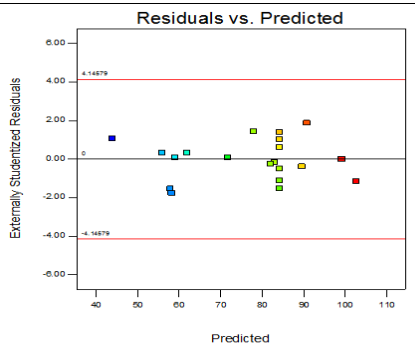

a3

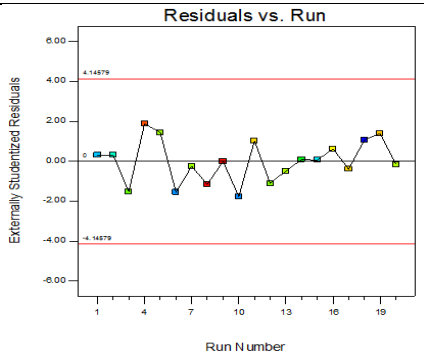

a4

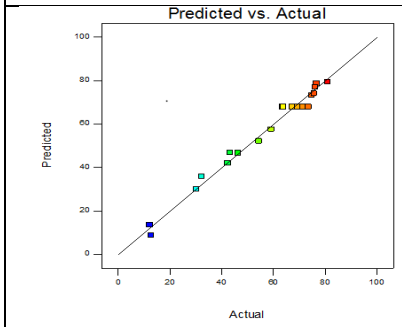

b1

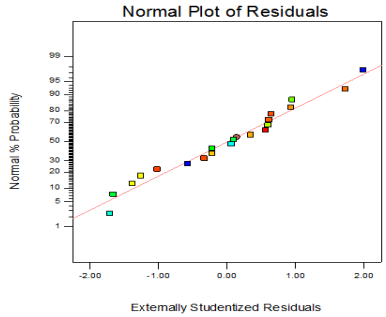

b2

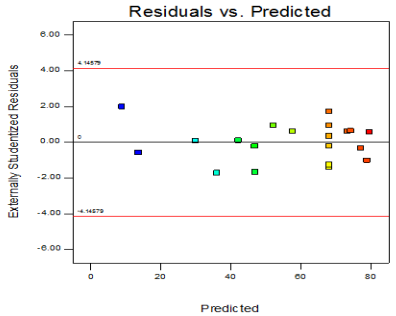

b3

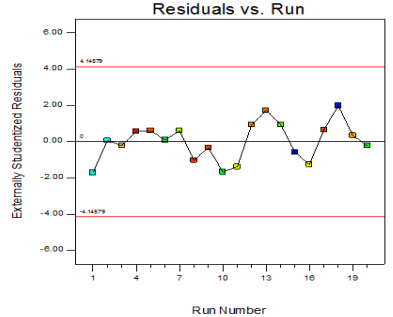

b4

Figure E1(i): Design expert diagnostic plots for a (turbidity) and b (COD)

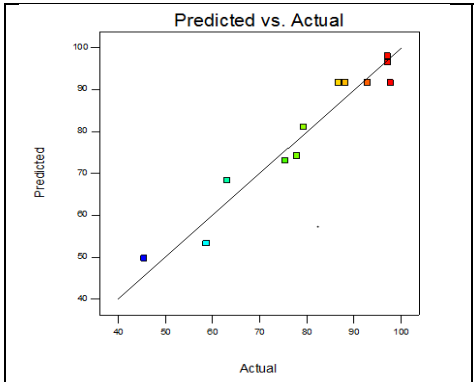

c1

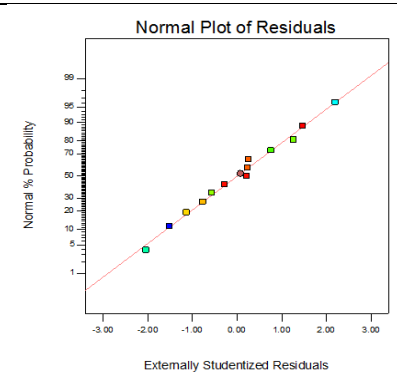

c2

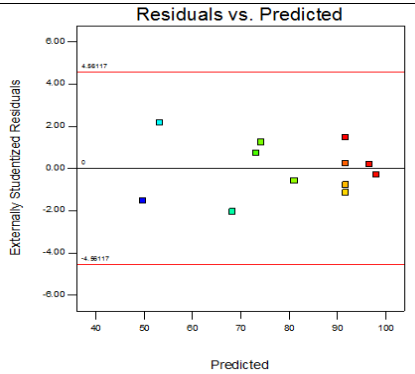

c3

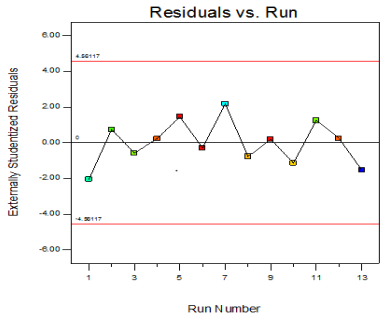

c4

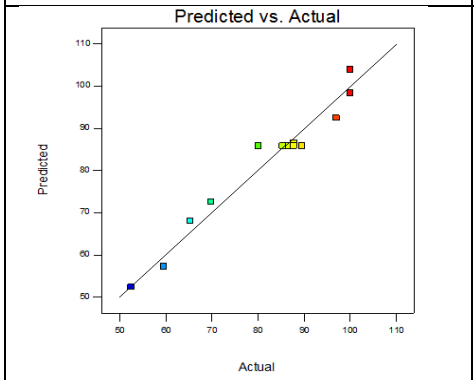

d1

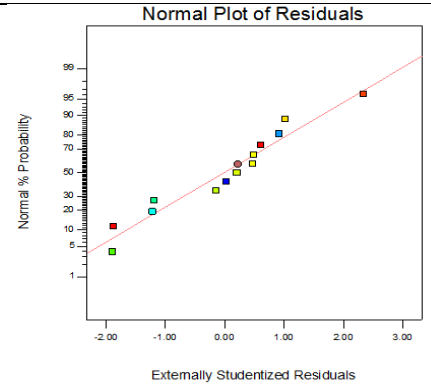

d2

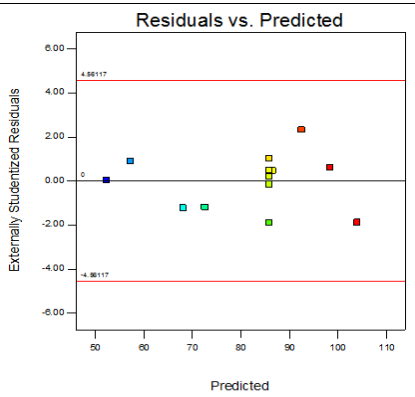

d3

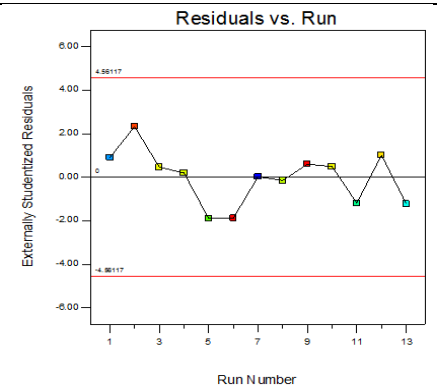

d4

Figure E1 (ii): Design expert diagnostic plots for c (lead) and d (chromium).

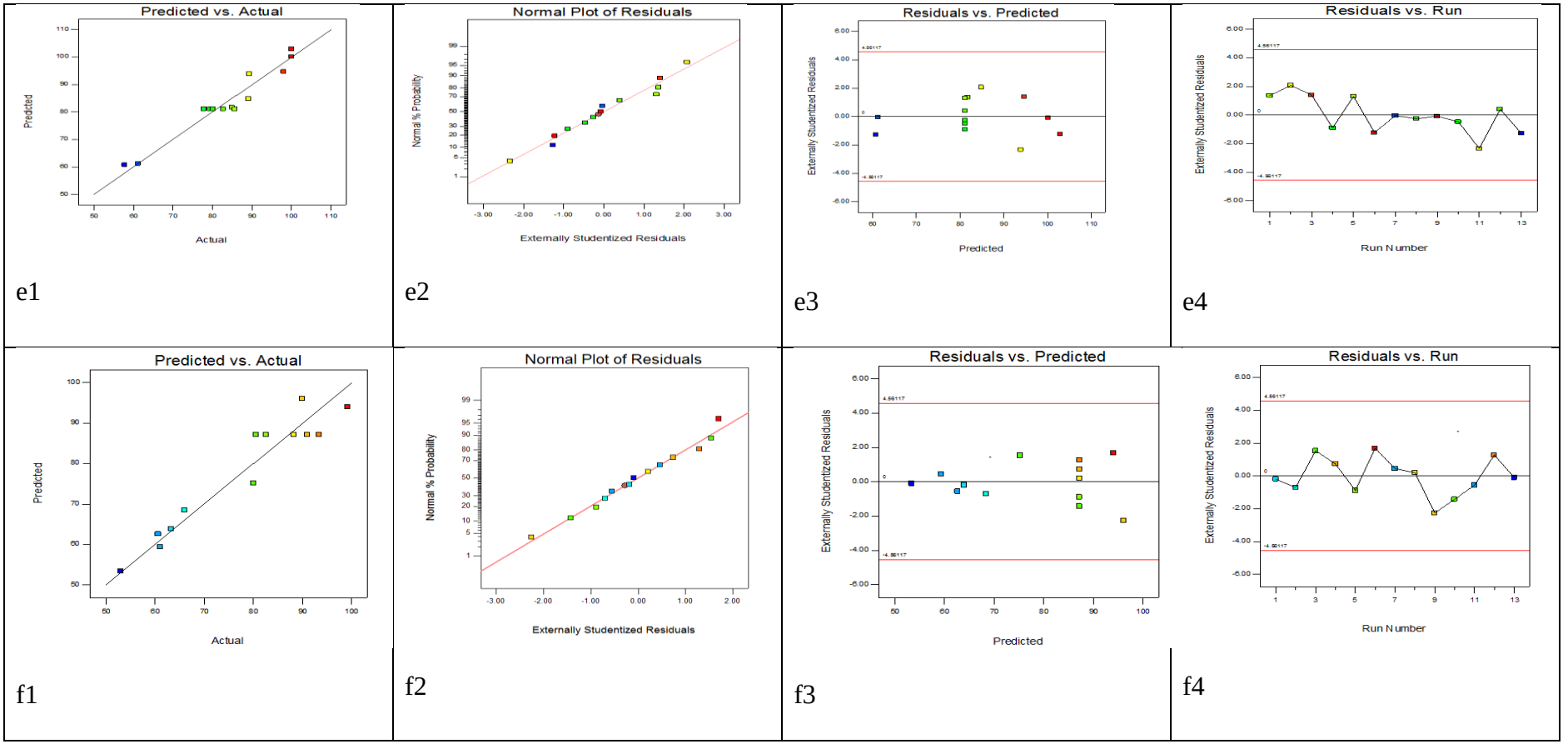

Figure E1 (iii): Design expert diagnostic plots for a (turbidity), b (COD), c (lead), d (chromium), e (zinc) and f (iron).

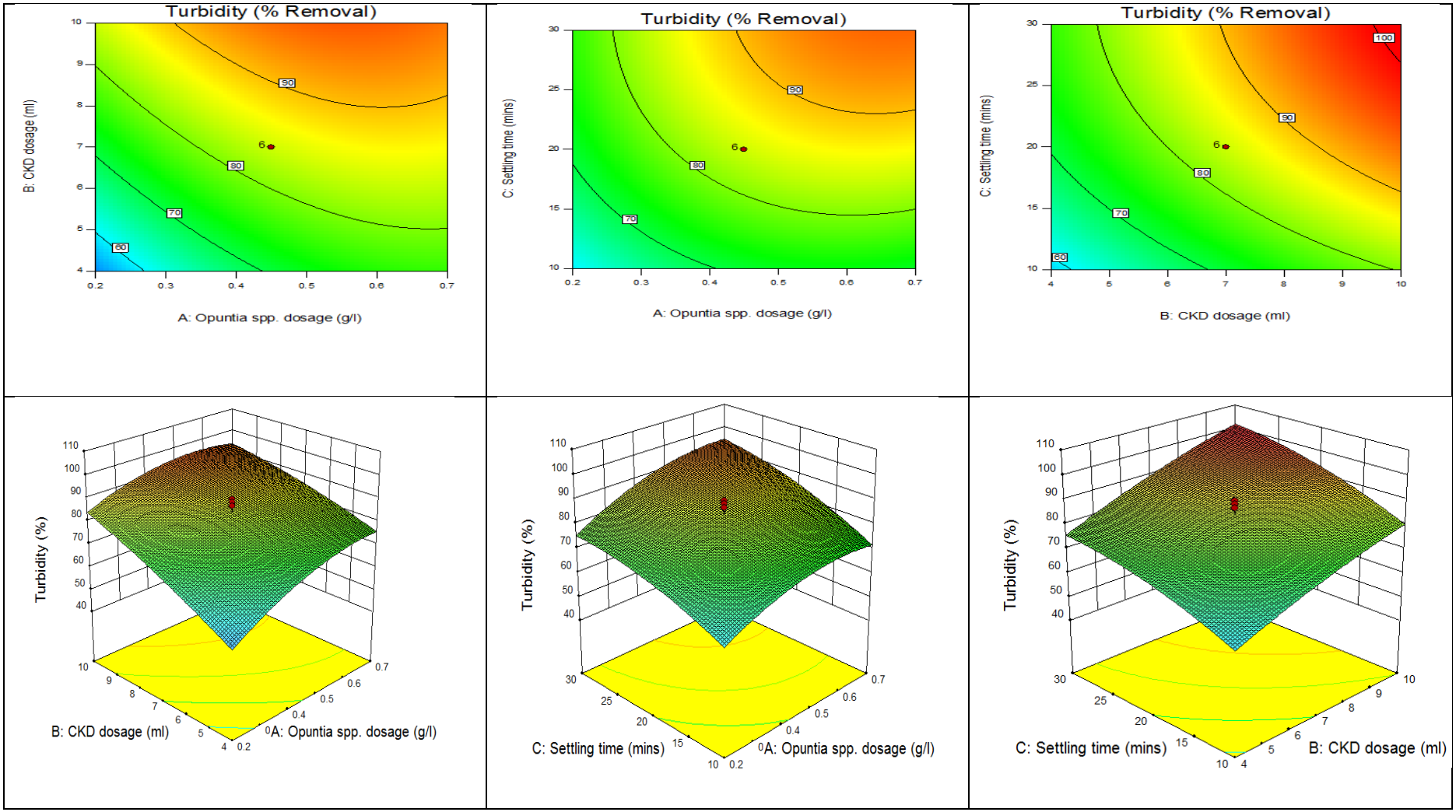

Figure E2: Contour and 3D plots for turbidity removal using Opuntia Spp. and CKD coagulant

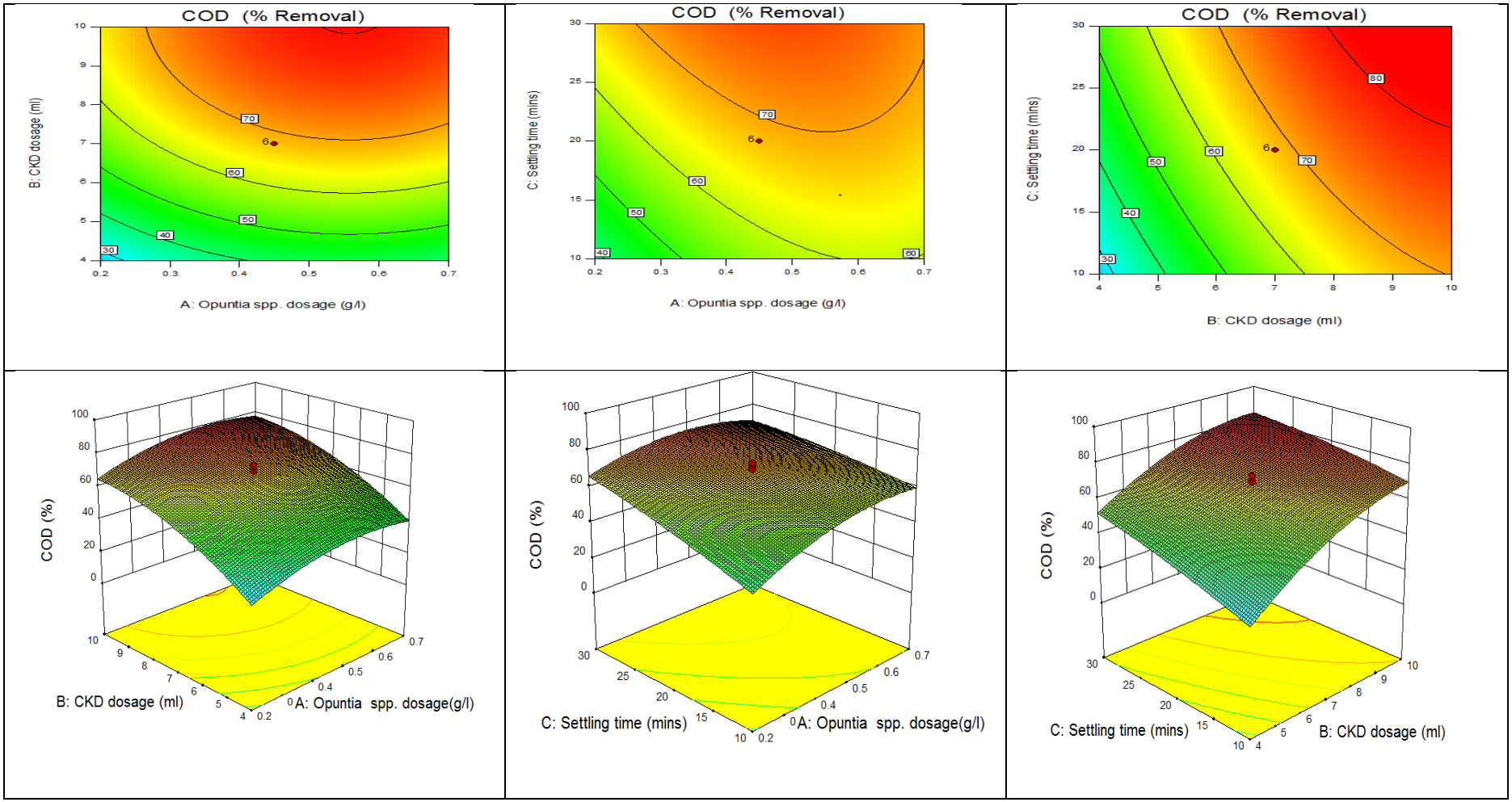

Figure E3: Contour and 3D plots for COD removal using Opuntia Spp. and CKD coagulant

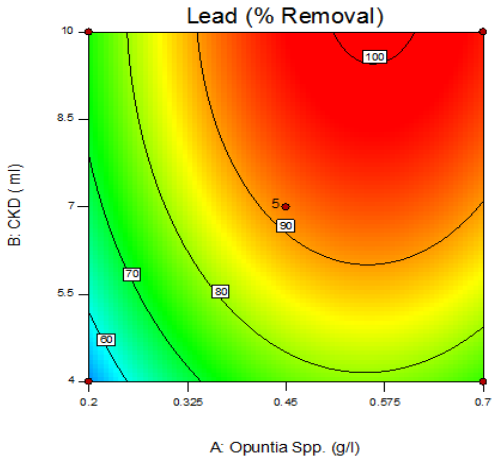

a1

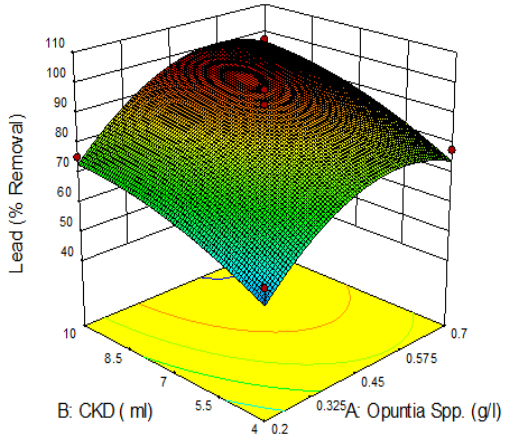

a2

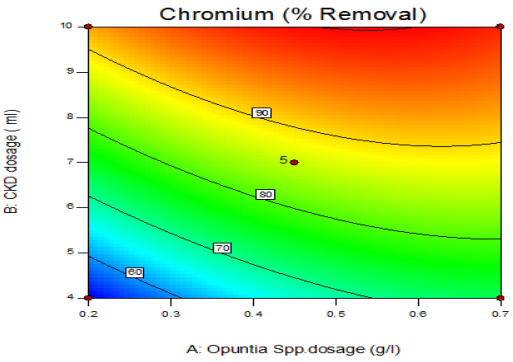

b1

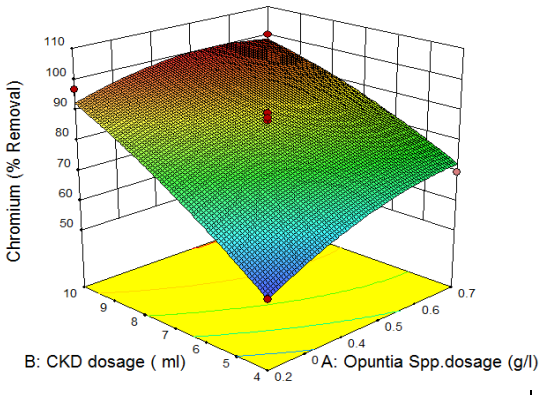

b2

Figure E4(i): Contour and 3D plots for a (lead) and b (chromium) removal using Opuntia Spp. and CKD

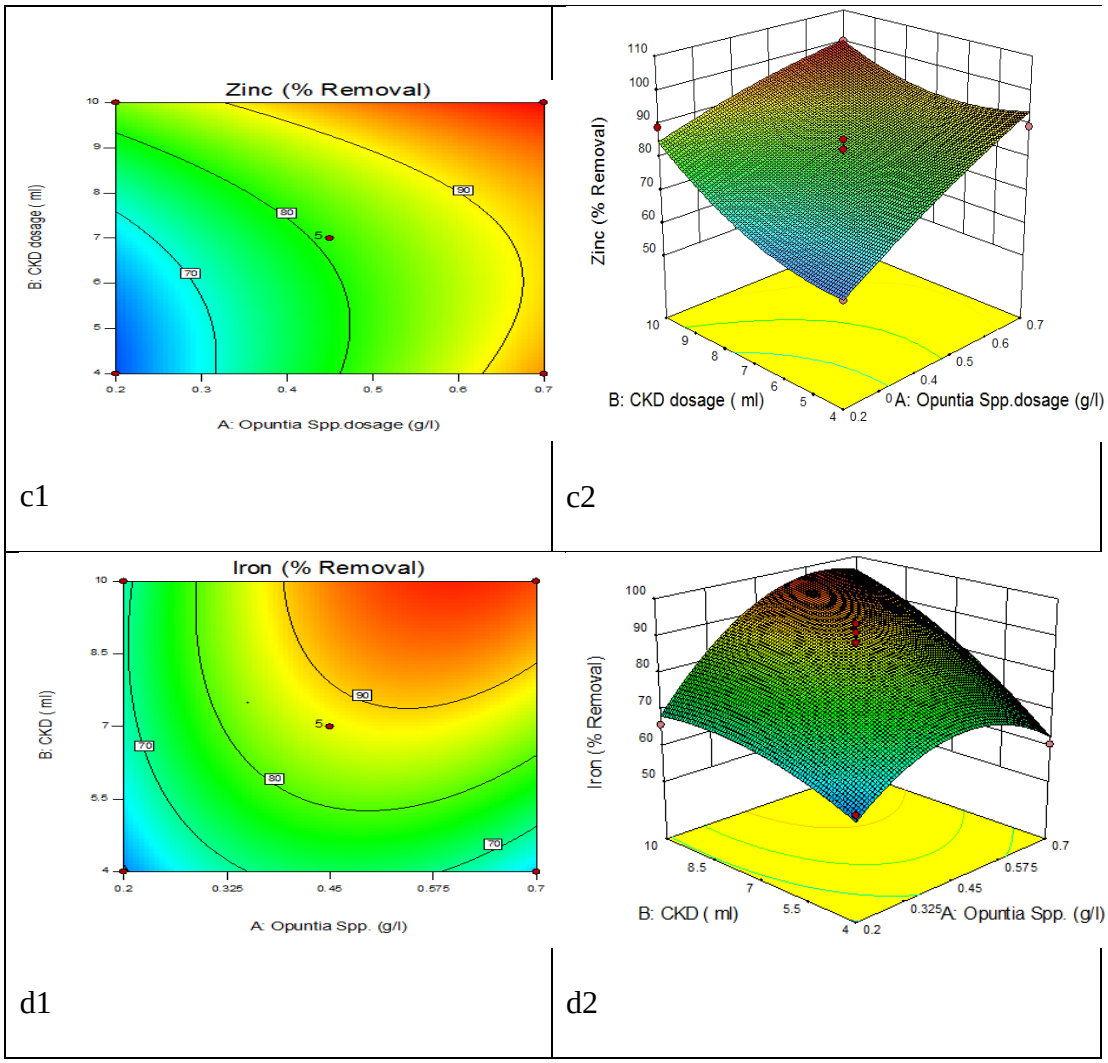

Figure E4 (ii): Contour and 3D plots for c (zinc) and d (iron) removal using Opuntia Spp. and CKD

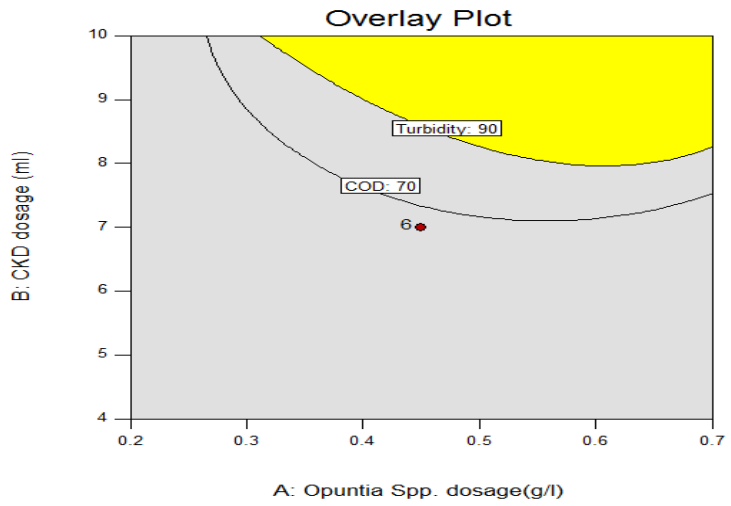

Figure E5. Design expert plot; overlay plot for optimal region for turbidity and COD using Opuntia Spp. and CKD coagulant

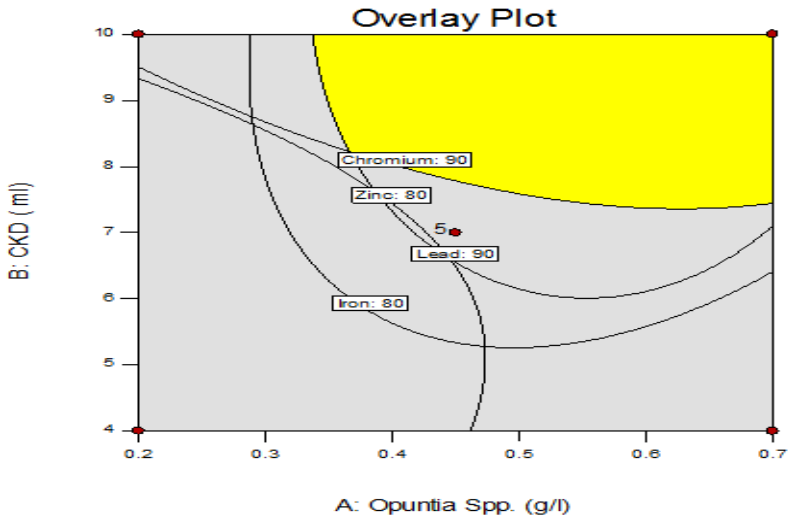

Figure E6: Design expert plot; overlay plot for optimal region for lead, chromium, zinc and iron using Opuntia Spp. and CKD coagulant.

Table E3: Predicted and verification results for multiple response analysis.

Optimized factors	Response	Predicted values	Experimental values	Error
Opuntia Spp. 0.52 g/l CKD of 9.32 ml, settling time 20 minutes	Turbidity	93.44	92.87	0.57
	COD	78.96	76.22	2.74
Opuntia Spp.0.52 g/l CKD of 8.45 ml	Lead	98.00	96.58	1.42
	Chromium	94.28	93.46	0.82
	Zinc	88.87	84.73	4.14
	Iron	93.53	92.91	0.62

Appendix F

Table F1: Percentage of contribution (PC) for each individual term in response quadratic models using Maerua Decumbent coagulant.

	Turbidity removal		COD				Lead		Chromium		Zinc		Iron	
Sources	Sum of Squares	PC (%)	Sum of Squares	PC (%)		Sources	Sum of Squares	PC (%)	Sum of Squares	PC (%)	Sum of Squares	PC (%)	Sum of Squares	PC (%)
A-Dosage	431.39	4.95	565.97	7.17		A-Dosage	9.31	4.10	178.11	15.62	242.73	62.50	380.83	45.62
B-pH	1868.34	21.42	2220.05	28.12		B-pH	17.72	7.80	765.16	67.12	88.85	22.88	143.9	17.24
C-Settling time	2432.11	27.88	2202.3	27.89		AB	0.11	0.05	*32.04*	2.81	7.02	1.81	0.4	0.05
AB	58.21	0.67	35.07	0.44		A^2	0.58	0.26	36.49	3.20	43.62	11.23	110.2	13.20
AC	0.32	0.00	39.83	0.50		B^2	199.57	87.80	128.2	11.25	6.13	1.58	199.49	23.90
BC	54.71	0.63	232.74	2.95		Total	227.29	100.00	1140	100.00	388.35	100.00	834.82	100.00
A^2	280.07	3.21	934.88	11.84										
B^2	844.66	9.68	467.58	5.92										
C^2	2753.15	31.56	1197.78	15.17										
Total	8722.96	100.00	7896.2	100.00										

Table F2: Percentage of contribution (PC) for each individual term in response quadratic models using Alum coagulant.

Sources	Turbidity removal		COD removal			Sources	Lead removal		Chromium removal		Zinc removal		Iron removal	
	Sum of Squares	PC (%)	Sum of Squares	PC (%)			Sum of Squares	PC (%)	Sum of Squares	PC (%)	Sum of Squares	PC (%)	Sum of Squares	PC (%)
A-Dosage	6735.56	72.03	4038.9	69.21		A-Dosage	2761.3	73.77	1420.3	55.11	1077.2	30.00	1131.4	50.80
B-pH	1124.95	12.03	683.3	11.71		B-pH	2.6	0.07	585.44	22.71	116.93	3.26	65.02	2.92
C-Settling time	817.05	8.74	425.23	7.29		AB	73.44	1.96	*83.72*	3.25	129.5	3.61	103.94	4.67
AB	16.59	0.18	127.52	2.19		A^2	708.58	18.93	484.45	18.80	203.4	5.66	157.42	7.07
AC	5.38	0.06	67.51	1.16		B^2	197.44	5.27	3.46	0.13	2063.5	57.47	769.22	34.54
BC	45.22	0.48	0.16	0.00		Total	3743.3	100.00	2577.4	100.00	3590.5	100.00	2227	100.00
A^2	438.3	4.69	366.18	6.27										
B^2	37.73	0.40	8	0.14										
C^2	129.64	1.39	118.85	2.04										
Total	9350.42	100.00	5835.65	100.00										

Table F3: Percentage of contribution (PC) for each individual term in response quadratic models using Alum and banana pith Coagulant.

Sources	Turbidity removal		COD removal			Sources	Lead removal		Chromium removal		Zinc removal		Iron removal	
	Sum of Squares	PC (%)	Sum of Squares	PC (%)			Sum of Squares	PC (%)	Sum of Squares	PC (%)	Sum of Squares	PC (%)	Sum of Squares	PC (%)
A-Alum dosage	*1927.3*	14.08	*3216.23*	23.35		*A-Alum dosage*	*692.18*	48.91	*342*	32.66	*758.2*	38.85	*284*	17.46
B-Banana dosage	*759.04*	5.55	*127.28*	0.92		*B-Banana dosage*	*207.97*	14.70	*306.2*	29.25	*325.9*	16.70	*913*	56.14
C-pH	*2443.19*	17.85	*4289.36*	31.13		*C-pH*	*89.87*	6.35	*174.4*	16.66	*42.14*	2.16	*7.87*	0.48
D-Settling time	*4437.68*	32.42	*2069.63*	15.02		*AB*	*200.2*	14.15	*11.93*	1.14	*0.021*	0.00	*75.09*	4.62
AB	*292.84*	2.14	*375.49*	2.73		*AC*	*1.84*	0.13	*9.53*	0.91	*475.1*	24.34	*6*	0.37
AC	*51.23*	0.37	*1.59*	0.01		*BC*	*22.85*	1.61	*0.79*	0.08	*8.38*	0.43	*55.81*	3.43
AD	*125.5*	0.92	*0.51*	0.00		A^2	*102.71*	7.26	*25.22*	2.41	*0.036*	0.00	*266*	16.36
BC	*20.27*	0.15	*31.33*	0.23		B^2	*92.37*	6.53	*110.5*	10.55	*139.3*	7.14	*13.74*	0.84
BD	*16.06*	0.12	*3.2*	0.02		C^2	*5.08*	0.36	*66.34*	6.34	*202.7*	10.39	*4.8*	0.30
CD	*16.5*	0.12	*0.028*	0.00		Total	1415.07	100.00	1046.84	100.00	1951.79	100.00	1626.33	100.00
A^2	*1233.76*	9.01	*1033.24*	7.50										
B^2	*744.67*	5.44	*895.88*	6.50										
C^2	*23.25*	0.17	*90.74*	0.66										
D^2	*1597.02*	11.67	*1642.16*	11.92										
Total	13688.31	100.00	13776.668	100.00										

Table F4: Percentage of contribution (PC) for each individual term in response quadratic models using Opuntia Spp and CKD Coagulant.

Sources	Turbidity removal		COD removal			Sources	Lead removal		Chromium removal		Zinc removal		Iron removal	
	Sum of Squares	PC (%)	Sum of Squares	PC (%)			Sum of Squares	PC (%)	Sum of Squares	PC (%)	Sum of Squares	PC (%)	Sum of Squares	PC (%)
A-Opuntia spp. dosage	*824.97*	17.27	*566.36*	6.53		*A-Opuntia Spp.*	*981.28*	30.72	*340.5*	12.42	*1152*	60.19	*477.9*	18.67
B-CKD dosage	*1934*	40.50	*4851.57*	55.90		*B-CKD*	*886.03*	27.74	*2175*	79.34	*448.7*	23.45	*907.6*	35.47
C-Settling time	*1279.34*	26.79	*1283.14*	14.78		*AB*	*1.56*	0.05	*51.05*	1.86	*75*	3.92	*149.1*	5.83
AB	*71.1*	1.49	*3.13E-04*	0.00		A^2	*1199.5*	37.55	*126.7*	4.62	*19.82*	1.04	*908.7*	35.51
AC	*24.26*	0.51	*135.05*	1.56		B^2	*126.18*	3.95	*48.06*	1.75	*218.3*	11.41	*115.7*	4.52
BC	*7.01*	0.15	*62.89*	0.72		Total	3194.58	100.00	2741.5	100.00	1913.49	100.00	2558.98	100.00
A^2	*419.36*	8.78	*808.63*	9.32										
B^2	*45.99*	0.96	*929.23*	10.71										
C^2	*169.59*	3.55	*42.15*	0.49										
Total	4775.62	100.00	8679.02	100.00										